An integrated view of the essential eukaryotic chaperone FACT in complex with histones H2A-H2B

Maria Hondele

München 2013

Aus dem Adolf-Butenandt-Institut
Lehrstuhl: Physiologische Chemie
der Ludwig–Maximilians–Universität München
Vorstand: Prof. Andreas G. Ladurner, Ph.D.

An integrated view of the essential eukaryotic chaperone FACT in complex with histones H2A-H2B

Dissertation
zum Erwerb des Doktorgrades der Naturwissenschaften
an der Medizinischen Fakultät
Institut für Physiologische Chemie der
Ludwig–Maximilians–Universität
München

vorgelegt von
Maria Hondele
aus München

2013

Gedruckt mit Genehmigung der Medizinischen Faultät der Ludwigs-Maximilians-Universität München

Betreuer: Prof. Andreas G. Ladurner, PhD

Zweitgutachter: Prof Dr. Peter B. Becker

Dekan: Prof. Dr. med. Dr. h.c. M. Reiser, FACR, FRCR

Tag der mündlichen Prüfung: 16. 12. 2013

Eidesstattliche Versicherung

Hondele, Maria

Name, Vorname

Ich erkläre hiermit an Eides statt,

dass ich die vorliegende Dissertation mit dem Thema

An integrated view of the essential eukaryotic chaperone FACT in complex with histones H2A-H2B

selbständig verfasst, mich außer der angegebenen keiner weiteren Hilfsmittel bedient und alle Erkenntnisse, die aus dem Schrifttum ganz oder annähernd übernommen sind, als solche kenntlich gemacht und nach ihrer Herkunft unter Bezeichnung der Fundstelle einzeln nachgewiesen habe.

Ich erkläre des Weiteren, dass die hier vorgelegte Dissertation nicht in gleicher oder in ähnlicher Form bei einer anderen Stelle zur Erlangung eines akademischen Grades eingereicht wurde.

Ort, Datum

Unterschrift Doktorandin/Doktorand

Contents

1 Summary

1.1 Summary: Structure of the FACT chaperone domain in complex with histones H2A-H2B, and a model for FACT-mediated nucleosome reorganization

Nucleosomes are the smalles unit of chromatin: two coils of DNA are wrapped around a histone octamer core, which neutralizes its charge and 'packs' the lengthy molecule. Nucleosomes confer a barrier to processes that require access to the eukaryotic genome such as transcription, DNA replication and repair. A variety of nucleosome remodeling machines and histone chaperones facilitate nucleosome dynamics by depositing or evicting histones and unwrapping the DNA.

The eukaryotic FACT complex (composed of the subunits Spt16 and Pob3) is an essential and highly conserved chaperone. It assists the progression of DNA and RNA polymerases, for example by facilitating transcriptional initiation and elongation. Further, it promotes the genome-wide integrity of chromatin structure, including the suppression of cryptic transcription. Genetic and biochemical assays have shown that FACT's chaperone activity is crucially mediated by a direct interaction with histones H2A-H2B. However, the structural basis for how H2A-H2B are recognized and how this integrates with FACT's other functions, including the recognition of histones H3-H4 and of other nuclear factors, is unknown.

In my PhD research project, I was able to reveal the structure of the yeast chaperone domain in complex with the H2A-H2B heterodimer and show that the Spt16M module in FACT's Spt16 subunit establishes the evolutionarily conserved H2A-H2B binding and chaperoning function. The structure shows how an α-helical 'U-turn' motif in Spt16M interacts with the α1-helix of H2B. The U-turn motif scaffolds onto a tandem pleckstrin-homology-like (PHL) module, which is structurally and functionally related to the H3-H4 chaperone Rtt106 and the Pob3M domain of FACT. Biochemical and *in vivo* assays validate the crystal structure and dissect the contribution of histone tails and H3-H4 toward FACT binding.

My results show that Spt16M makes multiple interactions with histones, which I suggest allow the module to gradually invade the nucleosome and ultimately block the strongest interaction surface of H2B with nucleosomal DNA by binding the H2B α1-helix. Together, these multiple contact points establish an extended surface that could reorganize the first 30 base-pairs of nucleosomal histone–DNA contacts.

Further, I report a brief biochemical analysis of FACT's heterodimerization domain. Its PHL fold indicates shared evolutionary origin with the H3-H4-binding Spt16M, Pob3M and Rtt106 tandem PHL modules. However, the Spt16D–Pob3N heterodimer does not bind histones, rather it connects FACT to replicative DNA polymerases.

The snapshots of FACT's engagement with H2A-H2B and structure-function analysis of all its domains lay the foundation for the systematic analysis of FACT's vital chaperoning functions and how the complex promotes the activity of enzymes that require nucleosome reorganization.

1.2 Zusammenfassung: Struktur der FACT Chaperon-Domäne im Komplex mit Histonen H2A-H2B, und ein Modell für die FACT-vermittelte Restrukturierung des Nukleosoms

Nukleosomen sind die kleinsten Bausteine des Chromatin: das DNA Molekül wickelt sich in zwei Windungen um einen Oktamer aus Histon-Proteinen, die seine Ladung neutralisieren und es ordentlich 'verpacken'. Deshalb sind Nukleosomen ein Hindernis für alle nukleären Prozesse, die Zugang zur DNA erfordern, wie zum Beispiel Transkription, Replikation oder Reparatur der DNA. Verschiedene Protein-Komplexe (ATP-abhängige 'Remodeler' und ATP-unabhängige Histon-Chaperone) halten Nukleosomen in einem dynamischen und zugänglichen Zustand, indem sie Histone aus- oder ein-bauen, oder die DNA vom Oktamer abwickeln.

Der eukaryotische FACT Komplex ist ein hochkonserviertes, heterodimeres Histon-Chaperon (aus den Unterheiten Spt16 und Pob3), das DNA und RNA Polymerasen unterstützt, durch Nukleosomen hindurchzuschreiben. Gleichzeitig stellt es sicher, dass die Chromatin-Integrität erhalten bleibt und unterdrückt dadurch z.B. Transkription von sogenannten kryptischen Promotoren.

Genetische und biochemische Experimente haben gezeigt, dass die Interaktion mit Histonen, vor allem mit dem H2A-H2B Histon-Dimer, entscheidend für die Funktionalität von FACT als Histon Chaperon ist. Es fehlten jedoch molekulare oder strukturelle Informationen wie die Histone gebunden werden und wie dies mit den anderen biologischen Funktionen von FACT zusammenspielt, wie zum Beispiel der Interaktion mit Histonen H3-H4 oder anderen nukleären Faktoren, und letztendlich wie das reorganisierte Nukleosom aussehen könnte.

In dieser Arbeit habe ich die H2A-H2B bindende Domäne von FACT, Spt16M, identifiziert und ihre Struktur im Komplex mit H2A-H2B gelöst. Die H2A-H2B Bindung habe ich biochemisch verifiziert, verfeinert und den Phänotyp von wichtigen Spt16M-Aminosäuren *in vivo* in Hefe analysiert. Ein strukturell und funktionell konserviertes, neuartiges 'U-turn' (Kehrtwende) Motif interagiert mit der α1-Helix des globulären Kerns von Histon H2B; diese hydrophobe Interaktion mit mikromolarer Affnität ist essentiell für die Komplex-Stabilität. Ein konservierter 'acidic patch' ('negativ geladene Partie') interagiert zusätzlich mit dem unstrukturierten N-terminalen Ende von H2B und stabilisiert dadurch den Komplex kinetisch.

Das Spt16M U-turn Motif ist auf ein Tandem-PHL (pleckstrin-homology like) Modul aufgebaut, das hohe strukturelle Verwandtschaft zu den Histon-Chaperonen Rtt106 und Pob3M aufweist. Wie Rtt106 und Pob3M bindet auch Spt16M Histone H3-H4. Die Interaktion wurde biochemisch auf die αN-Helix von H3 eingegrenzt.

Zusammenfassend bindet Spt16M an drei Stellen auf der Histon-Oktamer Oberfläche des Nukleosoms. Diese bilden eine zusammenhängende Fläche, welche die ersten 30 Basenpaare der nukleosomalen DNA koordiniert. Vermutlich erfolgt die Interaktion von Spt16M mit dem Nukleosom schrittweise: Zunächst bindet Spt16M über das frei zugänglichen N-terminale Ende von H2B an das Nukleosom. Dort 'verharrt' das Chaperon bis die beiden stärkeren Interaktions-Stellen (die αN Helix von H3 und die α1 Helix von H2B), welche meist von DNA bedeckt sind, durch spontanes Ablösen der DNA freigelegt werden. Letztendlich würde die vollständige Bindung von FACT an das Nukleosom die ersten 30

Basenpaare DNA verdrängen und dadurch das Nukleosom destablisieren, so dass andere nukläere Prozesse (z.B. Polymerasen) auf die DNA Stränge zugreifen können.

Des Weiteren habe ich die Heterodimerisierungs-Domäne von FACT biochemisch analysiert. Spt16D-Pob3N besteht ebenfalls aus PHL Domänen, diese können jedoch keine Histone binden. Stattdessen koppeln sie den Chaperon-Komplex an die DNA Replikations-Maschinerie.

Die vorgestellten Ergebnisse legen den Grundstein für strukturelle und mechanistische Studien wie der holo-FACT Komplex mit dem Nukleosom interagiert, und wie sich dies in den Replikations- und Transkriptions-Prozess eingliedert.

2 Introduction

2.1 Chromatin packs, protects and regulates access to DNA

2.1.1 DNA storage requires dynamic packing

Genomic DNA, the principal carrier of a cell's hereditary information, is an acidic bio-molecule of great linear length that requires careful but dynamic packing to maintain its integrity. To facilitate the folding of DNA, mechanisms have evolved that neutralize most of its charges and that wrap DNA into a tight but flexible assembly whose condensation can be regulated. This ensures faithful genome inheritance and biochemical readout during DNA transcription, replication and repair.

Eukaryotes establish chromatin by assembling an octameric structure of basic histone proteins, which in general wrap 146 basepairs of DNA into nucleosome particles, the minimal repeating biochemical unit of chromatin structure. Nucleosomes establish higher-order chromatin structures and crucially affect the relative accessibility of the underlying DNA sequence to the cellular machinery.

2.1.2 Chromatin structure: histones and nucleosomes

Histone proteins share a common fold and are highly conserved in evolution

Histones are among the most highly conserved eukaryotic proteins. Although the four canonical histones H2A, H2B, H3 and H4 show almost no sequence similarity to each other, they share a common 'histone fold' [**?**] that was also found in other proteins, including TAFs ($TATA$-box binding protein $associated$ $factor$) [**?**]. Their 80 - 90 residue core consist of three α-helices connected by short loops ($\alpha1$ – L1 - $\alpha2$ – L2 - $\alpha3$). The shorter helices $\alpha1$ and $\alpha3$ fold back across the longer middle helix $\alpha2$. Histones have relatively long, less conserved, unstructured N-terminal extensions (20-35 amino acids, usually referred to as 'histone tails') that are rich in basic amino acids and subject to many regulatory modifications. Special structural features of individual histones are specified in Figure 2.1a.

The histone core fold and formation of the nucleosome octamer

Histones occur as obligate dimers, H2A pairing with H2B and H3 with H4 [**?**]. The dimer forms a crescent-shaped handshake-motif, with the $\alpha2$ helices crossing over such that the L1 and L2′ loops (L1L2′ and L1′L2 sites, the ′ refers to the histone partner within the dimer) and the N-termini of the $\alpha1$ helices ($\alpha1\alpha1'$ site) are in close proximity (Figure 2.1b).

In the nucleosome core particle (NCP), two copies of each histone dimer assemble to an octameric disc (Figure 2.2). $(H3\text{-}H4)_2$ assembles into a W-shaped, stable tetramer through formation of a symmetric four-helix bundle of the H3 $\alpha1$ and $\alpha2$ helices; this defines the symmetry 'dyad' axis of the nucleosome. At the tetramer edges, a similar

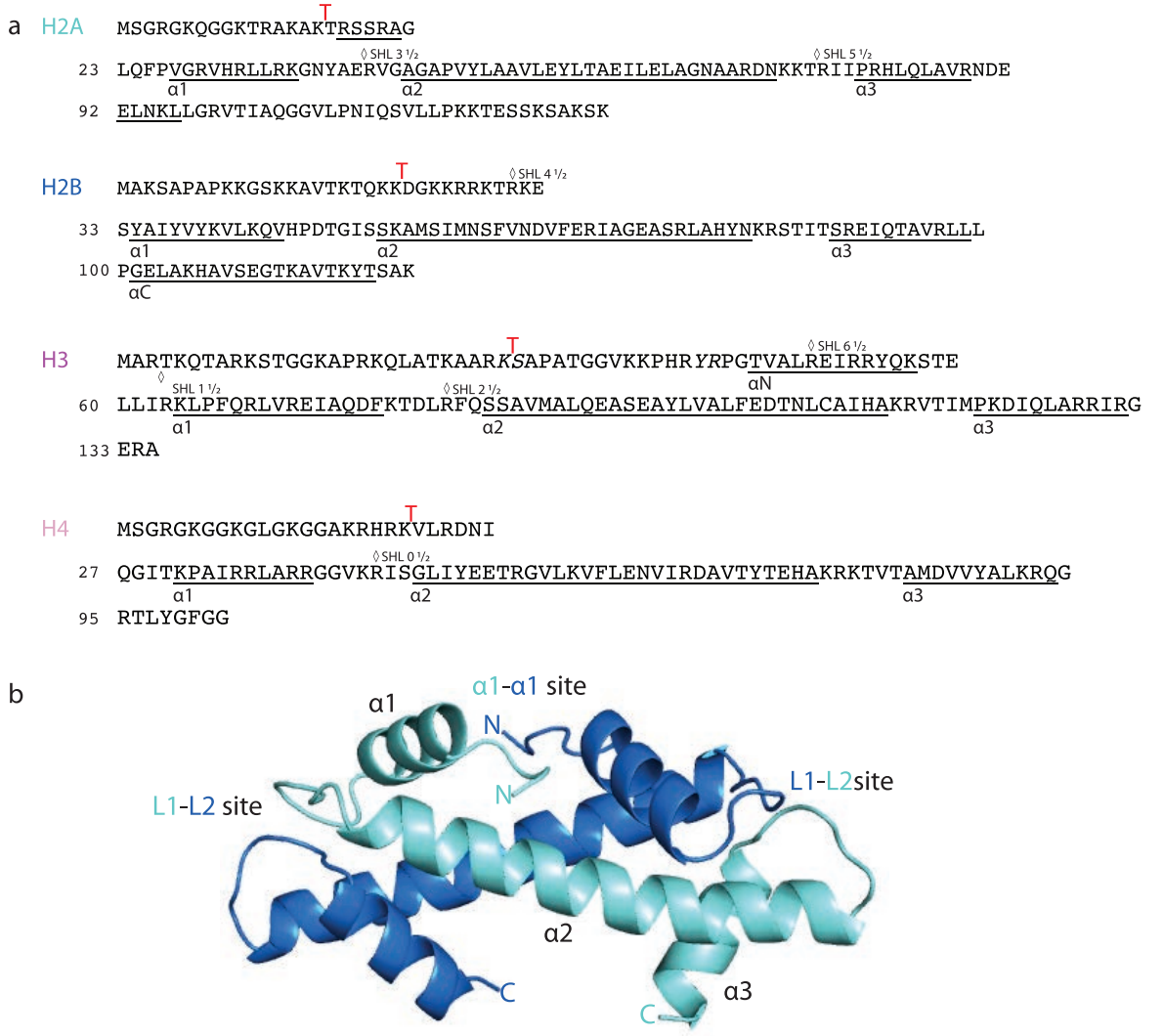

Fig. 2.1: **Sequence and structure of the four canonical histones.**
(a) Histone sequences. 1^{st} line: N-terminal tail, 2^{nd} line: histone core, 3^{rd} line: C-terminal tail. Helical parts are underlined. Arginines inserted into the DNA minor groove are marked by diamonds. Red T marks trypsin cleavage sites; downstream sequences are part of the globular core histones. (b) Histone dimer 'hand-shake' fold. DNA contact sites ($\alpha1\alpha2$, L1L2) are labeled.

but weaker 4-helix-bundle is formed between H4α1/α2 and H2Bα2/α3. In addition, the unstructured hydrophobic C-terminal tail of H2A (the 'docking domain') reaches out to contact the other H3′-H4′ dimer. H2A and H2A′ come to lie roughly atop of each other and have a minor contact opposite the dyad, bridging the two histone-halfdiscs.

The histone protein interfaces are mostly hydrophobic, therefore the octamer is stable in high salt conditions (∼1 M salt) but dissociates into H2A-H2B dimers and H3-H4 tetramers (or dimers [**?**]) in physiological salt (∼150 mM NaCl).

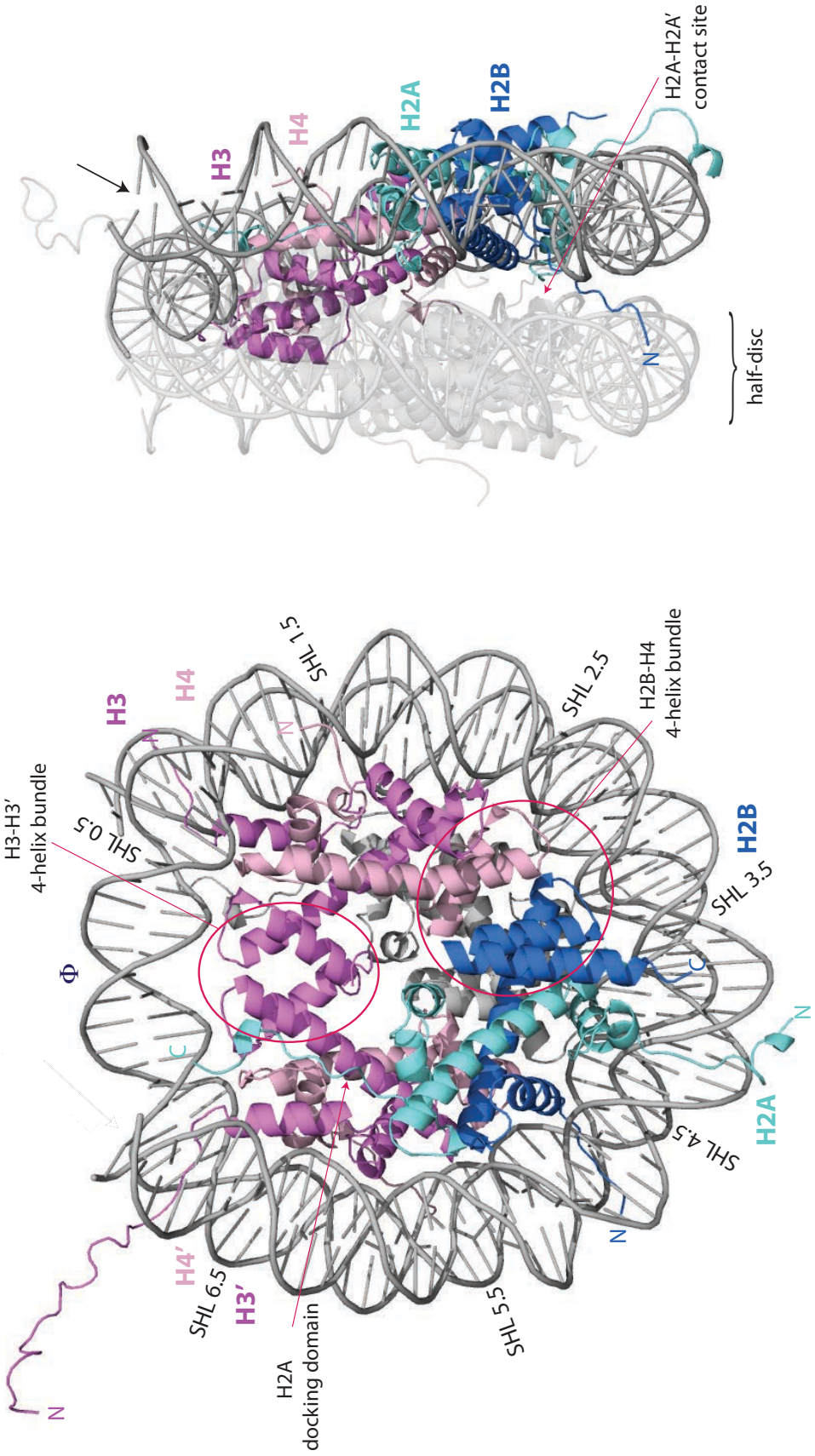

Fig. 2.2: **Structure of the nucleosome core particle (NCP).**
Structure after [**?**], PDB 1AOI. H2A (*turquois*), H2B (*blue*), H3 (*violet*), H4 (*light pink*), DNA (*grey*), Φ dyad. SHL locations are indicated for the top DNA strand.

Histone-DNA contacts occur periodically around the octamer, independent of the nucleotide sequence

Roughly 146 base pairs (bp) of DNA are wrapped around the histone octamer in 1.67 left-handed turns. The minor groove makes 14 contacts with the octamer, each with contributions from both strands and ∼10 bp periodicity (per DNA strand). Starting from the dyad axis, there are six contact points with the core histone dimers, e.g. the two L1-L2 and the $\alpha 1\alpha 1$ sites of both H3-H4 and H2A-H2B. A seventh contact that stabilizes the ultimate 10 bp of DNA at the nucleosome entry / exit site is supplied by the αN helix of H3; acetylation of H3 K56 in H3αN disrupts this contact [**?**]. The tails of H2B and H3 pass through the two DNA gyres (jargon for the 'turns' of the DNA double helix around the histone octamer) in a 'random coil' conformation [**?**].

Typical DNA-histone contacts are hydrogen bonds and salt bridges from main-chain amide nitrogens, basic residues and helix dipoles as well as through insertion of an arginine side chain into the minor groove. About half of the contacts are water-bridged; this allows deviations from the idealized double helix conformation (e.g. by inter-basepair angle restraints) [**??**].

Nucleosome positions are set by the DNA sequence and modified through nucleosome remodeling and transcription

Although all histone-DNA contacts are nucleotide-nonspecific, the primary DNA sequence strongly influences the local flexibility of the DNA sequence. Nucleosomes preferentially locate to more flexible DNA sequences, which are bent with less energy input and are thus thermodynamically more stable positions. Therefore the primary DNA sequence influences the position of the nucleosome and the location of histone-DNA contacts [**??**]. The most bendable dinucleotides are AT and TA, and a 10 bp periodicity of these was observed for alomst every nucleosome position in *in vivo* high-precision mapping studies [**?**]. In contrast, long tracks of poly(dA:dT) or poly(dG:dC) are quite stiff and exclude nucleosomes; these sequences are found in the promoter regions of many species, e.g. yeast [**?**].

DNA sequence is not the only determinant of nucleosome positioning: *in vitro* salt-dialysis of histone octamers onto *S. cerevisiae* genomic DNA recapitulates most, but not all aspects of the pattern observed *in vivo* [**??**]. Addition of yeast crude lysate and ATP to the assembly reaction, which allow for nucleosome remodeling, improves the positioning of the +1 and -1 nucleosomes flanking the nucleosome-free region at promoters, and establishes a regularly spaced pattern within open reading frames [**?**]. Active transcription further improves the reconstituted pattern: first, there seems to be a strict distance relationship between the +1 nucleosome and the pre-initiation complex (PIC), which associates with the TATA-element and is thus precisely positioned [**?**]. Second, active transcription establishes a regularly spaced nucleosome pattern throughout the coding region, either directly or through recruitment of remodellers [**?**].

2.1.3 Higher order chromatin structure

The 10 nm solenoid fiber: a string of nucleosomes

Nucleosomes occur every 200 ± 40 bp along the DNA, which was first seen in electron microscopy (EM) and described as a 'beads on a string' fiber with ∼10 nm diameter [**??**] (Figure 2.3a, from **?**). The 10 nm fiber compacts intrinsically to a regular 30 nm solenoid [**?**] which is folded into less structurally defined loops by attachment to a nuclear protein scaffold.

The 30 nm fiber: a regular helix

For 30 nm fiber folding, two structural models are commonly discussed (Figure 2.3b). A two-start / ZigZag helix was observed in cryo-electron microscopy (cryoEM) studies of *in vitro* assembled samples with a wide range of linker lengths, in physiological Mg^{2+} concentrations (1.6 mM) and in the presence of linker histone. Upon removal of linker histone and an increase in Mg^{2+}, the structures convert to one-start helices [**?**] that resemble the crystal-structure of a tetranucleosome (which was determined in high Mg^{2+}) [**?**]. Interactions between basic residues in the H4 N-terminal tail and the H2A-H2B 'acidic patch' on the surface of a neighbouring nucleosome are important for both intra-fiber ('compaction') and inter-fiber ('oligomerization') interactions [**??**]; the acetylation of H4 K16, which neutralizes the positive charge of the lysine residue, prevents both compaction and oligomerization [**?**].

Recent cryo-EM studies of native chicken erythrocyte chromatin, which is fully silenced and saturated with linker histone, observed a 30 nm solenoid fiber that forms a left-handed two-start helix with a 'hexagonal' pattern of 6.5 nucleosomes per turn; The structure has a diameter of 32 nm and a helical pitch of 22.8 nm, but the regular fold rarely extends over more than 3 nucleosome gyres [**?**] (Figure 2.3c). The nucleosomes of the two helix strands are juxtaposed, not directly above each other, but also not interdigitated, which leaves a lot of open space between the nucleosome cores that might be invaded by e.g. transcription factors or chromatin remodelling factors.

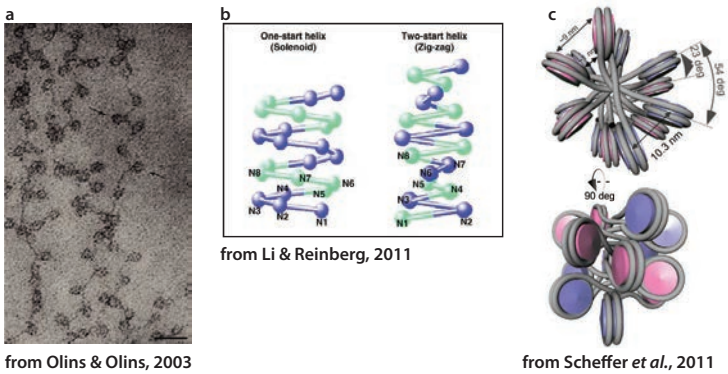

Fig. 2.3: **Higher order chromatin structure.**
(a) Electron microscopy picture of the 'beads on a string' 10 nm nucleosome fiber from **?**. (b) Models for 30 nm fiber folding, from **?** (c) CryoEM reconstitution of native chicken erythrocyte chromatin reveals a two-start solenoid fiber, from [**?**].

Heterochromatic 30 nm fiber compaction competes with euchromatic 10 nm fiber oligomerization.

Compaction and oligomerization may compete with each other: the compacted 30 nm fiber is present in interphase chromosomes ('diluted' conditions, which favour intramolecular assembly), while in mitotic chromosomes ('concentrated' conditions), more oligomerized 10 nm fibers and less or no 30 nm compaction was observed [**??**]. Since the acidic patch is important for efficient fiber compaction, histone variants with differing acidic patch surfaces stabilize either the 30 nm fiber (H2A.Z, enlarged acidic patch) [**?**] or interfiber oligomerization (H2A.Bbd, no acidic patch) [**?**].

HMG box proteins are a class of ubiquitous non-histone proteins that strongly influence the local chromatin structure: they bend DNA, break the regular solenoid folding pattern and therefore decrease the compactness of the chromatin fiber; this increases accessibility of chromatin to regulatory factors [**?**].

Every interphase chromosome occupies a certain 'territory' within the nucleus

Within the interphase nucleus, each chromosome occupies a certain 'territory' that is hardly invaded by neighboring chromosomes (Figure 2.4). The radial distribution of those territories seems to be conserved [**?**], but it is not clear wether this is also true for the relation between chromosomes and to nuclear landmarks (e.g. the nucleolus) [**?**]. Chromosome positioning can occur through direct interactions with the nuclear envelope: the nuclear lamina interacts with heterochromatic domains [**??**], and components of the nuclear pore complex were found to dynamically associate with active chromatin [**???**].

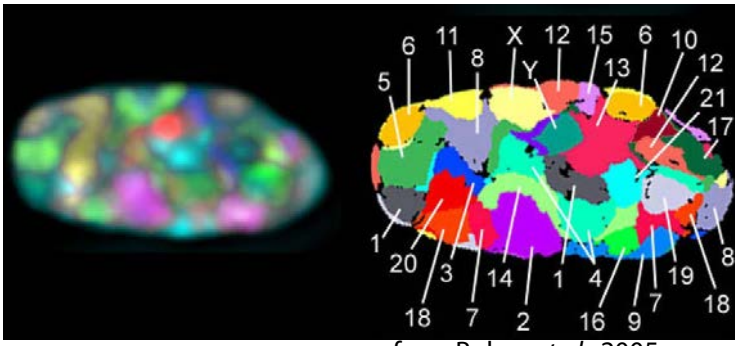

Fig. 2.4: **Nucleosome territories.**
The picture was taken and modified from **?**. FISH (Fluorescence *in situ* hybridisation) probes stain all 24 human chromosomes of a interphase fibroblast cell in different colours.

The mitotic chromosome is the most compacted form of chromatin

For the proper segregation of chromosomes during mitosis, the long strands of DNA are further compacted: chromatin fibers form 'loops' with attachment sites on a nuclear matrix scaffold (made of specialized proteins, e.g. nuclear lamins) (Figure 2.5). Chromatin looping is also observed outside mitosis, where dynamic 'regulatory looping' correlates with gene activity, e.g. to bring long-distance enhancers in close proximity of the promoter [**?**]. Historically, mitotic chromosomes were already figuratively described in the mid 19th century by e.g. Rudolf Virchov (1857), but the first understanding of their biological nature was probably written down by Anton Schneider in 1873, who observed that *" .. [der*

Zellkern sich bei der Zellteilung] in einen Haufen feinlockig gekrümmter, auf Zusatz von Essigsäure sichtbar werdender Fäden verwandelt. An Stelle dieser dünnen Fäden traten endlich dicke Stränge auf, zuerst unregelmäßig, dann zu einer Rosette angeordnet, welche in einer durch den Mittelpunkt der Kugel gehenden Ebene (Äquatorialebene) liegt." (the nucleus converts to a pile of finely curled, crooked fibers which become visible upon addition of acetic acid. Over time, the thinner fibers develop into thicker threads, at first with irregular placement, later on ordered rosette-like in an equatorial plane.) Walther Flemming observed in 1882 that these 'chromosomes' (from greek chroma (colour) and soma (body), to describe the dye-attracting particles in the nucleus) migrate during cell division, and in 1883, Wilhelm Roux proposed that faithful segregation of the chromosomes is extremely important for proper transmission of inheritable features, without yet knowing what genes are.

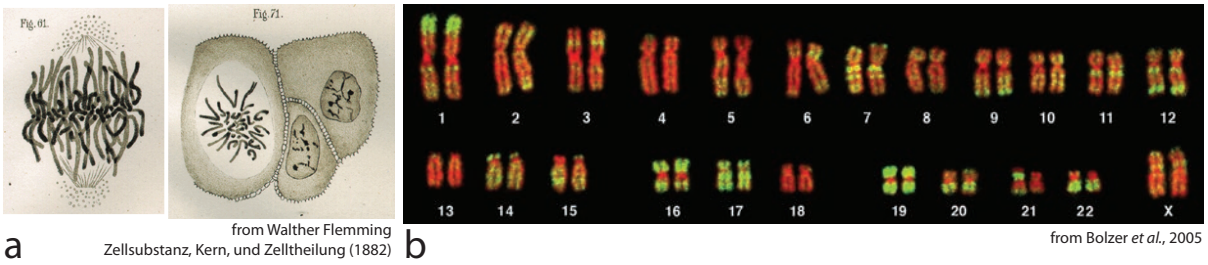

Fig. 2.5: **Mitotic chromosomes.**
(a) Early descriptions and drawings of chromosomes by Walther Flemming (1882) from **?**. (b) Light microscopy image of the karyotype of a human fibroblast, from **?**. Cytogenetic analysis of the number, shape (e.g. length, or position of the centromere) and banding pattern of the chromosomes is used in clinical medicine (e.g prenatal diagnostics) to detect chromosomal aberrations, and in evolutionary biology to study the relationship between different species.

2.1.4 Histone variants

Incorporation of structural histone variants (mostly of H3 and H2A) can functionalize a nucleosome, e.g. by making it more or less stable or by recruiting certain proteins and thereby affect the activity of the underlying DNA sequence. Unlike canonical histones, which are incorporated during S-phase, histone variants mostly require specific activities (chromatin remodelers and / or histone chaperones) for targeted integration into chromatin and are mostly incorporated outside S-phase [**?**].
Several examples are briefly described below:

- At centromeres, the chaperones Scm3 (yeast) or HJURP (higher eukaryotes) incorporate a specialized H3 variant (**Cse4** in yeast, **CenpA** in higher eukaryotes) that is required for kinetochore attachment and faithful chromosome segregation [**??**].

- In higher eukaryotes, the replication-independent **H3.3** variant differs from canonical H3.1 in only four amino acids but gets incorporated selectively at transcriptionally active genes and telomeric heterochromatin; this process requires the H3.3 specific histone chaperone HIRA [**?**], or the chaperone DAXX and the remodeler ATRX [**?**].

- Phosphorylation of the variant **H2A.X** around DNA breaks recruits the repair machinery. Further, the phosphorylated form marks the inactive sex chromosome [**?**].

- **H2A.Z** is a ubiquitous, quite diverged histone variant that gets inserted by the Swr1 remodeler in yeast (or the Tip60 remodeler-HAT(histone acetyl transferase) complex in human [**??**]). In higher eukaryotes, its presence is positively correlated with transcriptional activity [**?**]. Surprisingly, both H2A.Z and H3.3, representative for active chromatin, were also found enriched at genes targeted by PRC2 (polycomb repressive complex 2), which is known to silence gene activity, in embryonic stem (ES) cells [**?**].

- In **macroH2A**, the core histone fold is extended by a C-terminal globular 'macro' domain that can bind ADP-ribose [**??**]. This histone variant is enriched in the facultative heterochromatin of the inactive X chromosome [**?**] and may regulate or be involved in ADP-ribosylation networks [**?**].

- **H2A.Bbd**, absent from the inactive X-chromosome, lacks the C-terminal tail and the acidic surface patch of canonical H2A; it destabilizes the nucleosome and organizes only ∼120 bp of DNA [**?**].

2.1.5 Histone modifications and their 'readers'

Another way to vary and specify the default nucleosomal template are posttranslational modifications (PTMs) of the histone proteins and the DNA. For histone modifications, the most common ones are methylation (me) of arginine and lysine residues, acetylation (ac) of lysine, ADP-ribosylation of aspartates and lysines, phosphorylation of serines and threonines, ubiquitylation or sumoylation of lysines, but many more exist. These modifications have 'regulatory' function by either directly affecting chromatin structure (e.g. H4 K16 acetylation prevents chromatin compaction, see above) or recruiting chromatin modulating / modifying factors and transcription factors. Some modifications are characteristic of active (H3 K4me3, H3 K9ac, H3 K14ac) or inactive (H3 K9me3, H3 K27me3) chromatin.

Certain globular domains have evolved to 'read' these epigenetic marks [**?**]. For example, bromodomains recognize acetylated histone lysine residues [**?**], while chromodomains recognize di- and tri-methylated lysine residues [**?**] (Figure 2.6). In contrast to these highly specified readers, specific PHD (plant homeo domain) fingers can recognize various modfications, e.g. H3 K4 either in the tri-methylated (BPTF [**?**]) or in the unmodified form (BHC80, part of the demethylase complex LSD1 [**?**]) or acetylated H3 K41 (DPF3b [**?**]). Recently, the tandem PH (pleckstrin homology) domain of the histone chaperone Rtt106 has been described to recognize H3 K56ac [**?**]; the modification increases the affinity for recombinant H3-H4 dimers from 1.5 μM (unmodified) to 0.08 μM (K56 ac).

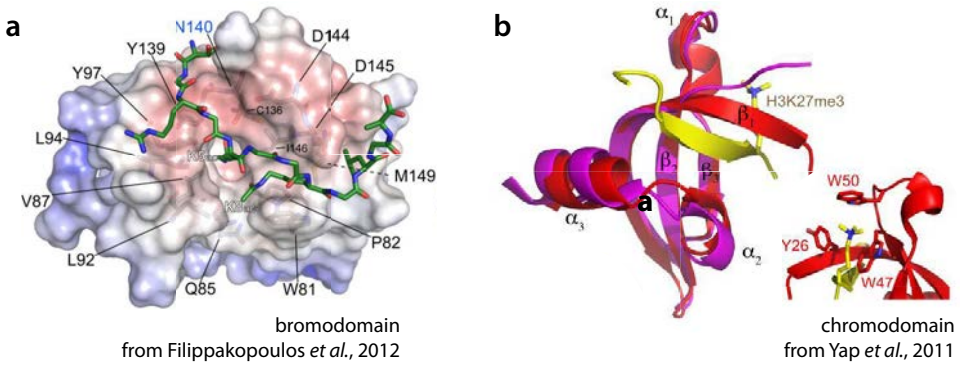

Fig. 2.6: **Histone modifications and their readers.**
(a) Di-acetylated H3 peptide bound to a bromodomain, from **?**. (b) Tri-methylated H3 peptide bound to HP1, from **?**.

2.1.6 Intrinsic chromatin dynamics

Nucleosomal DNA ends constantly detach from the octamer core ('breathing')

The nucleosome is not a static particle but a dynamic assembly. Still, breaking the histone-DNA contacts represents an energetic threshold for any process requiring access to DNA. High-resolution optical tweezer 'unzipping' experiments reveal three predominant, relatively broad regions of strong DNA-histone interaction. The strongest is located around the nucleosome dyad, two weaker ones around 40 bp away from the dyad, at the super-helical location (SHL, the double-helix contact points with the histone octamer) ± 4.5, where H2Bα1 interacts with the DNA [**?**].

In the crystal structure of the fully hydrated nucleosome, about 10-15 % of the DNA, in particular the ends, are dissociated from the histone octamer [**?**]. Consistently, restriction enzyme accessibility is highest at the DNA ends [**?**], also in nucleosome arrays of different compaction states [**?**].

Initial single-particle FRET studies showed that DNA peals off the histone octamer in about 3 % of all cases (nucleosome 'breathing') (Figure 2.7a), with a lifetime of 120 ms [**?**]. Subsequent, better resolved studies showed that displacement of nucleosomal DNA is 'progressive', with the ends being unwrapped in 20-60 % of cases, but only 10 % up to SHL ±4.5 [**?**].

While PTMs near the dyad affect nucleosome stability and promote nucleosome disassembly, PTMs near the DNA entry / exit site (e.g. acetylation of H3 K56 or the H2A-H2B tails) affect breathing [**??**].

Nucleosome 'gaping', lexosomes and further dynamics of the octamer core

Besides movements of the DNA, nucleosome 'gaping' was theoretically postulated as an oyster-shell like spreading of the nucleosome half-discs around the H3-H3′ dyad 'hinge' (Figure 2.7b); this would break the H2A-H2A′ contact [**?**].
During transcription *in vivo*, frequent turnover of histones H2A-H2B is observed, while histones H3-H4 seem to be rather stable [**??**]. On a molecular level, loss of one H2A-H2B dimer results in a 'hexasome' particle, which was observed *in vitro* when Pol II transcribes through nucleosomes [**??**]. Further, many histone chaperones were found to evict an H2A-H2B dimer to promote transcription elongation, e.g. FACT [**?**] and nucleolin [**?**]. Recent *in vitro* preparation and structural studies of recombinant hexasome particles [**?**] show

that they are rather stable particles wrapping ~112 bp of DNA, thus releasing ~40 bp. Nevertheless, small-angle X-ray scattering (SAXS) experiments suggest little structural change of overall particle shape compared to canonical octameric nucleosomes.

Several models exist for more 'open' octameric nucleosome structures, where DNA and the histone proteins are more accessible to modifying enzymes and the DNA and RNA polymerases. The most prominent are the lexosome (an extensively 'gaped' nucleosome where the nucleosome half discs are split at the dyad axis [**??**]), and more recently a dissasembly intermediate where H2A-H2B dissociates from the H3-H4 tetramer but is still associated with DNA (0.2-3 % of nucleosomes in physiological salt, ΔG = 2-4 kcal/mol) [**?**].

Various controversial models exist for centromeric nucleosomes, including structures containing only one copy of each histone (in *Drosophila*) [**?**] or only the CenpA-H4 tetramer plus Scm3 (in yeast, but it is still debated whether Scm3 is an integral part of the centromeric nucleosome or a histone chaperone) [**?**] and right- or left-handed DNA paths [**?**]. Two recent studies report that centromeric nucleosomes exist as tetramers throughout most of the cell cycle, e.g. in complex with the histone Scm3 [**?**], and convert to octamers during replication [**??**].

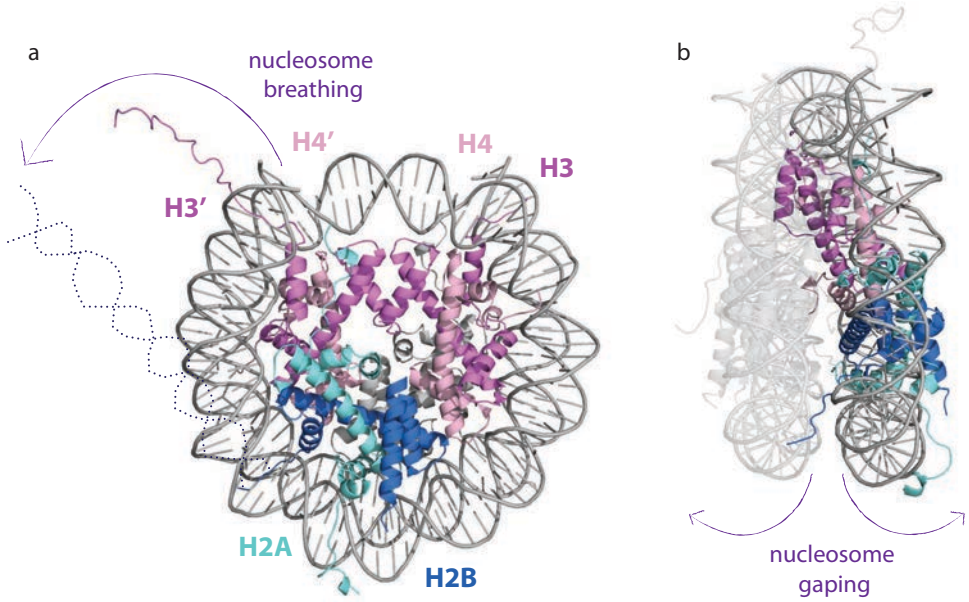

Fig. 2.7: **Intrinsic NCP dynamics.**
Nucleosomes are subject to spontaneous movements (indicated by arrows) such as (a) 'breathing', detachment of the DNA ends from the histone octamer surface, and (b) 'gaping', an oyster-shell like movement around the H3-H3′ hinge. H2A (*turquois*), H2B (*blue*), H3 (*violet*), H4 (*light pink*), DNA (*grey*).

2.1.7 Chromatin dynamics through ATP-driven nucleosome remodeling machines

Remodeling machines use ATP to translocate nucleosomal DNA around the octamer core

Nucleosome remodelers are ATP-driven motor protein complexes that translocate DNA around the histone octamer and thus give access to sites of DNA and/or move the

nucleosome along the DNA. They usually consist of several subunits, including a SWI2 / SNF2-type ATPase domain (see **?** and **?** for review).

Whether DNA translocation around the histone octamer occurs by 'twist diffusion' or 'loop / bulge propagation' is still a matter of debate [**??**] (Figure 2.8). In either case, the remodeler uses energy from ATP to introduce a disturbance into the DNA structure (either an additional supercoil (twist) or a loop made of additional nucleotides 'pumped' into the nucleosome) that disrupts some of the DNA-histone contacts. Propagation of the disturbance around the nucleosome into the linker DNA will restore the thermodynamically most stable state (with a maximum of DNA-histone contacts) and also translocate DNA.

In contrast to histone chaperones which preferentially bind histones and in particular the DNA-binding surfaces of histones (see below), remodelers seem to primarily recognize nucleosomal DNA, the accessible flat nucleosome surface and / or the linker DNA [**?**].

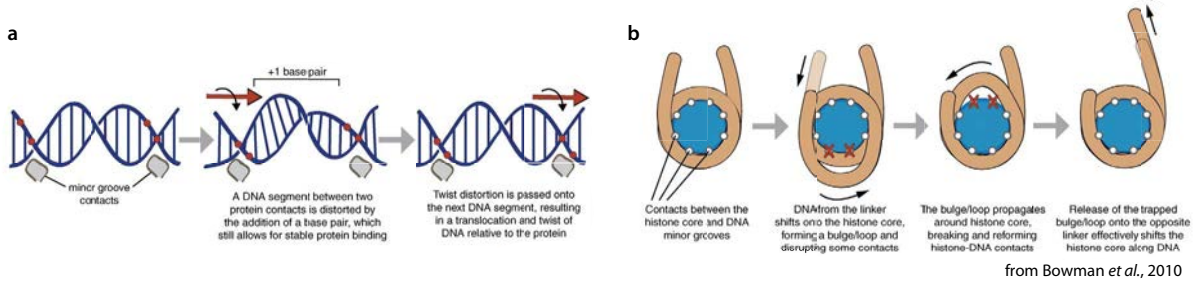

Fig. 2.8: **Models for ATP-driven nucleosome-remodeling.**
from **?** (a) Twist-diffusion model. (b) Loop-propagation model.

Classification and structure of remodeling complexes

Remodeling complexes are classified according to the ATPase subunit architecture. The SWI / SNF and RSC family are large complexes (8-14 subunits) that form multilobal structures with a large cavity to receive the nucleosome [**??**]. Monomers of the ISWI family (e.g. *Drosophila* CHRAC) appear in EM as a convex disc; two of them sandwich the nucleosome with their flat side [**?**].

Many of the remodeling complexes harbor protein domains that recognize specific histone modifications, e.g. SWI / SNF contains a bromodomain to recognize acetylated histone tails (see **?** for review) and human CHD1 a N-terminal double chromodomain that recognizes H3 K4me [**?**] and has been suggested to block ATPase activity in the absence of a nucleosomal substrate [**?**]; this indicates the presence of allosteric regulation mechanisms for these enzymes.

2.1.8 Transcription through chromatin

RNA Pol II requires 'help' to transcribe through nucleosomal DNA templates

RNA polymerase II (Pol II) by itself cannot transcribe through positioned nucleosomes *in vitro* since it cannot efficiently break the strong DNA attachment sites around the dyad and SHL 4.5 [**??**]. Several factors help to overcome the nucleosome barrier [**??**], for example:

- **high salt** disrupts the ionic histone-DNA contacts

- Pol II transcription factors **TFIIF** and **TFIIS** stimulate the catalytic activity of Pol II and restart stalled polymerase molecules until the nucleosome gets eventually disrupted [**???**]

- the histone chaperone **FACT** dissociates histones H2A-H2B from mono-nucleosomal templates to create a 'hexasome' (a nucleosomal particle containing six instead of eight histone proteins), which can more easily be traversed by the polymerase [**?**], also in subsequent rounds of transcription [**??**].

The θ-loop model: detachment of the distal 50 bp of DNA is sufficient for polymerase progression

As an alternative model to complete nucleosome disassembly, Studitsky and colleagues recently proposed that during transcription through the nucleosome, a small DNA loop is formed that contains the polymerase [**?**] (Figure 2.9). In this model, detachment of the DNA from the distal H2A-H2B dimer is necessary to avoid steric clashes of DNA with the enzyme. Strict recovery of histone-DNA contacts behind the progressing polymerase is tightly coupled with disruption ahead of the polymerase to stabilize the loop and to prevent nucleosome translocation.

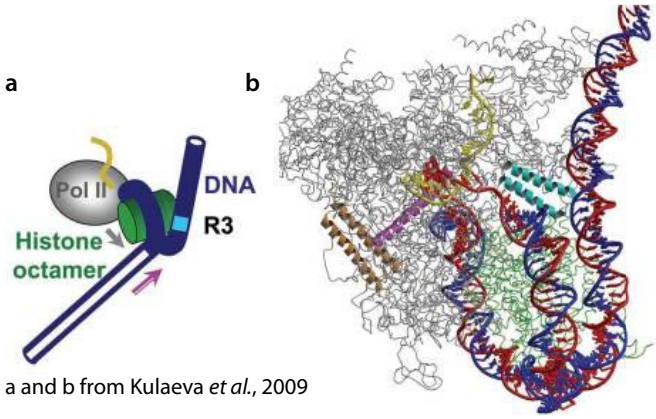

Fig. 2.9: **The θ-loop model for Pol II transcription through the nucleosome.** from **?**. Regular DNA-histone contacts are established before and after the enzyme, but the distal ~50 bp of DNA must be unwrapped to avoid steric clashes with the polymerase molecule. (a) Schematic representation. (b) Superposition of Pol II and NCP crystal structures.

Transcription through chromatin *in vivo* is aided by chromatin remodeling machines and histone chaperones

The transcription rate ('speed') of RNA Pol II is equivalent on chromatin *in vivo* and on naked DNA *in vitro* (1-4 kbp/min) [**?**] and sequences that impede polymerase progression *in vitro* are not necessarily a problem *in vivo* [**?**]. Thus, the cell must have established efficient mechanisms to overcome the nucleosome barrier. Prime candidates are chromatin remodelling machines, histone chaperones and PTM-induced changes of chromatin structure and stability.

Chromatin remodelers such as SWI / SNF [**??**], ISWI [**?**] and CHD1 [**?**] are present at active promoters and ORFs, where they are required for loss of histones, incorporation of

histone variants (e.g. H3.3 [**?**]) and maximal elongation speed. ISWI and CHD1 together establish a regularly spaced nucleosome pattern that somehow seems to facilitate Pol II elongation [**?**].

Histone chaperones such as Nap1, Asf1 and FACT cooperate with remodelers [**??**] or with PTMs (e.g. H3 K14 acetylation [**??**]) to promote nucleosome disassembly. In the wake of Pol II passage, the chaperones FACT and Spt6 are thought to reassemble nucleosomes; this function is vitally important since failure to reassemble the intact chromatin structure will uncover cryptic initiation sites within ORFs and disturb gene expression [**?**].

2.1.9 Open questions

Having determined the most prominent players in the 'chromatin circus', I want to understand mechanistically how nucleosomes and chromatin are shaped and reorganized, to gain or prevent access to the underlying DNA template in different states of activity. Several cryo-EM structures of chromatin remodelers [**????**] in complex with nucleosomes are available and have helped to understand the mechanism of ATP-driven remodelling processes.

For example, the group of Timothy Richmond used a combination of X-ray crystallography, cryo-EM and photocrosslinking techniques to study the interaction of the yeast remodeler ISW1a with a dinucleosome substrate [**?**] (Figure 2.10a). The Ioc3 subunit of ISW1a binds between the DNA strands exiting from the 'static' nucleosome. Isw1, the other subunit, consists of the HAND / SANT / SLIDE (HSS) domains which bind along the linker DNA towards the next, 'mobile', nucleosome. This mobile nucleosome is translocated backwards by the Isw1 ATPase domain until it reaches the HSS domains, which therefore acts as a length ruler for nucleosome spacing.

The nucleosome was crystallized in complex with a couple of peptides and proteins.

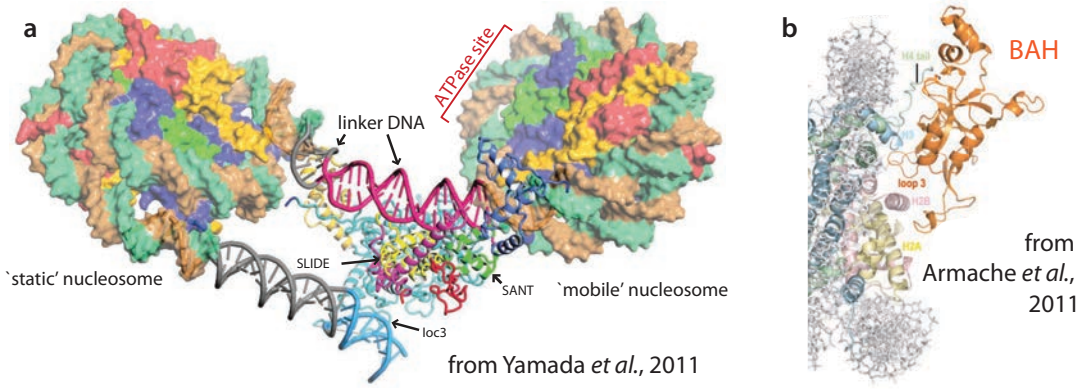

Fig. 2.10: **Model of the ISW1a remodeler bound to a dinucleosomal template, and Sir3-BAH bound to the nucleosome.**
(a) Modified from **?**. Crystal structures of the NCP and Ioc3-Isw1(HSS) were fitted into the cryo-EM maps and combined to a model for interaction of the remodeler with a di-nucleosomal template. The ATPase domain of Isw1 translocates the 'mobile' nucleosome towards the 'static' nucleosome, until there is a steric clash with the Ioc3-HSS 'length ruler'. (b) Modified from **?**. Structure of the Sir3 BAH domain bound to the NCP.

The viral LANA peptide [**?**] and RCC1, a signalling protein [**?**], use an unstructured loop to bind to the acidic patch on H2A-H2B and thus have a relatively small interaction inter-

face. In contrast, the BAH (bromo-associated homology) domain of the silent information regulator Sir3 binds a broad, DNA-free region on the octamer surface (Figure 2.10b) [**?**]. This includes the H4 tail, which becomes folded upon binding, a region on histones H3, H4 and H2B important for the establishment of silent chromatin in genetic screens, as well as the acidic patch. Acetylation of H4 K16, characteristic of active chromatin, strongly decreases the affinity, while methylation of H3 K79, which has been implicated in silencing, enhances the interaction.

Further, several structures of histone chaperones (mostly only peptide stretches) in complex with their histone substrate have been solved in the past years [**?**]. The globular chaperone Asf1 was crystallised in complex with histones H3-H4 [**??**] (Figure 2.11), and recently the structural basis of how the chaperone DAXX distinguishes between H3.1 and H3.3 has been understood [**?**]. However, for most of the histone chaperones and remodeling machines, the precise molecular mechanism of nucleosome reorganization is still unclear, and there is no structural insight at all on the interaction with H2A-H2B for any chaperone.

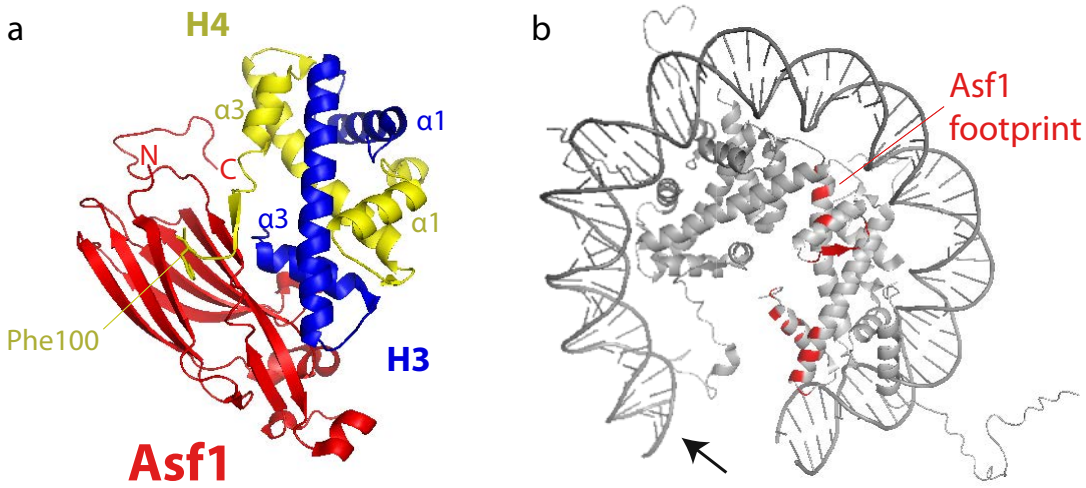

Fig. 2.11: **Crystal structure of the histone chaperone Asf1 in complex with H3-H4.** The picture was published in **?**. (a) Crystal structure of Asf1(*red*) in complex with histones H3 (*blue*) and H4 (*yellow*), as solved by **?** (PDB code 2HUE). (b) Structure of the nucleosome core particle (PDB code 1AOI, [**?**]), with histone residues contacted by Asf1 marked (*red*).

2.2 Histone chaperones escort histones and reorganize nucleosomes

2.2.1 Histones are abundant, but they need to be escorted

Histones are among the most abundant proteins in the cell, since they are needed to wrap the vast majority of a eukaryote's large genome. It is therefore critical for cells to ensure a timely and sufficient supply of histones, e.g. during DNA replication. Further, emerging evidence also suggests that histone supply levels play a determining role in faithful chromosome segregation [**?**] and organismal aging [**?**].

Since histone proteins carry a high number of positive charges, they readily bind DNA, but also carry a detrimental potential to make unwanted interactions with all nucleic acids and other cellular components. Therefore, several mechanisms ensure that histones properly assemble with DNA into chromatin. Histones not bound to DNA need to be escorted by histone chaperones, proteins that shield their charge, interact with their hydrophobic histone-histone and histone-DNA contact surfaces, promote their controlled transfer during nucleosome assembly or reorganization, and in doing so help histones avoid local energy minima or off-pathway structures on the folding pathway toward native chromatin. As a direct consequence, it has been estimated that free histones comprise only 1 - 5% of the total cellular pool [**?**].

2.2.2 Histone chaperones are a broad family of histone-safeguarding proteins

As a family, histone chaperones are generally abundant and highly conserved proteins involved in all chromatin-related cellular processes, from histone synthesis, transport and modification to the assembly or disassembly of nucleosomes, remodelling, gene activation, chromatin integrity, transcription, DNA replication and repair. In contrast to the ATP-dependent chromatin remodelling machines that interact primarily with the DNA substrate, chaperones are histone-binders. Depending on their specificity towards particular histones, they can function quite broadly in many biological processes centered on chromatin structure, such as the eukaryotic FACT complex (facilitates chromatin transcription), or they may fulfill highly specific, restricted functions, such as yeast Scm3 (suppressor of chromosome missegregation 3) and human HJURP (Holliday junction recognition protein) which mediate the establishment or maintenance of centromeric chromatin. Together with ATP-dependent nucleosome assembly and remodelling enzymes, histone chaperones procure an extensive, evolutionarily conserved escort network that guides the flow of histones from their synthesis to degradation based on the cell's actual need (for review, see **?**, **?** and **?**).

2.2.3 Chaperones are essential for storage of free histones

In 1978, Ron Laskey identified the first histone chaperone [**?**]: nucleoplasmin is the most abundant protein in *Xenopus* oocytes where it serves as a 'safe' storage for histone proteins, mainly H2A-H2B (H3-H4 is complexed by the chaperone N1/N2). Upon fertilization, the histones are rapidly mobilized for decompaction of the paternal genome and chromatin assembly during subsequent rapid cycles of replication.

Ron Laskey defined that such a histone 'chaperone' should, without requiring ATP,

prevent improper protein-DNA interactions, facilitate nucleosome formation and not be part of the final nucleosome product [?].

2.2.4 The role of histone chaperones in replication and nucleosome assembly

Histone chaperones ensure efficient recycling of parental histones during replication

Most nucleosome (dis)assembly and histone turnover occurs during replication, in lock-step with the replication machinery, to cover the duplicated amount of genomic DNA with chromatin. The role of histone chaperones in this pathway is well studied (Figure 2.12).

Since chromatin hinders access of DNA polymerases to the DNA template, it first needs to be disassembled. Nucleosomes are evicted by the DNA helicase complex MCM2-7 and immediately picked up by histone chaperones: H2A-H2B is probably collected by FACT, which associates with Mcm4 [?]. H3-H4 (bearing the 'parental' epigenetic marks H3 K9me3 and H4 K16ac) is received by Asf1, which initially forms a stable complex with the MCM helicase and then departs with the histones [?]. Both FACT and Asf1 stimulate the helicase activity of MCM [??]. After replication fork passage, intact nucleosome arrays have to be reassembled to ensure genomic stability and to preserve the epigenetic information. The histone source is half recycled parental histones and half newly synthesized histones. Parental histone H3-H4 dimers seem to get incorporated within 400 bp of their original location [?].

Newly synthetized histones get characteristically modified and are tightly escorted to different chromatin assembly pathways

Newly synthetized histones in the cytosol immediatly form heterodimers with their histone partner and are bound by chaperones; the chaperone-histone complex then gets imported into the nucleus through association with nuclear import factors, the karyopherins. In yeast, the H2A-H2B dimer is chaperoned by Nap1, which localizes to the cytosol in G2 and to the nucleus in S-phase [?], and gets imported to the nucleus with the karyopherin Kap114 [?]. Similarly, histones H3-H4 are chaperoned by Asf1 and imported with Kap123 [?].

Before incorporation into chromatin, fresh non-nucleosomal histones, in particular H3-H4, become acetylated by 'B-type' histone acetyl transferases (HATs). Asf1 presents histones H3-H4 to (fungal-specific) Rtt109 for H3 K56 acetylation [????], the HAT1 (yeast and higher eukaryotes) complex for H4 K5 and K12 acetylation [??], and other HATs for acetylation of the N-terminal tail of H3. The histone chaperone Vps75 presents the N-terminal tails of H3 to Rtt109 for acetylation of H3 K9 and K27 [????] and furthermore stimulates Rtt109 HAT activity [??]. Another H3-H4 chaperone, nuclear Hif1, is found in complex with the Hat1-Hat2 complex that modifies H4 K91 [?].

A histone chaperone 'escort network' for replication-coupled and replication-independent nucleosome assembly

In higher eukaryotes, Asf1 juggles histones H3-H4 into two independent pathways for nucleosome assembly: outside S-phase and independent of the replication process, the histone variant H3.3 is incorporated into transcribed chromatin by the chaperones HIRA,

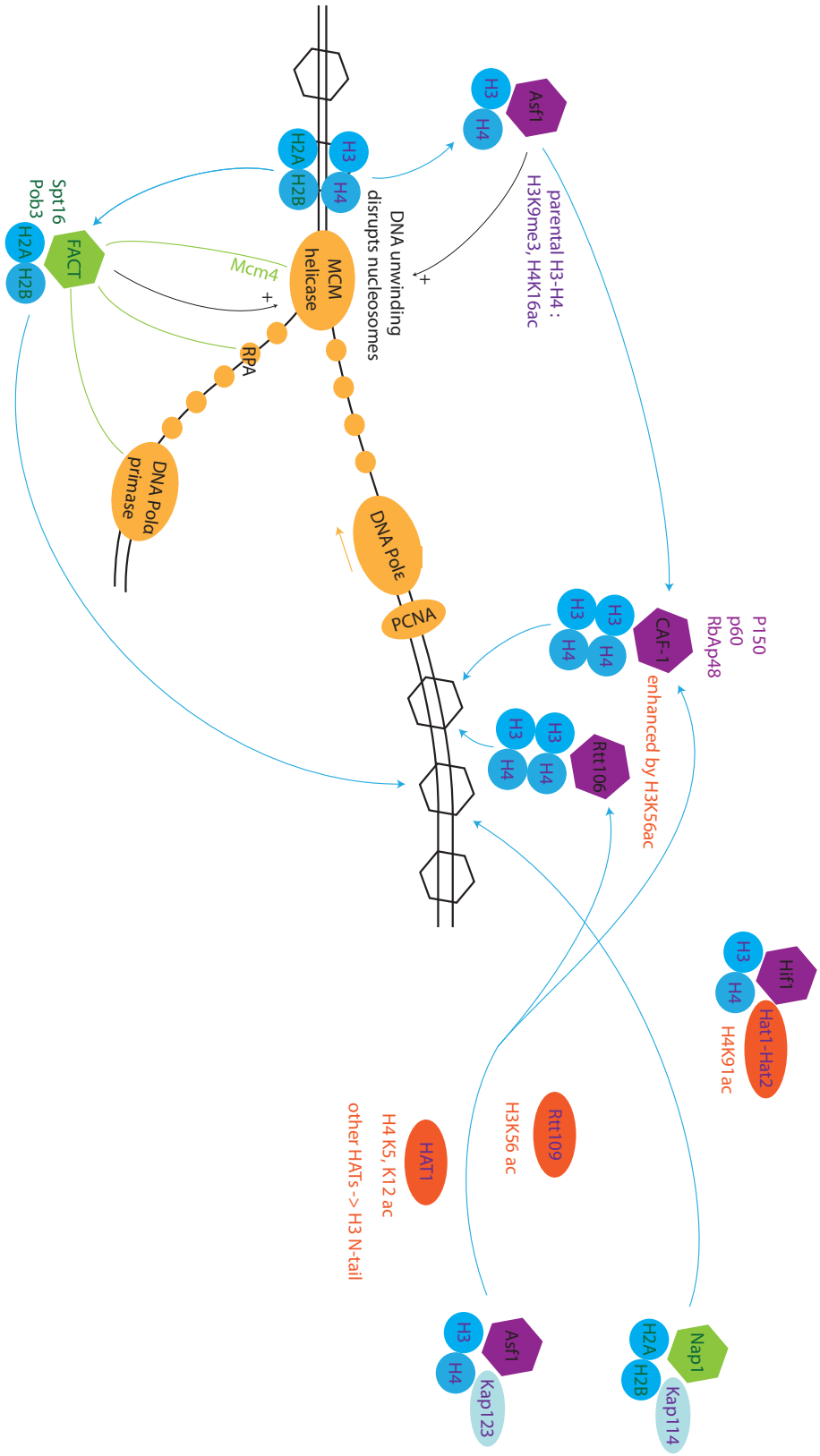

Fig. 2.12: **Replication-coupled nucleosome assembly.**
During S-sphase, histones are delivered to the sites of DNA replication to ensure simultaneous nucleosome assembly. DNA is represented as a double line, nucleosomes as hexagons. Individual proteins are marked as colored blobs. For detail, see text.

Daxx and DEK [??] and marks 'active' chromatin. S-phase restricted, replication-coupled nucleosome assembly of the H3.1 variant is mediated by the histone chaperone CAF-1, or fungal Rtt106. Transfer of histones to HIRA or CAF-1 is mutually exclusive since similar β-hairpin motifs of these chaperones bind to the same patch of Asf1 [??].

CAF-1 deposits H3-H4 tetramers during replication

The large subunit of CAF-1 (p150) physically interacts with the clamp loader PCNA and tethers the chaperone to the replisome machinery [?]. Earlier studies reported that monomeric CAF-1 (and also Rtt106) binds H3-H4 in the dimeric form [?]; the CAF-1 p150 subunit contains a dimerization domain that is critical for histone H3-H4 deposition, which occurs presumably as a tetramer [?]. In contrast, a recent study reported that monomeric CAF-1 binds at least two H3-H4 dimers and thus promotes tetramer deposition [?]. Most deposited tetramers contain either parental or newly synthetized H3-H4, but not a mixture thereof [???]. In human cells, CAF-1 shows a strong preference for the replication-dependent H3.1 isoform.

Binding of H3-H4 to both CAF-1 and Rtt106 is enhanced when H3 is acetylated on K56 [?], but acetylation of H3 N-terminal tails increases affinity only towards CAF-1 [?]. While acetylated H3 K56 is very abundant on newly synthesized histones in yeast, the modification (deposited by the acetyl-transferases CBP/p300 and/or Gcn5 [??]) is hardly detected in somatic cells from higher eukaryotes [?] except for human embryonic stem cells [?], so it is not clear whether the modification has the same signalling function in all those cells.

Both Asf1 and CAF-1 are essential in human cells; depletion of these chaperones activates the DNA replication checkpoint and stalls cells in S-phase, leading to chromosome segregation defects [???].

Certain acetylation PTMs make freshly assembled nucleosomes more malleable

Two acetylation PTMs, H3 K56ac and H4 K91ac, are very characteristic of newly synthetized histones and decrease nucleosome stability. H3 K56 is located at the DNA-entry / exit site of the nucleosome and, when acetylated (H3 K56ac) prevents formation of one DNA contact, thus facilitating 'breathing' of the DNA molecule and destabilizing the nucleosome core particle [??]. Similarly, H4 K91 sits at the interface of H4 and H2B and acetylation of this residue destabilizes the interaction between the H3-H4 tetramer and the H2A-H2B dimer.

It seems that first, less stable nucleosomal arrays (with H3 K56ac and H4 K91ac) are created that can easily be modulated and shaped by chromatin remodelling machines. Both acetyl modifications are then quickly removed (e.g. H3 K56ac is removed by the histone de-acetylases (HDACs) Sir2 in sub-telomeric regions [?] and Hst3/Hst4 elsewhere [??]), thus stabilizing the newly created and shaped nucleosomal array. Cells deficient in H3 K56 acetylation show defects in sister chromatid cohesion and high levels of spontaneous Rad52 foci, indicating that double-strand breaks are created during DNA replication [??].

2.2.5 The role of histone chaperones in transcription through chromatin

Transcription initiation

Histone chaperones can have both a positive and a negative effect on transcription initiation. At active genes, the chaperones Asf1, Spt6, FACT and Nap1 were described to keep nucleosomes in a 'dynamic' state and to promote nucleosome disassembly or assist in histone eviction (e.g. FACT and Asf1 [**?**]), often in cooperation with nucleosome remodelers [**???**]. On the other hand, they inhibit nucleosome turnover at inactive genes (e.g. Vps75) [**?**], mediate transcriptional repression (Asf1, Rtt106) [**?**] and reassemble chromatin during shut-down of gene expression (Spt6, HIR proteins) [**?**].

Nucleosomes flanking the promoter-associated nucleosome-free region (NFR) often contain the nucleosome-stabilizing histone variant H2A.Z. H2A.Z is specifically recognized and deposited by the chaperones Nap1 [**??**] and Chz1 [**?**].

Transcription elongation

Classical electron microscopy studies of Balbiani rings (large 'puffs' (as observed by light-microscopy) on midge polytene salivary gland chromosomes, marking actively transcribed regions) suggest that nucleosomes are disrupted before the transcription machinery and reassembled behind [**?**]. Consistent with a prominent role for histone chaperones in this process, many chaperones, eg. FACT [**?**] or Asf1 [**?**] travel with RNA Pol II and disrupt nucleosomes ahead of the enzyme [**?**] (Figure 2.13).

In the wake of Pol II passage, chromatin needs to be re-assembled, since loss of chromatin structure would nonselectively uncover regulatory DNA elements and cryptic promoters, affect genome stability and erase the local epigenetic information stored in the histone proteins. Nucleosome reassembly is accomplished by histone chaperones as well, in particular FACT [**?**] and the H3-H4 chaperone Spt6. Thus, these two chaperones are essential to prevent aberrant initiation events from uncovered cryptic promoters within open reading frames [**?**].

Histone chaperones can also promote transcriptional repression: they recruit machineries that remove 'active' histone marks (e.g. Asf1 recruits the H3 K4me3 demethylase LID) [**??**] or deposit 'inactive' marks (e.g. Spt6 promotes H3 K36me2/3 deposition by Set2 [**?**]) and regulate access of chromatin remodelers (e.g. the Hir proteins block SWI / SNF (activating) binding [**?**] and recruit RSC (repressive) [**?**]).

2.2.6 General mechanisms of chaperone-mediated histone escort

Histone Chaperones belong to diverse structural families but share certain common structural features

Mechanistic insight into how histone chaperones contribute to chromatin structure has begun to emerge from structural studies of histone chaperones or of histone-binding modules within these chaperones. These include a set of crystal structures for the complex of several chaperones bound to histones or histone peptides [**???????**].

Although histone chaperones belong to diverse structural families, some general features recur. Most chaperones are composed of a globular β-sheet core displaying acidic patches crucial for histone binding [**?**], as well as low complexity sequences rich in acidic

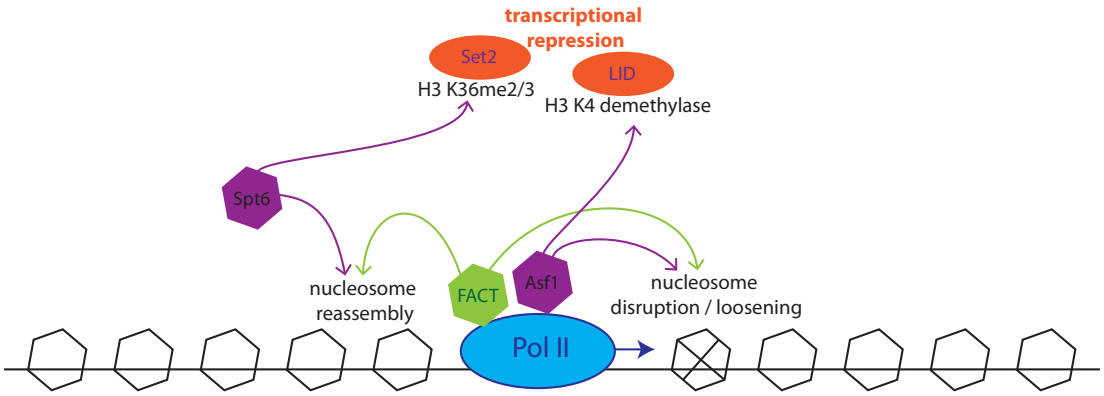

Fig. 2.13: **Transcription-coupled nucleosome dis- and re-assembly.**
Histone chaperones, some of which travel with elongating Pol II, assist in nucleosome dis- and re-assembly and recruit modifying enzymes that remove activating / destabilising histone marks to promote chromatin integrity. The model is based on **????**.

amino acid residues. These flexible acidic tails might provide more than charge complementation of histones by playing a role in promoting the transition of histones from chaperone to nucleosome and vice-versa [**?**].

For a more detailed description of individual chaperone-histone interactions, please refer to my review in *Current Opinion in Structural Biology* (COSB) in 2011 [**?**].

Histone Chaperones shield the charged and hydrophobic interaction surfaces of the histone proteins

Histone chaperones seem to use two general principles for histone binding: they shield charged (e.g. Nap1) [**?**] or hydrophobic interfaces (e.g. Asf1, DAXX, HJURP, Scm3) [**??**]. Formation of a chaperone-histone complex thus blocks nonspecific interaction with DNA and other cellular components and presents the histones in the respective 'correct' orientation e.g. for acetylation or nucleosome assembly. In some cases, chaperone binding distorts the histone dimer [**???**].

Chaperones funnel histone-DNA interactions for efficient nucleosome assembly

Nucleosome assembly is ultimately guided by a hierarchy of affinities between its components, the DNA and histone molecules [**???**]. Many of these interactions are electrostatic and very strong but rather unsprecific, thus pure mixing of DNA and histones will result in precocious and irreversible precipitation through non-productive interactions (Figure 2.14). Kinetic shielding of charged or hydrophobic histone-DNA and histone-histone interaction sites through formation of less stable histone-chaperone intermediates will allow the histones to slowly and gradually fold to the correct, DNA-bound structure of nucleosomes and chromatin and at the same time reduce the unwanted formation of mis-structured histone-DNA aggregates [**?**].

The 'sequential assembly' model for nucleosome assembly assumes that first the H3-H4 tetramer is deposited onto DNA, then the two H2A-H2B dimers. This model is supported by the fact that H3-H4 binds DNA with higher affinity than H2A-H2B [**?**] and *in vivo*, outside S-phase, the turnover rate for H2A-H2B is much higher than for H3-H4 [**?**]. It should be noted that according to this model, exchange or incorporation of histone H3

variants would require complete disassembly of the nucleosome.

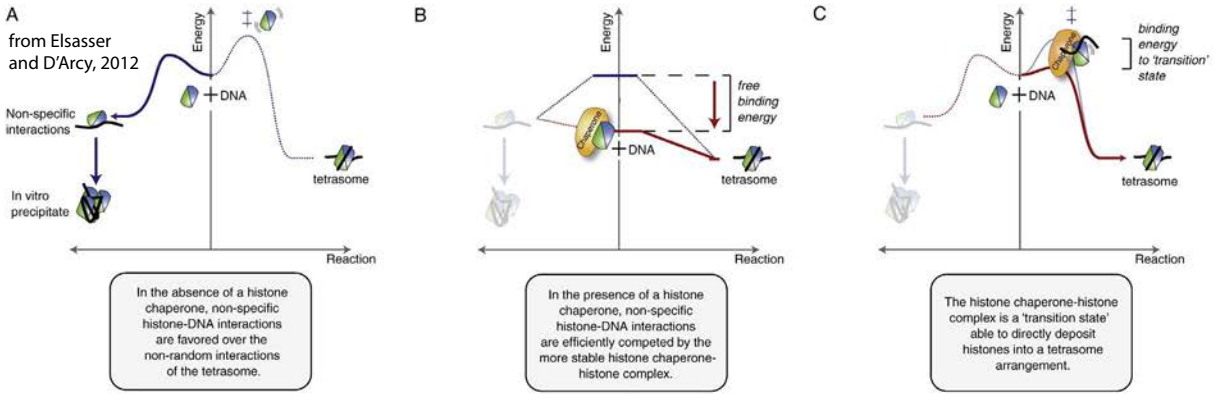

Fig. 2.14: **Chaperones thermodynamically funnel the assembly of nucleosomes.** from **?**. Histone chaperones guide histones and DNA through thermodynamically unfavoured intermediate states, to prevent non-specific aggregation and ultimately promote the assembly of a correctly folded nucleosome core particle.

Histone chaperones stabilize thermodynamically less stable, but more accessible forms of the nucleosome

Within fully assembled nucleosomes, the DNA ends of the nucleosome core particle transiently detach from the histone surface, either spontaneously as a function of the DNA sequence (which dictates bendability and therefore the strength of DNA-octamer contacts, as described above) [**?**], or aided by loop- or torsion-creating motors such as the distinct ATP-dependent remodelers. Such events, in principle, may provide temporary access to usually covered histone sites and give opportunity to histone chaperones to bind and conserve the 'open' state or further disassemble the nucleosome. Such destabilization of histone-DNA interactions will also promote the progression of RNA polymerase II [**?**].

2.3 FACT is an essential, ubiquitous H2A-H2B chaperone

FACT (*fa*cilitates *c*hromatin *t*ranscription) was identified in 1998 by George Orphanides and Danny Reinberg as a factor that allows transcription of chromatinized templates *in vitro* [**?**]. Human FACT is a native heterodimer of ∼230 kDa with two subunits, hSpt16 (p140) and hSSRP1 (p80; Pob3 in yeast) [**?**]. This chaperone is an abundant nuclear complex (∼20 000 molecules in yeast [**?**], compared to ∼70 000 nucleosomes) that localizes to the open reading frame of active genes [**??**]. *In vitro*, FACT reorganizes nucleosomes to facilitate Pol II passage and deposits histones onto DNA for nucleosome formation [**?**]. These 'chaperone' functions critically depend on the C-terminal domain (CTD) of (human) FACT, which forms a stable complex with histones H2A-H2B [**?**].

2.3.1 Molecular structure of the FACT complex

The four functional domains of yeast yFACT have been defined by partial proteolysis [**?**] and much effort has been made to characterize them structurally and biochemically (Figure 2.15).

- FACT dimerizes via the **Spt16D** and **Pob3N** domains. Spt16D is predicted to be partially unfolded [**?**]. The first half of Pob3N forms a PH-like domain (PDB 3F5R).
- **Pob3M** forms a tandem PH-like domain (PDB 2GCJ) [**?**] that interacts with the single-strand DNA binding protein RPA. Mutation of a conserved charged surface patch results in a *Spt-* phenotype (indicative of defects in transcription elongation) and HU sensitivity (indicative of defects in replication) [**??**].
- In addition to domains homologous to Pob3N and Pob3M, metazoan SSRP1 contains a C-terminal **HMG box** (PDB 1WXL [**?**]) which in fungi is encoded by a separate but structurally similar protein, Nhp6 (PDB 1LWM [**?**]). The HMG box interacts with DNA, mostly the minor groove, and inserts a sharp kink into the path of the double helix (NMR, PDB 1J5N [**?**]).
- **Spt16N** is composed of a peptidase-like and a pita-bread like fold (PDB 3BIQ, 3CB6), but the catalytic residues of the peptidase are not conserved [**??**]. The domain interacts with both the N-terminal tails and globular cores of histones H3 and H4 [**?**] and has a functional relationship with the H2A docking domain (synthetic lethality) [**?**]. It has been hypothetized that Spt16N destabilizes the dimer-tetramer interface [**?**].
- **Spt16M** shows sequence homology with Pob3M. Very recently, after this thesis has been written up, the structure of *S. cerevisiae* Spt16M was published by our competitiors [**?**]. They reveal the basic tandem PHL fold of the domain, which is very similar to our structures (presented in the results part of this thesis) and show that it interacts with histones H3-H4. Interestingly, they do not see interaction with histones H2A-H2B, maybe because their 'U-turn'-motif (the region I found to be crucial for interaction with H2A-H2B) is poorly defined, or because they use an inappropiate buffer.
- **Spt16C**, the unstructured C-terminal tail of the protein, is highly acidic: about half of its ∼75 residues are negatively charged, though in eukaryotes it is followed by a

positive stretch with putative regulatory function [?].
Pob3 is extended by a similarly acidic domain, **Pob3C**.

The Spt16M and Spt16C domains have been implicated in H2A-H2B binding, since a deletion construct lacking Spt16C and half of Spt16M is defective for binding and chaperoning histones H2A-H2B and does not facilitate Pol II progression [?].

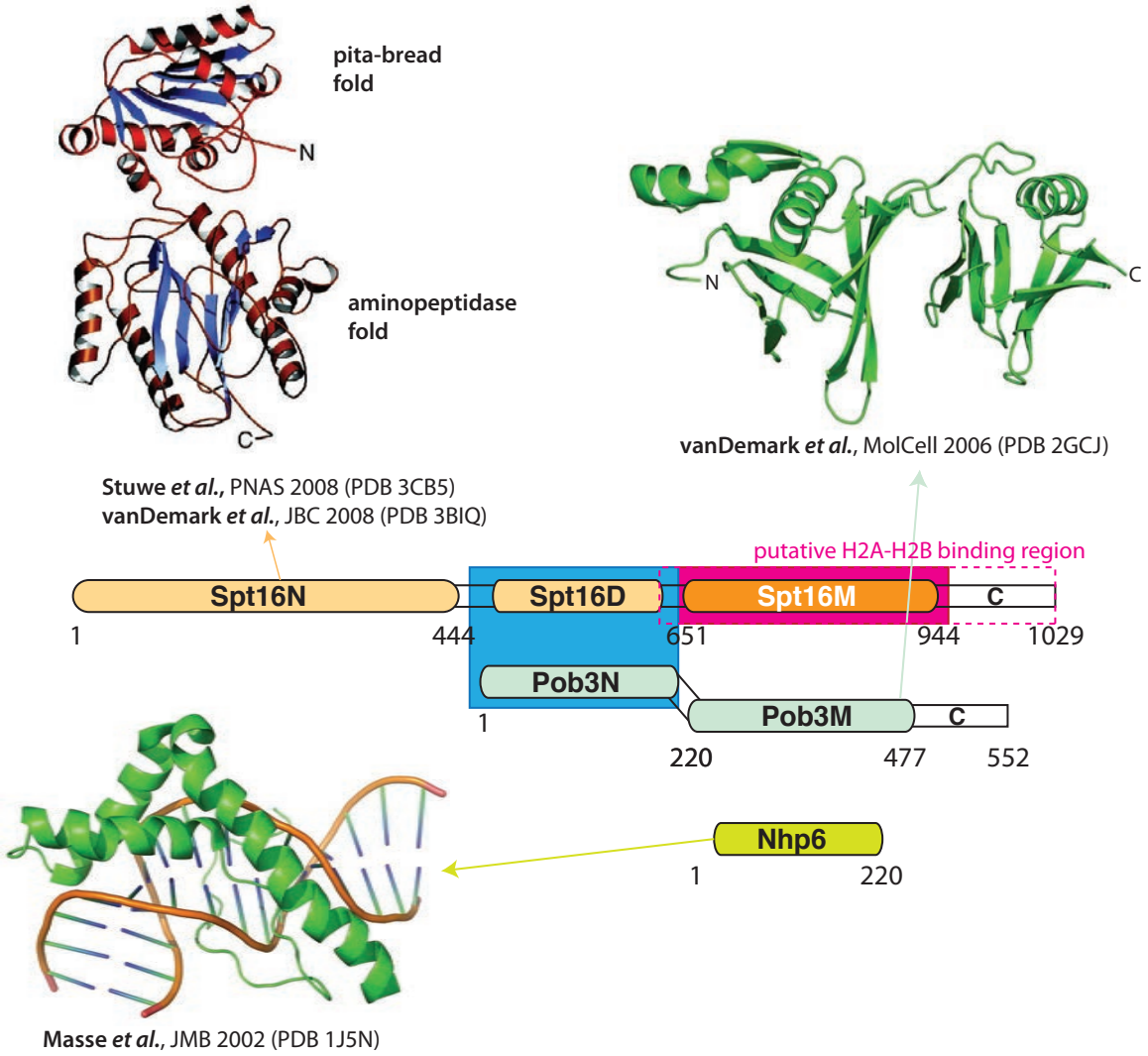

Fig. 2.15: **Domain structure of the histone chaperone FACT.**
Domains as proteolytically defined in the study by **?** are schematically represented with *C. thermophilm* sequence numbering; unstructured parts are non-colored. The published structures of Spt16N, Pob3M and Nhp6 are illustrated. The unpublished structures (our work) of Spt16D-Pob3N (*blue box*) and Spt16M (*pink box*) in complex with H2A-H2B are illustrated in the Results part of this thesis.

2.3.2 FACT in nucleosome reorganization

FACT binds and reorganizes nucleosomes [??]. This activity does not require ATP, and it does not translocate the nucleosome along the DNA [?]. How FACT reorganizes the nucleosome mechanistically has been a matter of much debate. Two models exist, the dimer eviction model [?] and the global-accessibility/non-eviction model [?] (Figure 2.16). In both cases, maximal FACT activity requires a near 1:1 ratio with nucleosomes.

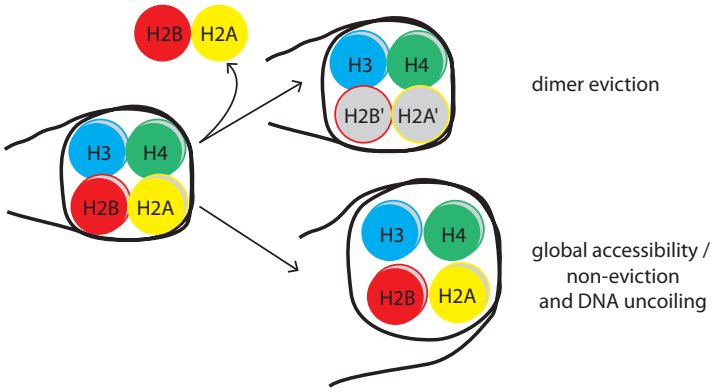

Fig. 2.16: **Models for FACT-mediated nucleosome reorganisation.**
FACT could mediate nucleosome reorganisation either by eviction of a H2A-H2B dimer [**?**], or by loosening histone-DNA and / or histone-histone contacts, thereby increasing the 'global accessibility' of the NCP with no loss of histones [**??**].

The 'dimer-eviction' model of FACT function

The dimer eviction model was suggested by the group of Danny Reinberg, in their initial biochemical characterization of FACT function. They suggest that the 'CTD' region of hSpt16 (encompassing Spt16C and half of Spt16M) binds H2A-H2B and displaces the dimer from the nucleosome; the remaining hexasome can be traversed by Pol II. After polymerase passage, Spt16 reinserts H2A-H2B [**?**]. H2A-H2B dissociation was observed for transcription of nucleosomal templates *in vitro* [**?**] and during transcription initiation *in vivo* [**?**]. After cross-linking of histone octamers with DMS, FACT activity and Pol II passage through the nucleosome was inhibited; the authors conclude that H2A-H2B dissociation is a prerequisite [**?**]. On mononucleosomal transcription-elongation templates, FACT relieves a subset of (energetic) nucleosome 'barriers', mostly in the promoter-distal region. In low salt conditions (40 mM KCl), only a hexasome is left after polymerase passage [**?**].

The 'global accessibility' model of FACT function

In the 'global accessibility / non-eviction' model [**?**], yFACT increases the overall accessibility of nucleosomal DNA and histones without necessarily displacing the H2A-H2B dimer. Tim Formosa and colleagues suggest that first, ∼10 molecules of Nhp6 bind the nucleosomal DNA and induce small conformational changes so that ySpt16-yPob3 can bind (formation of a 'SPN' (Spt16-Pob3-Nhp6) particle [**?**]). This causes more dramatic reorganization of the nucleosome, but the components — DNA and histones — are tethered (to the FACT complex and to each other) so they do not get lost. After FACT dissociation, the original nucleosome is restored [**?**].

In support of their model, the authors find that in complex with FACT, the nucleosomal DNA template is 'globally' more accessible at all sites to hydroxy radicals or nuclease digestion, and the otherwise clear 10 bp periodicity of DNA-octamer contacts becomes blurry. Displacement of H2A-H2B is observed, but the authors reason that it is a side-product of nucleosome reorganization since more nucleosomes get reorganized to the accessible state than dimers displaced [**?**]. Further, the GAL-10 promoter gets activated without significant loss of H2A-H2B *in vivo* [**?**].

In their very detailed study, the authors also observed that the source of histones

affects the affinity of FACT towards H2A-H2B and the overall stability of the histone octamer [**?**]. Thus, it is possible that species-specific differences exist for the FACT chaperoning mechanism [**?**].

A recent publication from the Luger, Reinberg and Studitsky labs further refines this model: they suggest that FACT helps to partially uncoil the DNA from the histone octamer core; this facilitates transcription through the nucleosome [**?**]. Using *in vitro* Pol II transcription assays of nucleosomal templates, the authors observe that FACT action requires the presence of H2A-H2B dimers in the nucleosomal particles, that the H2A-H2B dimer does not get evicted, that pausing sites corresponding to strong histone-DNA contacts get alleviated, and that the interface between the H2A-H2B and the H3-H4 tetramer is not disturbed (nor accessibility required). In conclusion, they suggest that the primary target of FACT is histone-DNA contact sites, which constitute the major thermodynamic barrier to polymerase progression.

2.3.3 The FACT complex embraces the nucleosome through multiple 'synergistic' interactions

Human FACT binds histones H2A-H2B, H3-H4 and DNA in vitro

FACT not only binds H2A-H2B but makes 'multiple synergistic interactions' [**?**] with the nucleosome. Spt16N binds the tails and core domains of H3-H4, although the function of this interaction is unclear [**?**], and Pob3M binds H3-H4 as well as DNA [**??**]. Karolin Luger and colleagues showed that the C-terminal domain (CTD) of hSpt16 (encompassing Spt16C and half of Spt16M) binds mostly the tails but also the globular cores of H2A-H2B [**?**], with an affinity (31 nM) that lies in between those of H2A-H2B for DNA (44 nM) or the tetrasome (13 nM). Deletion of the CTD strongly decreases H2A-H2B binding [**?**]. Full-length FACT can outcompete DNA from H2A-H2B binding; FACTΔCTD instead forms a FACTΔCTD·H2AB·DNA complex. The authors suggest a two-step model for FACT binding to the nucleosome: first, some non-CTD part binds an accessible H2AB site and then the CTD displaces DNA to access a previously covered binding site [**?**].

Mutations in the nucleosomal H2A-H2B : H3-H4 interface suppress mutants of yFACT in genetic studies

Recently, the group of David Stillman identified histone mutants that suppress the hydroxyurea (HU) (and weaker the *Spt-*) phenotype of the *spt16-11* mutant (*S. cerevisiae* T828I P859S, corresponding to P815 P846 in the Spt16M PHL-2 core, see below). The suppressor mutations localize to the octamer core or to the H2A-H2B : H3-H4 interface and destabilize the histone octamer (with an increased loss of H2A-H2B dimer). Surprisingly, no mutants of H3 or H4 were identified, but still the authors conclude that FACT-mediated nucleosome reorganization primarily destabilizes the interface between H2A-H2B and the tetrasome [**?**].

2.3.4 Ubiquitination of H2A or H2B has opposing effects on FACT function but is likely an indirect effect of chromatin structure

FACT has multiple regulatory interactions with ubiquitin. At active genes, FACT, the PAF complex and **H2B monoubiquitination** (on H2B K123 by Rad6 / Bre1 in yeast

[????] or K120 by hBre1 / RNF20 / RNF40 in human [??]) cooperate to stimulate transcriptional elongation [?]. FACT stimulates the formation of H2Bub1; the modification in turn retains the chaperone at the open reading frame (ORF). When the FACT – H2Bub1 interaction gets disrupted (e.g. by mutation of H2B K123 or depletion of Spt16), loss of chromatin integrity gives way to cryptic initiation [?].

In contrast, **monoubiquitination of H2A** (5-15 % of all H2A) by 2A-HUB (H*2A* - *h*istone *ub*iquitin ligase) blocks FACT recruitment and elongation [?].
Therefore, the positive effect of H2Bub1 on FACT recruitment is probably not a consequence of a direct interaction between ubiquitin and FACT, but rather of a more accessible chromatin structure: H2Bub1, but not H2Aub, interferes with chromatin compaction and maintains an open and accessible chromatin fiber [?]. Consistent with this hypothesis, H2Bub1 is enriched in linker-histone depleted, micrococcal nuclease (MNase) -sensitive regions of chromatin *in vivo* [?]. Further, H2Bub1 stabilizes individual nucleosomes *in vitro* and *in vivo*, at promoters and within the ORF [?].

The H2Bub1-Spt16 system seems to operate at highly transcribed genes in yeast [?] whereas long, infrequently transcribed genes are regulated by Spt6 and H3 K36 methylation [?].

2.3.5 FACT in replication

FACT is required for successful replication of chromatin in *Xenopus* egg extracts [?], and yeast FACT mutants show sensitivity to hydroxyurea and synthetic phenotypes with other components of the replication machinery [??].
FACT recruits to replication origins in a biphasic pattern: a first wave of recruitment before origin licensing is rapid, but binding is unstable and the chaperone dissociates quickly. A second wave of recruitment occurs after licensing, and this pool remains stably associated and travels with the replication fork [??].

Several physical interactions connect FACT to the replication machinery

Yeast Pob3 was purified as a DNA polymerase I associated protein [?], and its Pob3M domain interacts with RPA (replication protein A, which binds single-stranded DNA at replication forks) [?]. Depletion of human SSRP1 provokes a delay in S-phase; this is rather a consequence of slowed replication fork progression than delayed origin firing [?]. Human FACT interacts with the MCM helicase and promotes replication initiation [?]. The interaction is dependent on mono-ubiquitination of Spt16D by the Rtt101 Cullin-E3 ligase and seems to be important for initiation of early replication origins [?].

Further, the N-terminal, non-catalytic domain of yeast POL1, the catalytic subunit of the DNA Polymerase I α / primase complex, interacts with FACT and Ctf4, a sister-chromatid cohesion factor [?]. Ctf4 and FACT binding is mutually exclusive. Mutation of the highly conserved Gly493 residue in POL1 abolishes FACT binding; Ctf4 is still recruited although with altered kinetics [?]. Here, the FACT - POL1 interaction seems to be important for replication elongation of late origins, in heterochromatin [?].

2.3.6 FACT in DNA repair: ribosylation-dependent chaperone recruitment and histone variant exchange

DNA breaks get rapidly marked by phosphorylation of H2A.X (the modified form is named γH2A.X) around the DNA lesion; this can extend to mega-basepair stretches in higher eukaryotes. γH2A.X disrupts nucleosome and higher order chromatin structure and signals for recruitment of the DNA repair machinery. Poly [ADP-ribosoe] polymerase 1 (PARP1)-mediated ribosylation of Spt16 triggers dissociation of FACT from chromatin *in vivo* and prevents chaperone-mediated removal of (γ)H2A.X from nucleosomes *in vitro* [**?**]. After successful repair, non-ribosylated FACT promotes the exchange of γH2A.X for canonical H2A. Depletion of the H2Bub1 modifying enzyme RNF40 decreases FACT recruitment and γH2A.X turnover [**?**]. Further, depletion of RNF40 decreases the presence of the repair proteins RPA1 and RAD51, suggesting that FACT contributes to chromatin disassembly preceding the repair process [**?**].

Further, human FACT's SSRP1 subunit colocalizes with DNA-PK at sites of DNA damage, co-purifies with Ku86 (a subunit of DNA-PK) in a DNA-dependent manner [**?**] and stimulates phosphorylation and activation of p53 [**?**].

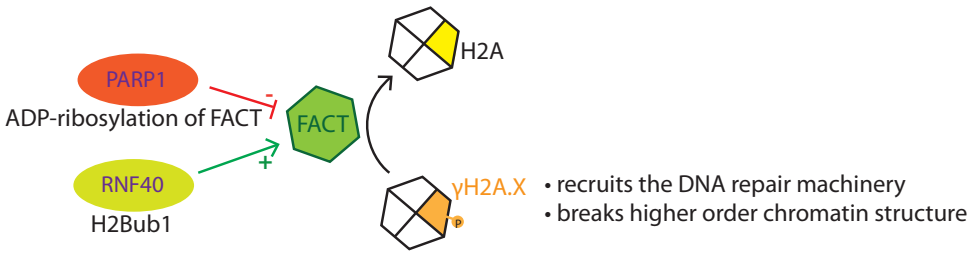

Fig. 2.17: **During DNA repair, FACT exchanges γH2A.X for canonical H2A.** FACT activity during DNA repair is regulated by ribosylation of Spt16, and removal of γH2A.X signals for the end of the repair process. The model is based on **??**.

2.3.7 FACT in transcription: evidence at the cellular level

FACT promotes transcription initiation

FACT recruits to the promoter of active genes [**?**]. The chaperone promotes recruitment of the TATA-box binding protein (TBP) and RNA Pol II to the GAL1 promoter region; recruitment is antagonised by the chromatin remodeler Chd1 and the methyl transferase Set2 [**?**]. yFACT is only required for the expression of genes with 'strong' promoter nucleosomes with very high affinity for the underlying DNA sequence [**?**], and depletion of human FACT affects the expression of only a small subset of genes(∼1.3 %). Interestingly, those transcripts can be up- or down- regulated upon depletion of FACT, and SSRP1 seems to affect some targets independently of Spt16 [**?**]. yFACT cooperates with the H3-H4 chaperone Asf1 to evict histones during activation of the HO locus [**?**] and with Spt6 for nucleosome assembly or maintenance to repress SER3 activation [**?**].

FACT is present throughout transcribed ORFs and promotes transcription elongation

FACT colocalizes with many transcription elongation factors [**?**] and travels with the elongating polymerase [**?**]. It is recruited to the transcribing polymerase by the PAF complex and/or HP1c in higher eukaryotes [**????**]. A high-resolution genome-wide ChIP profile of the Pol II elongation complex showed that Spt16 associates with all transcribed genes [**?**]. While most elongation factors associate with the ORF about 50 nt downstream from the TSS, Spt16 enters ∼30 nt more upstream, maybe through interaction with the +1 nucleosome. Apart from the different entry points, its profile across the ORF is very similar to Paf1 and the CTC kinases Bur1 and Ctk1, all of which peak in the middle of the coding region and dissociate before the polyA site [**?**].

Mutants of yFACT display elongation defects (*Spt-* phenotype) [**?**] and initiation from cryptic promoters within ORFs, presumably as a result of disrupted chromatin structure and nucleosome loss [**?**]. This may explain why mutant versions of Spt16 can suppress deletion of TFIIS (Δppr2) and Spt4, two canonical transcription elongation factors that stimulate RNA Pol II activity [**?**].

SSRP1 and Spt16 also colocalize and copurify with actively elongating RNA Pol I and Pol III complexes and promote Pol I transcription through nucleosomal templates *in vitro* [**?**].

2.4 Aims of this PhD thesis

Long before gene transcription was detected biochemically, it had been postulated theoretically [**?**]. Transcription transforms genetic information from its storage form DNA to the chemically more active messenger molecule, RNA. RNA is the molecular gadget that converts genetic information into biological function, either directly as a ribozyme and non-coding RNA or indirectly as a blueprint for translation into protein.

Four decades of research have identified most of the biochemical steps and individual factors that are required for the transcription process *in vitro*, on a naked DNA template (for a review, see [**?**]). Yet, we lack an in depth molecular understanding of how transcription occurs in its natural context, the chromatin-embedded DNA template. The regulatory influence of the DNA's 'wrapping', the chromatin, on nuclear processes is a very exciting and active field of research. In particular, I am interested in dissecting how RNA polymerase deals with repressive nucleosomes and in obtaining a more complete molecular and mechanistic understanding of nucleosome reorganization during transcription.

One of the first factors identified (biochemically) to allow RNA polymerase to transcribe through chromatinized DNA templates was the histone chaperone complex FACT [**??**], which has attracted quite some scientific interest, also in other fields of chromatin research. For example, it was shown to be essential for the maintainance of an intact chromatin structure over transcribed open reading frames. This is essential for the cell since loss of nucleosomes over ORFs would uncover cryptic promoter sites [**?**] and erase the 'epigenetic memory' of PTMs stored in the histone proteins, which signal for certains states of (transcriptional) activity.

But how can a single chaperone fulfill two such different functions - nucleosome disruption to permit polymerase passage, and nucleosome stabilization to prevent loss of the chromatin's structural integrity?

It was clear that FACT is (mainly) a histone H2A-H2B chaperone: *in vitro*, it binds histones H2A-H2B and it can disrupt the nucleosomal structure by substracting one H2A-H2B dimer [**?**].

Still, very little was know about the molecular mechanism of how FACT reorganizes nucleosomes, and which part of the multi-domain complex are vital to this chaperone function. Thereferore, I decided to study the complex using a structural-biochemical approach. Through a detailed analysis of how this essential complex interacts with histones, in particular H2A-H2B, and nucleosomes, I hoped to gain a better and more defined picture of its nucleosome reorganization mechanism and in consequence how it allows transcription to progress through chromatin.

3 Material & Methods

3.1 Materials

3.1.1 Media

Bacterial Media

LB (Lysogeny broth) 1 liter

10 g	tryptone
5 g	yeast extract
10 g	NaCl

M9 minimal medium 1 liter (5x)

Na_2HPO_4	450 mM
KH_2PO_4	110 mM
NaCl	43 mM
NH_4Cl	93 mM

PSB (Pete's Super Broth) rich medium 1 liter (10x)

Bactotryptone	100 g
Casamino acids	20 g
Yeast extract	20 g
NaCl	855 mM
NH_4Cl	187 mM
KH_2PO_4	220 mM
Na_2HPO_4	423 mM
Glucose	222 mM
$MgSO_4$	10 mM

Medium A, per 1 liter

100 ml	M9 medium (10x)
10 ml	Trace element solution (100x)
20 ml	20 % (w/v) Glucose
1 ml	1 M $MgSO_4$
0.3 ml	1 M $CaCl_2$
4 ml	Biotin (1 mg/ml)
3 ml	Thiamine (1 mg/ml)

Trace elements solution (100x), per 1 liter

EDTA	5 g
$FeCl_3$	0.83 g
$ZnCl_2$	84 mg
$CuCl_2 \cdot 2\ H_2O$	13 mg
$CoCl_2 \cdot 6\ H_2O$	10 mg
H_3BO3	10 mg
$MnCl_2 \cdot 6\ H_2O$	1.6 mg

Yeast Media

YPDA

10 g	Bacto yeast extract
20 g	Bacto peptone
20 g	Glucose monohydrate
40 mg	Adenine hemisulfate
20 g	Bacto Agar (only for making YPDA/agar plates)
800 ml	ddH_2O

Dissolve everything by stirring, add ddH_2O to 1l final, then autoclave and store at 4°C.

SD

Make amino acid solutions as required (all amino acids were purchased from Sigma). For 100 ml of a 100x solution take:

200 mg	arginine HCl
300 mg	isoleucine
300 mg	lysine HCl
200 mg	methionine
500 mg	phenylalanine
2000 mg	threonine
300 mg	tyrosine
200 mg	uracil
1500 mg	valine
6.7 g	Yeast nitrogen base without amino acids
20 g	Agar (for plates only)
850 ml	ddH_2O

Add amino acids as required, mix by stirring and bring to 950ml with ddH_2O. Adjust to pH 5.8 and autoclave, then cool to ∼55°C and add 50ml 40 % glucose (final 2 %) and store at 4°C.

FOA plates

For one litre of the respective SD plate media solution, add 1.0 g of FOA (5-Fluoroorotic Acid) after autoclaving, when cooled to ∼55°C, and stir for 30 min to 1 hour at ∼55°C.

PBS buffer

NaCl	137 mM
KCl 2.7	0.2 mM
$Na_2HPO_4 \cdot 2\ H_2O$	10 mM
KH_2PO_4	2 mM

Adjust to pH 7.4.

10x LiAc

1 M LiAc
10 X TE (0.1 M Tris-HCl, 10 mM EDTA pH 7.5)
Adjust to pH 7.5 with dilute acetic acid and autoclave.

1x PEG

50 % PEG 4000 in 1x LiAc solution
Filter sterilize.

3.1.2 Gel buffers

SDS protein sample loading buffer
125 mM Tris-HCl pH 6.8
10 % β-mercaptoethanol
4 % SDS
20 % glycerol
0,004 % Bromphenol Blue.

Laemmli running buffer
63 mM Tris HCl
10 % glycerol
2 % SDS
0.0025 % Bromophenol Blue pH 6.8

4x upper / stacking gel SDS buffer
500 mM Tris-HCl; pH 6.8
0.4 % SDS

4x lower / separating gel SDS buffer
1.5 M Tris-HCl; pH 8.8
0.4 % SDS

Western Blot transfer buffer
3.1 g/l Tris base
14.4 g/l glycine
15 % MeOH

Native gel mix
0.2x TBE
5 % acrylamide 37:1 (acrylamide : bis-acrylamide)

TAE buffer
40 mM Tris
20 mM acetic acid
1 mM EDTA

TBE buffer, 5x stock solution (1 liter)
4 g Tris base
27.5 g boric acid
20 ml 0.5 M EDTA
Adjust to pH 8.

3.1.3 Kits

Item	Manufacturer, Specification
Plasmid preparation	Miniprep, Qiagen
Gelextraction	PCR Purification and Gelextraction Kit, Qiagen
Silver Staining	Invitrogen SilverQuest
NuPAGE precast gels and buffers	Invitrogen

3.1.4 Chemicals

Item	Manufacturer, Specification
α-D-Glucose	Sigma
Acetic Acid	Fisher Scientific
Acetone	Fisher Scientific
Acrylamide	BioRad
Agarose	Denville Agarose HS
Ammonium chloride (NH_4Cl)	Fluka
Ammonium persulfate	Bio-RAD
Ammonium sulfate (NH_4SO_4)	Fluka, ultra pure
Ampicillin	Sigma
β-mercapto Ethanol (β-ME)	Fluka
Bacto Tryptone	BD
Biotin	Sigma
Bis-Acrylamide	Bio-RAD
Boric acid $B(OH)_3$	Sigma
Bromphenol Blue	Sigma
BSA	Sigma
Cacodylate sodium salt	Fluka, ultra pure
Calcium Chloride ($CaCl_2 \cdot 2\ H_2O$)	Merck
casaminoacids	BD
Chloramphenicol	Sigma
Cobalt Chloride ($CoCl_2$ anhydrous)	Fluka
Coomassie G250 and R250	Sigma
Dithiothreitol (DTT)	Biomol
Ethylendiamine tetra acetate (EDTA)	Sigma
Ethanol (EtOH)	Pharmaco-AAPER
Ethidium Bromide (EtBr)	Bio-RAD
fish sperm DNA	Sigma
5-Fluoroorotic Acid (5-FOA)	Zymo Research
Formaldehyde (35 %)	Merck
Formic acid	Fisher Scientific, ultra pure
Glutathione reduced (GSH)	Sigma
Glycerol	Fisher Scientific, ultra pure
Guanidine HCL	Sigma
HEPES	Sigma
Imidazole	Sigma
IPTG	Gold Bio Technology, Inc

Iron Chloride ($FeCl_2$)	Merck
Isopropanol	Fisher Scientific
Kanamycin	Sigma
Lithium Acetate (LiAc)	Sigma
Luria Bertani medium LB Broth	Miller, EMD
Magnesium Sulfate ($MgSO_4 \cdot 7\ H_2O$)	Sigma
Manganese Chloride ($MnCl_2 \cdot 4\ H_2O$)	Sigma
Methanol (MeOH)	Pharmco-AAPER
Nickel sulfate ($NiSO_4$)	Sigma
Nonident P-40 (NP40)	Fluka
Polyethylenglycole 8000 (PEG8000)	Hampton
Polyethylenglycole 4000 (PEG4000)	Merck
Phenylmethylsulphonylfluoride	Fluka
poly-L-lysine	Sigma
Potassium chloride (KCl)	Fisher Scientific
Potassium (di)Hydrogen Phosphate (KH_2PO_4)	Sigma-Aldrich
Riboflavine	Sigma
Sodiumdodecylsulfate (SDS)	Sigma
Sodium chloride (NaCl)	Sigma, Fluka
Sodium Fluoride (NaF)	Sigma
(di)Sodium Phosphate (Na_2HPO_4)	Sigma-Aldrich
Superblock in TBE	Pierce
TCEP	Sigma
Thiamine	Sigma
TRIS Base	Sigma
Triton X-100	Fisher Scientific
Tween20	Sigma
Urea	Fisher Scientific
Yeast extract	Fisher Scientific
Zinc chloride (ZnCl)	Fluka

3.1.5 Antibodies

Antibody	Manufacturer, Specification
anti-V5	abcam, ab27671
anti-TAP	Thermo Scientific, CAB1001
goat anti-rabbit HRP	Jackson Immuno, 111-035-144
goat anti-mouse HRP	BioRad, 170-6516
V5 affinity agarose	Sigma

3.1.6 Instruments

Instruments	Manufacturer, Specification
Centrifugation bottles	1l Beckman, poly-carbonbate
Crystallization robot	Rigaku Phoenix
Spectrofluorometer	Horiba Fluorolog-3
FPLC	Äkta Purifier10, Äkta FPLC
ITC	GE / Microcal, VP-ITC or ITC200
PCR-machine	Biometra T-Gradient
PCR-machine	MJ Research PTC-200
pH-meter	inoLab pH-meter
Peristaltic pump	Rabbit pump
Pipettes	Denville, Gilson, RAININ
Rotors	Sorvall, SS 34
Table-top centrifuges	Denville 260D; Sorvall RT7 Plus; TOMY MC140
Ultra centrifuge	Sorvall instruments, RC5C
Western blot	Wet or Semi trans blot, BioRad

Consumables	Manufacturer, Specification
Centrifugation bottles	1l Beckman, poly-carbonbate
Concentrators	Amicon Ultra, Millipore
Concentrators	Vivaspin (Hydrosart membrane; 3, 10 and 30 kDa MWCO), Sartorius
Cover slips	Hampton Research (HR3-229)
Crystallization plates	VDXplates-Hampton 22 mm (HR3-170)
Dry Air	Servisol, Aero duster 100
Dialyzing membrane	ZelluTrans, Roth (6, 14 and 23 kDa MWCO)
Filter	Stericup, Millipore, 50 ml Bottle Top Filter, 0,22 μm PES
Filter	Millipore, Type GV 0.5 μm and 0.2 μm
Glass beads	Sigma, 425-600
Pipette tips	1-50 ml Costar
Pipette tips	TipOne USAScientific, RAININ
Plates	Fischerbrand, Falcon
Reaction tubes	Eppendorf, volumes 1.5 ml and 2 ml
Snake skin	Pierce, MWCO 8 kDa
Syringes	BD Syringe, 5 ml, 10 ml, 20 ml and 60 ml
Table-top centrifuge	USA Scientific

3.2 General Methods

3.2.1 Protein expression and purification

Bacterial protein expression was performed using the *E. coli* 'Rosetta' strain which expresses several tRNA genes from a plasmid (with chloramphenicol-resistance) for optimized codon usage. Chemically competent cells were transformed with the expression plasmid and 50 ml precultures grown over-night in LB with respective selection antibiotics. Expression was performed in 1 l PSB (1x) medium per 6 l Erlenmeyer flasks, shaking at 200 rpm. The media was inoculated with 10 ml preculture and grown at 37°C to OD_{600nm} = 0.8; cells were induced with 400 mM IPTG and shifted to 18°C for over-night protein expression. The cultures were harvested in 1 l Beckman centrifugation bottles in a JA 8.1000 rotor at 4°C, 4000 rpm for 12 min and resuspended in 15 ml resuspension buffer per liter of culture (500 mM NaCl, 50 mM Tris pH7.5, 15 mM imidazole with protease inhibitors, e.g. 1 tablet of Roche Complete EDTA-free per 2 to 3 l of culture). Cells were lysed by one freeze-thaw cycle and sonication (Bruker, four times 2 minutes on ice at 50 % output) and the lysate cleared by centrifugation (Thermo Scientific SS-34 rotor or similar, 1.5 h at 18000 rpm, 4°C).

Standard protein purification was performed at 4°C using the Aekta Purifier liquid chromatography system. A typical purification constisted of:

- **affinity purification** of the epitope-tagged protein (His- or GST-tag) from crude lysate using Ni-NTA (high-performance Ni-sepharose, GE Healthcare) or glutathione S-transferase covered sepharose (GE Healthcare) beads. Usually, this step was perforemed 'in batch', with ∼5 ml resin in a 50 ml tube (Falcon) and wash and elution steps performed by centrifugation at 1000 rpm. For crystallography-grade purification, the resin was packed into a column and wash and elution steps performed on the AEKTA system. Eluate was either dialyzed into imidazole-free buffer (typically 400 mM NaCl, 25 mM Tris pH 7.5 and 2 mM DTT; imidazole can form decay products (after reaction with radicals) that may harm the protein) or immediately subjected to size-exclusion chromatography (SEC).

- **size exclusion chromatography** (**SEC**) using the Superdex (SD) 75 or SD 200 resin columns (GE Healthcare) was performed to separate the protein of interest from aggregated protein (which comes down in the void fraction) and other impurities that non-specifically bind to the affinity resin. This step can also be used for moderate buffer exchange, e.g. to bring the protein into imidazole-free buffer or slightly lower salt (e.g. from 400 to 200 mM NaCl).

- The (more or less) pure protein fractions were pooled and incubated with 1 ml 1 mg/ml recombinant **TEV** (Tabacco Edge Virus) protease per 50 mg protein, which cleaves a recognition site (ENLYFQ(G/S) inserted into the expression construct between the epitope tag and the protein of interest. The mixture was dialyzed into low salt buffer (∼200 mM NaCl) for more efficient TEV cleavage and better binding to ion exchange resins in the next step.

- **ion exchange chromatography** on MonoQ or MonoS columns (GE Healthcare) was performed to further purify the protein from all contaminants or degradation products. The protein was bound in low salt buffer (∼ 200 mM NaCl, 25 mM Tris pH 7.5, 2 mM DTT), washed with 10 column volumes of low salt buffer and eluted

with a long gradient into high salt buffer (∼60 min from e.g. 200 to 1000 mM NaCl at 1 ml / min).

- The cleanest fractions were pooled and dialyzed into the desired buffer (e.g. 200 mM NaCl, 25 mM Tris pH 7.5, 2 mM DTT). **Protein concentration** (usually to the solubility limit) was performed using centrifugation devices with appropriate molecluar weigth cut-off (MWCO) (from Vivaspin or Millipore), spinning at 4°C, 4000 rpm in a Falcon centrifuge. Protein concentration was monitored by absorbance at 280 nm (nanodrop system). Extinction coefficients were calculated with the Expasy ProtParam online tool. Small aliquots (50 μl or less in a 0.6 ml eppendorf tube) were snap-frozen in liquid nitrogen and stored at -80°C.

3.2.2 Protein separation and visualization

For separation of proteins according to size by **SDS-PAGE**, protein samples were mixed with Laemmli SDS loading buffer and boiled at 100°C for 1 min. The samples were separated on self-cast BioRad Mini gels (acrylamide concentration varying from 8 - 16 %, run in Laemmli SDS buffer) or precast gradient gels (Invitrogen NuPage, 4-12 % in Tris-Glycine buffer (purchased, Invitrogen), run in Invitrogen 1x MES or 1x MOPS buffer) at 160 V.

Proteins were visualized in gel by staining with Coomassie Brilliant Blue (stain with 1 g/l Coomassie R250, 10% acetic acid, 40 % MeOH, destain in a equivalent solvent solution without the dye) or silver (Invitrogen Silver Quest kit).

Alternatively, proteins were specifically detected by **Western blot**. The proteins were transferred at 60V for 60 minutes at 4°C onto a nitrocellulose membrane in transfer buffer. After blocking with 5 % milk in TBST (TBS buffer with 0.05 % Tween20), proteins were incubated with protein- or epitope-specific primary antibodies (in 5 % milk TBST, for 1 h at room temperature or 4°C over-night), washed (3 times 5 minutes) with TBST, incubated with HRP-coupled secondary antibodies (in 5 % milk TBST, 30 min at room temperature), washed 3 times 5 minutes and detected by chemoluminescence.

3.2.3 Native PAGE

Native gel electrophoresis was performed using the BioRad Mini gel system. Samples were supplemented with 5 % glycerol and separated on a native gel (5 % acrylamide, 0.2x TBE), run in 0.2x TBE at 4°C and 100 V.

After the run, DNA was detected by either Ethidium bromide (EtBr) (after staining 5 min in a 0.01 g/l EtBr in TAE buffer and subsequent 5 min wash in TAE), radioactivity (DNA was labelled with ^{32}P by either PCR synthesis with radioactive nucleotides (α-GTP or ATP) or by direct labelling of the oligonucleotide with T4 plynucleotide kinase (PNK) and radioactive γ-ATP (radiactive nucleotides from Perkin Elmer)) or fluorescence (Cy5 labelled DNA, synthesis by PCR with a Cy5-labelled oligomeric primer (purchased from Metabion)).

Proteins were detected by Coomassie or silver stain, as described for SDS-PAGE.

3.3 Methods related to the Spt16M - H2A-H2B complex

3.3.1 Protein Expression and Purification

Purification of Spt16M

The *Chaetomium thermophilum* Spt16M domain (Spt16M, residues 651–944) was amplified from cDNA and cloned into the pETMCN-6xHis vector, carrying an N-terminal 6x-His tag and tobacco etch virus (TEV) protease-cleavage site (leaving an N-terminal overhang of the residues Gly-Met-Glu, where Glu corresponds to residue 647 of Spt16M). The chaperone domain by itself purifies nicely as follows: prufication from lysate via Ni-NTA affinity either in batch or over a self-cast column; SEC of the eluate in 400 mM NaCl, 25 mM Tris pH7.5, 2 mM DTT; dialysis into 200 mM NaCl buffer with addition of TEV protease and incubation for 1 day; ion exchange chromatography over a MonoQ and elution with a gradient of 200 to 1000 mM NaCl. Site-specific mutations were introduced by PCR and purified as for wild-type Spt16M.

Purification of the Spt16M-linker-H2B - H2A complex

For expression of the complex, the Spt16M construct was fused to a 12-residue GGSGGS linker and the globular domain of H2B (residues 24–122). The construct was co-expressed with globular H2A lacking the hydrophobic C-terminus (residues 13–106). The complex was purified as follows: cell lysate was loaded onto a self-packed Ni-NTA column, washed with 5 volumes of lysis buffer (500 mM NaCl, 50 mM Tris pH 8.0, 10 mM imidazole), and eluted in the same buffer with a linear gradient of imidazole from 10 to 500 mM. Fractions containing both the Spt16M-H2B fused construct and H2A were run over a Superdex 200 HR26/60 column column in 400 mM NaCl, 25 mM Tris pH 7.5, 2 mM DTT. Complex fractions were pooled and the 6xHis tag was cleaved with TEV protease for 20 h at 4° C and dialysed into a buffer containing 25 mM Hepes pH 8.5, 500 mM NaCl, 2 mM DTT. The protein was bound to a MonoS HR10/10 ion exchange column and eluted running a linear gradient of 50 column volumes of elution buffer containing 25 mM Hepes pH 8.5, 1 M NaCl, 2 mM DTT. Fractions were pooled and dialyzed against 25 mM Hepes pH 8.5, 500 mM NaCl, 1 mM TCEP.

3.3.2 Crystallization and data collection

For crystallization of Spt16M - H2A-H2B, tetragonal crystals of the native complex were grown at 4°C or 10°C from hanging drops composed of 1 μl protein (15 mg/ml) and 1 μl crystallization buffer (7.25 % [vol/vol] PEG8000, 0.2 M $MgCl_2$, 0.1 M Tris pH 7.8) suspended over 1 ml of the latter. Crystals were frozen by stepwise soaking in crystallization buffer containing increasing glycerol up to 20 %, and frozen in liquid N_2. High-resolution datasets were collected at beamlines PXIII (SLS, Villigen, Switzerland) and ID23-2 (ESRF, Grenoble, France). Data processing and scaling were done with XDS and Scala [**???**].

3.3.3 Structure determination and refinement

For the structure of the complex, a PHASER [**?**] molecular replacement solution was determined using the phases of Spt16M as determined by Tobias Stuwe and the histone H2A-H2B heterodimer from the structure of the canonical nucleosome core particle

[?]. The structure was finalized by iterative cycles of model adjustment in COOT and refinement in Refmac and PHENIX [???]. Structural visualization was done using Pymol. Electrostatic surface potentials were calculated using APBS [?]. Structural superpositions were calculated with 3dSS [?].

3.3.4 Sequence alignments

ClustalW sequence alignments were performed on the EBI server with the default settings (slow alignment, protein weight matrix Gonnet, gap open penalty = 10, gap extension penalty = 0.2, gap distance penalty = 5, no end gaps penalty = no, iteration = none, numiter = 1, clustering = NJ)

3.3.5 Isothermal titration calorimetry

Binding affinities were determined at 25°C or 4°C using an ITC calorimeter (either VP-ITC or ITC200, both MicroCal). Proteins and peptides were dialyzed in one beaker against ITC buffer (typically containing 25 mM Tris and NaCl (between 75 and 500 mM, as indicated) and no DTT. Protein and peptide were adjusted such that the ligand concentration (syringe solution, 40 μl plus 20 μl extra for laoding) was in roughly 10-fold molar excess over the cell solution (total volume $\sim$ 240 μl, plus 60 μl extra for loading). Injections consisted of 1 or 2 μl of ligand at 3 to 5 min intervals. Data were analyzed using Origin software (version 5.0).

3.3.6 Histone refolding

Recombinant histones were purified and refolded as described [?], with modifications: full-length and globular histones were mixed at equimolar ratios to a final concentration of 1 mg/ml and refolded in 25 mM Tris pH 7.5, 150 mM NaCl and 5 mM DTT. H2A-H2B dimers as well as $(H3\text{-}H4)_2$ tetramers were subsequently purified by gel-filtration chromatography using a Superdex 200 HR16/60 column.

3.3.7 Size exclusion chromatography (SEC)

For SEC of histone-chaperone complexes, proteins were mixed at equimolar ratios and incubated on ice for 30 min. Proteins were separated on a Superdex 75 10/300 GL column in 300 mM NaCl, 25 mM Tris pH 7.5 and 5 mM DTT.

3.3.8 V5 Immunoprecipitations

A total of 15 μl of anti-V5-agarose beads (Sigma) was incubated with 40 μg of recombinant, purified V5-fused protein for 30 min rotating at 4°C in 200 mM NaCl, 25 mM Tris pH 7.5 and 0.05% Nonident P-40 detergent. Beads were washed three times with 1 ml buffer. Next, beads were incubated with refolded H2A-H2B in 5-fold excess of histone for 1 h at 4°C and afterwards washed five times with buffer. Bound proteins were eluted by either directly boiling the beads in SDS-loading buffer or by incubation for 30 min with 25 μl V5 peptide (2 mg/ml) (sequence: Ac-YGKPIPNPLLGLDST) at room temperature. Samples were subsequently analyzed by SDS-PAGE.

3.3.9 Electrophoretic Mobility Shift Assay (EMSA)

A radioactive 150 bp PCR product of the 'Widom 601' [**?**] sequence was generated with a polynucleotide-kinase (PNK) labeled radioactive primer. In a total volume of 20 μl, proteins (amount as indicated) were mixed with about 100 ng DNA for 1 h at 37°C. Glycerol was added to a final concentration of 3.5 %. Samples were run on a 20x20 cm native acrylamide gel (4 % acrylamide, 0.2 % bisacrylamide, 5 % glycerol, 2 mM $MgCl_2$, 0.5x TBE) for 4 h / 150 V at 4°C, dried on Whatman filter paper, exposed to a phosphoimager storage screen and read with a Fuji Phosphoimager.

3.3.10 DNA–histone interaction assays

A radioactive 150 bp PCR product of the "Widom 601" sequence was generated with an PNK-labelled primer and diluted to 20 μM. The respective amount of histones was diluted into 10 μl buffer (100 mM NaCl, 25 mM Tris pH 7.5, 5 mM DTT and 0.2 mg/ml BSA final concentration). The reactions were mixed with 10 μl Spt16M or protein buffer and incubated at 37°C for 30 min. 1 μl of DNA was added, mixed briefly and incubated at 37°C in a incubation oven to prevent condensation. Glycerol was added to a final concentration of 3 %. Samples were run on a 20x20 cm native acrylamide gel (4 % acrylamide, 0.2 % bisacrylamide, 5 % glycerol, 2 mM $MgCl_2$, 0.5x TBE) for 20 min / 150 V plus 12 h / 50 V at 4°C, dried on Whatman filter paper, exposed to a phosphoimager storage screen and read with a Fuji PhosphoImager.

3.3.11 Yeast methods

Transformation of *S. cerevisiae*

50 ml of yeast culture at OD_{600} = 0.5 to 1.0 were spun down (5 min 2000 rpm at room temperature) and washed twice with autoclaved water. The pellet was resuspended in 1x LiAc (200 μl per transformation). 0.5 μg plasmid DNA or 10 μl PCR product were mixed with 18 μl pre-heated (boiled) carrier DNA (e.g. fish sperm, 10 mg/ml) in a sterile reaction tube. 200 μl of the yeast mixture were added and vortexed. 1.2 ml 1x PEG was added and vortexed and the mixture was incubated at 42°C for 1 h. After that, cells were spun down, washed once with sterile water, and plated on the respective selective media plates. Cells were cultivated at 30°C or 24°C.

Phenotypic analysis in *S. cerevisiae* (Tuepfeltest)

To determine the effect of Spt16M mutations on yeast cell growth, Spt16 was deleted from *S. cerevisiae* strain W303 by homologues recombination introducing a TRP cassette as selection marker. The associated lethal phenotype was rescued using a plasmid (YPLac33) carrying wild-type Spt16 from *S. cerevisiae* as well as the URA3 gene that was co-transformed using the lithium acetate / PEG method.
A first set of mutant plasmids was generated as follows: a chimeric Spt16 gene was generated replacing the Spt16M domain from *S. cerevisiae* with the Spt16M domain (or point-mutants thereof) from *C. thermophilum* and cloned into YCplac111 carrying the LEU2 gene as selection marker.

Since these mutants could not be unambiguously distinguished from endogenous wild-type protein by western blot, a second set of mutants was cloned with a N-terminal V5-tag

and the full-length *C. thermophilum* sequence (wild-type of mutants thereof).

Resulting constructs transformed into the Δ*spt16* strain with the URA rescue plasmid. Transformants growing on SD –Leu plates (so the plasmid containing the mutant proteins cannot get lost) were grown over-night in –LEU SD medium and subsequently plated by spotting 10 μl of 10-fold serial dilutions onto –LEU 5-Fluoroorotic Acid (5-FOA) plates and incubated at 30°C or 24°C for 3 days. 5-FOA is toxic if cells contain the URA3 gene and thus only cells that can loose the URA3 / wild-type Spt16 rescue plasmid and live with only the LEU2 / (mutant) Spt16 plasmid can survive.

Immuno-precipitation (IP) from yeast whole-cell lysate (WCL)

100 ml yeast culture at OD_{600} = 0.5 was spun down (5 min 2000 rpm) and washed once with sterile water. The cell pellet was resuspended in 0.5 ml ice-cold yeast extraction buffer (10 mM sodium phosphate pH 8, 1 % NP40, 200 mM NaCl, 2 mM EDTA, 50 mM NaF, 1x roche complete EDTA-free protease inhibitor cocktail) and cells were broken by vortexing 5 times 1 min with 0.5 ml glass beads (0.2 mm diameter). The lysate was taken off the beads and spun for 20 min at 14000 rpm, 4°C. and the supernatant transferred to a fresh reaction tube (whole cell lysate, WCL).

For IP, the supernatant was diluted 1:4 with TAP-IP buffer (50 mM Tris pH 7.5, 100 mM NaCl, 0.15 % NP40, 1.5 mM $MgCl_2$, 0.3 mM DTT and 1x protease inhibitor cocktail). Recombinant, V5-tagged proteins were bound to V5 affinity agarose (20 μl per reaction) and incubated with 1 ml of the diluted WCL for 2 h rotating at 4°C. Beads were washed 5 times with TAP-IP buffer and bound protein eluted with reducing-agent-free loading buffer (0.08 g SDS and 0.4 ml 100 % glycerol per 1 ml).

Fixing and immuno-staining of yeast cells for microscopy

10ml of a yeast culture at OD_{600} = 0.3 was spun down, washed once with sterile water and transferred to a 1.5 ml reaction tube. Cells were fixed with 5 % formaldehyde for 15 minutes at room temperature. Cells were pelleted, washed twice with PBS and spun down again to estimate the 'packed cell volume' (pcv, usually less than 20 μl).
Cells were resupended in 100 μl lyticase digestion solution (100 μg/ml lyticase (Sigma L4025), 3 μg/ml PMSF, 2 μl/ml β-ME) and spheroblasted for 30 min at 30°C. Spheroblasted cells were washed twice with 1ml PBS (spin 5 min 2000 rpm at 4°C).

The cell pellet was resuspended in 20 pcv PBS, and 10 μl of this solution spotted onto polylysine-coated cover slips and left to dry for 20 min at room temperature. Slides were washed twice with PBS (4°C), then fixed in MeOH (5 min, -20°C) and acetone (20 min, -20°C) and dried over-night at room temperature.

For immunostaining, the slide was washed twice with PBS (4°C), once in PBS / 0.1 % Triton X-100, and blocked with BSA (2 % BSA, 0.1 % Tween20 in PBS) for 60 min at 4°C. The first antibody was applied at the appropriate dilution in blocking solution for 2 h at room temperature; afterwards the slide was washed 10 times with PBS. Similarly, the second (fluorescent) antibody was applied for 1 - 2 hours at room temperature in the dark and washed.

For DAPI staining of the nuclear DNA, a 10 μg/ml DAPI was applied for 5 min at room temperature and the slide washed twice with PBS.

4 Results and Discussion I: Structure of the FACT chaperone domain in complex with H2A-H2B

4.1 FACT is a conserved H2A-H2B chaperone

FACT is well-known for its ability to chaperone histones H2A-H2B during transcription and replication. Deletion of the C-terminal part of Spt16 (termed FACTΔC in the literature, which encompasses half of Spt16M plus Spt16C as defined by proteolysis, Figure 4.1) is lethal in human cells and abrogates chaperone function [**???**] (Figure 4.1). Mutants of the yeast Spt16 gene with *Spt-* (transcription) or HU (replication) phenotype predominantly map to the Spt16M domain (Figure 4.1).

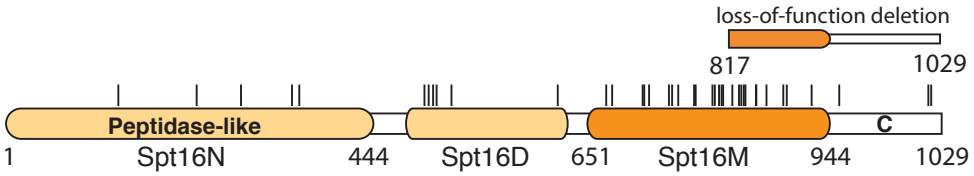

Fig. 4.1: **Domain organization of ySpt16.**
Residue numbers refer to the sequence of *C. thermophilum*. Black lines indicate the positions of HU and *Spt-* mutants isolated in *S. cerevisiae*. A loss of function truncation of the human protein is indicated (the construct for the remaining human sequence was termed FACTΔC [**??**]).

Despite this knowledge, molecular details about how FACT binds H2A-H2B were missing. Since such knowledge would allow mechanistic conclusions about FACT-mediated nucleosome reorganization, I decided to study the interaction in a biochemical – structural approach. In particular, I wanted to

- define the 'chaperone' domain of FACT that interacts with histones H2A-H2B and study the biochemistry and biophysics of this interaction;
- solve the structure of the FACT chaperone domain (Spt16M) in complex with histones H2A-H2B;
- study the interaction of Spt16M with histones H3-H4;
- and combine all these results to describe a model for FACT-mediated nucleosome reorganization.

The project was started with Tobias Stuwe, a former PhD student in the lab. Together, we designed and discussed the analysis of the Spt16M domain. I performed most of the biochemistry, and Tobias solved the structure of free Spt16M. After Tobias had left the lab, I designed the construct for the Spt16M – H2A – H2B complex, solved its structure and verified the observed interaction biochemically.

4.1.1 Spt16M is the only globular domain of FACT that binds H2A-H2B

For the experiments described below, I used the Spt16 and Pob3 sequences of the thermophile yeast *Chaetomium thermophilum*. The RNA and cDNA of this recently sequenced organism was a kind gift from Ed Hurt, BZH Heidelberg [**?**]. This species lives in soil and compost heaps and tolerates temperatures up to 60°C. It seems that these conditions promoted the evolution of stable protein forms opportune for structural studies.

First, I analyzed by pull-down assays which of the four globular 'functional' domains of the yeast FACT complex (Figure 4.1) interacts with histones H2A-H2B. To this purpose, the individual FACT domains with an N-terminal V5-tag were recombinantly expressed in *E. coli*, purified, bound to V5-affinity agarose and incubated with an excess of histone dimer. After extensive washes (200 mM NaCl, 25 mM Tris pH 7.5, 0.05 % NP40 at 4°C), bound proteins were analyzed by SDS-PAGE and Coomassie staining. Only full-length Spt16 and the Spt16M domain were able to interact with the histone dimer (Figure 4.2a).

Spt16M also purified with histones H2A-H2B in size exclusion chromatography (Superdex75 10/300 in 300 mM NaCl, 25 mM Tris pH 7.5, 2 mM DTT) as a stoichiometric complex of higher molecular weight than the individual domains (Figure 4.2b). Therefore Spt16M is sufficient for interaction with the histone H2A-H2B dimer and presumably the sought-for 'H2A-H2B chaperone' domain of Spt16 or FACT.

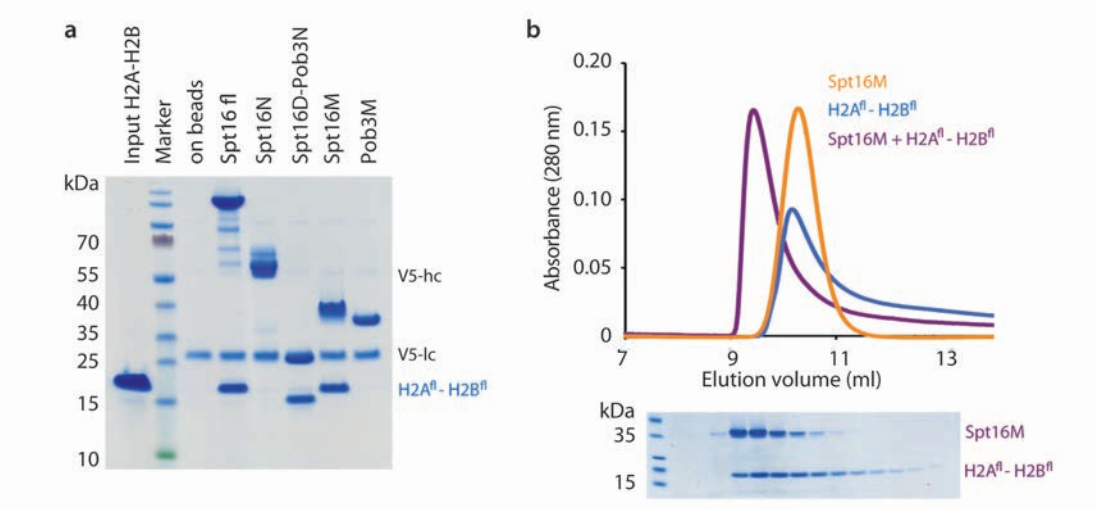

Fig. 4.2: **The Spt16M domain of FACT forms a complex with histones H2A-H2B.** (a) Spt16M, but none of the other globular FACT domains, interacts with recombinant histones H2A-H2B in V5-immunoprecipitation assays. V5-hc / lc = V5 antibody heavy / light chain. (b) SEC elution profile (top) of the individual proteins and of the chaperone-histone complex, and SDS-PAGE (bottom) of the eluted fractions for the complex. Spt16M forms a stable complex with full-length H2A-H2B dimers, resulting in a lower retention time than the individual proteins.

To get an impression of how conserved the chaperone domain is, I performed a sequence alignment of selected Spt16M sequences, from yeast to human (Figure 4.3). The domain is highly conserved, in particular the second half, indicating that many of the residues are crucial for function (or folding) of the protein. This explains why many functional mutants map to this domain.

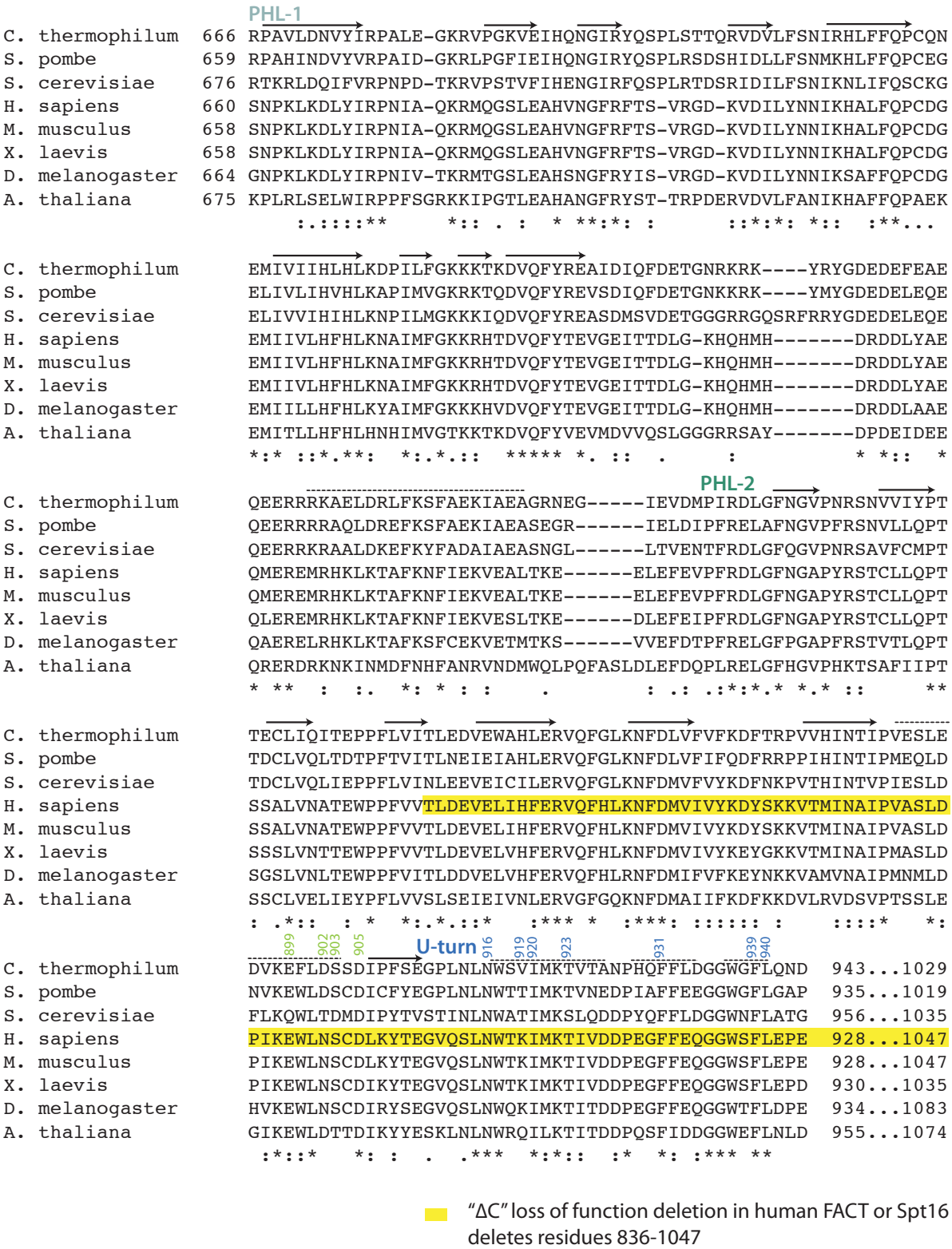

Fig. 4.3: **Alignment of Spt16M sequences.**
Sequences of the Spt16M domain from different species were aligned with ClustalW2. Functionally important residues are marked using *C. thermophilum* sequence numbering.

4.1.2 H2A-H2B binding is conserved for human Spt16M

To verify that H2A-H2B binding is a conserved function of Spt16M, I cloned, expressed and purified also the human Spt16M domain (residues 643-929). As for the yeast protein, human Spt16M was sufficient to interact with H2A-H2B in pull-down assays (Figure 4.4) and therefore Sp16M is an evolutionary conserved H2A-H2B binding module.

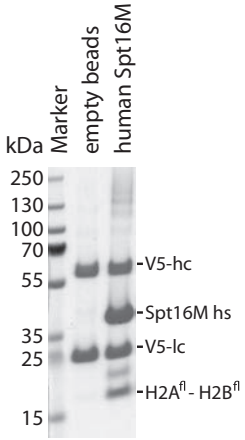

Fig. 4.4: **Human Spt16M interacts with H2A-H2B.**
Recombinant human Spt16M interacts with recombinant histones H2A-H2B in V5-immunoprecipitation assays. V5-hc / lc = V5 antibody heavy / light chain.

4.2 Crystal structure of the Spt16M – H2A-H2B complex

4.2.1 Construct design and purification, crystal optimization and structure determination

Rationale for construct design: how to find a balance between loss of floppy tails and loss of complex stability.

All my attempts to obtain crystals of isolated Spt16M in complex with H2A-H2B were unsuccessful. The complex with full-length histones could be stoichiometrically purified, but the unstructured tails are probably too 'floppy' to allow formation of a crystal lattice. The complex with tailless histones fell apart in chromatography (see below, section 4.3), thus I had to rely on mixing and did not obtain crystals either (maybe because I could not achieve perfect stoichiometry, or because the complex was too unstable).

Therefore, I decided to fuse the C-terminal extension of *C. thermophilum* Spt16M to globular *X. laevis* H2B via a short linker sequence (Figure 4.5), as has been done for other chaperone-histone complexes, e.g. Asf1 [**?**], Chz1 [**?**] or Scm3 [**?**]. From pull-down and ITC experiments I had performed beforehand (see below, section 4.3) I could assume that the C-terminus of Spt16M and the N-terminus of H2B should be in close proximity. Constructs of two linker lengths were tested - six and twelve residues - which both gave initial crystal hits, but the quality of the latter was much better and was used for further crystal optimisation.

This construct was co-expressed with tail-less *X. laevis* H2A; H2A was also lacking the C-terminal hydrophobic tail (which did not contribute to the interaction in ITC mea-

surements (see section 4.3)), since I had observed that deletion of this rather hydrophobic stretch strongly increased the solubility of the histone when expressed by itself.

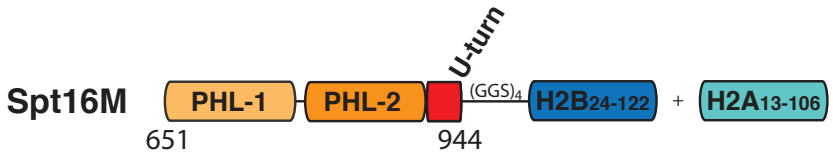

Fig. 4.5: **Design of the Spt16M - H2A-H2B expression construct.**
Schematic representation of the construct design. *C. thermophilum* Spt16M (*orange* and *red*) was linked to globular *X. laevis* H2B (*blue*) and coexpressed with globular *X. laevis* H2A (*light green*) lacking the hydrophobic C-terminal tail.

Protein expression and initial crystal setup

The described construct (Figure 4.5) gave high yields of protein (about 20 mg per liter *E. coli* culture) and the complex could be purified to stoichiometry via His-affinity, size exclusion and ion exchange chromatography (Figure 4.6).

The protein concentration was strongly dependent on temperature and salt. After several buffer optimization steps, conditions of high salt (500 mM NaCl) and an elevated pH (10 mM Hepes pH 8.5) allowed concentration to ∼15 mg/ml at 4°C. This protein preparation was used for crystallization set-up.

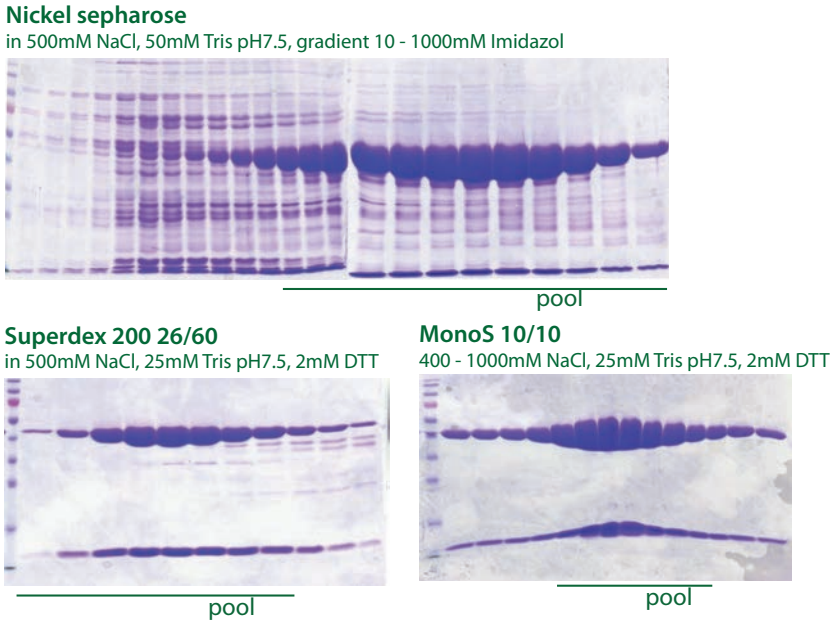

Fig. 4.6: **Crystal-grade purification of the Spt16M-H2B - H2A complex.**
Filtered *E. coli* cell lysate was run over a Nickel Sepharose column for His-affinity purification. After TEV cleavage of the His-tag, the protein was further purified by size exclusion (Superdex 200) and ion exchange (MonoS) chromatography. Eluted fractions were analyzed by SDS-PAGE / Coomassie staining and the cleanest fractions pooled.

Protein complex at 15 mg/ml in 500 mM NaCl, 10 mM Hepes pH 8.5, 1 mM TCEP was screened by robot (at the MPI for Biochemistry) over six standard screens (Wizard I / II, Qiagen PACT, Qiagen JSCG +, Hampton Research (HR) Index, Qiagen Complex, Crystal Platform Magic I), both at room-temperature (20°C) and 4°C. Three initial 'crystal hit' conditions were found (Figure 4.7):

- 0.2 M $MgCl_2$, 0.1 M Tris pH 8.5, 10 % (w/v) PEG8000, 4 °C (Wizard I / II)
- 0.2 M $CaCl_2$, 0.1 M Tris pH 8.0, 20 % (w/v) PEG6000, 20 °C (PACT)
- 1 M Na_3Citrate, 0.1 M CHES pH 9.5, 20° C (Wizard I / II)

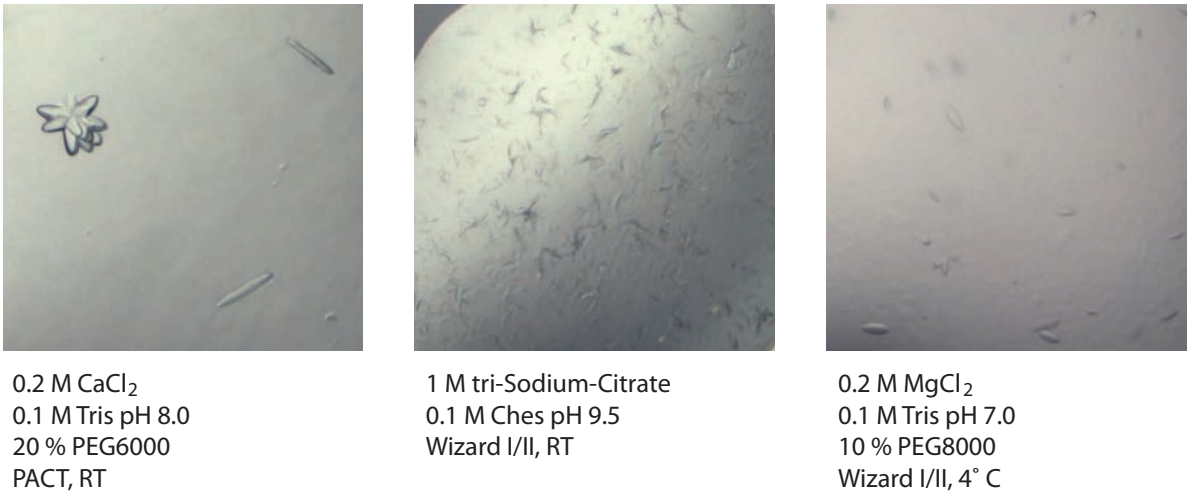

Fig. 4.7: **Initial crystal 'hits'.**
Pictures were taken by the screening robot; screen and buffer conditions are indicated.

Optimization of initial crystal hits

The Mg^{2+} crystals looked most promising and could be reproduced manually by hanging drop setup. Initial crystals were boat-shaped and had terminal growth defects. A sample thereof was washed and analyzed by SDS-PAGE / silver staining. This verified that they contained all components of the complex, e.g. the linked Spt16-H2B protein and H2A (Figure 4.8a).

The initial crystals were optimized by systematic screening of buffer conditions (to an optimal 7.25 % [vol/vol] PEG8000, 0.2 M $MgCl_2$, 0.1 M Tris pH 7.8), variation of the nucleation temperature (10°C instead of 4°C) and micro-seeding (Figure 4.8b). For cryo-freezing, crystals were successively soaked in increasing glycerol concentrations, up to 30 % (v/v) in crystallization buffer, since they were very fragile and burst when immediately subjected to high concentrations of cryo-protectants.

Structure determination

I collected crystal diffraction data at the ESRF (Grenoble, France) and SLS (Villigen, Switzerland) synchotron beamline. The crystal lattice contained one copy of the complex per asymmetric unit cell (space group $P4_32_12$, dimensions a, b, c ($\AA$): 108.4, 108.4, 117.8). The structure was solved by molecular replacement with the Spt16M phases from Tobias Stuwe. The structure was refined at 2.35 $\AA$ resolution to an R-factor of 0.205. XDS, the CCP4 suite, Phenix and COOT were used for data processing.

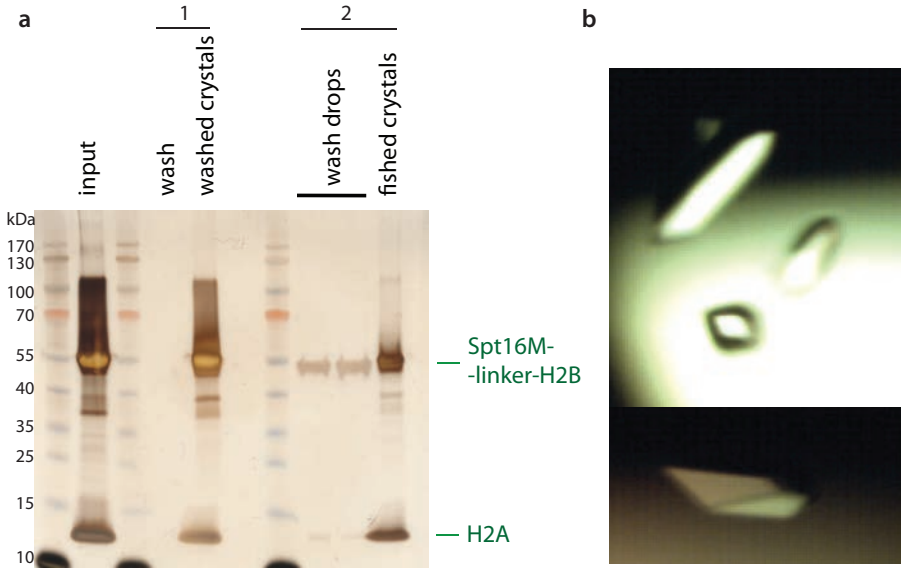

Fig. 4.8: **Optimized crystals.**
(a) Crystals were washed 1) by sucking up the surrounding liquid and washing the crystals with well buffer or 2) by fishing crystals into a drop of well (wash) buffer. Crystals were dissolved in ddH_2O and their content analyzed by SDS-PAGE / silver stain. (b) Picture of an optimized crystal.

4.2.2 Crystal structure of the Spt16M - H2A-H2B complex: a 'U-turn' motif embraces the α1 helix of H2B

Spt16M domain consists of a tandem PHL domain with a novel C-terminal motif, the 'U-turn'

Tobias Stuwe solved the crystal structure of isolated Spt16M. I used his structure to create a picture to illustrate details of the isolated Spt16M domain (Figure 4.9). Spt16M consists of three folds: two pleckstrin homology-like (PHL) domains (residues 653-911) and a novel, α-helical, U-shaped fold (residues 912-943), which I termed the 'U-turn motif' (Figure 4.9a). The structure is almost identical to the recently published crystal structure of *S. cerevisiae* Spt16M by **?**. The PHL domains, PHL-1 (residues 653-816) and PHL-2 (residues 817-911), consist of two perpendicular anti-parallel β-sheets capped by an α-helix.

Spt16M displays a distinct surface charge distribution: PHL-1 has basic surface patches and a long unstructured insertion rich in basic amino acids (between the ultimate blade and the capping helix) that might bind DNA (discussed in section 4.7). PHL-2 displays a conserved acidic patch, as seen for many other histone chaperones, e.g. Nap1 [**??**] which presumably neutralizes the positive charge of histones proteins, and histone tails in particular (Figure 4.9b,c).

The U-turn motif consists of three short α-helices and is closely associated, or rather 'built atop of', PHL-2. The groove formed by the three helices is lined with highly conserved, hydrophobic residues. The sequence of the U-turn is the most conserved part of the Spt16M domain (Figures 4.3) and 4.9b, e). Some of these highly or completely conserved residues contribute to the structural integrity of the hydrophobic core of the Spt16M domain (e.g. Phe931, Leu915 / Trp917 or Gly935 / Trp937), others such as Asn916, Val920, Ile921, Asp934, Phe939 and Leu940 mediate the interaction with the H2A-H2B dimer,

as seen in the crystal structure of the chaperone-histone complex (Figure 4.10), and are essential for yeast viability (see section 4.8).

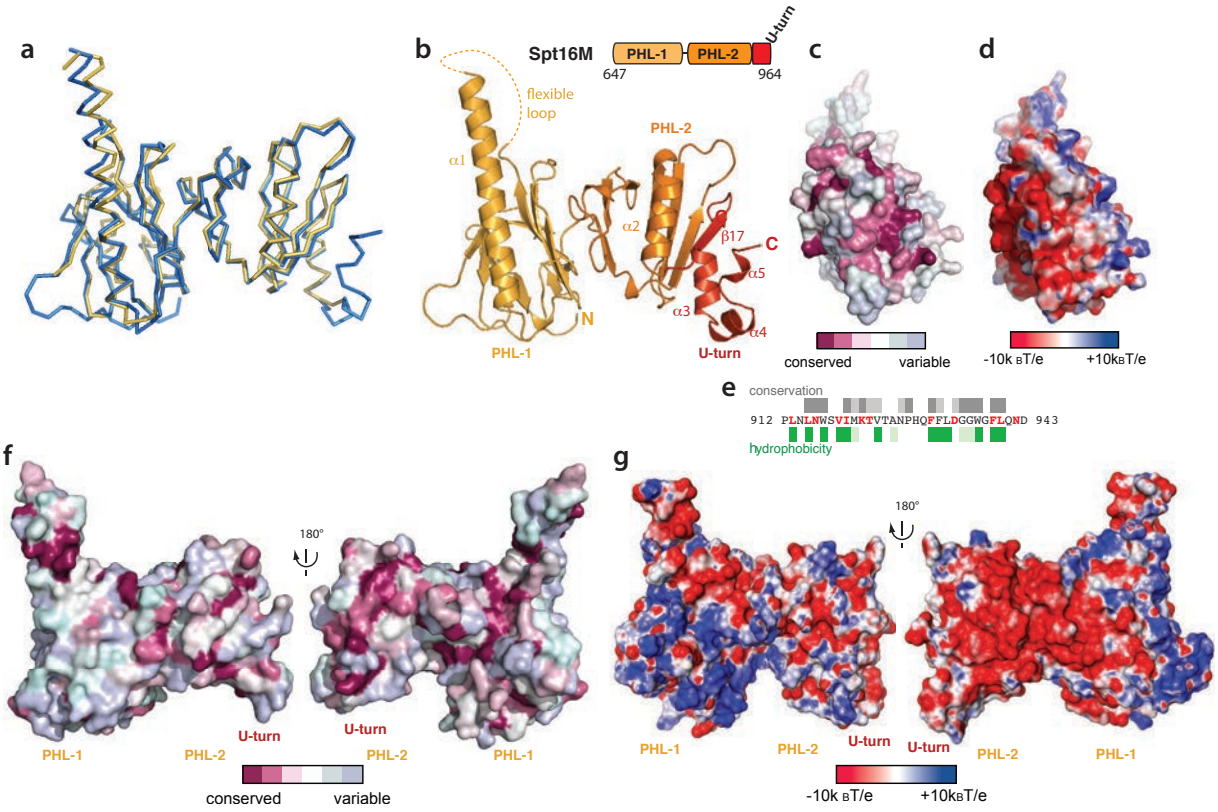

Fig. 4.9: **Structure of the Spt16M domain.**
(a) Superposition of the crystal structures of free Spt16M from Tobias Stuwe (blue) and **?**. (b) 2.0 Å resolution crystal structure of *C. thermophilum* Spt16M in ribbon representation. PHL-1 (*light orange*), PHL-2 (*dark orange*), U-turn motif (*red*). (c) Conservation view of the U-turn motif; completely or highly conserved residues are coloured *pink*. The color code for the conservation is based on a ClustalW2 alignment of 18 Spt16 sequences ranging from yeast to humans. (d) Electrostatic surface potential of the U-turn motif. Contour levels from -10kBT/e (*red*) to 10kBT/e (*blue*), neutral / hydrophobic regions appear white. The electrostatic potential was calculated using APBS. (e) Sequence of the U-turn motif; conserved residues are marked in *grey* and hydrophobic residues in *green*, bold residues are completely conserved and hydrophobic. (f) Surface sequence conservation of Spt16M in two orientations. (g) Electrostatic surface potential of Spt16M in two orientations.

The U-turn of Spt16M forms a tight interaction with a hydrophobic patch on the α1-helix of H2B

My new structure of the chaperone-H2A-H2B complex reveals extensive interactions between the Spt16M U-turn motif and a hydrophobic patch on H2Bα1 (Figure 4.10). The 12 residue linker sequence, as well as several residues at the C-terminus of Spt16M (1 residue) and N-terminus of H2B (6 residues) are unstructured and not visible, indicating that the linker is flexible and not constrained.

H2B's N-terminal α1-helix, L1 loop and α2-helix, establish a surface complementary to the U-turn motif (Figure 4.11a,b). The hydrophobic H2B residues Ile36 and Tyr39 stack into the Spt16M groove formed by the conserved Leu915, Val919, Ile920, Phe931, Phe939 and Leu940 (Figure 4.11d). H2B Ile51 and Met56 are in close contact to Phe939 in helix α4 of the U-turn extension. Electrostatic contacts stabilize the interaction: Spt16 Asp934 forms a salt bridge to H2B Lys43 and a hydrogen bond to H2B Tyr39 (Figure 4.11c). Further hydrogen bonds are formed between H2B Lys40 and Spt16 Thr923 (OH group) and Val919 (main chain carbonyl), as well as H2B Ser53 and Spt16 Asn942 (amide group). H2A complements the interaction with Arg77 (side chain) H-bonding Spt16 Leu933; an additional set of hydrogen bonds mediated by a chloride ion (yellow dot) links Spt16 Asn916 to H2B S33 and I36 (Figure 4.11c).

In total, the hydrophobic and electrostatic interactions between the U-turn motif and the histones establish an interface of $\sim$660 $\AA^2$ with a free energy potential of -7.1 kcal/mol, revealing the molecular basis for FACT's H2A-H2B interaction.

The protein backbone path of both the U-turn and H2A-H2B does not change much upon binding

Comparison of the complexed and uncomplexed structures of Spt16M or the histone H2A-H2B dimer (atomic coordinates from PDB 1AOI, [**?**]) revealed little structural changes upon binding (Figure 4.12). The α-helix of PHL-1, which is unusually extended in the uncomplexed structure (possibly through involvement in crystal lattice formation) is reduced to standard PHL domain length. In the U-turn motif and on H2Bα1, some of the interacting residue side chains deviate from their initital position (Figure 4.12b,c). The terminal residues of the U-turn motif deviate slightly, but it is not clear whether this is due to linker attachment or histone binding, since mutation of these residues did not show any effect on histone binding in ITC (see below, Figure 4.18a on page 69). In summary, this suggests a 'rigid fit' binding mode where the partners do not change conformation upon binding.

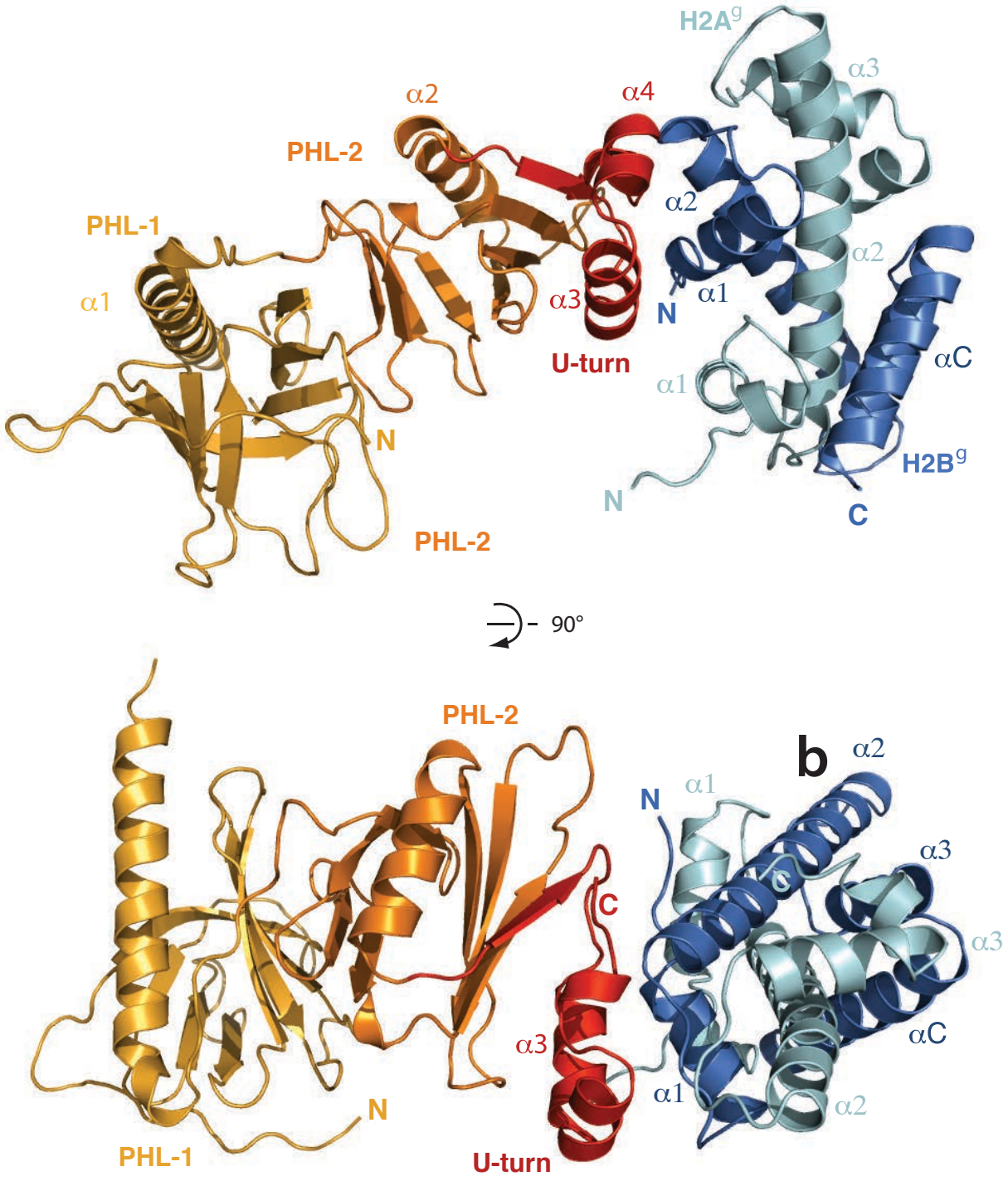

Fig. 4.10: **Structure of the Spt16M–H2A-H2B complex.**
Two orientations of the 2.35 Å resolution crystal structure of *C. thermophilum* Spt16M (residues 651-944) – H2B (24-122) and H2A (13-106) in ribbon representation. Spt16M PHL-1 (*light orange*), Spt16M PHL-2 (*dark orange*), U-turn motif (*red*); H2B (*blue*), H2A (*light green*), N-termini (N), C-termini (C).

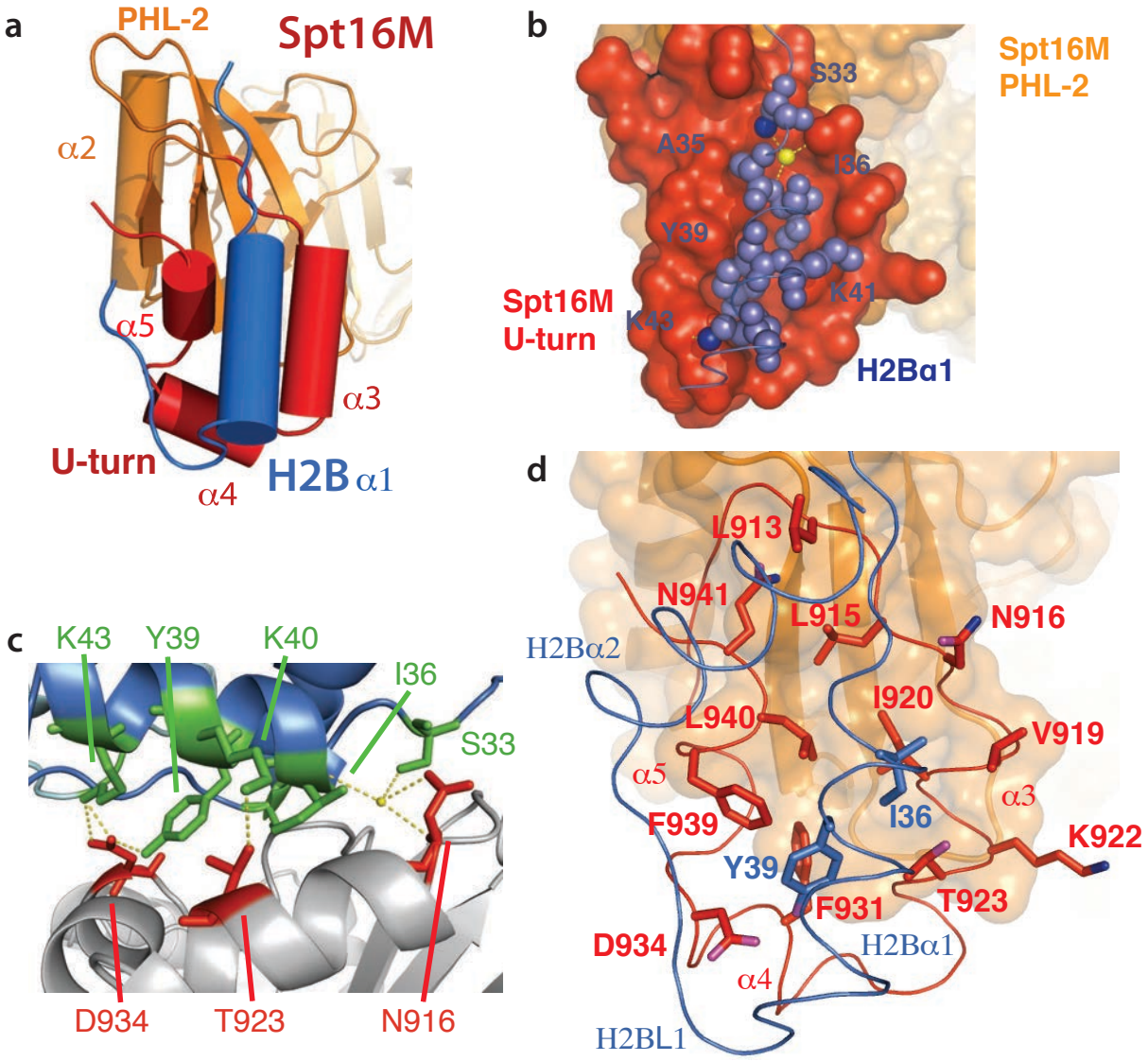

Fig. 4.11: **Close-up view of the Spt16M – H2B / H2A interface.**
(a) H2B's α1 helix stacks into the groove formed by the three helices of the Spt16M U-turn. (b) Side chains of the H2B α1-helix nestle into the hydrophobic groove formed by the Spt16M U-turn motif. Spt16M *orange*, U-turn motif in *red*, H2B α1 ribbon backbone (*blue*), important residues (labeled with the residue number) in spheres. A chloride ion (*yellow*) contributes bridging polar contacts. (c) Polar contacts formed between Spt16M and histone H2B residues. H2B (*blue*), crucial residues (*green*); Spt16M (*grey*), crucial residues (*red*). Cl^- ion (*yellow*). (d) Overview of residues involved in the chaperone-histone interaction. Spt16M PHL-2 *orange* (cartoon and surface), Spt16M U-turn motif *red*. α1 and α2 of H2B are shown as Cα ribbon backbone (*blue*).

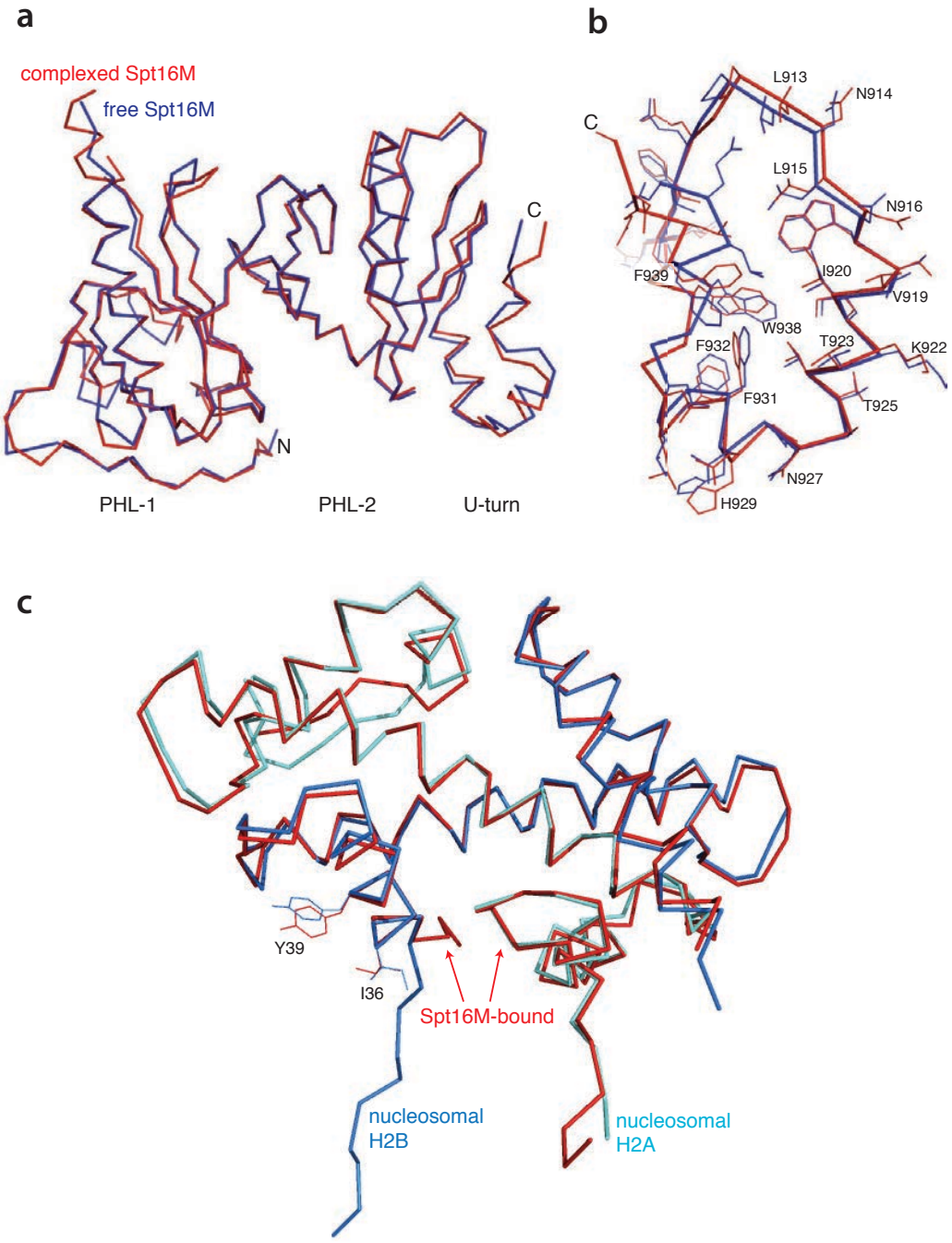

Fig. 4.12: **Superposition / RMSD of the Spt16M–H2A-H2B subunits relative to the free or nucleosomal state.**
(a, b) Superposition of the Spt16M as crystallized in the free form (*blue*) and in complex with H2A-H2B (*red*). (c) Superposition of the H2A-H2B dimer as part of the nucleosome (*turquois / blue*) or Spt16M-complex (*red*) crystal structures. Average r.m.s.d. of 1.095 Å on 193 Cα-atoms.

4.3 Biochemical mapping of the interaction of Spt16M with histones H2A-H2B

4.3.1 The U-turn, together with PHL-2, is sufficient for interaction with histones H2A-H2B

As described in detail below, Spt16M harbors a tandem PHL domain highly similar to the chaperones Rtt106 and Pob3M, and all three chaperones bind histones H3-H4 (section 4.6). Crucially, only Spt16M – but not Pob3M (Figure 4.2a) or Rtt106 [**?**] – recognizes H2A-H2B. The U-turn motif is highly conserved (Figure 4.9c, d) and specific to Spt16, and therefore already from an evolutionary point of view a good candidate for the H2A-H2B interaction.

To verify that the interaction between the U-turn and H2Bα1 observed in the crystal structure was not an artefact, I mapped the interaction biochemically. For initial pull-down experiments, I cloned and expressed truncated constructs of the Spt16M domain, encompassing either the PHL-1 or the PHL-2 domain together with the U-turn. Constructs of the U-turn itself, or a PHL-2 construct lacking the U-turn, could not be purified since the proteins were aggregate, presumably because both folds contribute to the shared hydrophobic protein core essential for correct folding of the domain. The recombinant V5-tagged PHL-1 and PHL-2 constructs were bound to V5-affnity agarose beads and incubated with excess of full-length or tail-less H2A-H2B dimers. After extensive washes, bound protein was analyzed by SDS-PAGE and Coomassie staining. PHL-2, together with the conserved U-turn motif, was sufficient and necessary to bind full-length histones H2A-H2B as well as the globular cores thereof (Figure 4.13). In perfect agreement with my crystal structure, the 'minimal' complex for pull-down assays consists therefore of PHL-2 with the U-turn motif and globular H2A-H2B.

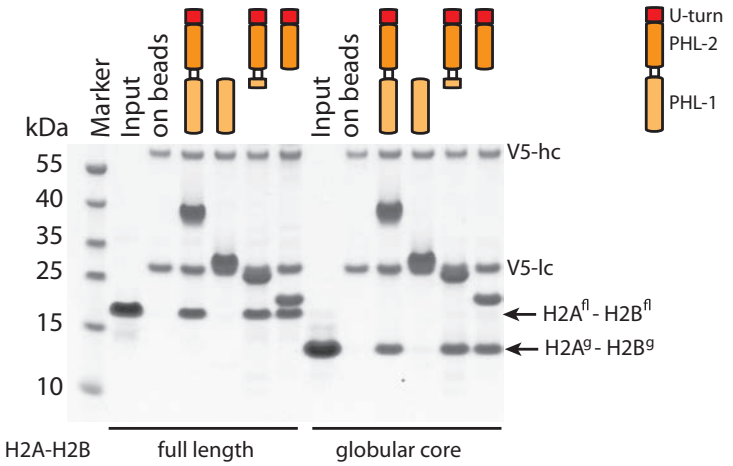

Fig. 4.13: **Spt16M PHL-2 interacts with the globular core of H2A-H2B.** V5-tagged proteins were bound to V5 affinity agarose, incubated with excess of histone H2A-H2B dimer (full-length or tailless) and washed with 200 mM NaCl, 25 mM Tris pH 7.5, 0.05 % NP40. Precipitated protein was separated by 4-12 % SDS-PAGE.

4.3.2 ITC reveals an endothermic, low micromolar affinity interaction between Spt16M and H2Bα1

To characterize the Spt16M-H2A-H2B interaction more quantitatively, I measured the affinity of interaction by isothermal titration calorimetry (ITC) with various histone constructs (Figure 4.14). Both full-length and globular H2A-H2B bound to Spt16M with about equal affinity (0.4 μM). This confirmed that the globular H2A-H2B core harbors the main site of interaction, as already observed in pull-down assays (Figure 4.13). Interestingly, the heat of reaction was endothermic, hinting towards a hydrophobic mode of interaction. On Spt16M, the groove formed by the U-turn motif is the only conserved hydrophobic surface area (Figure 4.9) and therefore the only strong candidate for such an interaction.

The value I determined is much higher than the K_D of ~30 nM (full-length H2A-H2B) or ~200 nM (globular H2A-H2B) measured by **?**, but their system differs drastically from ours: they use a low-salt buffer, full-length human protein and a fluorescence-based, thermodynamic equilibrium method.

In the crystal structure, the U-turn interacts with a hydrophobic patch on H2Bα1 (Ile36 and Tyr39) which contacts DNA in the nucleosome (Figure 4.11d). On the nucleosome, I identified two more hydrophobic areas that could form a hydrophobic interaction with the U-turn: the C-terminal tail of H2A and a region of H2B contacting H4 (around H2Bα3; Tyr80) [**?**] (Figure 4.14a). I tested all three sites by ITC: neither deletion of the H2A C-tail nor mutation of the H2B-H4 contact site (H2B Y80E) strongly affected the affinity of interaction. In contrast, mutation of the H2B-DNA contact site (I36E) increased the K_D by a factor of ~30 to 13 μM (Figure 4.14c) and a H2B [26-48] peptide (spanning this region) binds with relatively strong affinity (~2.6 μM). In contrast, a peptide spanning the hydrophobic C-terminal tail of H2A [105-120] did not. Thus, Spt16M binds the hydrophobic site of H2B around H2Bα1 / L1 that contacts DNA when part of a nucleosome.

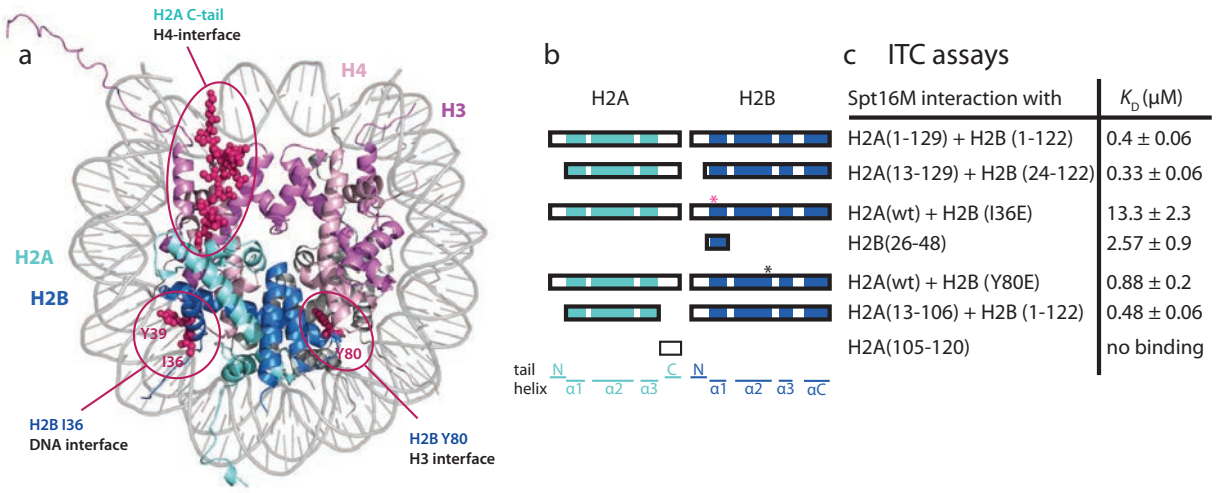

Fig. 4.14: **Spt16M binds a hydrophobic patch on histone H2B.**
(a) Schematic view of the three candidate hydrophobic patches (*pink* spheres) on the nucleosome; H2B (*blue*), H2A (*light green*). (b) Overview of H2A and H2B fragments tested for binding to Spt16M. Below, a schematic representation of the H2A and H2B histone fold. (c) Equilibrium dissociation constants (K_D) were determined using equilibrium ITC measurements at 25°C in 200 mM NaCl, 25 mM Tris pH 7.5 (4°C).

4.3.3 The interaction between Spt16M and histones is not stabilized in high salt, as expected for a hydrophobic interaction

To validate the observed hydrophobic interface between Spt16M and H2A-H2B on the chaperone side, I created a series of point mutants. I targeted conserved residues of the U-turn motif, which contribute to the crystal interaction. As a first approach, residues were mutated to either alanine (a small, rather 'neutral' residue; this aimed at eliminating any specific 'chemical' contribution of the mutated residues) or arginine (a rather large, basic residue, to repulse the equally basic histone surface).

Initially, I tried pull-down experiments in various buffer conditions, but could never reproducibly detect decreased interaction for U-turn motif mutants. Salt concentrations (NaCl or KCl) ranged from 100 to 1000 mM, but since the interaction was not solely hydrophobic, it was not stabilized in high salt (which is the case for e.g. Asf1, HJURP, Scm3, DAXX [**?**]) (Figure 4.15). Since Spt16M displays a distinct acidic patch that might nonspecifically interact with the basic histone proteins, I also tried to vary the pH (pH 5 – 10.5) and buffer substances (Tris / MES / CHES / Sodium-Phosphate) but could still not detect any differences between U-turn motif mutants and wild-type protein (*data not shown*). In contrast, an 'acidic patch' mutant showed decreased affinity in most pull-down experiments so I assumed that the result was dominated by electrostatic, somewhat 'unspecific', non-equilibrium interactions (see below, section 4.5). Therefore, I switched to equilibrium methods to analyse the chaperone-histone interface.

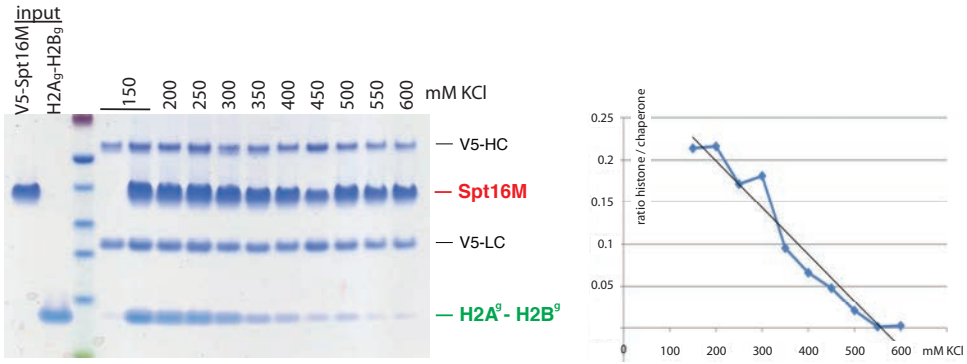

Fig. 4.15: **Salt-dependency of the Spt16M – H2A-H2B interaction.**
Pull-down experiments between V5-Spt16M and globular H2A-H2B were performed with washes of increasing KCl concentration. The interaction is salt-dependent and not stabilized in high salt, as expected for purely hydrophobic interactions and as observed for other histone chaperones (e.g. Asf1, DAXX) [**?**].

4.3.4 Double point mutations in the U-turn abrogate binding, as measured by tryptophan fluorescence quenching

Having observers three tryptophan are part of the U-turn or buried in between the U-turn motif and the PHL-2 domain, I tested and verified that H2A-H2B binding increased the fluorescence emission intensity of those tryptophan residues (Figure 4.16a). Binding of Spt16M to increasing amounts of H2A-H2B was assayed in high-salt to destabilize the electrostatic component of the interaction between the acidic Spt16M (pI = 5.25) and the basic H2A-H2B (pI = 10.69) proteins. 10 μM Spt16M was incubated with *X. laevis* full-length H2A-H2B dimers (0, 1, 2, 3, or 4-fold molar excess of histones over Spt16M) in 500

mM KCl, 10 mM Hepes pH7.5, 2 mM $MgCl_2$ buffer for 30 minutes at room temperature. Tryptophan emission of wild-type and mutants as indicated was quantified in triplicate at 350 nm after excitation at 280 nm wavelength. After subtraction of histone background emission, results were normalized to the 'no histone' value.

Spt16M showed increasing emission intensity saturating near equimolarity (Figure 4.16 b). In contrast, mutation of hydrophobic U-turn residues abolished fluorescence changes and thus binding of hydrophobic H2A-H2B surfaces. As a negative control, a protein with mutations in the conserved acidic patch behaved like wild-type (Figure 4.16). These assays corroborated the structural evidence that the Spt16M–H2A-H2B interaction locates to the U-turn motif. However, the changes are rather small and the assay not generally accepted in the community, so it did not seem to be particularly suited for the analysis of the interaction within the complex.

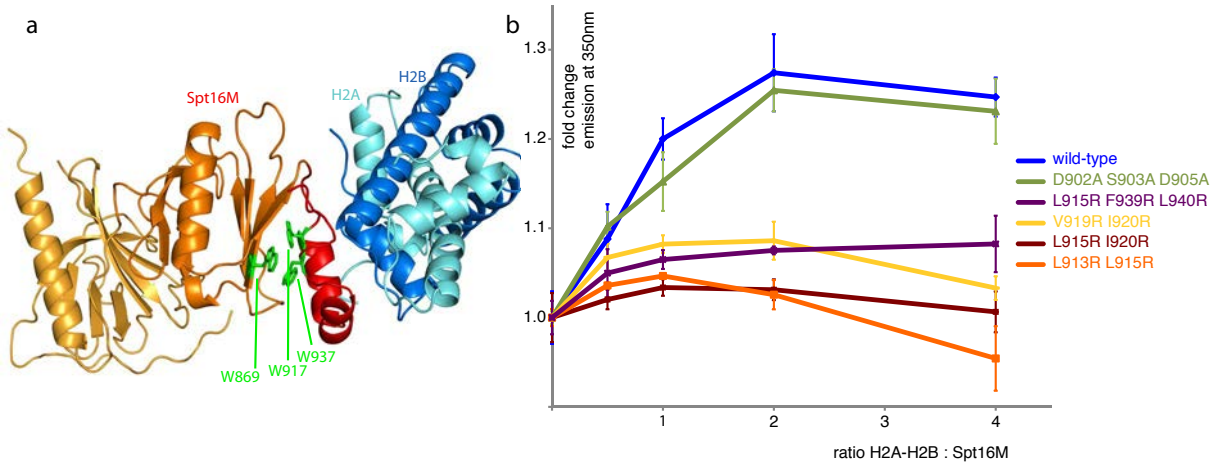

Fig. 4.16: **Surface point mutation analysis of the Spt16M–H2A-H2B interaction by tryptophan fluorescence emission.**
(a) Three tryptophan residues are buried between PHL-2 and the U-turn motif. (b) 350 nm fluorescence emission of these Trp residues (after excitation at 280 nm) changes upon histone binding. Wild-type protein and a mutant of the acidic patch bound full-length histones H2A-H2B, saturating around equimolarity; mutants of the U-turn motif did not show a change in emission and therefore did not bind.

4.3.5 A strong mutant of the U-turn is required to abrogate binding by ITC or SEC

None of the mutants tested by tryptophan fluorescence emission was sufficient to disrupt complex formation in ITC or SEC. Thus I screened other, more drastic point mutations of the interaction interface.

In ITC, mutation of multiple (seven) conserved hydrophobic residues to alanine dramatically changed the enthalpy (ΔH) and entropy (ΔS) values, but the affinity (K_D) was unchanged (Figure 4.17) and those chaperone proteins still formed a complex with H2A-H2B in SEC (*data not shown*). The methyl group of alanine (or the long aliphatic side chain of arginine) is fairly hydrophobic and might be sufficient to maintain the hydrophobic character of the wide interaction interface.

	N	K_D µM	Δ*H* cal/mol	Δ*S* cal/mol/deg
WT	0.82	0.37	4407	44.85
U-turn ->A	0.80	0.40	1272	33.80

Fig. 4.17: **Mutation of U-turn residues to alanine changes the biophysics of interaction, but not the overall affinity.**
ITC values (stoichiometry (N) enthalphy (ΔH), entropy (ΔS) and affinity (K_D)) for several Spt16M wild type and a U-turn mutant, N916A V919A I920A T923A D934A F939A L940A.

Therefore, I mutated those conserved residues to serine, the hydroxyl group of which should reduce the hydrophobic character of the U-turn's surface. I tried mutation of residues on either the left or the right half of the U-turn. While mutation of residues on the second and third α-helix of the U-turn (D934, F939, L940) had little effect on K_D and complex formation (Figure 4.18a), mutation of residues in the first α-helix (N916, V919, I920 and T923) drastically changed the ITC profile and disrupted complex formation in SEC (Figure 4.18b). Hence, the interaction between the chaperone and H2A-H2B critically depends on those four U-turn residues. Together with the ITC data for histone mutants, this fully verifies the observed crystal contact between the U-turn and H2B α1 as the major site of interaction between Spt16M and the H2A-H2B.

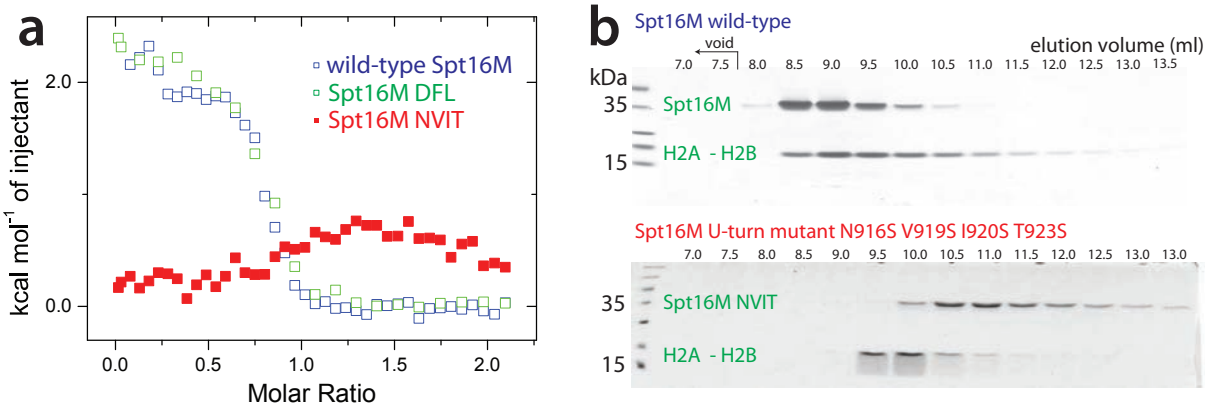

Fig. 4.18: **A strong U-turn mutant disrupts complex formation in ITC and SEC.**
(a) ITC profiles of wild-type Spt16M and point mutants thereof (DFL = D934S / F939S / L940S and NVIT = N916S / V919S / I920S / T923S) b) SEC fractions (SD 75 10/300, Coomassie-stained) of wild-type and U-turn NVIT mutated Spt16M with full-length histones H2A-H2B. The NVIT U-turn mutant disrupted binding in both ITC and SEC.

4.4 Other parts of Spt16 contribute to H2A-H2B binding, but only Spt16M is essential for chaperone function

4.4.1 Regions outside Spt16M contributes to H2A-H2B binding

Previous data have shown that the C-terminal region of human Spt16 is required for H2A-H2B binding, chaperone activity and viability [**??**]. However, in addition to the acidic C-terminal tail of Spt16 (Spt16C), the construct used in those studies (FACTΔC) lacked a vital portion of the H2A-H2B binding Spt16M module, including the 'U-turn' and half of PHL-2 (Figure 4.1). To dissect the contribution of the Spt16M domain, I designed and a expressed a construct of Spt16 lacking only the Spt16M domain (Spt16ΔM). To test for interaction by pull-down, I bound V5-tagged Spt16 full-length, Spt16ΔM and Spt16M to beads and incubated them with soluble H2A-H2B. The recombinant Spt16ΔM protein bound histones H2A-H2B, similar to Spt16M itself (Figure 4.19), and therefore some region of Spt16 other than Spt16M contributes to the interaction.

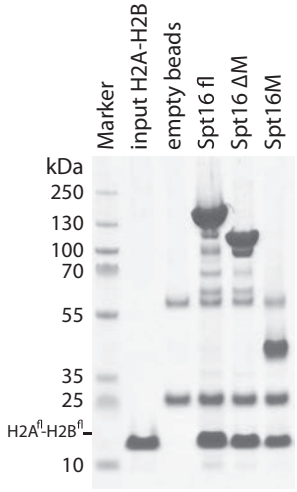

Fig. 4.19: **Spt16 lacking Spt16M binds H2A-H2B.**
V5-immunoprecipitations showed that a construct containing the unstructured acidic Spt16C tail but lacking the Spt16M module (Spt16ΔM) was capable of binding recombinant H2A-H2B.

To better characterize the interaction of Spt16 with H2A-H2B, I performed ITC with full-length Spt16 (Spt16 fl) and various truncated constructs (Figure 4.20). Both Spt16M and Spt16M plus acidic C-terminus (Spt16MC) display an endothermic binding site (KD ∼400 nM). However, Spt16MC adds a second, exothermic binding site (KD ∼30 nM; Fig. 3b), consistent with an independent, electrostatic histone interaction site mediated by Spt16C. These values compare favorably with the 30-90 nM H2A-H2B affinity reported for holo-FACT and full-length Spt16 using independent methods [**?**]. Further, Spt16N and Spt16D together (Spt16ND) bind H2A-H2B exothermically, albeit with low affinity (KD 10-100 μM). ITC profiles of full-length Spt16 and of Spt16 lacking Spt16M (Spt16ΔM) combine the characteristics of the isolated Spt16M, Spt16MC and Spt16ND domains. Thus, quantitative ITC reveals two high affinity sites: the hydrophobic interaction seen in our Spt16–H2A-H2B complex and an electrostatic Spt16C interaction.

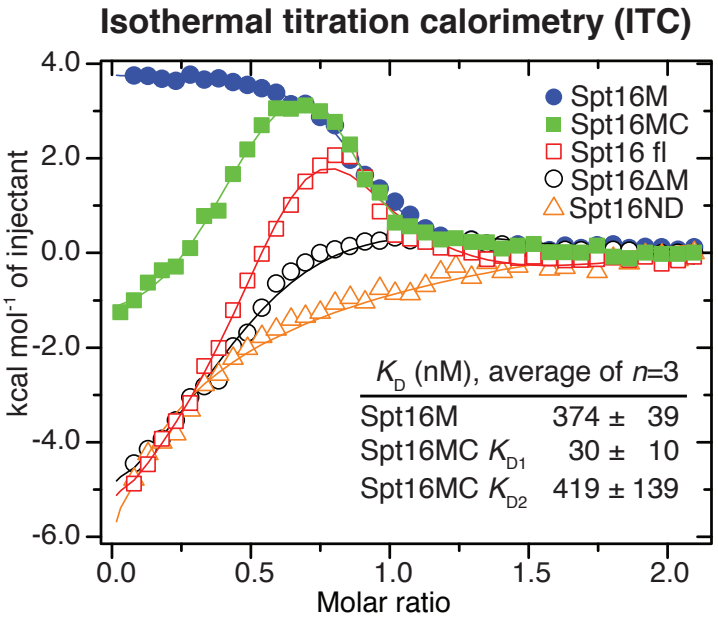

Fig. 4.20: **ITC of full-length Spt16 and truncated versions with H2A-H2B.** ITC of various (truncated) Spt16 constructs shows that domains other than Spt16M contribute exothermically to the overall interaction with H2A-H2B. K_D values for Spt16M and Spt16MC were calculated from three independent measurements fitted with a 1-site (M) or 2-site (MC) model. The curves for Spt16 fl, ΔM and ND are complex and were fitted using a model for 4 / 3 / 2 sequential (cooperative) binding sites, but not evaluated quantitatively.

4.4.2 Spt16ΔM cannot chaperone histones H2A-H2B from aggregation with DNA

Nevertheless, I found that the Spt16M domain was absolutely necessary and sufficient for 'chaperoning' of histones H2A-H2B and DNA. The following 'chaperoning' experiment was performed by my postdoctoral colleague Dr. Andrew Bowman (Figure 4.21).

Mixing of H2A-H2B with an excess or molar equivalent of DNA resulted in a discrete band in Native PAGE, corresponding to a defined H2A-H2B-DNA complex (Figure 4.21a). When the amount of H2A-H2B was increased, the DNA precipitated (the H2A-H2B-DNA band disappeared, the resulting precipitate did not enter the gel or wells).

Preincubation of histones with full-length Spt16 prior to addition of DNA mostly prevented such precipitation and rescued the soluble H2A-H2B-DNA complex. In contrast, the same molar amount of Spt16ΔM had little ability (13 % (above the background control) of full-length Spt16, Figure 4.21b) to prevent precipitation of DNA in the presence of excess histone dimers. Spt16M in contrast rescued 50 % of the chaperone activity.

This finding suggested that although Spt16ΔM may be able to bind H2A-H2B, interaction with the core histone fold mediated by Spt16M is more important for the resolution of histone-DNA aggregates. Thus, Spt16M harbors the major 'chaperone' activity of the FACT complex. Pure electrostatic interactions are not sufficient to chaperone the histones from aggregation with DNA.

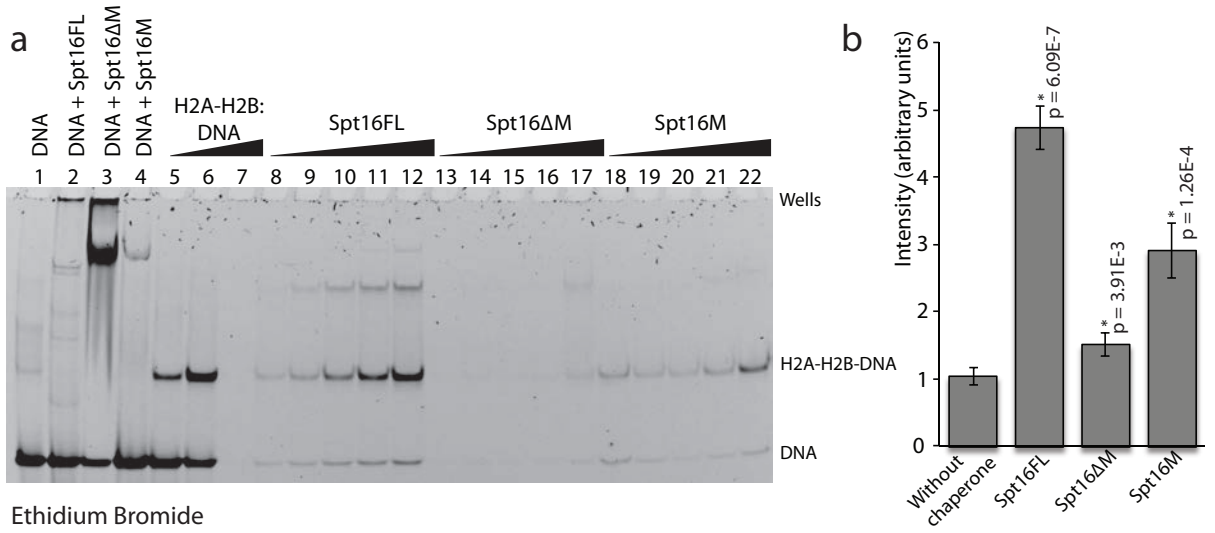

Fig. 4.21: **Only Spt16M reproduces the chaperone function of FACT and prevents H2A-H2B from aggregating with DNA.**
(a) Chaperoning assay: increasing the ratio of H2A-H2B to DNA causes a histone-driven precipitation of a 54 base pair DNA fragment (lanes 5-7). Pre-incubation of H2A-H2B with full-length Spt16 (Spt16FL) prior to adding DNA prevents precipitation and rescues the soluble H2A-H2B–DNA complex in a Spt16 concentration-dependent manner (lanes 8-12). Similar 'chaperoning' activity was seen for Spt16M alone (lanes 18-22), but was essentially absent in Spt16ΔM (lanes 13-17). In addition, two higher migrating species that did not correspond to any band in the minus histone control, were observed (compare lanes 8-12 and 17, 22 with lane 2), suggesting that Spt16 may also form a stable multimeric assembly between H2A-H2B and DNA. Complexes were separated by Native PAGE and DNA visualized with Ethidium Bromide. (b) Quantification of the H2A-H2B-DNA complex under the same conditions shown in lanes 7, 12, 17 and 22 (final titration point) carried out in quadruplicate was performed using a Fusion-FX7 Advance (PeqLab) imaging system; statistics were calculated on with a two-tailed t-test assuming equal variance. Asterisks indicate p-values of less than 0.05 when compared to the without chaperone control; actual p-values are given. The experiment was performed by Andrew Bowman.

4.5 A conserved 'acidic patch' on Spt16M's PHL-2 interacts with the N-terminal tail of H2B

During the biochemical analysis of the interaction between Spt16M and histones H2A-H2B, I used size-exclusion chromatography (SEC) to monitor complex formation. Since the main crystal interface is formed between Spt16M's U-turn and the globular, tailless core of H2A-H2B, and since globular H2A-H2B have the same affinity like full-length histones in ITC assays, I tested whether I can form and purify a complex of Spt16M and tailless H2A-H2B by SEC. This reduced system would minimize non-specific electrostatic interactions between the basic histones (pI = 10.7) and the the acidic chaperone (pI = 5.3) that may affect the interaction values measured. Surprisingly, these studies resulted in the identification of a second, electrostatic interface between Spt16M and the histone H2A-H2B dimer.

4.5.1 Deletion of the H2B-tail disrupts the complex in SEC

To analyze elution profiles of the complex and its components by SEC, samples were mixed with 1.1 fold excess of histone over chaperone, incubated on ice for 30 min and run over a Superdex 75 10/300 size exclusion column in 300 mM NaCl, 25 mM Tris pH 7.5, 2 mM DTT. Similar results were obtained in 200 mM NaCl or with a Superdex 200 resin (*data not shown*).

Spt16M formed a stable complex with full-length H2A-H2B (Figure 4.22a). In contrast, globular histones did not co-elute as a complex, but the peak of both Spt16M and the histone dimer was shifted to slightly higher molecular weight. I speculate that the complex was initially formed but fell apart when diluted during the chromatography run. To determine whether one of the histone tails makes specific contribution, I mixed the chaperone with histone dimers lacking either the H2A or the H2B tail. While deletion of the H2B tail was sufficient to dissociate the complex, deletion of the H2A tail was not. Since similar 'amounts' of charge were deleted (7 of 28 positive residues for H2B, and 5 of 27 positive residues for H2A), it is rather a H2B-tail specific than a nonspecific electrostatic interaction (Figure 4.22b). Therefore, the H2B tail is essential for complex formation in SEC, which is in contrast to the results from pull-down and ITC experiments. I do not think that the lower salt concentration (200 mM NaCl) of the described pulls-down and ITC experiments is the major reason for this discrepancy since SEC runs in 200 mM did not result in complex formation between Spt16M and globular H2A-H2B (*data not shown*). Rather, I think that pull-down and equilibrium ITC measurements can capture more transient or kinetically unstable complexes, which dissociate during chromatography runs.

4.5.2 Multiple positively charged residues of H2A interact with an 'acidic patch' on Spt16M in a second crystal contact

The structure of the complex reveals an electrostatic crystal contact (450 Å^2, free energy potential of +1.2 kcal/mol) mediated by Glu899, Asp902, Asp905 on PHL-2's acidic patch and Arg residues on the H2A N-terminal tail and α1-helix (Figure 4.23). I speculated that this fortuitous crystallographic interaction (mutation of which did not affect the interaction with histones as measured by tryptophan fluorescence (Figure 4.16))

may serve as a 'placeholder' for the N-terminal tail of H2B. The H2B tail was missing from my crystal constructs but contributed to complex stability in SEC (Figure 4.22). The H2B tail could easily extend from the H2B α1-helix sitting in Spt16M's hydrophobic groove to the acidic patch (Figure 4.23), replacing the H2A arginine residues with some of its numerous positively charged residues.

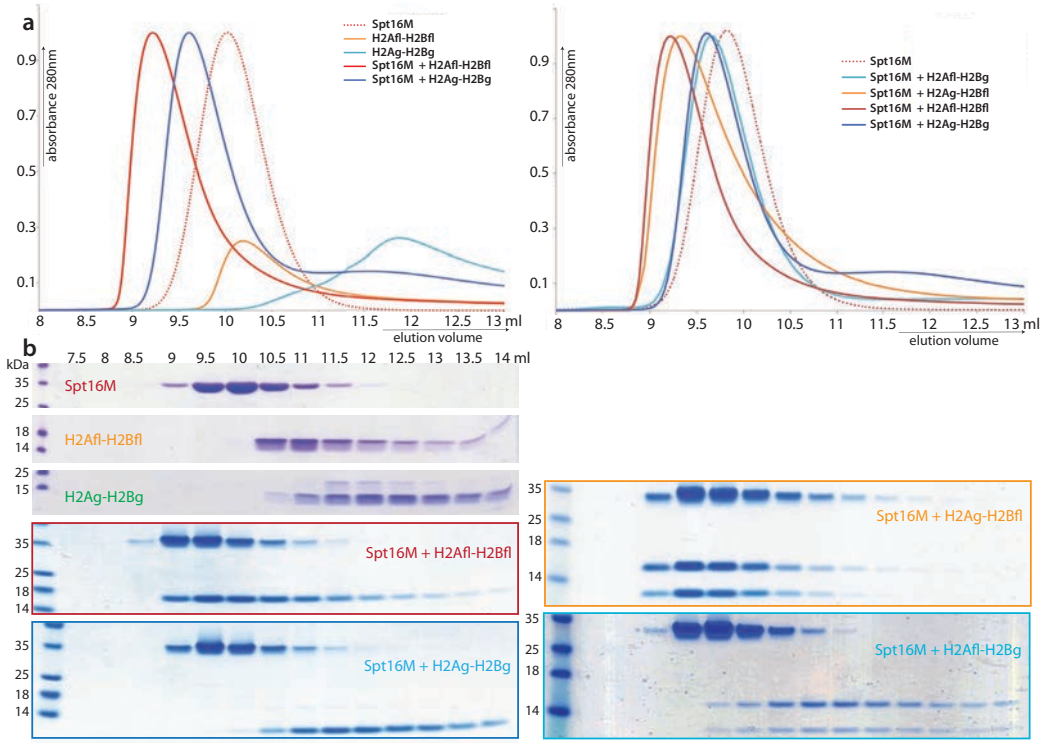

Fig. 4.22: **The H2B N-terminal tail stabilizes the complex in SEC.**
(a) SEC elution profiles (SD75 10/300 in 300 mM NaCl, 25 mM Tris pH 7.5, 2 mM DTT (4°C)) and (b) Coomassie-stained SDS-PAGE fractions thereof. While full-length H2A-H2B formed a complex with Spt16M, the globular cores of the histones, or a histone dimer lacking solely the H2B tail, were not sufficient for complex formation.

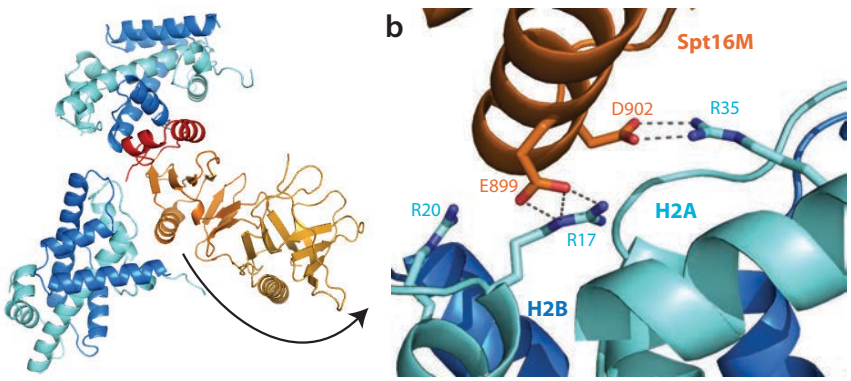

Fig. 4.23: **An acidic patch of Spt16M forms a crystal contact with basic H2A residues.**
(a) Spt16M forms crystal contacts with two H2A-H2B dimers (linker not visible). Stp16M *orange, red*, H2A *turquois*, H2B *blue*. (b) Close-up view of the crystal contact between an acidic patch on Spt16M PHL-2 and basic residues in H2A. Salt bridges are shown as dashed lines.

4.5.3 A peptide spanning H2B residues [11-30] interacts with the acidic patch

I thus tested whether I could detect binding of synthetic H2B tail peptides to Spt16M. Initial trials by ITC were unsuccessful, possibly because the Spt16M protein is very prone to aggregation in low salt conditions (e.g. 75 mM NaCl) and thus the concentration of the protein had to remain very low. Therefore, I decided to test for interaction by peptide pull-down assays, where Spt16M can be immobilized and 'individualized' as single molecules on beads.

V5-tagged recombinant Spt16M or mutants thereof were bound to V5-affinity agarose beads and incubated with excess of synthetic H2B tail peptides (*X. laevis* sequence). After washes (75 mM NaCl, 25 mM Tris pH 7.5, 0.05 % NP40), bound peptide was eluted with high salt, separated on a gradient gel and detected by silver staining. Spt16M interacted with a peptide spanning H2B residues [11-30], but not [1-20] (Figure 4.24a). Mutation of the conserved acidic patch (*green* label) abolished binding to H2B [11-30], but a mutant of the U-turn (which disrupted the interaction with H2A-H2B full-length dimers) bound to the peptide similar to wild-type Spt16M. From these results I concluded that the H2B tail interacts with the conserved acidic patch on Spt16M.

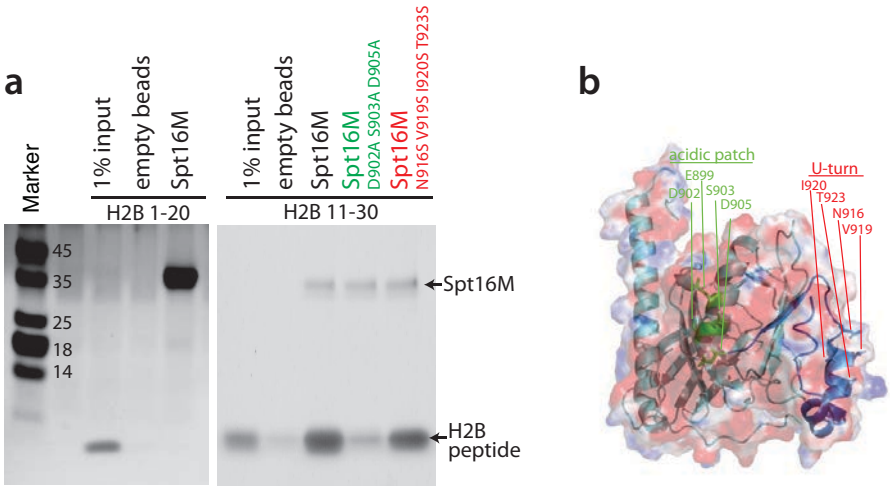

Fig. 4.24: **The acidic patch of Spt16M interacts with a H2B [11-20] peptide.** (a) V5-immunoprecipitation of Spt16M with synthetic H2B tail peptides. A peptide spanning residues [11-30], but not [1-20], interacted with wild-type Spt16M. Mutation of a conserved 'acidic patch' disrupted interaction with the H2B [11-30] peptide, while mutation of the U-turn had no effect. (b) Location of the acidic patch (*green* label) and the U-turn (*red* label) mutants, mapped onto the electrostatic Spt16M surface.

4.5.4 Truncation of the H2B tail accelerates disassembly of the complex in 'kinetic' pull-down experiments

Since deletion of the N-terminal tail of H2B did not affect equilibrium K_D values in ITC but triggered complex disassembly during SEC, I speculated that this interaction may contribute to the kinetic stability of the complex. To test whether the k_{off} rate was strongly increased for complexes lacking the H2B tail, I performed 'kinetic pull-down' experiments.

I assembled complexes of chaperone and respective histone dimers on V5-affinity agarose for 1 h at 4°C , spun down the beads and washed them with a large volume of buffer (200 mM NaCl, 25 mM Tris pH7.5, 2 mM DTT, 2.5 % glycerol, rotating at room-temperature) in a time-course experiment. At the indicated time points, beads were spun down and bound proteins analyzed by SDS-PAGE. The intensity of the Coomassie bands was quantified with a Fuji Phosphoimager. After background substraction, the amount of bound histone was normalized to the amount of chaperone and the 0 min value. $H2A^{fl}$-$H2B^{fl}$ was analyzed as one band, $H2A^{fl}$ and $H2B^{g}$ were analyzed separately. As expected, histone dimers lacking the H2B tail dissociated much more quickly than full-length histone dimers (Figure 4.25), confirming my hypothesis that the H2B N-terminal tail is required for the kinetic stability of the Spt16M – H2A-H2B complex.

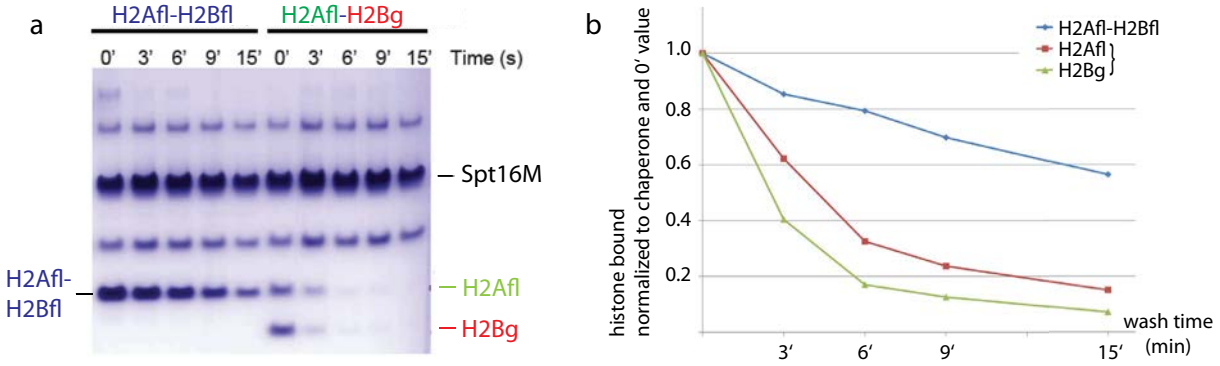

Fig. 4.25: **H2A-H2B dimers lacking the H2B tail dissociate more quickly from Spt16M than full-length H2A-H2B.**
(a) Chaperone-histone complexes were assembled on affinity agarose and washed for the indicated time. Bound proteins were analyzed by SDS-PAGE. (b) For quantificiation, the intensity of bound histones was normalized to background, amount of chaperone and the 0 min value.

4.5.5 Mutation of the acidic patch also destabilizes the chaperone-histone complex 'kinetically'

Since the H2B tail binds a conserved acidic patch (Figure 4.24), I tested whether mutation of the 'acidic patch' also destabilizes the complex both in pull-down experiments and size-exclusion chromatography (Figure 4.26).

Highly purified Spt16M D902A/S903A/D905A ('DSD') was incubated with full-length or globular H2A-H2B (1.1 fold excess of histone) on ice for 30 min and run over a Superdex 75 10/300 chromatography column in 300 mM NaCl, 25 mM Tris pH 7.5, 2 mM DTT (4°C). The DSD mutant by itself eluted identical to the wild-type Spt16M protein (Figure 4.26a). DSD formed a complex with full-length H2A-H2B, but the peak was shifted to later elution times or lower molecular weight than for the wild-type complex, indicative of an altered complex shape. When mixed with tailless H2A-H2B, the peak of the isolated wild-type protein (with no histones associated) elutes shifted to higher molecular weight, maybe because some initial unstable complex is formed which falls apart during the run (see above); this effect is much less pronounced for the DSD mutant (Figure 4.26a). Together, these results indicate that mutation of the acidic patch destabilizes the complex in SEC.

In pull-down experiments, I had observed that the DSD mutant interacted weaker than wild-type protein with full-length histones H2A-H2B (Figure 4.26b). Therefore, I tested whether this is also a 'kinetic effect', as observed for assays with histone dimers lacking the H2B N-terminal tail. As expected, H2A-H2B was washed away more quickly from the DSD mutant than from wild-type protein in kinetic pull-down experiments (Figure 4.26c). Thus, the interaction between the H2B tail and the acidic patch of Spt16M is required for kinetic stability of the complex, and mutation of these interfaces accelerates disassembly of the complex (Figure 4.25).

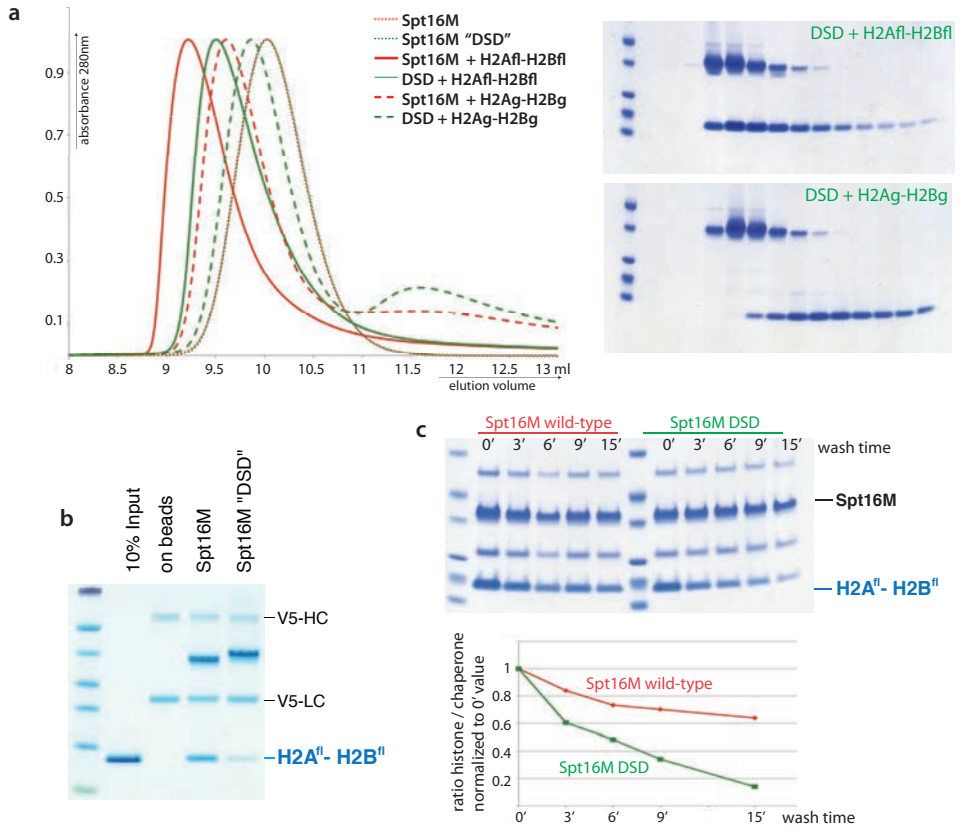

Fig. 4.26: **Mutation of three residues in the 'acidic patch' region diminishes H2A-H2B binding.**
Highly purified Spt16M D902A / S903A / D905A ('DSD') was analyzed for H2A-H2B binding in (a) SEC (elution profiles and SDS-PAGE of the eluted fractions for the runs with full-length and tail-less histones), (b) pull-down experiments and (c) 'kinetic pull-down' experiments, with quantification.

4.5.6 Spt16M and the H2A-H2B heterodimer have two distinct interfaces with different biophysical properties

From the data above I concluded that Spt16M interacts with histones H2A-H2B through two interfaces: First, the extended, mostly hydrophobic interaction of the U-turn and H2Bα1-helix and second, the electrostatic interaction between the Spt16M acidic patch and the H2B N-terminal tail.

Mutants of both interfaces affected ITC profiles in 200 mM salt buffer: the acidic patch mutant (D902A S903A D905A) showed decreased affinity, but the interaction enthalpy was even more endothermic than wild-type, hinting that the hydrophobic interaction with

H2Bα1 was undisturbed (Figure 4.27a,b).

In contrast, the U-turn mutant that disrupted complex formation in SEC (N916S V919S I920S T923S) showed a complicated ITC profile (Figure 4.27a); the slight increase in signal towards the later injections might have been caused by moderate protein aggregation or other secondary effects. A milder variant of this mutant (mutation of the respective residues to alanine instead of serine) had a curve shape and therefore K_D similar to wild-type protein, but the enthalpy values were strongly decreased and the entropy was strongly increaseds, hinting that the hydrophobic binding interface was disturbed but not disrupted (Figure 4.27b). Combination of the U-turn and acidic patch mutant gave 'combined' results: the K_D is changed like in the acidic patch mutant, the ΔH and ΔS values are similar to the U-turn mutant. This further indicates that binding to the U-turn and acidic patch are independent events in equilibrium conditions.

In high salt conditions (500 mM NaCl), the electrostatic interaction between the H2B tail and the acidic patch should be disrupted. Consistent with this, the acidic patch mutant behaved almost like wild-type. The U-turn mutant profile was close to baseline in these conditions, which indicated that there was no binding interaction or precipitation (Figure 4.27a).

In summary, the two interfaces of the chaperone with the hydrophobic patch on H2Bα1 and the N-teriminal tail of H2B both contribute to the overall affnity and the shape of the ITC profile of the binding reaction in physiological salt conditions.

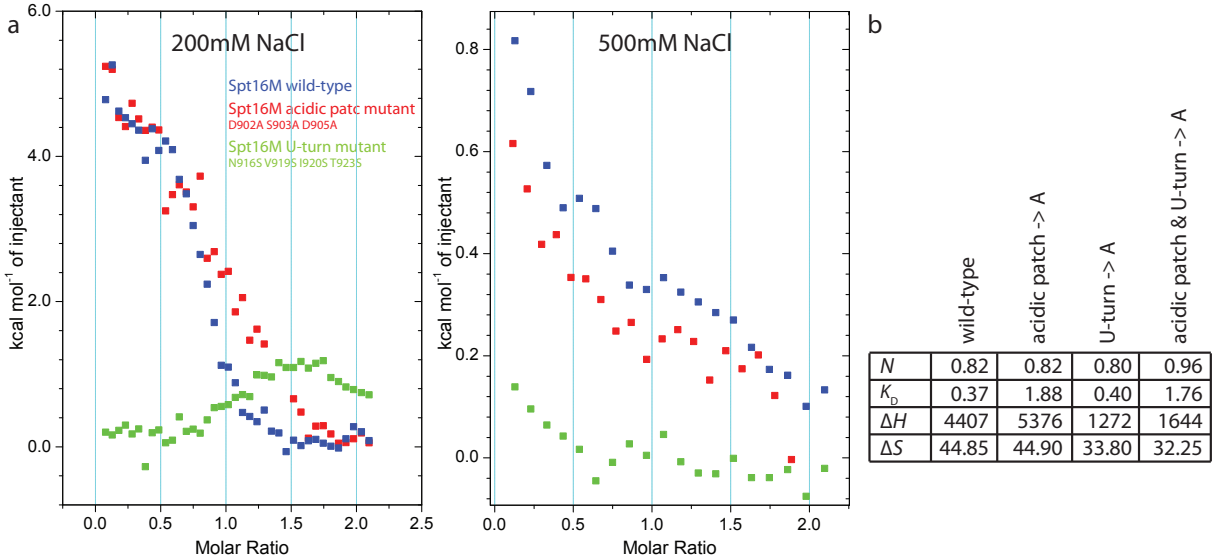

	wild-type	acidic patch -> A	U-turn -> A	acidic patch & U-turn -> A
N	0.82	0.82	0.80	0.96
K_D	0.37	1.88	0.40	1.76
ΔH	4407	5376	1272	1644
ΔS	44.85	44.90	33.80	32.25

Fig. 4.27: **ITC analysis of the acidic patch and the U-turn mutant.**
(a) ITC profile for wild-type Spt16M (*blue*) as well as mutants of the acidic patch (*red*) and the U-turn(*green*) in two buffer conditions (low and high salt). (b) ITC values (stoichiometry (N) enthalphy (ΔH), entropy (ΔS) and affinity (K_D)) for several Spt16M constructs, measured in 200 mM NaCl. Acidic patch = D902 S903 D905, U-turn = N916 V919 I920 T923 D934 F939 L940.

4.6 The tandem PH modules of Rtt106, Pob3M and Spt16M are a conserved family of histone H3-H4 chaperones

The Spt16M tandem PHL domain shows high structural homology to two other histone chaperones, the FACT domain Pob3M [**?**] (Figure 2.15) and the fungal H3-H4-binding chaperone Rtt106 [**???**] (Figure 4.28a). Therefore, I analyzed whether these three proteins share conserved surface patches that might be functionally important, and whether Pob3M and Spt16M can also bind histones H3-H4.

4.6.1 Literature overview: Structural and functional characterization of Rtt106

Rtt106 consists of a small N-terminal heterodimerization domain (residues 1-42), a tandem PH chaperone domain (residues 68-315) and a C-terminal acidic unstructured stretch (residues 316-455). Three groups recently solved the structure of the chaperone domain and studied the function of conserved surface patches, but came to different conclusions (Figure 4.28).
? identified a stretch of conserved basic residues across both PH domains in Rtt106 and Pob3 that binds DNA. They further mapped histone binding to an 'ITRLT' motif in a loop region of the second PH domain; an adjacent conserved 'acidic patch' might neutralize the histone charge.
? showed that the heterodimerization domain forms a V-shaped 2-helix bundle that binds histones H3-H4 (K_D = 0.6 μM). Acetylation of the H3 K56 residue strongly increased the affinity (K_D = 0.08 μM); the modification is recognized by a conserved pocket in PHL-2 that can be blocked by a lysine residue in a 'flexible helical' C-terminal extension (residues 302-315), but the functional relevance of this intra-molecular interaction is unclear.
? genetically identified two separate, conserved histone-binding regions, a basic patch on PHL-1 for H3-H4 binding and the two threonine residues in the 'ITRLT' motif mapped by **?** that contribute specifity for acetylated H3 acetylated on K56. Both patches are important for replication and HMR silencing. The basic patch on PHL-1 is conserved in Pob3M; solely the sum of positive charge seems to be important to bind the 'correct' amount of histones H3-H4 whereas deviations cause a *Spt-* phenotype.

4.6.2 Structural and functional comparison with Spt16M

The structures of the tandem PH domains of Rtt106 (PDB ID = 3TO1), Pob3 (PDB ID = 2GCL) and Spt16M, especially the second PH domain, have high structural homology (Figure 4.28a). Using the Spt16M coordinates from the chaperone-histone complex and Pob3M (PDB ID = 2GCL, [**?**]) and Rtt106 (PDB = 3TO1, [**?**]) from the PDB database, I calculated the the Root-mean-square deviations (r.m.s.d.) of backbone atoms for the superimposed proteins:

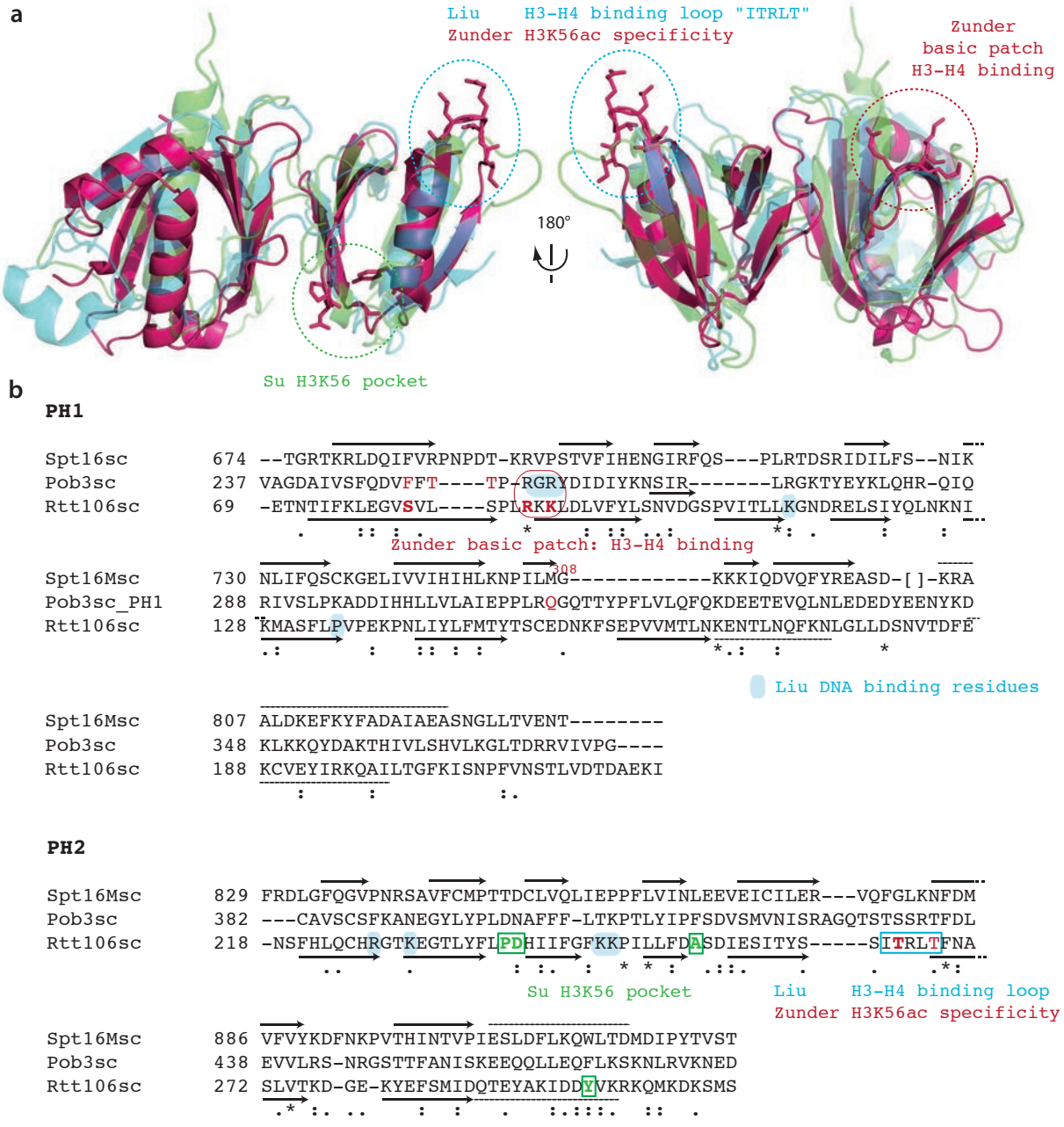

Fig. 4.28: **Alignment of tandem PHL sequences from Spt16M, Pob3M and Rtt106.** (a) ClustalW2 alignment of the PHL domains of Spt16M, Pob3M and Rtt106 (*S. cerevisiae*). β-strands are marked as arrows, α-helices are marked as dashed lines. The unstructured loop in PH-L1 connecting the last β-strand to the capping α-helix was omitted. (b) Structural alignment of the tandem PHL domains of Spt16M (*green*, our structure), Pob3M (*light blue*, PDB ID = 2GCL) and Rtt106 (*pink*, PDB ID = 3TO1).

tandem PHL domains	Spt16M – Pob3M	3.3 Å
	Spt16M – Rtt106	3.6 Å
	Pob3 – Rtt106	2.9 Å
PH1	Spt16M – Pob3M	no score calculated
	Spt16M – Rtt106	3.1 Å
	Pob3M – Rtt106	2.8 Å
PH2	Spt16M – Pob3M	2.1 Å
	Spt16M – Rtt106	1.9 Å
	Pob3M – Rtt106	1.4 Å

Two of three 'basic patch' residues (PHL-1, [**?**]) are present in Spt16M (Figure 4.28b) and are highly or completely conserved (Figure 4.3). Although there is no direct sequence homology to the 'ITRLT' motif, the corresponding loop region is very conserved in Spt16M as well (Figure 4.3). Mutation of several residues ("RV. . . .N.D") was lethal in *S. cerevisiae* (section 4.8), and from superposition of the complex structure onto the nucleosome, it looks as if this region would be close to or collide with protein and DNA around the H3-H4 (L1-L2) DNA contact (section 4.10). The phenotype and biochemistry of point mutant proteins of these regions remains to be tested, in particular for their ability to interact with histones H3-H4 or H3 K56 (see below).

4.6.3 Spt16M interacts with histones H3-H4

4.6.4 Pob3M and Spt16M bind recombinant H3-H4

Since both Rtt106 and full-length Pob3 bound histones H3-H4, I tested whether this functionality was conserved in the tandem PHL domains of Spt16M and Pob3M (at this time, the paper by **?** that mapped H3-H4 binding to Pob3M had not yet been published). I first tested GST-tagged constructs of Pob3M and Spt16M, but found that H3-H4 interacted strongly with GST itself (*data not shown*). Thus, I decided to use the V5 epitope tag instead which has little charge under physiological pH (IP (V5)= 6.25).

V5-tagged recombinant Spt16M and Pob3M was bound to V5-affinity agarose beads, incubated with excess refolded full-length histones H3-H4 (*X. laevis*) and washed extensively (300 mM NaCl, 25 mM Tris pH7.5, 0.05 % NP40). Bound proteins were eluted with SDS-PAGE loading buffer. Spt16M bound both full-length and tail-less histones H3-H4 (residues H3 [28-135] and H4 [21-102]) (Figure 4.29a). Since Pob3M tends to aggregate when mixed with the histone H3-H4 dimer, I decided not to elute denaturating with loading buffer but instead eluted 'native' with V5-peptide; I found that Pob3M formed a stoichiometric complex with the histone dimer (Figure 4.29b). The interaction with Spt16M was stable up to 500 mM NaCl, whereas Pob3M binding was already strongly reduced at 400 mM NaCl (Figure 4.29c). Thus, interaction with histones H3-H4 is a conserved function of tandem PH like chaperone modules.

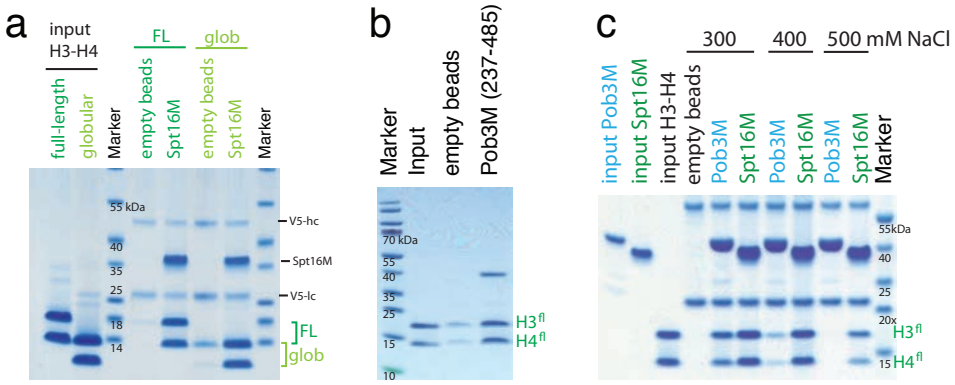

Fig. 4.29: **Spt16M and Pob3M bind histones H3-H4.**
(a) Spt16M interacted equally well with full-length (FL) and globular (glob) histones H3-H4. (b) Pob3M formed a stoichiometric complex with histones H3-H4, after elution with V5-peptide. (c) The interaction of H3-H4 with Spt16M was stable at higher salt concenctrations than with Pob3M.

4.6.5 Spt16M's PHL-2 and U-turn are sufficient for interaction with H3-H4

I mapped the interaction of Spt16M with histones H3-H4 in more detail by pull-down assays. On the chaperone side, a construct of PHL-2 with the U-turn motif was sufficient for interaction with full-length H3-H4 (Figure 4.30). On the histone side, the globular cores of H3-H4 were sufficient for interaction with Spt16M (Figure 4.30). Thus, the H3-H4 binding function is conserved in all three tandem PH domains, but in my hands the interaction mapped to Spt16M PHL-2, not to PHL-1 as in Pob3M and Rtt106 [**?**].

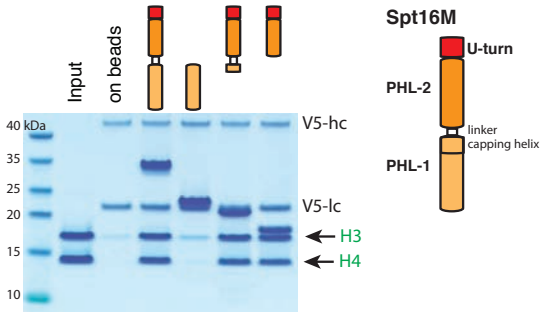

Fig. 4.30: **PHL-2 of Spt16 is necessary and sufficient for H3-H4 binding.**
V5-tagged proteins were bound to V5-affnity agarose, incubated with excess of full-length histones H3-H4 dimer and washed with 300 mM NaCl, 25 mM Tris pH 7.5, 0.05 % NP40. Precipitated protein was separated on a 4-12 % SDS-PAGE.

4.6.6 H3-H4 outcompetes H2A-H2B for binding to Spt16M in SEC

Since Spt16M binds both H2A-H2B and H3-H4, I wanted to know whether both histone dimers can bind simultaneously. Equal amounts of H3-H4, H2A-H2B and Spt16M or stoichiometric 1:1 and 1:1:1 complexes of the chaperone and histone dimer(s) were mixed in a buffer containing 300 mM NaCl, 25 mM Tris pH 7.5 and 2 mM DTT, incubated on ice for 30 min and analyzed by SEC. Both H2A-H2B and H3-H4 can bind to Spt16M

when only one histone dimer is incubated with the chaperone. In contrast, when Spt16M was mixed with both H2A-H2B and H3-H4 at the same time, only the chaperone-H3-H4 complex was formed and outcompeted H2A-H2B (Figure 4.31).

To test whether H3-H4 and H2A-H2B compete for the U-turn as a common histone binding site, I mixed the H3-H4 dimer with the U-turn mutant that disrupted complex formation with H2A-H2B in SEC. Complex formation between H3-H4 and the U-turn was not disturbed, and therefore the U-turn is presumably not the site of the chaperone that interacts with histones H3-H4. Nevertheless, the experiments described above gave a little insight to where on the chaperone H3-H4 might be bound: when mixed with Spt16M and H3-H4, full-length H2A-H2B did not elute like free protein but was shifted to slightly higher molecular weight, just as had been observed for histone dimers lacking the H2B tail when run with Spt16M (Figure 4.22). I thus speculate that H3-H4 binding might displace H2B's N-terminal tail from the acidic patch, which would be sufficient to disrupt the Spt16M-H2A-H2B complex in SEC.

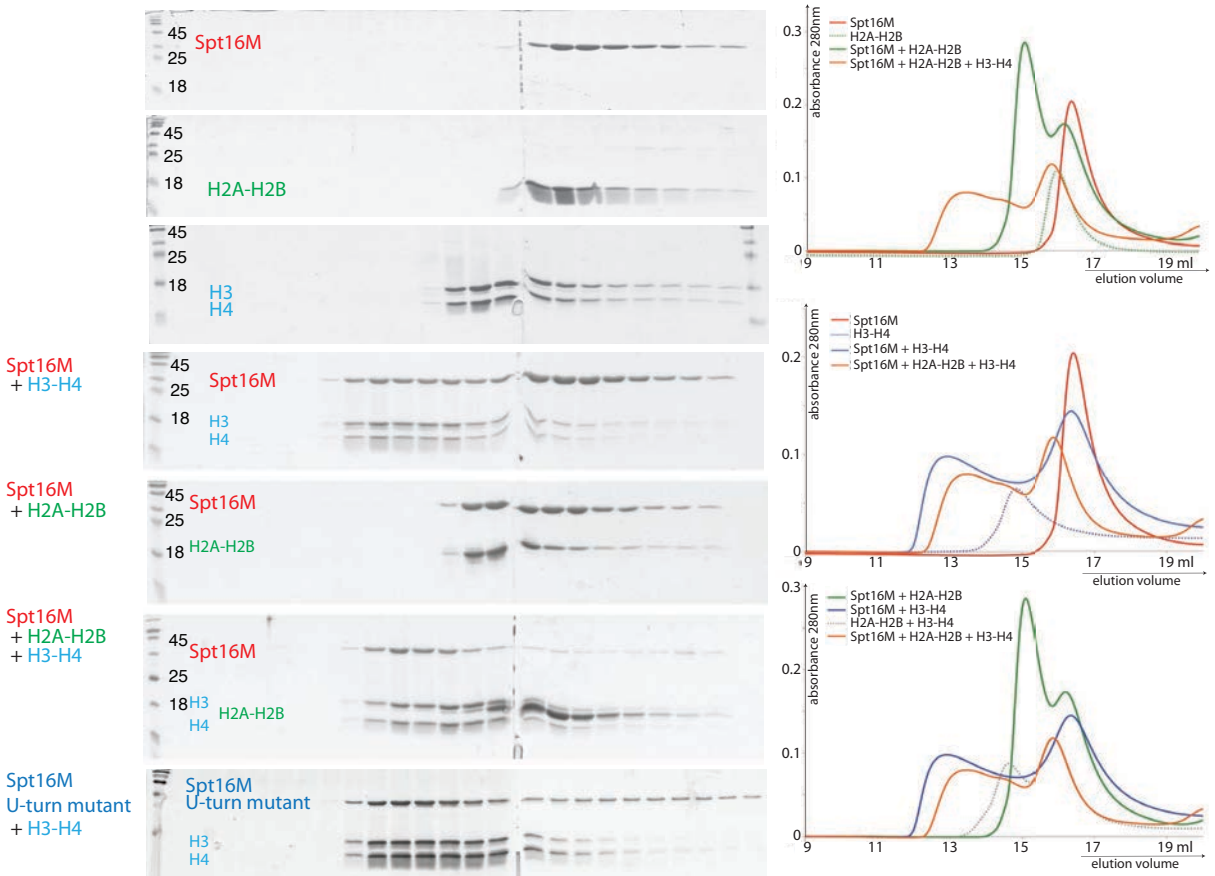

Fig. 4.31: **H3-H4 outcompetes H2A-H2B in SEC for binding to Spt16M.** H2A-H2B, H3-H4, Spt16M (wild-type or the 'NVIT' U-turn mutant) and stoichiometric complexes thereof were separated on a SD 200 10/300 column in 300 mM NaCl, 25 mM Tris pH 7.5, 2 mM DTT. Eltuion profiles and SDS-PAGE of eluted fractions for the individual proteins and the complexes are shown.

4.6.7 Mapping the H3-H4 site (1): Spt16M recognizes a H3 [26-45] peptide

To map which part of H3-H4 is recognized by Spt16M, I tested which peptides of H3 would be bound by the chaperone.

First, I tried whether I could detect significant binding of Spt16M to peptides on an ActiveMotif MODified histone peptide array. The peptide chip was incubated with V5-tagged Spt16M (50 μM, 1.7 mg/ml) in 75 mM NaCl, 10 mM $MgCl_2$, 25 mM Tris pH7.5, 0.05 % Tween20 over-night and washed for several days in 100 mM NaCl, 2 mM $MgCl_2$, 25 mM Tris pH7.5, 0.05 % Tween20. Bound protein was detected by immuno-affinity (anti-V5 primary antibody and a fluorescent secondary andibody) and analysed using a Li-Cor quantitative fluorescence reader. Some of the signals are discussed later on in section 4.9.3.

Spt16M strongly bound any peptide (modified or unmodified) covering the sequence H3 [26-45] (Figure 4.32). Except for the first two residues, this region is part of both globular and full-length histones H3-H4. In the nucleosome structure, it is unstructured and lies between the two gyres of DNA, at the DNA entry / exit site and might thus be transiently accessible during nucleosome breathing (Figure 4.32b).

It was recently shown that a peptide of the same sequence is recognized by human FACT [**?**], which is in agreement with my results. These authors further showed that interaction is disrupted by acetylation of H3 K36, a repressive chromatin mark. In conclusion, the interaction between FACT and H3 not modified on K36 would recruit the chaperone mostly to 'active' chromatin.

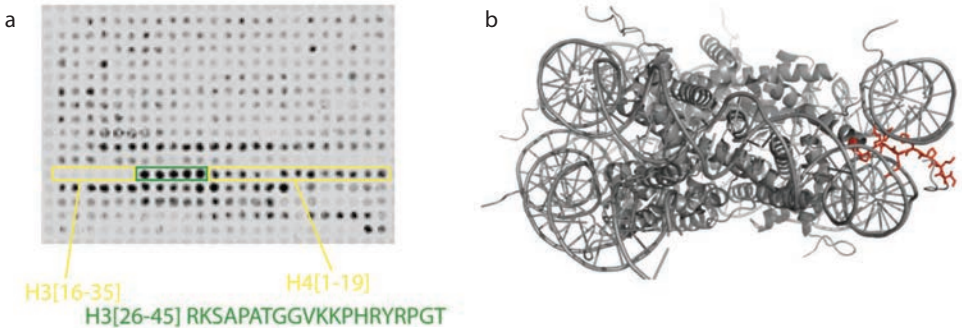

Fig. 4.32: **Mapping of the Spt16M bound H3 peptide on a histone peptide ChIP.** (a) A peptide encompassing H3 [26-45] interacts strongly with the Spt16M domain. The stretch of strongly interacting peptides is marked in green, neighboring peptides of different sequence are marked in yellow. (b) The H3 [26-45] stretch comes to lie inbetween the DNA gyres in the nucleosome structure (1AOI).

4.6.8 Mapping the H3-H4 site (2): like Rtt106, Spt16M binds a H3 [46-65] peptide

As a parallel approach, I bound soluble biotinylated peptides to streptavidin dynabeads and analyzed which of them would pull down recombinant Spt16M in TBS 0.05 % NP40. Besides a weak interaction with the the N-terminal 20 residues of histone H3, strong binding was observed for a peptide covering H3 resiudes [47-66] (Figure 4.33); the interaction was stable in 300 mM NaCl (*data not shown*). This sequence covers the H3 K56 residue which is recognized by the structurally homologous Rtt106 chaperone, and

thus Spt16M and Rtt106 might share a evolutionary conserved binding site on H3.

The sequence detected by biotin-pulldown assays was not covered on the histone peptide chip. *Vice versa* I did not have a biotinylated [26-45] peptide available. Therefore, I was unable to verify any of my results by the complementary method. Nevertheless, it is worth noting that I could not pull down any Spt16M with the biotinylated [17-36] peptide, which shares residues [26-36] with the Active Motif peptide sequence. Although the experiments cannot be directly compared, I speculate that Spt16M recognizes the C-terminal [37-45] of the Active Motif peptide sequence, which is adjacent to the biotinylated peptide [46-65] that strongly pulled down Spt16M. The real recognition sequence might thus extend over both sequences.

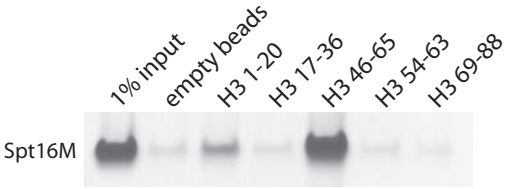

Fig. 4.33: **Mapping of the Spt16M bound H3 peptide by peptide-pulldown assays.** Spt16M interacts with H3 peptides [1-20] and [46-65]. Biotinylated peptides were bound to dynabeads and incubated with recombinant Spt16M in TBS 0.05 % NP40. After washing, bound protein was analyzed by SDS-PAGE and Coomassie staining.

4.6.9 Spt16M interacts with both an unmodified and a K56-acetylated H3 peptide

Since Rtt106 preferentially binds acetylated K56 [**??**], I tested whether this modification affects interaction with Spt16M. V5-tagged Spt16M was bound to beads and incubated with H3 [46-65] peptides, either acetylated on K56 or unacetylated, in a buffer containing 150 mM NaCl, 25 mM Tris pH7.5, 0.05 % NP40. After washing, bound peptide was eluted with high salt buffer (1 M NaCl) and analyzed by SDS-PAGE and silver staining. Both peptides bound to Spt16M (Figure 4.34). However, it remains to be determined whether the affinity changes (e.g. by ITC) and whether K56 acetylation is essential for interaction with the chaperone *in vivo*, as observed for Rtt106 (but not Pob3M) [**?**].

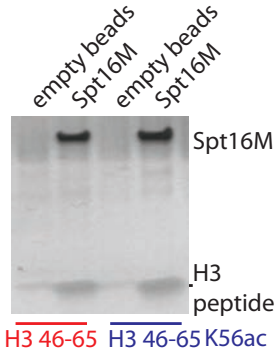

Fig. 4.34: **Spt16M binds H3 [46-65] independent of K56 acetylation.** V5-Spt16M was bound to beads and incubated with soluble peptides; after washing, bound peptides were analyzed by SDS-PAGE / silver staining.

4.7 Spt16M interacts with dsDNA

Spt16M displays distinct positively charged surface patches on the PHL-1 domain (see Figure 4.9). Thus, I tested whether Spt16M, and in particular PHL-1, could bind DNA. Purified Spt16M or the individual domains were incubated with a short fragment of radiolabeled DNA; the reactions were analysed by Native PAGE and detection of the radioactive DNA. In the reactions with the tandem PHL domain or isolated PHL-1, but not PHL-2, distinct bands of higher molecular weight appeared. I concluded that Spt16M and PHL-1 were able to bind DNA (Figure 4.35a), just like the structurally homologous Pob3M and Rtt106 [**?**].

In fungal Spt16 protein sequences, the unstructured loop between the last β-sheet and the capping α-helix is enriched for positive residues, these are good candidates for the interaction with DNA. A homologous stretch of positively charged residues is absent or less distinctive in higher eukaryotes. I speculate that it was functionally replaced by the DNA-binding HMG box of SSRP1 during evolution, which is not present in the yPob3 protein (Figure 4.35b).

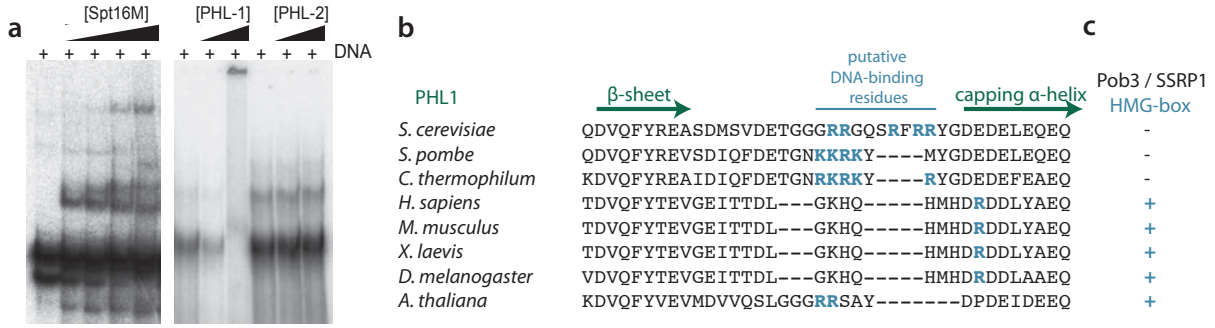

Fig. 4.35: **The Spt16M domain can bind double-stranded DNA.**
(a) Spt16M, in particular its PHL-1 domain, shifts double-stranded DNA in electrophoretic mobility shift assays. (b) Alignment of selected PHL-1 residues of different species. Secondary structure elements are marked above the sequence. (c) Fungal Pob3 does not contain a HMG box, but the SSRP1 protein of higher eukaryotes does; the order of sequences is the same as for the PHL-1 sequence alignment.

4.8 Mutations that affect H2B binding *in vitro* also decrease viability in yeast *in vivo*

4.8.1 Experimental design: testing mutants for viability in a Δ*spt16* background strain

To test the relevance of the observed contacts between Spt16M and H2A-H2B *in vivo*, I screened for the ability of mutant Spt16 proteins to rescue lethality in *S. cerevisiae* Δ*spt16*. Since Spt16 is an essential gene, I created a Δ*spt16* deletion strain that carried a rescue plasmid under URA selection with wild-type Spt16, expressed from it's endogenous promoter. Mutants of Spt16 were cloned into a similar plasmid with LEU as a selection marker; these constructs I transformed into the Δ*spt16* strain with the URA rescue plasmid. After several days of growth in media lacking leucine, I spotted the yeast on FOA (5-Fluoroorotic Acid) plates so cells that depend on the wild-type URA plasmid would die (the URA3 gene transforms FOA into the toxic substance 5-fluorouracil) (Figure 4.36a). Single or double mutations within the helical Spt16M U-turn motif were mostly lethal, so a functional U-turn and presumably H2A-H2B binding are essential for viability. One of the mutants, Q930R, was not lethal but displayed a severe growth phenotype; this residue is not directly involved in the interaction with the histones. Acidic patch mutants could weakly rescue viability, but grew very slowly at 24°C (Figure 4.36).

Several highly conserved residues of Spt16M were tested in the first round of experiments that do not directly map to the H2A-H2B interaction surfaces identified *in vitro*: The 'basic loop' in PHL-1 might be involved in DNA binding (Figure 4.35). Residues R862, V863, N869 and D871 correspond roughly to the 'ITRLT' motif of Rtt106 involved in H3-H4 / K56 recognition (Figure 4.28) and might 'clash' with H3-H4 when the complex is superimposed onto the nucleosome structure (section 4.8). Since all of those mutations have a lethal phenotype *in vivo*, the respective Spt16M proteins should now be analysed *in vitro* for protein stability, and for their ability to interact with histones and DNA.

4.8.2 Mutation of the U-turn or acidic patch does not affect protein stability *in vivo*

The first set of mutants carried no epitope-tag and thus could not be distinguished from wild-type protein in western blot. To verify that the mutant proteins were properly expressed, I created a new set of mutants with a N-terminal V5-tag. While expression of the U-turn mutant (NVIT→S)was compromised at 30°C (*data not shown*), all proteins were expressed to the same level as wild-type protein when cells were grown at 24°C (Figure 4.37b). Thus, any *in vivo* experiment should be performed at the lower temperature.

The viability experiment was performed as described above (Figure 4.36a). As expected, mutation of residues crucial for H2A-H2B interacion *in vitro* was lethal *in vivo* (Figure 4.37a) so the U-turn has an essential function, presumably the interaction with histones H2A-H2B. The V5-tagged acidic patch mutant did not seem to be able to rescue viability any more, as observed for the untagged protein. One explanation could be that both the N-terminal Spt16N domain ([**?**], affected by the newly introduced V5 epitope tag) and the acidic patch might be involved in interaction with histones H3-H4.

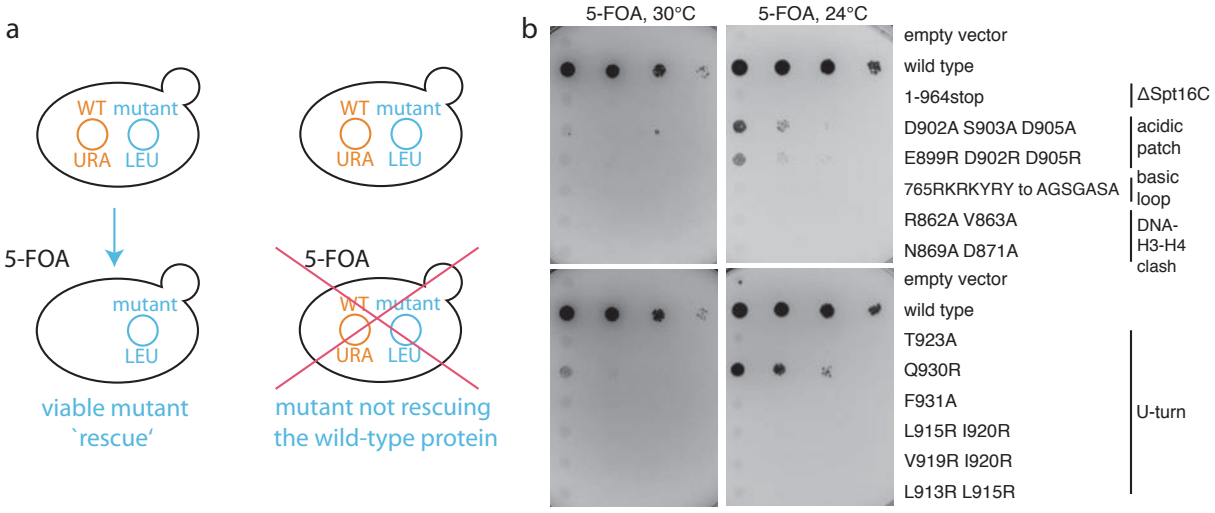

Fig. 4.36: ***In vivo* analysis of selected Spt16M mutants in *S. cerevisiae*.**
(a) The plasmid-shuffle system. The Spt16 gene was deleted in a yeast strain carrying a URA rescue plasmid (with a chimeric version of Spt16 where *S. cerevisiae* Spt16M was replaced by the *C. thermophilum* Spt16M module). Mutants (in the same chimeric background) were transformed on a LEU plasmid. On FOA, cells that cannot survive with the mutant version of Spt16 only but require the wild-type gene for vitality cannot survive because the URA3 gene will convert FOA to a toxic substance. (b) Yeast was analyzed for growth at 24°C and 30°C. Mutants in the U-turn motif were lethal; mutants of the acidic patch had severe growth defects.

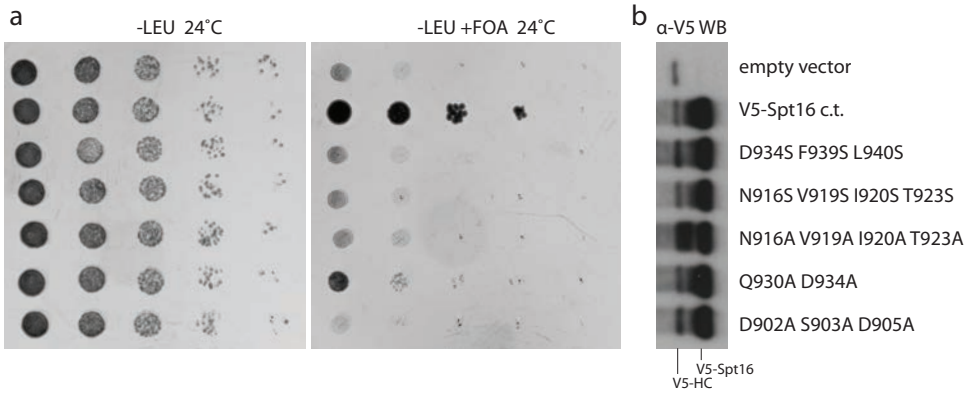

Fig. 4.37: ***In vivo* analysis of selected V5-tagged Spt16M mutants in *S. cerevisiae*.**
(a) On -LEU at 24°C, all strains grow like wild-type. On FOA, only cells that do not rely on the URA3 rescue plasmid containing wild-type Spt16 can grow. U-turn and acidic patch mutants (under LEU selection) are not viable or strongly growth-deficient. (b) Wild-type and mutant proteins are expressed to similar levels, as tested by Western Blot against the N-terminal V5-tag. Spt16 from equal cell counts was enriched by IP before SDS-PAGE for better signal intensity, the heavy chain of the V5 antibody reacts with the secondary antibody and is visible as well.

4.8.3 Spt16C contains a putative NLS

Previous data had shown that the C-terminal region of human Spt16 is required for H2A-H2B binding, chaperone activity and viability [**??**]. However, the construct used in these studies lacked both the unstructured Spt16C domain and a large part of the H2A-H2B binding Spt16M module, including the U-turn motif (Figure 4.1). Therefore, I designd a construct that contained the full Spt16M chaperone domain but lacked the unstructured Spt16C part and tested whether it could rescue growth of the Δ*spt16* strain, which it could not (Figure 4.38a). One reason might be that the sequence of Spt16C contains a predicted nuclear localization sequence (NLS) which is conserved across most species (except for *S. cerevisiae*) (Figure 4.38b). Therefore, I tested whether the Spt16 proteins with and without Spt16C localize to the nucleus of a yeast cell by immuno-fluorescence. Yeast cells were fixed, incubated with a fluorescent antibody against the N-terminal V5 tag of Spt16, and imaged. While full-length Spt16 and a construct encompassing the Spt16M and C domains (Spt16MC) localized to the nucleus, deletion of the Spt16C domain (Spt16M construct) delocalized the protein to the cytoplasm (Figure 4.38c). I concluded that the Spt16C domain with the predicted NLS is required for nuclear localization, and thus we cannot judge whether the Spt16C domain is also essential for some nuclear function, e.g. histone binding.

Apart from containing a putative NLS, I speculate that the Spt16 acidic tail might also have a mechanistic role: for the histone chaperone Nap1, it was described that such long, unstructured acidic stretches facilitate nucleosome destabilization and reorganization, presumably by directly competing with the acidic DNA molecule [**?**].

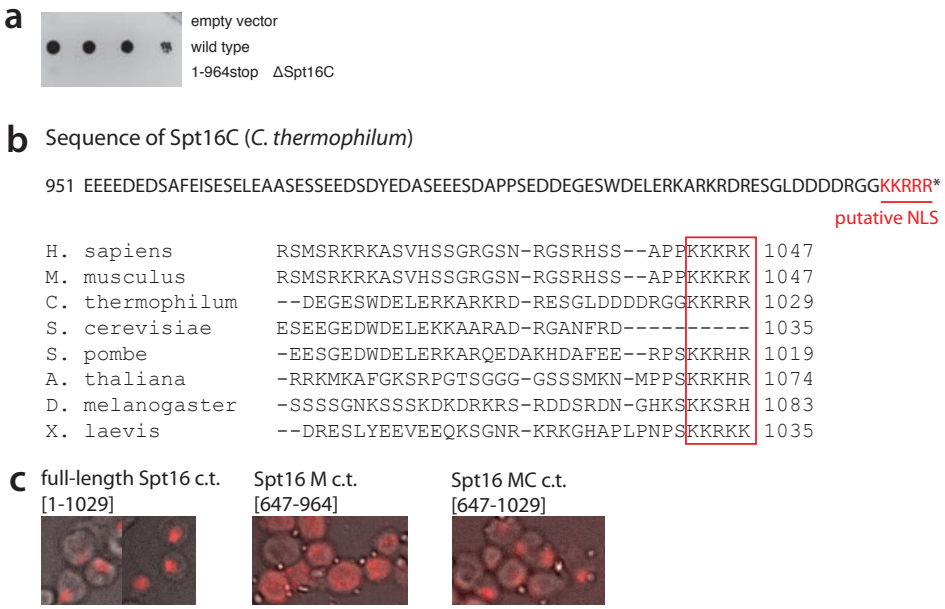

Fig. 4.38: **Spt16C contains a putative NLS.**
(a) Deletion of Spt16C is lethal in a FOA growth assay (as described in Figure 4.36a) (b) Spt16C *c.t.* contains a C-terminal stretch of basic residues, a putative NLS (* = end of protein sequence) which are quite conserved (ClustalW2 alignment), except for *S. cerevisiae* (c) Immuno-fluorescence of fixed yeast cells, with antibodies against the V5-tag (*red*). Full-length Spt16 c.t. (*C. thermophilum*) or a construct encompassing Spt16M and Spt16C (Spt16MC) localize to the nucleus, Spt16M alone does not.

4.9 Spt16M is a 'universal' reader of the H2A-H2B core but might be regulated by PTMs of the histone tails

4.9.1 Ubiquitination of H2A or H2B probably does not directly interfere with FACT binding

During transcription elongation, FACT shows functional interaction with histone ubiquitination modifications. Ubiquitination of H2A (on K119 in mammals) blocks FACT recruitment and inhibits transcription elongation [**?**]. In contrast, FACT promotes ubiquitination of H2B K123 in yeast (K120 in mammals) and is in return retained at actively transcribed ORFs by this modification. Together with the PAF complex, FACT and H2Bub1 cooperate to promote transcription elongation [**?**] and preservation of intact chromatin [**?**].

Neither H2A K119 nor H2B K123 are visible in our structure: H2A K119 is not part of our construct since the rather hydrophobic H2A C-terminal tail was deleted to increase solubility; the H2B K123 residue is unstructured (no sufficient electron density). However, both ubiquitination-sites locate to the C-terminus of the histone proteins, opposite to where Spt16M binds H2Bα1 (Figure 4.39). Thus, the modifications will probably not directly influence FACT binding but rather promote a chromatin state more accessible or inaccessible to the binding of the chaperone, as discussed in 2.3.4.

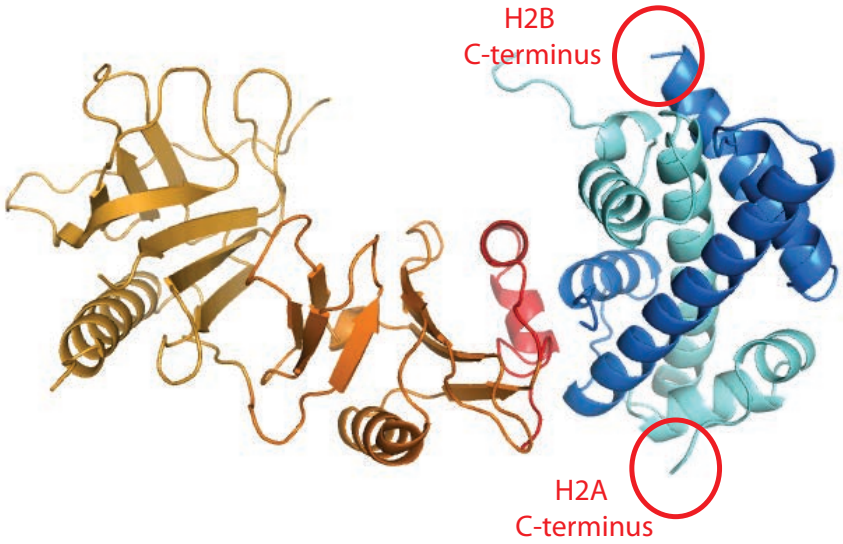

Fig. 4.39: **H2A and H2B ubiquitination and Spt16M binding locate to opposite sides of the histone dimer.**
The ubiquitination sites H2A K119 and H2B K123 lie C-terminal of the visible structure. Spt16M (*orange, red*), H2A (*turquois*), H2B (*blue*); C-termini of the histones are marked with red circles.

4.9.2 Histone conservation, variants and modifications do not influence the Spt16M-H2B contact

Almost all of the interacting residues of H2B are completely conserved over evolution. A notable exception is Ile36 that nestles into the hydrophobic Spt16M U-turn in the chimeric complex structure but is substituted by a non-hydrophobic Serine in yeast sequences (Figure 4.40).

H2A's Arg77, which contributes an electrostatic interaction (Figure 4.11), is also conserved apart from *S. pombe* (by a chemically similar Threonine, *data not shown*).

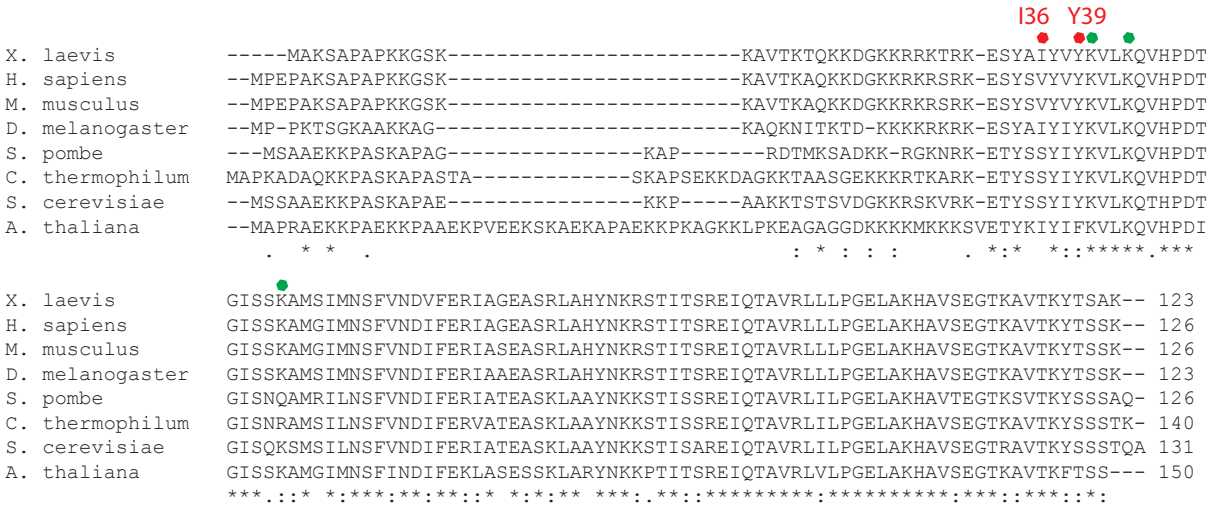

Fig. 4.40: **Alignment of histone H2B sequences.**
Alignment of H2B sequences with ClustalW2. Hydrophobic residues stacking into the U-turn of Spt16M are marked with red dots. Lysine residues contributing electrostatic interactions (K40, K43, K54) are marked with green dots.

Recent mass spectrometry analysis has detected quite a few modifications for H2B. However, only a few of them were verified to be somehow 'functional' [**??**]. Only one of them, phosphorylation of H2BSer33 (found in *D. melanogaster*) localizes to the interface with Spt16M. In the crystal structure, this residue makes electrostatic contacts with a chloride ion that is further coordinated by Sp16M Asn916 and H2B I36 atoms (Figure 4.11). The negatively charged phosphate group might replace these interactions and could stabilize the complex to promote transcriptional activation [**?**].

Only very few, and only rare histone variants of H2B are known, and none of these sequence variations localizes to the interfaces. Sequence variance for histone variants of H2A localize to the C-teminus of the protein, which is far from the interaction site (Figure 4.39). Thus, in summary, FACT is a general H2A-H2B chaperone that can recognize any histone H2A-H2B dimer.

4.9.3 Spt16M 'reads' histone modifications on a histone peptide Chip

For initial tests of which histone peptides might bind the Spt16M domain, I used a ActiveMotif MODified Histone Peptide array which covers all N-terminal tails, with various

modifications. Besides strong binding to a H3 tail peptide I found that several modifications were significantly recognized (minimum sixfold over background) (Figure 4.32 on page 84). The strongest hit was **H3K36**, either acetylated or mono-/di-/tri-methylated. These modifications are known to promote transcriptional activation and elongation, although methylation seems to prevent FACT binding [**?**]. But since H3 K36 is part of the peptide stretch that might bind Spt16M (see Figure 4.32) I could not conclude that binding is modification-dependent. A more detailed analysis of the binding affinity (etc. by ITC) would be required.

Strong interaction was also found with **acetylated lysine residues of the H4 tail** (K5, K8, K12, K16) but not with unmodified control peptides of the same sequence (Figure 4.32). Modification of these four residues was implicated in transcriptional activation [**?**] and histone deposition, e.g. at sites of DNA repair [**?**]. Interestingly, a mutant allele of Spt16 (*spt16-11*, T828I P859S (*S. cerevisiae*) in the core of the Spt16M PHL-2 domain) cannot grow when combined with non-acetylable lysine-to-arginine mutations of K5 & K12 or K12 & K16 (which by themselves do not affect growth) [**?**]. Acetylation-mimicking Lysine-to-Glutamate mutations did not prevent growth. Thus, acetylation of the H4 tail lysines and FACT should act in parallel genetic pathways to activate transcription elongation or, since FACT seems to bind these residues, stabilize interaction of the 'weak' mutant protein at the ORF. As for the H3 K36 peptides, a more quantitative analysis by ITC or peptide pull-down studies would be required to determine whether the chaperone can really distinguish between acetylated and non-acetylated H4 lysine residues. If so, the surface area of Spt16M responsible for recognition of the modification should be identified, and the pathway where this interaction is relevant, for example by studying the sensitivity of the mutant protein to certain drugs (e.g. hydroxy-urea (HU) for DNA replication, methyl methanesulfonate (MMS) or Cisplatin for DNA damage response, and 6-azauracil (6AU) for transcription elongation phenotypes).

4.10 A model for FACT-mediated nucleosome reorganization

4.10.1 Spt16M facilitates nucleosome 'breathing' through interaction with three proximal octamer surfaces that organize the first 30 bp of nucleosomal DNA

My high-resolution snapshot of the Spt16M–H2A-H2B complex serves as a structure-based platform for determining the mechanism(-s) through which FACT couples H2A-H2B recognition to nucleosome reorganization. This can be illustrated by superposition of our Spt16M–H2A-H2B complex onto the canonical nucleosome core particle (NCP) (Figure 4.41).

My structural and biochemical analysis showed that Spt16M interacts with three proximal surface patches of the histone octamer, the H2B N-terminal tail, the H2Bα1 helix and the H3αN helix. The solvent-accessible H2B N-terminal tail exits from the nucleosome between the gyres of DNA and is therefore quite accessible. It may mediate first interactions of FACT with the nucleosome ([**?**] and our data). At that location, the Spt16M chaperone would be poised to capitalize on a highly dynamic property of the NCP, the constant and progressive unwrapping and rewrapping of the first ~30 base pairs from the nucleosome [**?**], to gradually invade the NCP and develop stronger interactions with two DNA-covered

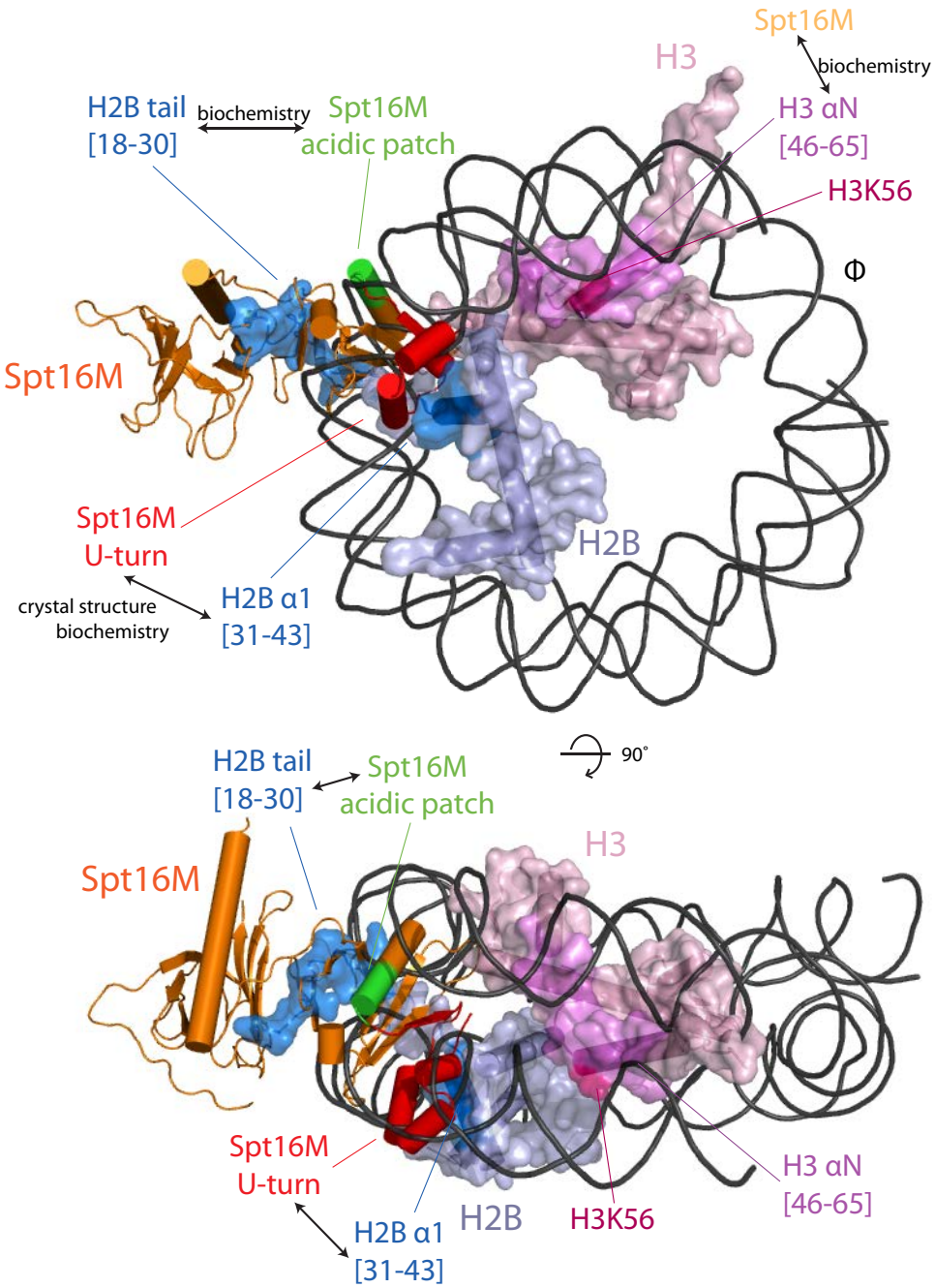

Fig. 4.41: **Summary of histone surface patches recognized by Spt16M.** Superposition of my Spt16M–H2A-H2B complex onto the structure of the nucleosome core particle. Spt16M (*orange-red*), H2B (*blue*), H3 (*violet*) and DNA (*grey*). Both copies of H2A and H4 and one copy of H2B and H3 were removed for clarity. Described interactions are based on my results from the crystal structure or biochemistry.

patches on the histone octamer. Specifically, the first 10 bp of DNA are detached about 20-60 % of the time (at the nucleosomal super-helix location (SHL) 6.5), and this decreases to 10 % at a position 27 bp into the nuclesome (SHL 4.5).

Spt16M interacts with both of the two first major DNA-octamer contacts, nameley the N-terminal αN helix of H3 at SHL 6.5 and the hydrophobic patch on H2B encompassing α1/L1/α2 at SHL 4.5, which together coordinate the outermost ~30 base pairs (Figure 4.19). Spt16M's primary interaction site on the H2B α1-helix at SHL 4.5 is one of the stronger DNA–histone contacts in the NCP [**???**]. This site becomes hypersensitive to enzymatic and chemical degradation in FACT's presence [**?**].

? describe that in protein-protein interactions, initial electrostatic and successively strong hydrophobic interactions often cooperate since the attractive forces of electrostatic interactions (which are not necessarily part of the main interaction interaface) have greater reach and promote faster complex assembly. The Spt16M—H2A-H2B interaction would perfectly fit into this model: both the highly charged H2B N-terminal tail and the Spt16C unstructured 'tail' could mediate first, 'attracting' interactions that will facilitate (hydrophobic) binding of the U-turn to H2Bα1.

My data provide a structural basis for how FACT could facilitate nucleosome 'breathing' through Spt16M [**??**] and stabilize a reorganized, more accessible NCP, supporting the conclusions of other studies [**???**].

4.10.2 Superposition of Spt16M onto the NCP predicts that FACT could facilitate nucleosome 'gaping'

Biophysical analysis of the NCP has predicted another intrinsic dynamic: nucleosome 'gaping', an oyster shell-like movement of two nucleosome half-discs around a H3-H3′ interface hinge [**?**] (this movement was illustrated in Figure 2.7 of the introduction).

Structural superposition of our Spt16M–H2A-H2B complex with the NCP identifies a steric clash between a Spt16M surface bulge and the H3′-H4′ dimer (L1 loop of H3′ and L2 loop of H4′) with the associated DNA gyre, which locate below the H2Bα1-helix bound by Spt16M's U-turn motif (Figure 4.42). The Spt16M residues involved locate around the N-terminus of the PHL-2 capping helix and a loop region connecting β-strands 14 and 15, near the U-turn opening. These residues are conserved and essential for yeast viability (Figure 4.36).

The steric clash could be resolved by flexibility in the Spt16M–H2A-H2B interface, nucleosome 'gaping', or by moving away the H2A-H2B dimer, thus breaking contacts to the H3-H4 dimer. In physiological salt, these contacts between H2A-H2B and H3-H4 are weak and the octamer is solely stabilized by the presence of DNA. Therefore, although Spt16M does not actively disturb contacts between the H2A-H2B dimer and the H3-H4 tetramer, Spt16M-induced displacement of DNA might be sufficient to release the H2A-H2B dimer from the nucleosome, as observed [**??**]. In my model, H2A-H2B released from the nucleosome but still bound by Spt16M could be retained close to the reorganized nucleosome through other parts of FACT: Pob3M ([**?**] or the positive surface patches on PHL-1 are well positioned to receive and neutralize DNA peeled off the octamer core, and Spt16M, the Spt16N 'aminopeptidase' [**?**] or Pob3M (Figure 4.29) all interact with histones H3-H4.

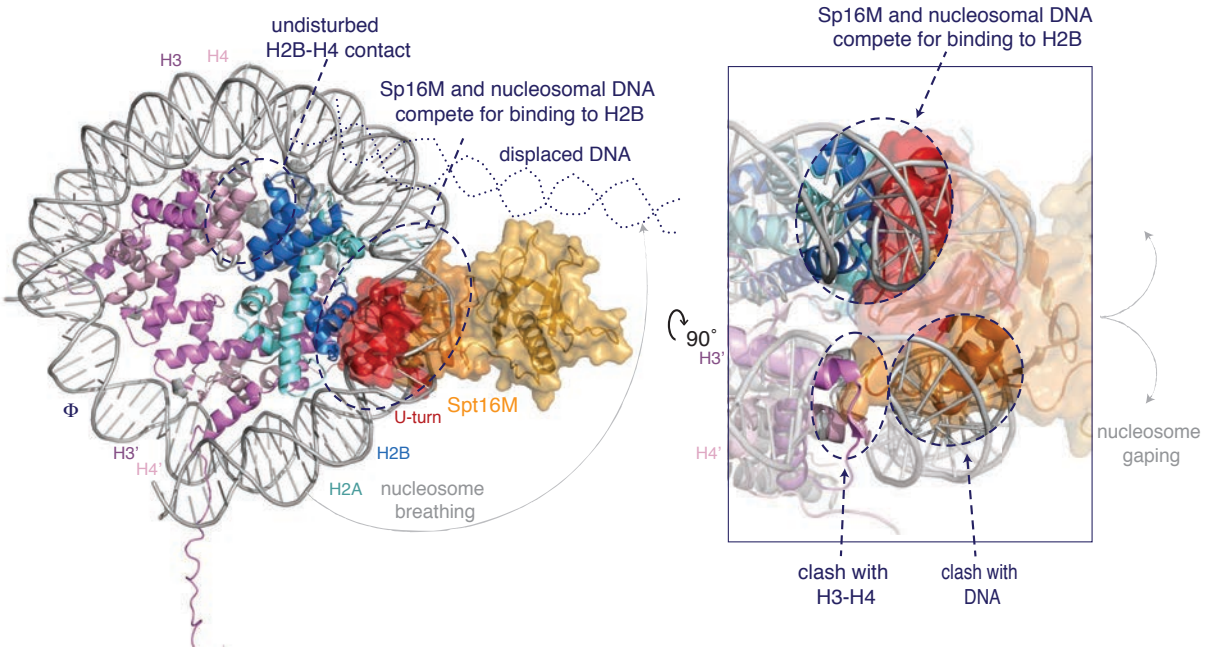

Fig. 4.42: **Model for FACT-mediated nucleosome re-organization.**
Superposition of our Spt16M–H2A-H2B complex onto the structure of the nucleosome core particle. Spt16M (*orange-red*), H2B (*blue*), H2A (*turquois*), H3 (*violet*), H4 (*light pink*) and DNA (*grey*). The U-turn motif of Spt16M competes with DNA for binding to the hydrophobic patch on α1 and α2 of H2B. A Spt16M surface bulge (residues 862-872 and 891-893) clashes with the DNA and histone H3-H4 dimer of the other nucleosome half.

4.10.3 Breaking the stronger octamer-DNA contacts at SHL 4.5 and 6.5 allows RNA Pol II progression

Prevention of DNA–histone interactions and shielding of the histones' DNA-interaction sites are likely a characteristic feature of histone chaperones [**??**]. This has implications for the transcription of chromatin, as RNA polymerase II itself cannot generate enough force to transcribe through nucleosomes *in vitro*. Yet, when contacts between nucleosomal DNA and the distal H2A-H2B dimer are broken, the energetic barrier is sufficiently lowered to permit Pol II progression [**?**]. Recently, it was shown that FACT helps to partially uncoil the DNA from the distal H2A-H2B dimer, and that it's presence is sufficient to facilitate transcription through the nucleosome [**?**]. This process does not necessarily evict the H2A-H2B dimer nor introduce major changes in overall octamer structure, e.g. the interface between H2A-H2B and H3-H4. Overall, it seems that the chaperone complex mostly lowers the thermodynamic barrier of histone-DNA contacts. A nucleosome-engaged Spt16M module, as illustrated in Figure 4.42 would fulfil all these criteria. It could thus catalyze Pol II's override of the nucleosome barrier without necessarily disassembling the nucleosome or the intact chromatin structure required for repression of spurious RNA transcripts [**?**].

5 Results and Discussion II: The FACT heterodimerization domain Spt16D-Pob3N

5.1 Structure of the Spt16D-Pob3N complex

5.1.1 The heterodimerization domain is composed of PHL domains

The structure of the Spt16D-Pob3N complex was solved by Tobias Stuwe and details of the structure are described in his thesis. Still, a biochemical and functional analysis of the domain was missing. I started on this project mostly because I wanted to find out why the complex occurs as a stoichiometric complex in yeast cells [**?**] and what happens when the interaction is artificially disrupted.

Like Spt16M and Pob3M, the FACT heterodimerization domain consists of PHL domains, one in Sp16D and presumably two in Pob3N, with the capping helix of the second missing from the construct (and structure) but predicted from the amino acid sequence (Figure 5.1 and 6.1). The interface between the two subunits is very large (2195 Å^2) and very salt stable (>0.6 M NaCl).

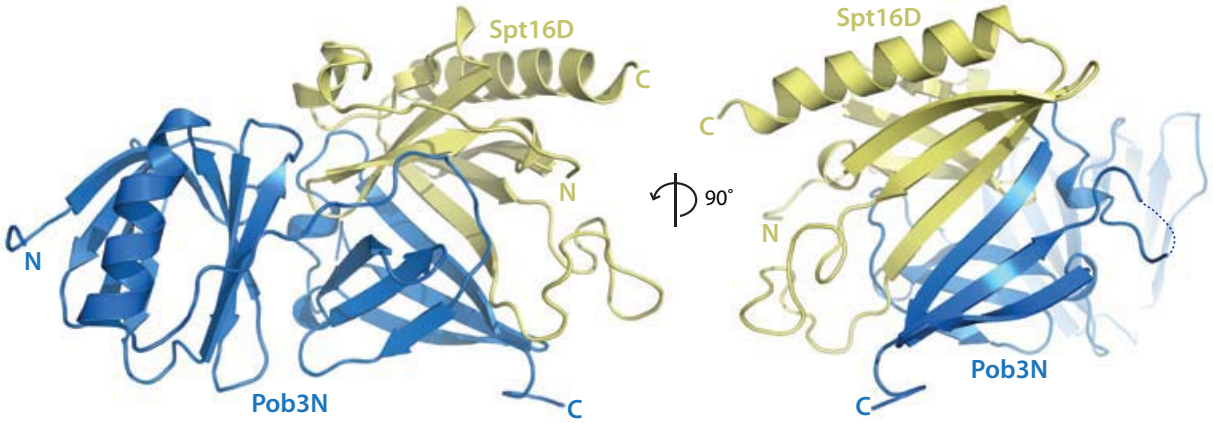

Fig. 5.1: **Structure of the FACT heterodimerization domain Spt16D-Pob3N.** Two different orientations of the Spt16D (*yellow*) - Pob3N (*blue*) complex in cartoon representation.

The interface between the two FACT subunits is highly conserved (Figure 5.2a). The same is true for a composite β-sheet formed by the β-barrels of both subunits, suggesting that this surface is used for some evolutionary conserved interaction (Figure 5.2c).

5.1.2 Mutation of two Spt16 interface residues disrupts the complex

So far, any function described for FACT is performed by individual domains, but nevertheless Spt16 and Pob3 form a strong heterodimer. Therefore, I wanted to create a mutant that would disrupt the complex and study the resulting proteins *in vivo*. To this

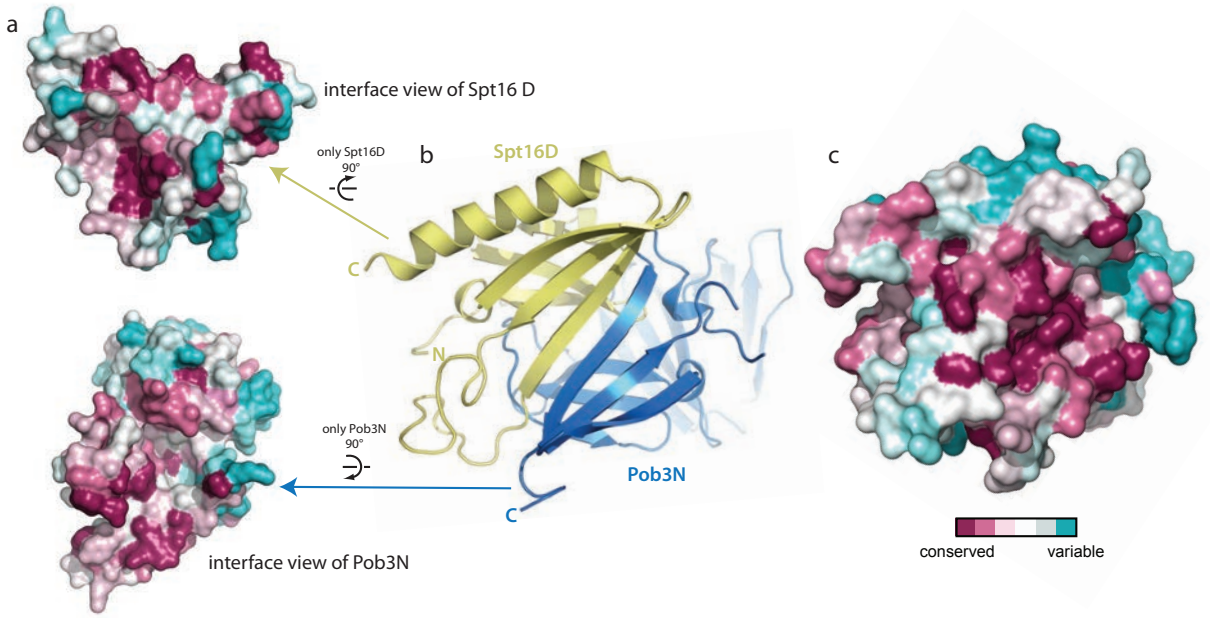

Fig. 5.2: **Conservation of the Spt16D-Pob3N surface.**
(a) Conservation surface view of the Spt16D and Pob3N interaction faces without the binding partner. Highly conserved residues in *pink* and variable residues in *green*. (b) Cartoon representation of Spt16D (*yellow*) and Pob3N (*blue*). (c) Conservation surface view in the same orientation.

goal, I created a series of interface point mutants and tested tested them for their ability to interact with the complex partner.

First, I screened the mutants by coexpression of His-V5-Pob3N and untagged Spt16D in *E. coli*. After lysis in high salt buffer (500 mM NaCl) and centrifugation, the cleared lysate (SN fraction) was incubated with Ni-NTA sepharose beads to enrich for the His-tagged Pob3N. After extensive washing, bound protein was eluted with imidazole (E fraction) and analyzed by SDS-PAGE and Coomassie staining. While wild-type Spt16D co-purified with Pob3N, two mutants of Spt16D (V624R L627R or V624E R625A L627E) did not (Figure 5.3a).

Next, I wanted to verify this result by pull-down with individually expressed recombinant V5-Pob3N and Spt16D. While Spt16 wild-type and the V624 L627 mutant could be purified by themselves, the triple mutant V624E R625A L627E was prone to aggregation (presumably because the protein fold is somehow disturbed) and not used further. Therefore, I worked only with the double mutant. V5-Pob3 was bound to beads and incubated with Spt16D (wild-type or mutants thereof) in 300 mM NaCl, 25 mM Tris pH 7.5, 0.05% NP40. After extensive washes with binding buffer, bound protein was analyzed by SDS-PAGE and Coomassie staining. While wild-type Spt16D co-precipitated with Pob3N, the interface mutant Spt16D V624R L627R did not (Figure 5.3b). Therefore, although the interface between Spt16D and Pob3N is very large and salt-stable, I it could be disrupted by mutation of only two interface residues, Val624→Arg and Leu627→Arg (Figure 5.3), which allows us to test the relevance of hetero-dimerization *in vivo*.

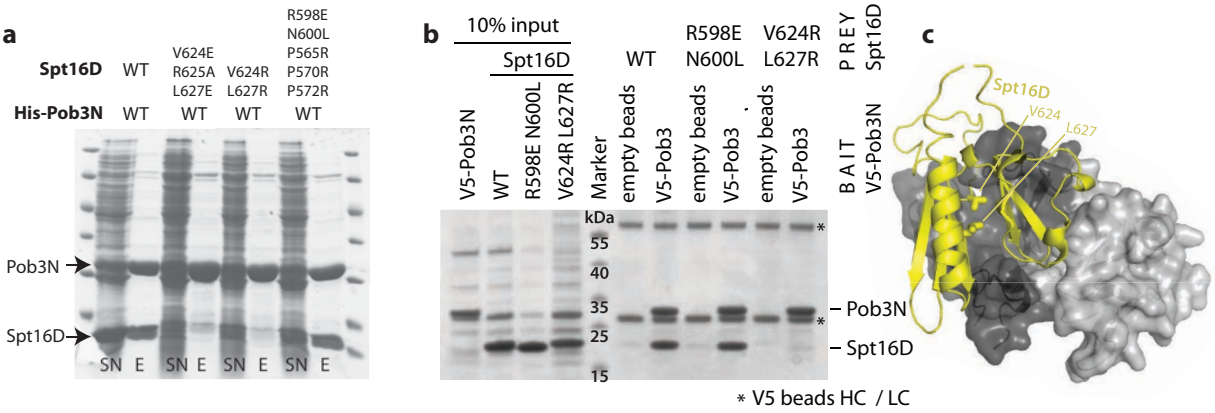

Fig. 5.3: **Mutation of two residues prevents interaction of Spt16D and Pob3N.**
(a) Coexpression of His-V5 tagged Pob3N with untagged Spt16D. SN = supernatant after centrifugation of the crude lysate, E = eluate from Ni-NTA-sepharose. While wild-type Spt16D co-purifies with Pob3N, interface mutants do not. (b) In V5-pulldowns, wild-type Spt16D coprecipitates with V5-Pob3N, but the interface mutant V624R L627R does not. (c) Location of Spt16 V624 and L627 (sticks); Spt16 D in *yellow* cartoon representation, Pob3N as *grey* surface.

5.2 Spt16D-Pob3N does not bind histones

Since Spt16D-Pob3N is formed of PHL domains just like Spt16M and Pob3M, I tested wether it binds histones like these. I had already shown that it did not interact with H2A-H2B in pull-down assays (Figure 4.1). Similarly, I tested for H3-H4 binding: recombinant V5-tagged FACT domains were bound to beads and incubated with soluble H3-H4; after extensive washing bound protein was analyzed by SDS-PAGE and Coomassie staining. H3-H4 bound strongly to Spt16M and weakly to Spt16N or Pob3M, but not to the heterodimerization domain Spt16D-Pob3N (Figure 5.4). Thus, although Spt16D and Pob3 share the same basic fold as the tandem PHL modules of Spt16M and Pob3M, they do not seem to be histone binders.

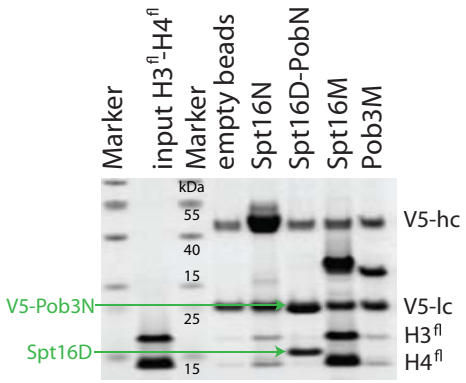

Fig. 5.4: **Spt16D-Pob3N is the only globular domain of FACT that does not interact with H3-H4.**
V5-immunoprecipitations of FACT's globular domains with full-length histones H3-H4. The assay was performed in 300 mM NaCl, 25 mM Tris pH 7.5, 0.05 % NP40; bound protein was analyzed by SDS-PAGE / Coomassie. The heterodimerization domain (Spt16D-Pob3N) does not recognize H3-H4.

5.3 The heterodimerization domain couples FACT to the replication machinery

FACT is known to interact with many non-histone proteins, I tested *S. cerevisiae* whole cell lysates (WCL) expressing TAP-tagged candidates for co-precipitation with the Spt16D-Pob3N heterodimer. Recombinant V5-tagged FACT proteins were immobilized on beads and incubated with the respective WCLs. After extensive washes (50 mM Tris pH 7.5, 100 mM NaCl, 0.15 % NP40, 1.5 mM $MgCl_2$, 0.3 mM DTT), bound protein was analyzed by SDS-PAGE and western blot with antibodies against the TAP-tag. Many tested TAP-tagged proteins were 'sticky' and bound nonspecifically to beads. In contrast, for the TAP-POL1 WCL, the result was very clean: the protein interacted (directly or indirectly) with full-length Spt16, the heterodimerization domain and Spt16D in particular (Figure 5.5). This suggested that Spt16D may couple the chaperone to the replication machinery, in addition to Pob3M binding to RPA (replication protein A) [**?**].

A region encompassing *S. cerevisiae* residues [469-717] was shown to interact with the replication machinery, through ubiquitination by the E3 ligase Rtt101 [**?**]. Their region covers most of the Spt16D domain (residues [521-642] in *C. thermophilum* and [533-651] in *S. cerevisiae*). This supports my results and implies that the interaction I observed might be ubiquitination-dependent.

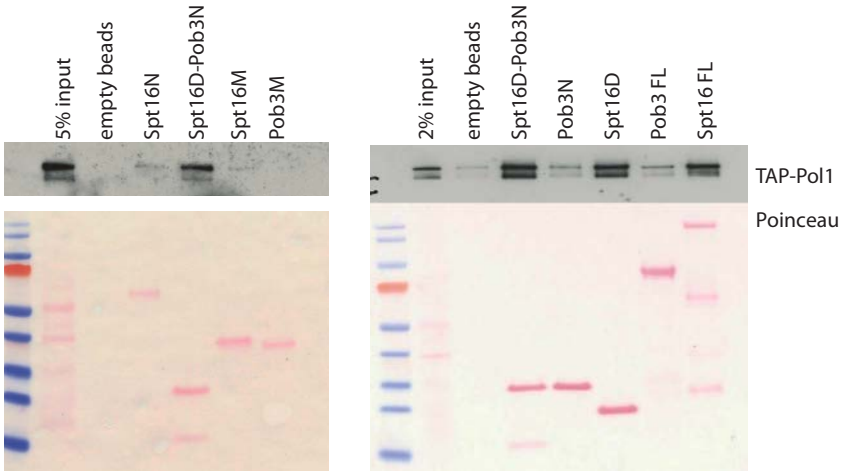

Fig. 5.5: **Spt16D interacts with POL1 from yeast whole-cell lysate.** Recombinant V5-tagged FACT proteins were bound to beads and incubated with WCL from yeast expressing TAP-POL1; bound proteins were analyzed by western blot against the TAP tag. As a loading control for bound V5-tagged proteins, the membrane was stained with Poinceau. Spt16D is sufficient for interaction with POL1.

6 Outlook

6.1 A domain-wise structural summary of the holo-FACT complex

Together with the published structures of Spt16N [**??**] and Pob3M [**?**], the structure of all globular domains of FACT have now been solved (Figure 6.1). All structures are based on yeast protein sequences, but since the sequence and the secondary structure predictions are very conserved, we can assume that the observed features also apply to the proteins from human and other species.

Apart from Spt16N, which adopts a pitabread / peptidase fold, all domains consist of PHL (pleckstrin homology like) domains, and thus might have originated from domain fold amplification during evolution. Pleckstrin homology (PH) domains are very common in the human proteome, and also occur several times in the yeast genome. Some of them, though less than 10 %, bind phosphoinositides for targeting to cellular membranes [**?**]. They also serve as interaction modules with other proteins, e.g. ubiquitin [**?**].

The linkers connecting the globular domains are predicted to be (at least) partially α-helical, but I assume that they are not rigidly connecting the globular domains. Thus, each domain may act as a more or less 'independent' unit that binds histones or other nuclear factors. Tethering the domains together might have recruiting function, or 'keep things in place' (e.g. the chaperone or bound proteins) and thus increase processivity of nuclear processes.

Although only one domain of FACT (Spt16M) can bind histones H2A-H2B, three out of the four globular domains interact with H3-H4: Spt16N interacts with both the tails and the globular core of the histone dimer [**?**]. Spt16M seems to be the strongest binder and recognizes primarily a peptide spanning H3 residues [46-65]. Which region of H3-H4 is recognized by Pob3M has not yet been mapped; it will be interesting to see whether it binds H3αN like Rtt106 and Spt16M or some other region. This might allow further mechanistic conclusions about holo-FACT interaction with the H3-H4 dimer and for reorganization of the nucleosome particle.

Two of the FACT domains were shown to interact with the replication machinery: Pob3M interacts with RPA, the single-stranded DNA binding protein [**?**], and Spt16D precipitates POL1 of the DNA primase complex from yeast whole cell extract (section 5.3). This suggests that it is very important to couple the chaperone to the replication machinery, where it might be involved in nucleosome (re-)assembly during DNA replication and chromatin duplication.

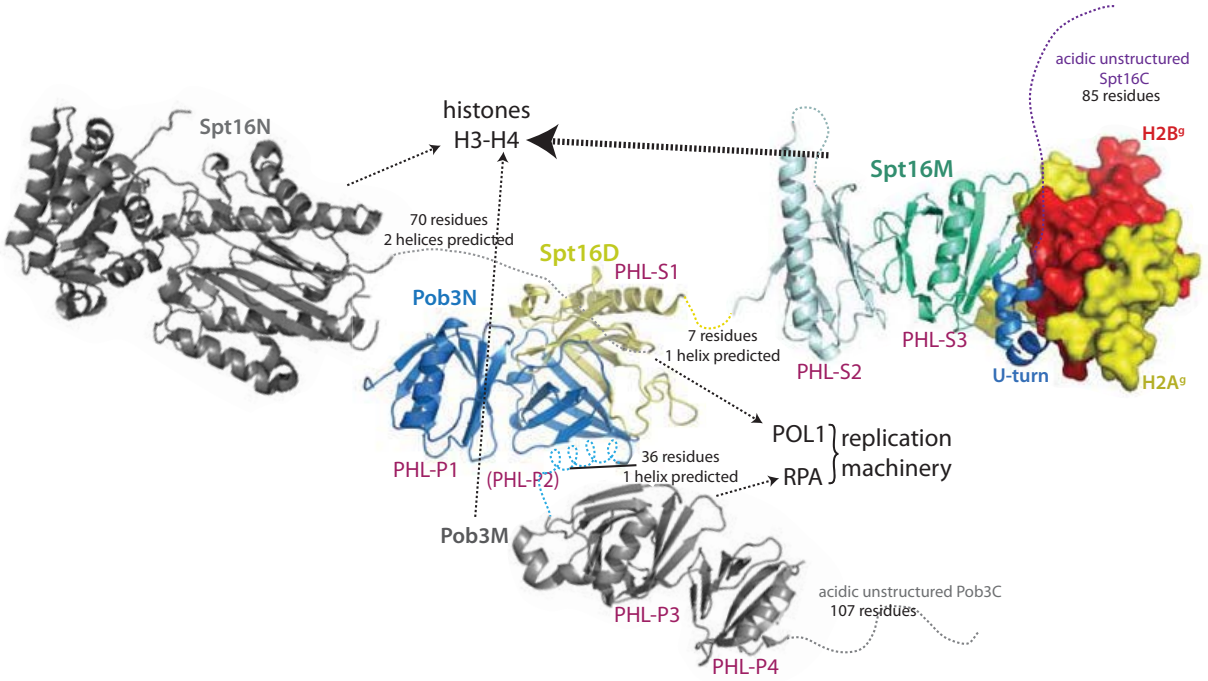

Fig. 6.1: **A domain-wise model of holo-FACT.**
The crystal structure of all FACT domains has been solved. Published structures in *grey*, new structures in *colour*. Spt16N (PDB code 3CB5), the heterodimerization domain Spt16D-Pob3N (PDB code 4KHB), Pob3M (PDB code 2GCJ), Spt16M in complex with H2A-H2B (this work, PDB code 4KHA). Linkers and unstructured regions are depicted as dotted lines. All globular domains except Spt16N consist of PHL domains with distinct molecular functions. The PHL domains are numbered according to the protein subunit, with PHL domains of Spt16 as PHL-S#, and PHL domains of Pob3 as PHL-P#. Spt16N, Pob3M and particularly Spt16M bind histones H3-H4. Spt16M engages histones H2A-H2B, as revealed by my crystal structure of the Spt16M–H2A-H2B complex. Spt16D and Pob3M bring the two subunits together and tether the comprehensive histone binding complex to the replication machinery.

6.2 The full picture: how does holo-FACT interact with the nucleosome?

6.2.1 Possible methodical approaches: SAXS, cryoEM and cross-linking/MS

The ultimate goal is to understand how holo-FACT interacts with the nucleosome and reorganizes its DNA-histone contacts, to allow progression of DNA and RNA polymerases, and at the same time keep chromatin intact. Towards this goal, I would like to have 'snaphots' of the full chaperone bound to the NCP, if possible at different stages of reorganization. Methods like **SAXS** or **cyroEM** would produce an envelope into which the crystal structures of the individual domains could be fitted. To allocate signal, it might be useful to work with a series of FACT truncation constructs and antibodies against individually tagged domains. **Crosslinking** studies, coupled to mass-spectrometric analysis of the resulting chimeric peptides, might help to refine the intra- and inter-molecular interactions.

6.2.2 A first glimpse: setting up a purification protocol suitable for cryoEM studies.

Initial experiments to prepare the FACT-NCP complex for cryoEM were performed. Using GraFix (density gradient-based mild crosslinking) [**?**], the complex could be purified to homogenity and gave promising initial negative stain or cryo-EM pictures (Figure 6.2).

Interestingly, while developing the purification protocol, I observed that Spt16 seems to oligomerize (weakly), since the protein itself forms distinct bands of increasing molecular weight (a 'ladder') when subjected to GraFix (Figure 6.2d). If this holds true *in chromatin*, it might help to tether the chaperone to the nucleosome fiber: FACT is very abundant and a ratio of one chaperone per nucleosome was estimated for transcribed regions, so oligomerization along transcribed ORFs is possible in terms of number. In consequence, this would also hold the histones in place and thus stabilize chromatin structure, as required for suppression of cryptic transcripts.

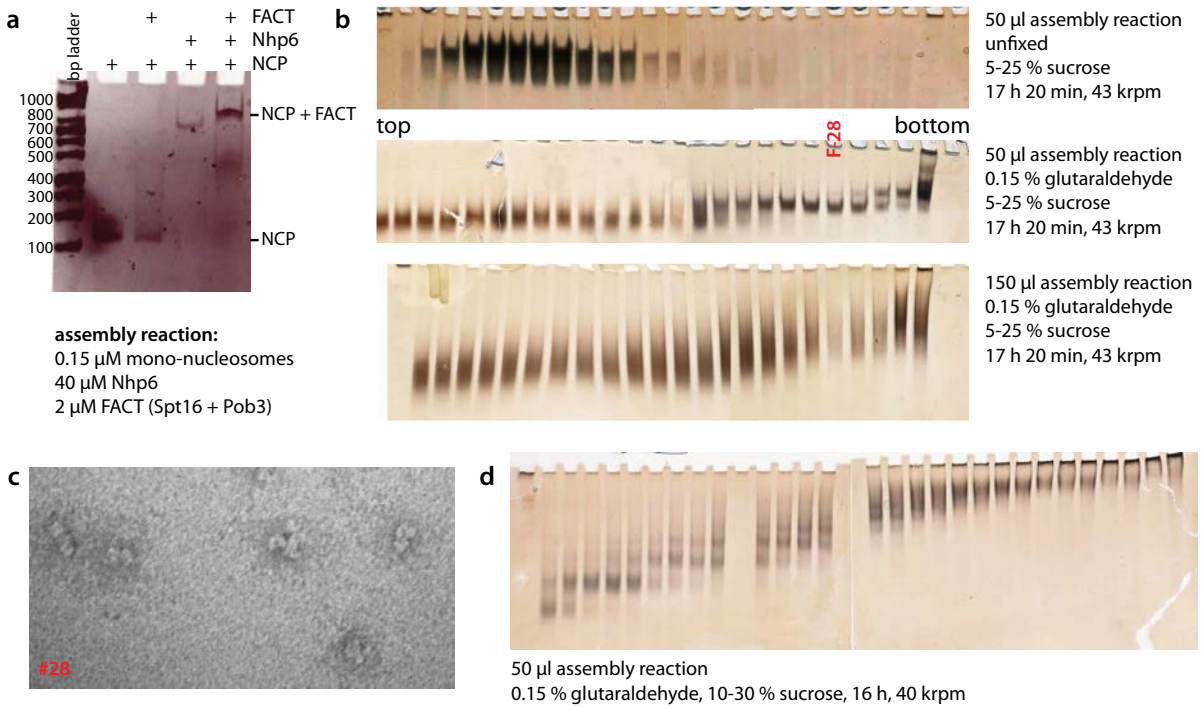

Fig. 6.2: **Purification of the FACT-NCP complex for cryoEM.**
(a) Assembly of the FACT-NCP complex from recombinant material and visualization by Native PAGE and Ethidium Bromide staining. (b) Purification of crosslinked complexes by GraFix gives fractions containing only one defined species (fraction F-28), as seen by Native PAGE / silver staining. 'top' and 'bottom' of the sucrose gradient are labelled. Increasing the amount of assembly reaction results in nonspecific cross-linking and 'smearing' of the bands. (c) Representative cryoEM Image for fraction F-28. (d) Higher molecular species of the GraFix mixture, which were unresolved at the bottom of the gradient in (b), can be resolved by a lower density sucrose gradient; the observed 'ladder' is probably caused by oligomerization of the Spt16 protein.

6.3 Immediate follow-up work on the structural and biochemical work described

Several experiments should follow up the work on Spt16M, to refine our knowledge of how such a complex chaperone interacts with histones H2A-H2B and H3-H4, and how these individual interactions complement and influence each other.

6.3.1 Refining the H3-H4 interaction with the Spt16M and Pob3M tandem PHL domains

First, it should be analyzed which parts of Spt16M contribute to H3-H4 binding. This would give insight into how H3-H4 binding cooperates or conflicts with H2A-H2B binding. Most information could be gained from a crystal stucture, e.g. by desinging a tethered construct similar to the one used for the complex with H2A-H2B, or by trying to obtain crystals with the [46-65] peptide (or truncated versions thereof). Insight might also come from detailed biochemical studies (e.g. peptide pull-down experiments with point mutants of Spt16M) or genetic studies (e.g. testing whether mutation of conserved residues changes the sensitivity to certain chemicals, which can be indicative of a defect in replication, transcription or heterochromatic silencing, as done by **?** for Pob3M).

Similar work should also be performed for Pob3M, especially on the histone side and biochemically on the chaperone, since **?** already did an extensive genetic mapping (section 4.6).

6.3.2 The effect of H3 K56 acetylation on Spt16M binding

Of great interest to the chromatin community is how histone modifications influence the interaction with 'reader' proteins. Acetylation of H3 K56 enhances binding to the Rtt106 chaperone *in vitro* and *in vivo* [**?**], and it would be interesting to see whether the same is true for Spt16M. Towards this goal, I am trying to study by ITC the interaction between Spt16M and H3 [46-65] peptides with or without the modification. Further, I want to see whether H3-H4 still co-precipitates with the chaperone when the histone acetyl-transferase for H3 K56 (Rtt109) is deleted and thus no K56 acetylated H3 present. **?** used this experimental setup to show that Rtt106 requires K56 acetylation to bind H3-H4 *in vivo*, while Pob3 functions independently of the modification.

As Tobias Stuwe already pointed out in his thesis, the PHL-1 of Spt16M contains a pocket lined by highly conserved, hydrophobic residues that looks a lot like a bromodomain acetyl-pocket. At the bottom, an asparagine (Asn713) residue might repulse unmodified, positively charged lysine residue (Figure 6.3).

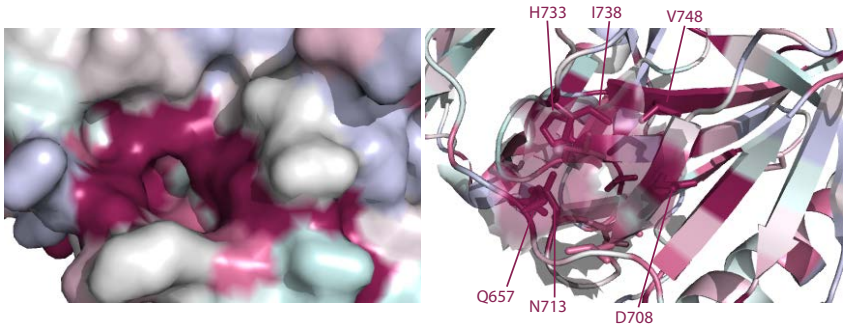

Fig. 6.3: **A conserved bromo-like pocket in PHL-1 might bind acetylated lysines.** Close-up view of the 'bromo-like' pocket on Spt16M PHL-1. Completely conserved residues are marked *pink*. Highly conserved residues that contribute to the putative acetyl-lysine binding pocket are labeled.

6.3.3 Defining the role of Spt16C in histone binding

Although we know that it adds a high-affinity exothermic component to the interaction between Spt16 and H2A-H2B, the relative contribution of Spt16C to histone H2A-H2B binding is not yet clearly defined, Since Spt16C could not be expressed and purified properly, it will be neceassary to compare Spt16M [651-944] to Spt16MC, encompassing residues [651-1029].

I suspect that Spt16C interacts mostly with the charged histone, therefore experiments to be performed include ITC, size exclusion chromatography and 'kinetic' pull-downs both with full-length and tail-less histones H2A-H2B. Further, I observed that H3-H4 could outcompete H2A-H2B from binding to Spt16M (section 4.6), and it would be interesting to test whether this holds true for the Spt16MC construct. Further, it should also be tested whether Spt16C contributes to binding of the H3-H4 dimer.

More detailed mapping might be possible through crosslinking studies; I presume that the flexibility of the Spt16C domain will prevent crystallization.

6.4 Systematic analysis of histone binding in yeast *in vivo*

One big goal for the detailed analysis of FACT function would be to transfer the biochemical results to an *in vivo* system, e.g. an analysis of the mutants deficient for histone binding *in vitro* for their phenotype *in vivo*. The *C. thermophilum* Spt16 constructs bearing an N-terminal V5-tag are suitable for most of the studies proposed. It seems to be necessary to work in a Δ*spt16* background, because otherwise expression of the Spt16 constructs is very low (*data not shown*).

I suggest to work with the following sets of Spt16 constructs:

- Insertion of the U-turn mutant, the acidic patch mutant and any other Spt16M mutant of interest, into the full-length Spt16 sequence, as already established for some (section 4.8). With these constructs, the effect of the individual patches to which a function could be ascribed *in vitro*, can be studied *in vivo*.

- A series of domain truncation constructs, first of each individual FACT domain (Spt16N, Spt16D (which will pull down Pob3N), Spt16M, and Pob3M) and second

a set of systematic deletions of one or two domains. With these constructs, the role of individual domains could be studied.

Experiments should include the following:

- **IP of H2A-H2B and H3-H4 from yeast whole cell extract**. Antibodies for the histones are available, but during initial tests I realized that the signal might be too weak (maybe because of the low expression of the V5-tagged Spt16 constructs in wild-type background, *data not shown*) and therefore, expression of tagged histones is preferential.

- **IP from yeast whole-cell extract, coupled to mass spectrometric analysis**. First, this experiment would allow one to see whether any histone modification is specifically enriched in the FACT-bound histone pool. Second, it might help to dissect with which FACT domain the many functional partners of the complex interact, and this might already hint towards a 'pathway' function for the individual domains.

- **Chromatin Immmunoprecipitation (ChIP) analysis.** First, it will be interesting to determine which domains of FACT actually localize to chromatin and thus might be recruiting the complex. Second, it would be interesting to see *where* the domains interact, e.g. at transcribed regions or replication origins. Third, one could study which parts of FACT contribute to the propagation of the complex from the promoter of a gene into the open reading frame.

6.5 FACT & nucleosome breathing

From the superposition of the Spt16M - H2A-H2B complex onto the nucleosome structure, I postulated that the chaperone could enhance 'breathing' of the nucleosomal DNA ends, and this could of course be tested.

FACT or Spt16 bind only weakly to NCPs, they require the presence of the helper protein Nhp6 (Figure 6.2a). Nhp6 itself distorts the DNA around the octamer core [**?**] and would thus blur the result, but this can presumably not be avoided and would hopefully not be stronger than the Spt16-Pob3 signal.
Possible experimental setups include:

- Increased **nuclease accessibility** of the nucleosomal DNA ends, as observed by [**?**]. In particular, the nucleosomes would be treated with DNA-digesting enzymes or chemicals. Incubation of the NCP with FACT should change the accessibility of the DNA at the sites where FACT is bound.

- **FRET** assays (Foerster Resonance Energy Transfer, either as ensemble or single-molecule studies) or **EPR** studies (Electron Paramagnetic Resonance), which are spectrometric methods to measure the distance between two dyes in the range of 20 - 70 (EPR) or 100 (FRET) $\mathring{A}$. If the dyes are e.g. positioned on the histone octamer and the DNA molecule, one would hope to see an increase in distance between the two dyes upon FACT binding. In parallel, a dye pair positioned on the octamer and on FACT, close to the Spt16M U-turn motif, could be used to verify that Spt16M binds the H2Bα1 helix also in the nucleosomal context.

6.6 Biochemical characterization of the FACT heterodimerization domain

6.6.1 Mapping the POL1 interaction

The Spt16D domain of FACT interacts with POL1, and the interaction might be regulated by ubiquitination of the domain [?]. Initial attempts to identify a point mutant that disrupts POL1 binding have failed so far (*data not shown*), but only a limited number of highly or completely conserved residues (∼20) was tested as single point mutants. Since the domain is not large (122 amino acids) I assume that it should be feasible to identify a mutant that disrupts POL1 binding, for example by testing all the most conserved residues in batches of three, or by specifically testing lysine residues (in compliance with the ubiquitin hypothesis). Such a mutant would be a great tool to study the role of FACT in replication.

One should also further map the interaction between Spt16D and POL1 on the polymerase side, and further test whether the mutually exclusive binding of FACT and Ctf4 to POL1 [?] holds true when only the Spt16D domain is used instead of the holo-complex.

6.6.2 Spt16D has structural homology to TFIIH, and they might share a evolutionary conserved interaction with TFIIE

A search for structural homologues of Spt16D on the DALI server [?] identified the pleckstrin-homology like domain in Tfb1, the large subunit of the TFIIH general transcription factor complex [?] (Figure 6.4a) (Z-score = 8.3, r.m.s.d. of superimposed backbone atoms = 3.4 $\AA$, 90 of 115 Tfb1 residues aligned with 10 % sequence identity). Interestingly, this protein interacts with Tfa1, a subunit of the TFIIE complex, through a conserved hydrophobic pocket [?] (Figure 6.4b, c). TFIIH contains a helicase that helps to 'melt' the promoter DNA double-helix and a kinase that phosphorylates the CTD of Pol II; TFIIE is also involved in melting promoter DNA. A structurally homologous interaction seems to couple human Tfb1 also to the DNA repair machinery (Rad2) and p53 (Figure 6.4c) [?].

The residues of Tfb1 interacting with Tfa1, Rad2 and p53 are conserved in Spt16D, both in sequence (Figure 6.4b) and in location (Figure 6.4d), and are highly conserved within the domain across evolution (Figure 6.4e). Thus, it is tempting to speculate that Spt16D might also interact with Tfa1 and Rad2 (p53 does not exist in yeast) and thereby couple the chaperone to the transcription machinery. An interaction between full-length FACT and Tfa1 has already been described [?]; if this truly maps to Spt16D this domain would couple FACT not only to the replication machinery (see section 5.3) but also to the transcription machinery.

It is worth noting that the human arginine residue (R569) corresponding to *Chaetomium* R598 was found mutated in certain cancers (COSMIC database: p.R569Q / c.1706G→A; carcinoma of the large intestine (1 sample) [?]).

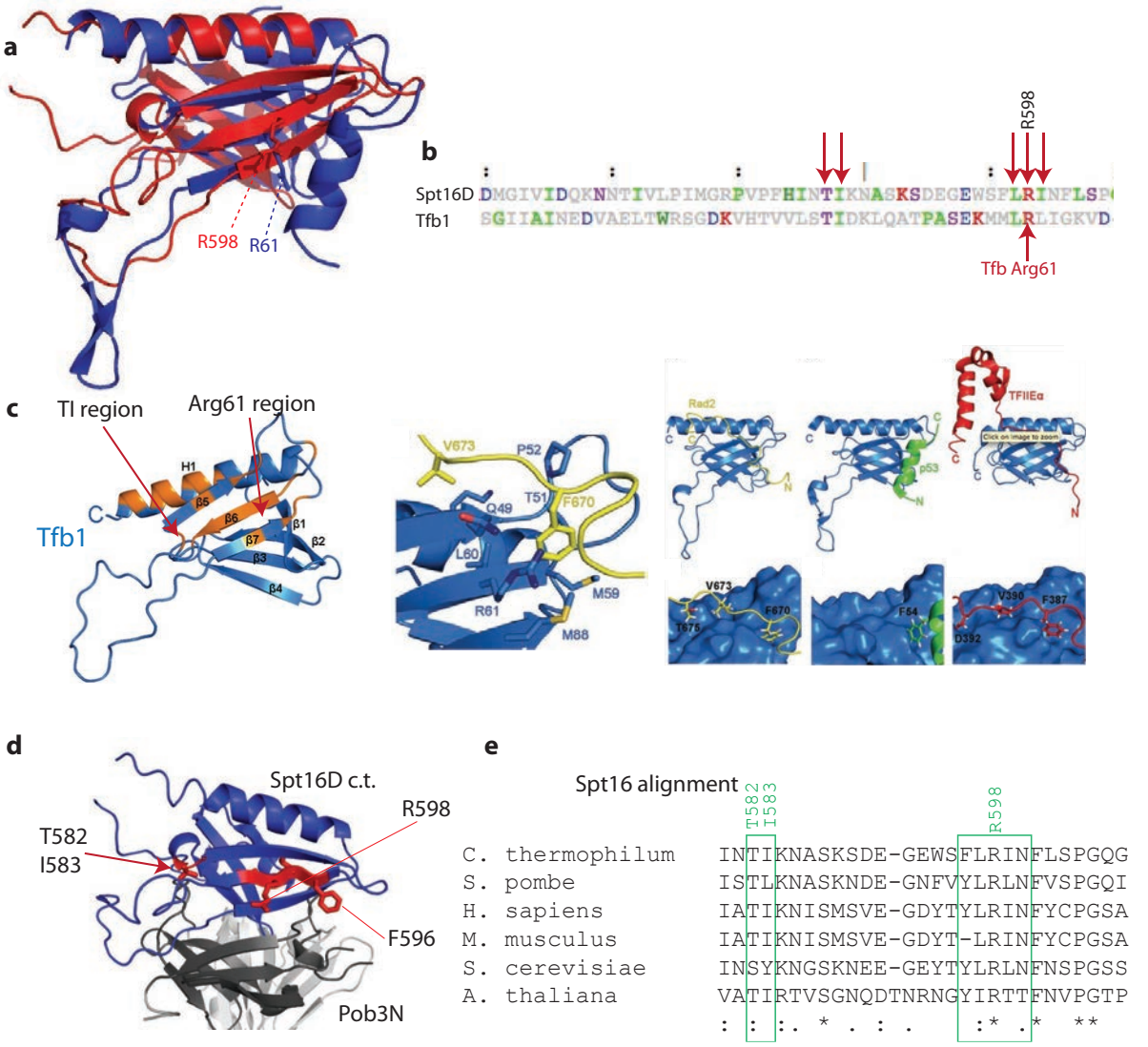

Fig. 6.4: **Spt16D is structurally homologous to Tfb1 of TFIIH and might couple FACT to the transcription initiation machinery.**
(a) A DALI search identified Tfb1 (*blue*) of the TFIIH complex as a structural homologue of Spt16D (*red*), the r.m.s.d. of superimposed backbone atoms is 3.4 *Å*. A highly conserved arginine residue is labeled. (b) They also share high sequence homology; residues involved in the interaction between Tfb1 and Tfa1 of the TFIIE complex (e.g. Arg61 of Tfb1) which are highly conserved (*red* arrows). (c) Tfb1 interacts with Tfa1 of the TFIIE complex and similarly with Rad2 and p53. Figures are taken from [**?**]. (d) Location of residues conserved between Spt16D and Tfb1 on the Spt16D structure. (e) ClustalW sequence alignment of partial Spt16D sequences. Residues involved in the Tfb1-Tfa1 interaction are structurally and evolutionary conserved in Spt16D.

6.7 Studies of the human FACT protein and its function in DNA repair

6.7.1 How is FACT recruited to sites of DNA repair?

FACT recruits to sites of DNA repair and promotes the exchange of phosphorylated γH2A.X for the unmodified form, and thus removes the 'recruiting' signal for the repair machinery [**?**]. PARP1-mediated ADP-ribosylation of FACT inhibits its histone exchange activity and stabilises H2A.X at sites of DNA damage repair [**?**]. Since my host lab intensively studies ADP-ribosylation and its role in DNA repair using biochemical, structural and in particular live cell imaging methods [**??**], it would be interesting to extend the studies to the FACT chaperone complex. We would like to study FACT's role in chromatin reorganization at sites of DNA repair, as well as its interactions with the repair machinery. As a starting point, I am currently cloning the human Spt16 and Pob3 proteins into suitable live cell imaging vectors.

6.7.2 Histone modifications might regulate the timely recruitment of FACT to sites of DNA repair

Upon DNA damage and double-strand break (DSB) formation, two histone residues seem to be methylated with signalling function: human H3 K36 gets methylated [**?**], and maybe also yeast or human H2B K46 [**?**]. H3 K36me1 was shown to disrupt FACT binding [**?**]. H2B K46 contributes to the electrostatic 'fence' that stabilizes the interface between Stp16M's U-turn and H2Bα1; methylation thereof should also decrease FACT binding to the histone. In addition, FACT was shown to get ribosylated during early DNA repair signalling, and ADP-ribosylation abrogates H2A-H2B binding [**?**]. Taken together, all these modifications prevent FACT from binding to sites of DSB in the 'early phase'.

After repair was successful, some signalling checkpoint will activate enzymes that remove the methylation and ribosylation marks. Subsequently, FACT can bind and exchange phosphorylated γH2A.X for the unmodified form; this signals for the end of the repair phase. The modifications would thus set the timer for a delayed FACT response that gives γH2A.X sufficient time to recruit the repair machinery and other factors.

It would be interesing to study this structure-bases hypothesis in a combined biochemical and cell culture / imaging approach, e.g. by observing the time course of histone modification occurence, their ability to repulse FACT binding, and to identify the enzymes that deposit and remove these modifications and study their knock-out phenotype.

List of Figures

7 Appendix I: List of abbreviations

α	alpha-helix (protein secondary structure)
ac	acetylation, histone modification
bp	base pair
ATP	adenosine tri-phosphate
DNA	deoxyribo-nucleic acid
DSB	double-strand break
EM	electron microscopy
FACT	facilitates chromatin transcription
H2A-H2B	histones 2 A and 2 B
HAT	histone acetyl transferase
HU	hydroxy-urea, a drug used to test for defects in replication
ITC	isothermal titration calorimetry
IP	immuno-precipitation
L	loop (protein secondary structure)
me	methylation, histone modification
MNase	micrococcus nuclease
MW	molecular weight
NCP	nucleosome core particle
ORF	open reading frame (of a gene)
PHL	pleckstrin homology like (domain)
PTM	post-translational modification
SD	Superdex, a gel filtration resin (dextran covalently attached to highly cross-linked agarose)
SDS-PAGE	SDS-Poly-Acrylamide-Gel-Electrophoresis
SEC	size-exclusion chromatography
SHL	super-helical location of the nucleosome = attachment point of the DNA double helix on the octamer surface
Spt-	yeast genetic phenotype; indicative of defects in transcription and disrupted chromatin structure.
Spt16M	Spt16 middle domain
TAP	tandem affinity purification (epitope tag), composed of calmodulin, a TEV cleavage site, and Protein A
TFII	transcription factor (RNA Polymerase) II
ub	ubiquitination, histone modification
V5	an epitope tag (GKPIPNPLLGLDST), derived from the RNA polymerase alpha subunit of simian virus 5
WCL	whole cell lysate

8 Appendix II: Constructs used in this study

Construct Name	Location	Selection
pETMCN HisV5 Spt16 c.t. 651-944	CL2538	Ampicillin
pETMCN His Spt16 c.t. 651-944	CL2537	Ampicillin
pETMCN His V5 Spt16 c.t. FL	CL2167	Ampicillin
pETMCN His V5 Spt16 c.t. 1-650, GSGSGS, 945-1029	CL3047	Ampicillin
pETMCN His V5 Spt16 c.t. 1-447	CL2564	Ampicillin
pETMCN His V5 Spt16 c.t. 651-818	CL2203	Ampicillin
pETMCN His V5 Spt16 c.t. 810-944	CL2202	Ampicillin
pETMCN His V5 Spt16 c.t. 772-944	CL2201	Ampicillin
pETMCN His V5 Spt16M c.t. 651-926	CL2929	Ampicillin
pETMCN His V5 Spt16 c.t. M 651 - 910	CL2938	Ampicillin
pETMCN His V5 Spt16 c.t. N916A V919A I920A T923A D934A F939A L940A	CL2935	Ampicillin
pETMCN His V5 Spt16 c.t. D934S F939S L940S	CL2950	Ampicillin
pETMCN His V5 Spt16 c.t. N916S V919S I920S T923S	CL2951	Ampicillin
pETMCN His V5 Spt16 c.t. 651-944 D902A S903A D905A	CL2264	Ampicillin
pETMCN His V5 Spt16 c.t. L915R F939R L940R	CL2907	Ampicillin
pETMCN His V5 Spt16 c.t. L913R L915R	CL2878	Ampicillin
pETMCN His V5 Spt16 V919R I920R	CL2875	Ampicillin
pETMCN His V5 Spt16 L915R I920R	CL2872	Ampicillin
pETMCN His V5 Spt16 h.s. 643-929	CL2940	Ampicillin
pETMCN His V5 Pob3 c.t.	CL2165	Ampicillin
pETMCN His V5 Pob3 c.t. 206-485	CL2563	Ampicillin
pETMCN His V5 Pob3 c.t. 1-192	CL2559	Ampicillin
pETMCN His Spt16 c.t. (1-944) - 6link (GGS)4 - H2B(24-122), H2A (13-106)	CL2811	Ampicillin
pETMCN His Spt16 c.t. (1-944) - 12link (GGS)4 - H2B(24-122) H2A (13-106)	CL2810	Ampicillin
pETMCN His Spt16 c.t. 521-642	CL2826	Ampicillin
pETMCN His V5 Spt16 c.t. 521-642	CL2811	Ampicillin
pETMCN His Spt16 c.t. 521-642 V624R L627R	CL2828	Ampicillin
pETMCN His Spt16 c.t. 521-642 R598E N600L	CL2827	Ampicillin
pETMCN untagged Spt16 c.t. 521-642	CL2558	Ampicillin
pETMCN untagged Spt16 c.t. 521-642 V624E R625A L627E	CL2747	Kanamycin
pETMCN untagged Spt16 c.t. 521-642 V624R L627R	CL2746	Kanamycin
pETMCN untagged Spt16 c.t. 521-642 R598E N600L P565R P570R P572R	CL2722	Kanamycin
YPLac33(-NheI)	CL2276	Amp / URA3
YPLac111(-NheI)	CL2277	Amp / LEU2
YPLac111(-NheI) Spt16 s.c. plus Spt16 c.t. 651-942	CL2301	Amp / LEU2
YPLac111(-NheI) Spt16 s.c. plus Spt16 c.t. 651-944 stop	CL2302	Amp / LEU2
YPLac111(-NheI) Spt16 s.c. plus Spt16 c.t. 651-942 Q930R	CL2916	Amp / LEU2
YPLac111(-NheI) Spt16 s.c. plus Spt16 c.t. 651-942 L913R, L915R	CL2915	Amp / LEU2
YPLac111(-NheI) Spt16 s.c. plus Spt16 c.t. 651-942 V919R, I920R	CL2914	Amp / LEU2
YPLac111(-NheI) Spt16 s.c. plus Spt16 c.t. 651-942 L915R, I920R	CL2913	Amp / LEU2
YPLac111(-NheI) Spt16 s.c. plus Spt16 c.t. 651-942 D902A S903A D905A	CL2444	Amp / LEU2
YPLac111(-NheI) Spt16 s.c. plus Spt16 c.t. 651-942 E899R D902R D905R	CL2912	Amp / LEU2
YPLac111(-NheI) Spt16 s.c. plus Spt16 c.t. 651-942 765 RKRKYRY→AGSGASA	CL2443	Amp / LEU2
YPLac111(-NheI) Spt16 s.c. plus Spt16 c.t. 651-942 N869A D871A	CL2442	Amp / LEU2
YPLac111(-NheI) Spt16 s.c. plus Spt16 c.t. 651-942 R862A V863A	CL2441	Amp / LEU2
YPLac111(-NheI) Spt16 s.c. plus Spt16 c.t. 651-942 F931A	CL2440	Amp / LEU2
YPLac111(-NheI) Spt16 s.c. plus Spt16 c.t. 651-942 T923A	CL2439	Amp / LEU2
YPLac111 V5 Spt16 c.t.	CL2924	Amp / LEU2
YPLac111 V5 Spt16 c.t. N916A V919A I920A T923A	CL3046	Amp / LEU2
YPLac111 V5 Spt16 c.t. N916S V919S I920S T923S	CL3002	Amp / LEU2

YPLac111 V5 Spt16 c.t. D934S F939S L940S	CL3001	Amp / LEU2
YPLac111 V5 Spt16 c.t. Q930A D934A	CL2978	Amp / LEU2
YPLac111 V5 Spt16 c.t. D902A S903A D905A	CL2977	Amp / LEU2
YPLac111 V5 Spt16 c.t. M 651-944	CL2932	Amp / LEU2
YPLac111 V5 Spt16 c.t. MC 651-1026	CL2931	Amp / LEU2
pET3a H2A x.l.	CL0103	Ampicillin
pETMCN untagged H2A x.l. 13-106	CL2622	Ampicillin
pET3a H2A x.l.13 - 129	CL3068	Ampicillin
pET3a H2B x.l.	CL0104	Ampicillin
pET3a H2B x.l. 24-122	CL3069	Ampicillin
pET3a H2B x.l. Y80E	CL2619	Ampicillin
pET3a H2B x.l. I36E	CL2617	Ampicillin
pET3a H4 x.l.	CL0106	Ampicillin
pET3a H3 x.l.	CL0105	Ampicillin

9 Appendix III: Manuscripts

9.1 *Review:* The chaperone-histone partnership: for the greater good of histone traffic and chromatin plasticity

Hondele M, Ladurner AG.

Curr Opin Struct Biol. 2011 Dec;21(6):698-708. doi: 10.1016/j.sbi.2011.10.003. Epub 2011 Nov 3.

Histones are highly positively charged proteins that wrap our genome. Their surface properties also make them prone to nonspecific interactions and aggregation. A class of proteins known as histone chaperones is dedicated to safeguard histones by aiding their proper incorporation into nucleosomes. Histone chaperones facilitate ordered nucleosome assembly and disassembly reactions through the formation of semi-stable histone-chaperone intermediates without requiring ATP, but merely providing a complementary protein surface for histones to dynamically interact with. Recurrent chaperoning mechanisms involve the masking of the histone's positive charge and the direct blocking of crucial histone surface sites, including those required for H3-H4 tetramerization or the binding of nucleosomal DNA. This shielding prevents histones from engaging in premature or unwanted interactions with nucleic acids and other cellular components. In this review, I analyze recent structural studies on chaperone-histone interactions and discuss the implications of this vital partnership for nucleosome assembly and disassembly pathways.

9.2 *News & Views:* A mitotic beacon reveals its nucleosome anchor

Hondele M, Ladurner A.

Mol Cell. 2010 Sep 24;39(6):829-30. doi: 10.1016/j.molcel.2010.09.001.

Mitosis, nuclear envelope formation, and nucleocytoplasmic transport require chromosomes to identify themselves by enriching Ran-GTP around the chromatin fiber. In a recent Nature report, Makde et al. (2010) describe the structure of the Ran activator RCC1 anchored onto nucleosomes.

10 Acknowledgements

This work was carried out at EMBL Heidelberg (October 2007 - April 2011) and the LMU Munich (May 2011 - February 2012). I am very grateful to many people who supported, advised and encouraged me along the way:

First and foremost, I would like to thank my supervisor Andreas Ladurner for his continuous support, scientific guidance and mentorship throughout all these years. I very much appreciate the scientific freedom and respect I enjoyed, to try and fail and succeed in a 'safe', inspiring and generously funded environment.

I am very grateful to my funding agencies, the Boehringer Ingelheim Foundation (BIF), the EU Marie Curie FP6 Research Training Network and the EMBL for their PhD fellowships. I was more than lucky to attend several training events, conferences and summer schools close and far, where I met amazing people that re-set my enthousiasm when it got lost over time and cloning. I would like to thank Claudia Walther (BIF) for her perpetual encouragement to pursue an academic career, this is a big compliment and motivation.

I would like to thank my thesis committee, Patrick Cramer, Darren Gilmour and Christian Häring, for their helpful scientific and strategic discussions.

Success is the ability to go from one failure to another with no loss of enthusiasm. - Winston Churchill
I was very lucky and happy in the 'Ladurner lab' - thanks to:
Tobias, Susanne, Elisa, Gytis and Andy for making all those long hours so enjoyable;
Christiane Kotthoff and Bianca Nijmeijer for their enthousiastic technical support;
Christine Werner, Marzia Sidri, Stephanie Wendlberger, Corey Laverty and Anton Eberharter for help with administration, organization, writing and emergency situations;
Zdenka, Peter, Gerd & Co for help with media and equipment;
Markus, Gyula, Dejana, Marta, Carla, Tamas, Ava, Hari, Barbara, Eva, Sigurd and all the other lab members for discussions and solutions, support and a great time.

I am very grateful to Corey Laverty, Anton Eberharter, Andrew Bowman and Eva Kowalinski for helpful comments on my thesis.

There is no problem so complicated that you cannot find a very simple answer to it if you look at it in the right way. - Douglas Adams
For advice and support on specific scientific techniques, I thank:
Felix Halbach and Markus Hassler for very patiently teaching me crystallography;
Jérôme Basquin and the MPI crystallization platform (Karina Valer & Sabine Pleyer) for generous support and accessibility;
Synchotron staff at SLS (Villigen, CH) and ESRF (Grenoble, FR);
Vladimir Rybin and the EMBL protein core facility for help with ITC and protein expression;
Jürg Mueller, Sandra Hake, Peter Becker, Gunnar Schotta and Silvia Dambacher for gift of peptides and helpful discussion thereof;
Dimitra Keramisanou, Achilleas Frangakis and Marco Faini for help with electron microscopy;
Joachim Griesenbeck, Christian Häring, Jan Medenbach, Sebastian Glatt, Alessandro Ori, Ingmar Schäfer and Fabien Bonneau for helpful discussions of biochemistry.

In the midst of winter, I found there was within me, an invincible summer. - Albert Camus
Flying is learning how to throw yourself at the ground and miss. - Douglas Adams
Life is like riding a bicycle. To keep your balance you must keep moving. - Albert Einstein
Agnes, Lukas, Ulli, Judith, Susi, Tobi, Evelyn, Sara, Lars, Wolfgang, Christian, Ronny, Achi, Selim, Julien, Felix, Sabine, Gytis, Andy, Ingmar, Eva, Maria, Ana, Fabien, Ric and many more: Thanks for being such great friends !

Do not worry if you have built your castles in the air. They are where they should be. Now put the foundations under them. - Henry David Thoreau
I dedicate this thesis to my parents, Maria and Alfred, and my sister Anna, who 'chaperoned', supported and accompanied me throughout my life.

Available online at www.sciencedirect.com

SciVerse ScienceDirect

Current Opinion in Structural Biology

The chaperone–histone partnership: for the greater good of histone traffic and chromatin plasticity

Maria Hondele and Andreas G Ladurner

Histones are highly positively charged proteins that wrap our genome. Their surface properties also make them prone to nonspecific interactions and aggregation. A class of proteins known as histone chaperones is dedicated to safeguard histones by aiding their proper incorporation into nucleosomes. Histone chaperones facilitate ordered nucleosome assembly and disassembly reactions through the formation of semi-stable histone–chaperone intermediates without requiring ATP, but merely providing a complementary protein surface for histones to dynamically interact with. Recurrent 'chaperoning' mechanisms involve the masking of the histone's positive charge and the direct blocking of crucial histone surface sites, including those required for H3–H4 tetramerization or the binding of nucleosomal DNA. This shielding prevents histones from engaging in premature or unwanted interactions with nucleic acids and other cellular components. In this review, we analyze recent structural studies on chaperone–histone interactions and discuss the implications of this vital partnership for nucleosome assembly and disassembly pathways.

Address
Department of Physiological Chemistry, Butenandt Institute of Physiological Chemistry, Faculty of Medicine, Ludwig-Maximilians-Universität München, Butenandtstrasse 5, 81377 Munich, Germany

Corresponding author: Ladurner, Andreas G (andreas.ladurner@med.uni-muenchen.de)

Current Opinion in Structural Biology 2011, **21**:698–708

This review comes from a themed issue on
Proteins
Edited by Cynthia Wolberger and Patrick Cramer

Available online 3rd November 2011

0959-440X/$ – see front matter

DOI 10.1016/j.sbi.2011.10.003

Introduction

Genomic DNA, the principal carrier of a cell's hereditary information, is an acidic biomolecule of great linear length that requires careful but dynamic packing to maintain its integrity. To facilitate the folding of DNA, over evolution mechanisms have evolved that neutralize most of its charges and that wrap DNA into a tight, but flexible assembly whose condensation can be regulated, ensuring faithful genome inheritance and its biochemical readout during DNA transcription, replication or repair.

Eukaryotes establish chromatin by assembling an octameric structure of basic histone proteins, which in general wrap 146 basepairs of DNA into nucleosome particles, the minimal repeating biochemical unit of chromatin structure. Nucleosomes establish higher order chromatin structures and crucially affect the relative accessibility of the underlying DNA sequence to the cellular machinery.

In the absence of DNA and at physiological salt the histone octamer dissociates into histone H2A–H2B dimers and H3–H4 tetramers (or dimers). Since eukaryotic genomes can be very large and a vast majority of our genome is wrapped by histones, they are highly abundant proteins. It is therefore critical for cells to ensure a timely and sufficient supply of histones to where they are required, such as during DNA replication. Further, emerging evidence also suggests that histone supply levels play a determining role in organismal aging [1].

Since histone proteins carry a high number of positive charges, they readily bind DNA, but also carry the potential to make unwanted interactions with all nucleic acids and other cellular components. Several mechanisms ensure that histones properly assemble with DNA into chromatin. As a direct consequence, free histones are basically nonexistent within the cellular context. Rather, histones need to be escorted by histone chaperones, proteins that shield their charge, interact with their hydrophobic histone–histone contact surfaces, promote their controlled transfer during nucleosome assembly or reorganization, and in doing so help histones avoid local energy minima or off-pathway structures on the folding pathway toward native chromatin.

As a family, histone chaperones are generally abundant and highly conserved proteins involved in all chromatin-related cellular processes, from histone synthesis, transport and modification to the assembly or disassembly of nucleosomes, remodeling, gene activation, chromatin integrity, transcription, DNA replication, and repair. In contrast to the ATP-dependent chromatin remodeling machines that interact primarily with the DNA substrate, chaperones are histone-binders. Depending on their specificity toward particular histones, they can function quite broadly in many biological processes centered on chromatin structure, such as the eukaryotic FACT (*fa*cilitates *c*hromatin *t*ranscription) complex, or they may fulfill highly specific, restricted functions, such as yeast Scm3 (*s*uppressor of *c*hromosome *m*issegregation 3) and human HJURP (*H*olliday *j*unction *r*ecognition *p*rotein) which mediate the establishment or maintenance of centromeric

chromatin. Together with ATP-dependent nucleosome assembly and remodeling enzymes, histone chaperones procure an extensive escort network that guides the flow of histones from their synthesis to degradation based on the cell's actual need (for review, see [2••,3••,4•]).

Mechanisms of chaperone-mediated histone escort

Mechanistic insight of how histone chaperones contribute to chromatin structure has begun to emerge from structural studies of histone chaperones (or of histone-binding modules within these chaperones), including a remarkable set of crystal structures for the complex of several chaperones bound to histones or histone peptides [2••,3••,5•,6,7•,8••,9••]. Although histone chaperones belong to diverse structural families, some general features recur. Most chaperones are composed of a globular β-sheet core displaying acidic patches crucial for histone binding [4•], as well as low complexity sequences rich in acidic amino acid residues. These flexible acidic tails might provide more than charge complementation of histones by playing a role in promoting the transition of histones from chaperone to nucleosome and vice versa [10]. In this brief review, we will present and discuss recent research on the structure of chaperone–histone complexes, providing new insight into how histones are recognized, unwanted interactions are prevented and the right contacts are made at the right time during nucleosome folding. Last but not the least, we will highlight the emerging role of histone chaperones in transforming nucleosome structure by helping to reorganize or dismantle the octameric assembly of histones proteins with DNA (Figure 1).

Asf1 prevents premature histone H3–H4 tetramerization

The first crystal structures of a chaperone–histone complex were solved for yeast Asf1 (*a*ntis*i*lencing *f*actor 1) [11••] and the human orthologue CIA-I (*C*CG1-*i*nteracting factor *A*-1) [12], a chaperone that delivers newly synthesized histones H3–H4 to the DNA replication fork. The interaction with histones H3–H4 is structurally conserved from yeast to human [3••], establishing a stoichiometric 1:1:1 complex *in vitro* [13] that is thought to represent the major storage form of free histones H3–H4 *in vivo* [14,15•]. The highly conserved, histone-binding core of Asf1 folds into a concave β-sheet sandwich with three small helices in the connecting loops, while the poorly conserved C-terminal part comprises several disordered coils and — in yeast and many other eukaryotes — also contains highly acidic stretches [16]. Binding of Asf1/CIA-I to histones H3–H4 masks two

Figure 1

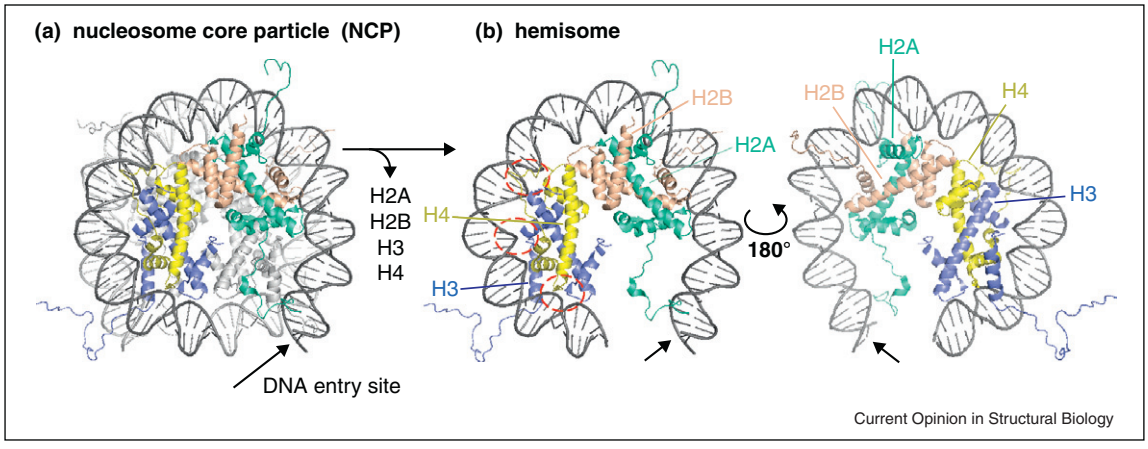

Structure of the nucleosome core particle and intermediate nucleoprotein assemblies. The individual histone core fold is composed of three helices (α1, α2, and α3) connected by two loops (L1 between α1 and α2, L2 between α2 and α3). Helices α1 and α3 cross over the ends of the middle helix α2. Two histone molecules (H3 and H4, or H2A and H2B, respectively) dimerize via their α2 and α1 helices in a 'hand-shake' fold. The H3–H4 dimer can stably tetramerize through a strong four-helix bundle of the H3 α1–α2 helices. Within the nucleosome core particle (NCP; PDB code 1AOI), H2A–H2B attaches to H3–H4 through formation of a four-helix bundle between the α2/α3 helices of H2B and H4, and in addition the shorter C-terminal tails of H2A and H4 form a short augmented β-sheet. Only very few contacts exist between the two H2A–H2B dimers in the complete octamer. Each of the 14 superhelical loops (SHL) in nucleosomal DNA is tightly associated with the histone octamer. The strong interaction energy compensates for the cost of bending the DNA. Interactions are mostly sequence-unspecific and base-unspecific, summing up to about 140 hydrogen bonds *per* NCP. Half of the hydrogen bonds, two to five per contact [53], are formed between protein-backbone and DNA-backbone atoms. Sidechain interactions, such as the insertion of arginine residues into the minor groove, further fix the structure. Each histone dimer provides three architecturally similar DNA attachment sites with the L1–L2′ contacts at the edge and the α1–α1′ in the middle of the histone dimer (e.g. for H3–H4, as marked with dashed circles in Figure 1b, H3L1 with H4L2, H3α1 with H4α1, and H3L2 with H4L1). The strongest contacts are located around the dyad axis SHL ± 0.5, numbered starting from the dyad axis. In addition, the αN helices of H3 organize the ultimate SHL ± 6.5 at the DNA entry/exit site [46,57•]. **(a)** Nucleosome core particle (NCP). H2A is labeled green, H2B ocre, H3 blue, and H4 yellow. The DNA entry site is marked with an arrowhead. **(b)** Two faces of a 'hemisome', a particle displaying only one set of histone proteins and half of the DNA molecule (dyad axis to the DNA entry site). DNA contact sites of the H3-H4 dimer are marked with dashed circles.

sites on the histone dimer that are essential for nucleosome formation [11••,12••]. First, the chaperone captures the H3–H4 dimer in such a way as to prevent its tetramerization. It does so by confiscating the H3 residues in helices α2 and α3 that are required for the formation of a four-helix-bundle between two partner histone H3 molecules. Second, the C-terminal tail of histone H4, which in the nucleosome core particle (NCP) folds back over the α3 helix of H4 to form a short parallel β-sheet with the C-terminal tail of histone H2A, switches almost 180° in orientation and is captured into an antiparallel β-sheet with the edge β-strand of the concave chaperone β-sandwich, thus extending the β-strand structure. In turn, during nucleosome disassembly reactions, the removal of the H2A–H2B dimer, would leave the C-terminal tail of histone H4 available as an Asf1 interaction site on the H3–H4 tetramer surface, suggesting that the Asf1 chaperone could dock a H3–H4 tetramer molecule by recognizing this accessible C-terminal tail of H4 through a 'strand capture' mechanism [11••]. Although Asf1 prevents H3–H4 tetramerization and interaction with histone H2A–H2B dimers, residues in the tails or core of the histone H3–H4 dimer are fully solvent accessible and thus could get post-translationally modified [12••]. This suggests that Asf1-bound H3–H4 could already be modified before incorporation into nucleosomes in a manner that would promote nucleosome assembly. The post-translational modifications would also ensure the appropriate inheritance of epigenetic marks following DNA replication. Biochemical evidence shows that Asf1 can promote the formation of DNA-associated H3–H4 tetrasomes and disomes (nucleosome particles lacking H2A–H2B dimers, composed of two or one H3–H4 dimer in complex with DNA, respectively), but it cannot efficiently disassemble preformed tetrasomes *in vitro*, even if they are thermodynamically weakened by histone H3 K56 acetylation [17], for example. Under low salt conditions, the affinity of Asf1 for soluble H3–H4 dimers was measured to be a remarkable 2.5 nM, similar to the histone's affinity for DNA at low ionic strength, potentially implicating Asf1 in a pivotal role for nucleosome assembly and disassembly [17] (Figure 2).

Histone-binding modules structurally related to those of Asf1/CIA-I exist in several other proteins. A wide-spread domain of similar structure is the conserved, globular YEATS domain which is found in protein complexes involved in transcriptional activation (TFIID and TFIIF) and in histone acetyltransferase complexes (SAS, NuA3, and NuA4), which acetylate the histone variant H2A.Z, for example, as well as nucleosome remodeling complexes, such as SWR1-C, which helps deposit H2A.Z at many euchromatic promoters, but also many other complexes including SWI/SNF, RSC and Ino80. The Yaf9 YEATS domain is a β-sandwich fold that is highly similar to Asf1, particularly in the histone-binding region, suggesting that this protein may recognize histone H3–H4 proteins in an analogous manner [18•].

Capture of histones through the Nap1 dimer

Histone synthesis in the cytoplasm is followed by their escort into the nucleus. This is catalyzed by the Nap1 (*n*ucleosome *a*ssembly *p*rotein 1) family of histone chaperones, which shield the charges and high hydrophobicity of histones during transport. Nap1 and related histone chaperone family members [including INHAT (*in*hibitor of *h*istone *a*cetyl*t*ransferase) and Vps75 (*v*acuolar *p*rotein *s*orting 75)] are obligate dimers that resemble the structure of a solid headset. Each monomer subunit provides a globular 'α/β earmuff' fold, joined by two long α-helices that align antidromically in between the two earmuffs. The central and bottom part of the earmuff fold are highly acidic, likely involved in histone binding [19]. *In vivo*, Nap1 has been shown to shuttle specifically histones H2A–H2B from the cytosol to the nucleoplasm [20], but *in vitro* recognizes the globular histone fold of all histones, with little specificity and high 1–10 nM affinity [21•]. This has made Nap1 a useful protein for *in vitro* chromatin reconstitution reactions. Furthermore, it can bind linker histone H1 and promote their chromatin incorporation [22]. In contrast, Vsp75 is specific for histones H3–H4, but has weaker, mid-nanomolar affinity. Both Nap1 and Vsp75 recognize histones H3–H4 in a tetrameric conformation, with the chaperone preserving and stabilizing the nucleosomal H3–H3′ interfaces [23•]. The histones bind in the earmuff cleft of Vsp75 [24,25,26•], and recent evidence that the H3α1 is flexible in solution allows and suggests a similar mode of binding for Nap1 [23•]. The histone variant H2A.Z is also a substrate for Nap1, but the association/dissociation rates are much higher than for canonical H2A, suggesting that Nap1 may not be an optimal chaperone and shuttle system for H2A.Z [27•] (Figure 4).

Ringfencing histones with beta-propeller scaffolds

Human RbAp46 (*Rb-a*ssociated *p*rotein 46) [7•] and *Drosophila* p55 [5•] are the histone chaperone subunits of the CAF-I (*c*hromatin *a*ssembly *f*actor 1) complex, the primary chaperone that not only deposits newly synthesized histones H3–H4 at the replicating fork, but also contribute histone chaperoning functionality to the nucleosome remodeling complexes NURF (*nu*cleosome *r*emodeling *f*actor) and NuRD (*nu*cleosome *r*emodeling and histone *d*eacetylation), as well as the histone modifying enzymes including HAT1 (*h*istone *a*cetyl*t*ransferase 1), ESH2/EED (*e*nhancer of *z*este *h*omolog 2/*e*mbryonic *e*ctoderm *d*evelopment) and the histone methyltransferase PRC2 (*p*olycomb *r*epressive *c*omplex 2 *h*istone *m*ethyl*t*ransferase). The chaperone domain of RbAp46/p55 adopts a seven-bladed β-propeller fold with two unusual features, a vertically attached N-terminal α-helix and — in near proximity — a long linker loop connecting the two C-terminal blades. The α-helix and the loop region together form a groove that can accommodate the isolated α1 helix of histone H4. For this to occur, the binding of

Figure 2

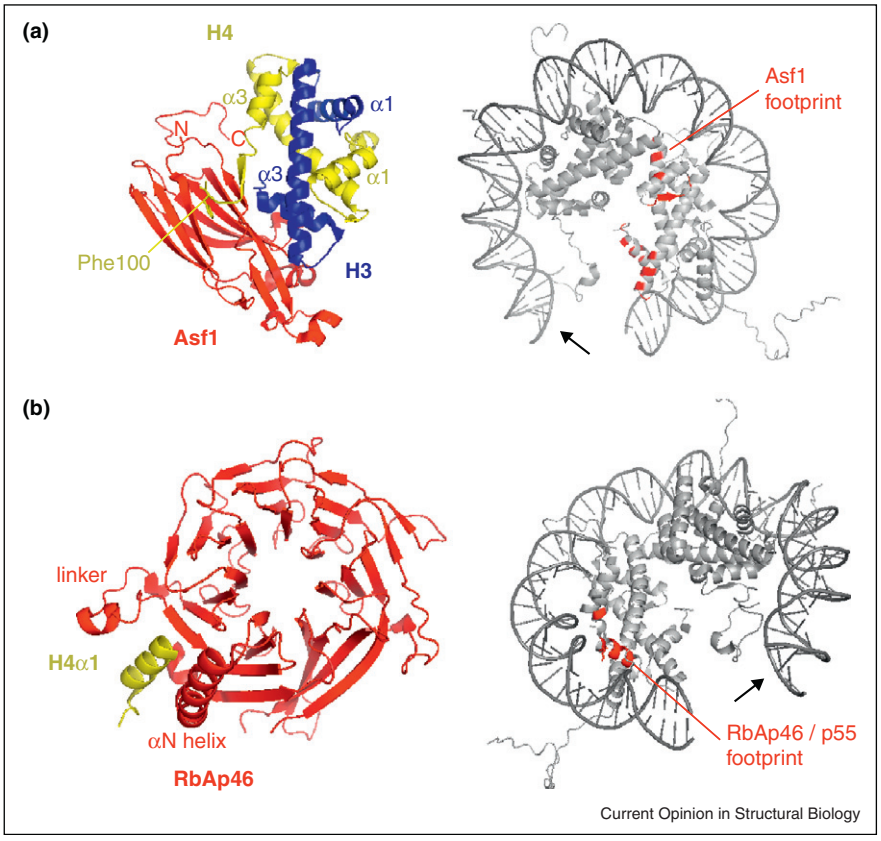

Histone chaperones in replicative nucleosome assembly. The histone chaperones are colored red (*left*), histone proteins are colored as in Figure 1 (H2A green, H2B ocre, H3 blue, and H4 yellow). Residues contacted by the chaperone are marked red ('footprint') on the hemisome surface (*right*). **(a)** Asf1–H3–H4 interaction. The Asf1 core (PDB code 2HUE, see also 2IO5) folds into a concave β-sheet sandwich with three small helices in the connection loop. H3α3 and the C-terminal part of H3α2 snuggle tightly into a hydrophobic groove in the concave face of the β-sandwich. Adjacent acidic patches stabilize the complex with numerous electrostatic interactions. The H4 C-tail forms a short antiparallel β-sheet with the edge strand of the concave chaperone β-sandwich. Phe100 in the H4 C-tail inserts into a hydrophobic pocket of the Asf1 sandwich core using a lock-and-key induced fit mechanism. In addition, the unstructured C-tail of Asf1 lies on top of the H4 core fold (helices α2 and α3). Interaction with both H3 and H4 is required for complex stability *in vitro* and histone chaperone functionality *in vivo*, including DNA damage repair, replication or transcription [11••,12••]. **(b)** Caf-I–H4 interaction. The seven-bladed β-propeller fold of CAF-I RbAp46 (PDB code 3CFS, for *Drosophila* p55 see PDB code 3C99) is supplemented with a vertical N-terminal α-helix (αN) and a long linker between the two ultimate blades that together form a groove. The amphiphatic H4α1 tightly fits into the groove, forming contacts with both the hydrophobic αN/seventh blade, as well as polar loop residues. Residues crucial for binding histones are conserved between RbAp46 and p55. The chaperone cannot bind 'canonical' free H3–H4 dimers, as seen in the NCP structure [46] because the hydrophobic face of the amphiphatic H4α1 helix is fixed to the α2 helices of both H3 and H4.

histone H4 to the CAF-I β-propeller requires a loosening of the normal histone fold, specifically the separation of the α1 helix of H4 from the remainder of the globular histone fold. Hydrophobic interactions between the α1-helix of H4 with the central α2-helices of H3 and H4 must be broken and the α1 H4 helix needs to rotate in order for highly related hydrophobic contacts to be established with the chaperone. Interestingly, the residues crucial for histone peptide binding are completely conserved across evolution. The interesting mode through which CAF-I interacts with histones H3–H4 by 'peeling away' the α1-helix of H4 from the globular histone core might promote increased flexibility within the H3–H4 dimer, thus impacting nucleosome remodel and chromatin modifying activities [7•]. It is not clear whether this pocket is the only site of interaction between H4 and human RbAp46, *Drosophila* p55 and related proteins, or whether histone H3 also contributes to binding between these proteins [5•]. The affinity of these interactions is low, in the high nanomolar [5•] to 1 μM [7•] range for both the H3–H4 dimer or the H4 peptide [7•]. Since subunits of the PRC2 complex [5•] appear to bind CAF-I through the same *Drosophila* p55 helix-loop-pocket that is recognized by histone H4 α1 (the first α-helix of H4), competition between PRC2 and H4 for the p55 pocket might have regulatory effects (Figure 2).

Nucleoplasmin/nucleophosmin form supermolecular assemblies

The nucleoplasmin/nucleophosmin (Np) family of histone chaperone proteins contain a central domain that forms an eight-stranded β-barrel which self-associates into a circular pentamer superassembly. Histones H2A–H2B binds to the flat face of the β-barrels, presumably via basic (e.g. arginine) residues in the C-terminal part of H2Bα2, a region of the histone dimer that contacts nucleosomal DNA [6]. Crystal structures indicate that two pentameric rings can dimerize into a large decameric assembly, while EM analysis argues for the existence of a structure formed by a single ring [6,28]. In contrast to many other histone chaperones, the surface charge of the β-barrel does not display distinct acidic patches. While nucleophosmin has mostly nucleolar functions, nucleoplasmin in the oocyte cytoplasm stores immense amounts of histone octamers, up to five octamers per Np decamer [6]. This feature likely plays an important role during the rapid decondenzation of sperm chromatin upon fertilization of an oocyte, where the nucleoplasmin-bound histones are relates and are replaced by sperm-specific chromatin proteins, allowing for a rapid supply of histones to the sperm chromatin as the zygotic genome assembles (Figure 4).

Peptidase-like and PH-like domains of histone chaperones FACT and Rtt106

The FACT complex [Spt16 (*sup*pressor of *T*y 16) and yeast Pob3 (*Po*l1 *b*inding 3)/metazoan SSRP1 (*s*tructure *s*pecific *r*ecognition *p*rotein 1)] is an abundant histone H2A–H2B 'evicting' [29] chaperone that can reorganize nucleosomes during transcription, replication and in addition has quite specialized functions. Indeed, FACT purifies with centromeric chromatin assemblies [30], and is required for centromeric chromatin structure [31], suggesting general and important roles in the assembly and/or maintenance of chromatin structure. FACT is a 'multi-chaperone', containing several globular domains implicated in histone binding. The N-terminal region of its subunit Spt16, Spt16N, exhibits the pita-bread fold domain typical of amino peptidase-like folds and not only binds the histone H3–H4 globular domains fold with 1:1 or 2:2 stoichiometry but can also recognize the H3 and H4 tails with low micromolar affinity [32]. The middle domain of Spt16, Spt16M (T Stuwe *et al.*, unpublished data), and the middle domain of Pob3, Pob3M [33] together with the recently identified histone chaperone Rtt106 (*r*egulator of *T*y1 *t*ransposition 106) [34], form a novel family of structurally related histone chaperone domains. These tandem pleckstrin-homology-like (PH-like) domains all can bind H3–H4, as well as DNA. More refined analysis shows that the second, C-terminal PH-like domain of Spt16M, Pob3M, and Rtt106M display strong structural similarity between each other and are sufficient for H3–H4 interaction. In the case of Rtt106M the interaction site was mapped to a short 'ITRLT' motif present in a surface loop region [34]. Interestingly, Spt16M differs in its function, since it can also bind histones H2A–H2B with high affinity. The C-terminal PH-like domain of the tandem Spt16M PH-like module exhibits special structural features that allow FACT to bind H2A–H2B, endowing the FACT complex with its well-known histone H2A–H2B chaperoning activity. In this case, a C-terminal 'U-turn' extension within the PH-like fold provides an Spt16M-exclusive, hydrophobic interaction site for residues on the α1 helix of H2B. H2Bα1 is the attachment site for nucleosomal DNA at superhelical location (SHL) ± 4.5 (helix turns counted from the nucleosome dyad axis). It is therefore possible that Spt16M might loosen up nucleosome structure by displacing the terminal 30 basepairs of the nucleosomal DNA (T Stuwe *et al.*, unpublished data), but without displacing or evicting the histone H2A–H2B dimer [35•]. Furthermore, the domain can prevent association of DNA with the histone (T Stuwe *et al.*, unpublished data) (Figure 4).

Working in concert with RNA polymerase — Spt6

The FACT subunit Spt16, as well as the chaperone and elongation factor Spt6, is essential for the restoration of intact chromatin structure during DNA transcription in the wake of RNA polymerase II enzyme passage through the nucleosome-wrapped gene [36]. Spt6 directly associates with the Ser2-phosphorylated form of the C-terminal domain of the large RNA polymerase II subunit Rpb1. This interaction is mediated by the C-terminal, tandem SH2 domain of Spt6 [37–39].

Both FACT and Spt6 bind nucleosomes only in the presence of the DNA-bending HMG-box protein Nhp6, suggesting that DNA needs to be distorted and lifted off the histone octamer surface before the chaperone binding site is available [40•,41]. Spt6 binds the histone H3–H4 core globular domain through a ~30 amino acid peptide stretch in its intrinsically disordered, acidic N-terminus [42]. Spn1 (*s*uppresses *p*ostrecruitment functions gene *n*umber 1), a frequent partner of Spt6, interacts with the same region of the Spt6 protein, thus competing with the chaperone for histone binding. Such a mutually exclusive interaction could help recycle Spt6 function for multiple rounds of nucleosome reorganization during transcription, providing a histone binding and chaperoning function to an elongating RNA polymerase II enzyme [40•,43]. Molecular details of how the histones interact with Spt6 are unknown. However, the structure of the Spt6 peptide in complex with Spn1 has been solved and reveals an extended helix-linker-helix conformation [40•,43] that may also occur upon histone H3–H4 binding.

Specialized functions of centromeric histone chaperones

The formation of kinetochores on chromosomes and the correct segregation of genetic information in eukaryotes critically depends on the function of a specialized cen-

tromeric chromatin structure. The hallmark of this is the incorporation of a distinct H3 variant into centromeric chromatin [known as cenH3, or CENP-A (*cen*tromere *p*rotein *A*) in mammals and Cse4 (*c*hromosome *se*gregation 4) in yeast]. Two recent structures provide molecular insight into how these dedicated, rather less abundant, histone chaperones selectively recognize cenH3 over canonical H3 [8••,9••]. Both the mammalian HJURP and yeast Scm3 protein contain an N-terminal histone chaperone domain of ~80 residues named CBD (CENP-A/Cse4 binding domain), which stoichiometrically binds a dimer of cenH3–H4 [44]. *In vitro*, free yeast CBD is an intrinsically disordered protein, but in complex with histones Cse4–H4 becomes structured and clamps the histone dimer with two extended α-helices connected by a long linker [9••]. Similarly, the human HJURP CBD twines along the α2 helix of CENP-A using a long, N-terminal α-helix and linker, and then caps the histone cenH3–H4 dimer with a small three-stranded β-sheet. In comparison to the soluble CENP-A–H4 [45] or nucleosomal H3–H4 [46] tetramer, the chaperone-bound histones show significant distortions. The structure of the yeast Scm3 CBD–H3–H4 complex would allow for the tetramerization of the cenH3-H4 dimer. In contrast, the complex of human HJURP with cenH3–H4 suggests that tetramerization may be prevented by HJURP, since the cenH3′ partner in the second cenH3–H4 dimer would clash with the chaperone domain of HJURP. Strikingly, both chaperones directly obstruct binding sites on H4L2 (the second loop region of the H4 histone core fold, between helices α2 and α3), for nucleosomal DNA (SHL ± 2.5). However, while this manuscript was under review, a crystal structure of yeast Scm3 in complex with Cse4–H4 was published, which shows remarkable similarity to the HJURP–CENP-A–H4 structure [47]. In contrast to the NMR study, this interaction would block not only DNA binding but also histone tetramerization. The authors suggest that the discrepancy between the NMR and the two crystal structures might likely be due to linked and truncated protein constructs in the first case.

Since centromeric histone variants occur at very low levels compared to the canonical histones H3.1/3.2 and the replication-independent histone variant H3.3 (yeast H3 is most closely related mammalian H3.3), the centromeric-specific histone chaperones have to be able to strongly discriminate cenH3 from canonical H3 isoforms. This occurs through a region in HJURP and Scm3 known as the CENP-A/Cse4 targeting domain (CATD), which helps to target the centromeric histone H3 variant to centromeric nucleosomes [30,48]. HJURP and Scm3 form strong hydrophobic contacts with two cenH3-specific residues that cannot be replaced by the corresponding residues in H3. These distinct features of cenH3 greatly increase cenH3-affinity for HJURP and Scm3, but by themselves cannot provide a distinguishing mechanism to counter-select against canonical H3. Discrimination is thus achieved outside of the CATD using a mechanism that leads to the repulsion of canonical H3. This occurs through a hydrophobic dint in the HJURP β-sheet cap that can nicely accommodate Ser68 of CENP-A, but not the corresponding Gln68 residues of H3 due to steric clashes [8••]. While this difference at position 68 of cenH3 is conserved in yeast, the existence of a repulsive discrimination mechanism needs to be verified (Figure 3).

Remodeling histone variant chromatin with Chz1

Chz1 (*c*haperone for *H*tz1/H2A–H2B dimer) is another variant-specific histone chaperone protein. As part of the histone-exchanging nucleosome remodeling complex SWR1, Chz1 binds the histone H2A.Z–H2B dimer with high nanomolar affinity and helps to incorporate the histone variant H2A.Z into or near the promoters of many active genes. An intrinsically disordered region of the Chz1 chaperone protein is stabilized into a regular secondary structure upon binding the histone dimer, forming two short α-helices connected by an extended linker region that roughly follows the shape of H2A.Z through multiple electrostatic interactions [49••]. The N-terminal α-helix of Chz1 shields arginine residues in the H2A.Z α1 helix that are crucial for interaction with nucleosomal DNA, and the basic half of the bipolar 'Chz motif' in the linker region occupies the 'acidic patch' on the H2A–H2B dimer surface. This acidic patch is important for H2A.Z variant incorporation [50] and, at least in canonical H2A, for the formation of the 30 nm chromatin fiber [46,51]. Some of the regions that Chz1 recognizes are freely accessible on the NCP and the chaperone might use these contact surfaces as a seizing point to anchor the SWR1 remodeling complex for subsequent DNA displacement and histone eviction (Figure 3).

Relaying histones

The distribution and flux of the histone pool from one chaperone to the next is determined by the relative binding constants and kinetic stabilities of the chaperone–histone complexes. These are subject to a variety of post-translational modifications, by the local availability of histone acceptors (proteins or DNA), as well as the accessibility of the chaperone binding sites on the histone or nucleosome surfaces. For example, both the chaperones Asf1 and Vsp75 directly interact with the histone acetyltransferase Rtt109 and present newly synthesized histones H3–H4 to Rtt109 for the acetylation of H3 K56 [24,25,26•,52]. In turn, acetylated H3 K56 is a preferred substrate for the chaperones Rtt106 and CAF-I [53], which perform replication-associated nucleosome assembly. While Asf1 is bound to H3–H4 dimers, the opposite tetramerization interface is freely available to other proteins, including residue H3 K56, which locates to the N-terminal α-helix of H3, as well as the α1 helix of H4 that is recognized by RbAp46/p55 proteins. CAF-I

Figure 3

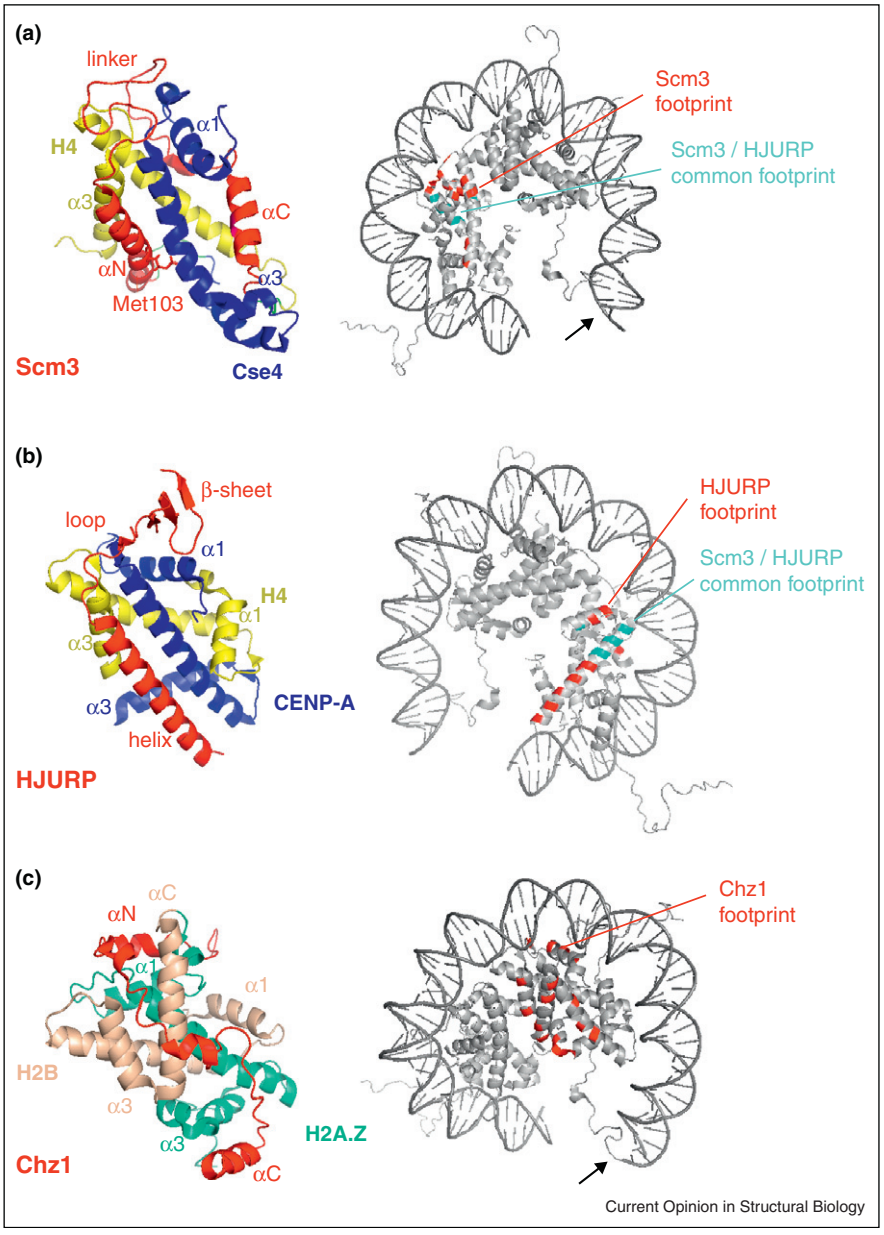

Variant-specific histone chaperones. **(a)** Centromeric chaperones: Scm3. In complex with the centromere-specific H3 variant Cse4 and histone H4, Scm3 (PDB code 2L5A) folds into two α-helices (αN and αC) connected by a long linker. The Scm3 αN helix makes major hydrophobic contacts with the Cse4-α2 and H4-α3. The extended 34-residue linker twines to the opposite face of the dimer, on its way there it interacts with Cse4L1, H4L2, and the C-terminal part of H4α2. The Scm3-αC helix contacts the N-terminal part of H4α2. Clamping by Scm3 loosens the Cse4–H4 dimer: tight hydrophobic interactions between the central α2 helices as well as contacts between H4L2 and Cse4L1 are broken. Met103 in the αN helix of Scm3 kinks Cse4α2 in the middle and the H4 C-terminus becomes structured by helical extension of α3. In general, the disordered H4 C-termini adopt regular secondary structure upon binding Scm3. Both centromeric histone chaperones induce helical extension of the H4 α3-helix. In sharp contrast, the chaperone Asf1 [11••,12••] and histone H2A (as part of the nucleosome) [46] induce a mini-β-strand as part of an augmented β-sheet. **(b)** Centromeric chaperones: HJURP. HJURP is a human histone chaperone specific for the centromeric H3 variant CENP-A. The HJURP-CBD (CENP-A binding domain) (PDB code 3R45) forms a long helix, a 15-residue loop and a three-stranded antiparallel β-sheet. HJURP αA runs along the central CENP-A α2 helix with tight hydrophobic interactions, and the HJURP linker and β-sheet cap the histone dimer by contacting the H4 L2 and CENP-A L1 and α1 region. In complex with HJURP, the C-termini of both CENP-A and H4 become more ordered by helical extension. The C-terminal part of H4α2 bends by 10° toward CENP-A α1, and concomitantly CENP-A L1 is flipped away from H4 L2. **(c)** Chz1. The H2A.Z-specific chaperone Chz1 (PDB code 2JSS) is relatively unstructured in solution, but becomes structured in complex with the H2A.Z–H2B histone dimer. Two short α-helices (αN and αC) and an extended linker (containing the bipolar 'Chz motif') roughly follow the H2A.Z shape. Chz1 forms extended electrostatic interactions with the histone dimer, thereby sequestering residues involved in various intra-nucleosomal and inter-nucleosomal contacts: Chz1αN shields arginine residues crucial for nucleosomal DNA interaction and the basic part of the bipolar Chz motif occupies the 'acidic patch' on the histone dimer surface.

Figure 4

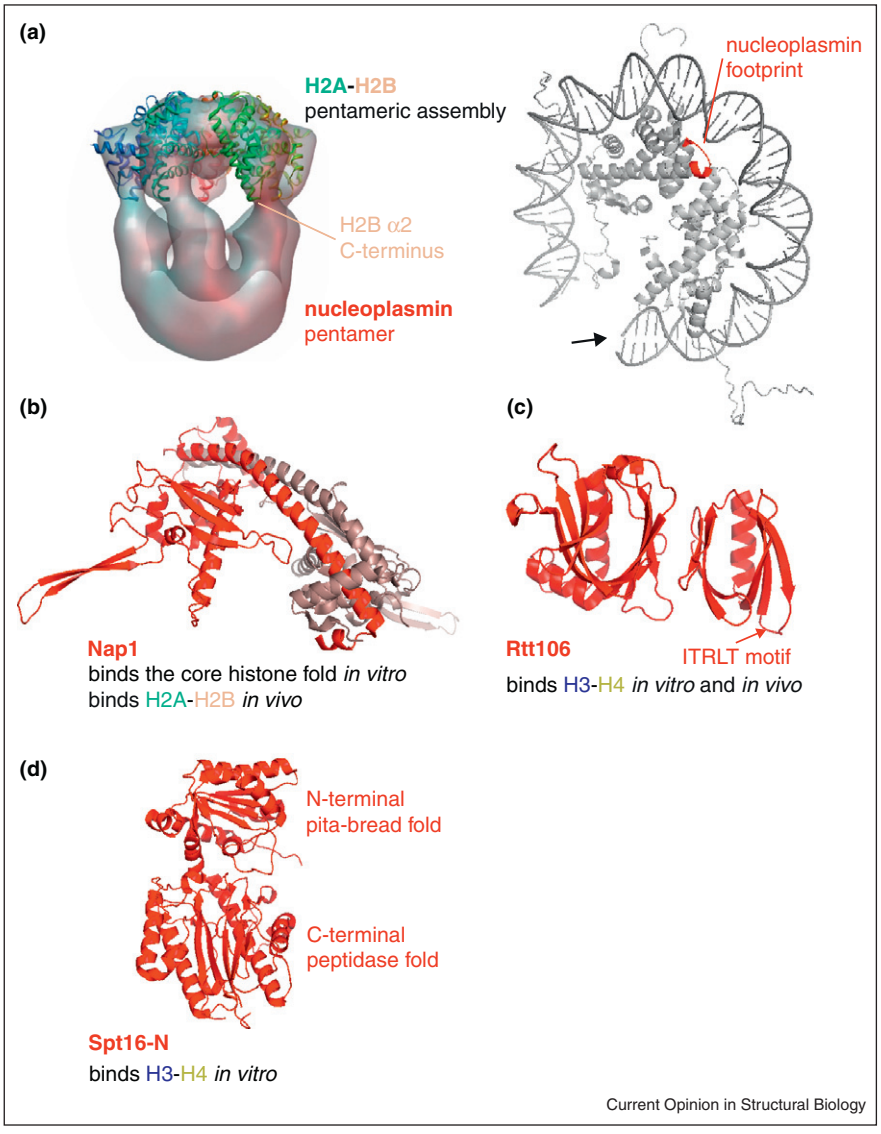

Chaperones with pleiotropic function in histone metabolism. **(a)** nucleoplasmin/nucleophosmin. The chaperone core of the nucleoplasmin/nucleophosmin family folds into an eight-stranded β-barrel; five barrels associate to a circular pentamer. Histones H2A–H2B bind the distal face of the chaperone assembly, presumably through the H2Bα2 C-terminus, and electrostatic interdimer contacts stabilize the complex (electron microscopy data bank code EMDB-1777). **(b)** Nap1. The Nap1 family of histone chaperones [Nap1 (PDB code 2Z2R, this figure), INHAT (PDB code 2E50), Vps75 (PDB codes 3C9D and 3DM7)] is obligatorily dimeric, in complex resembling a solid headset. The novel, globular 'α/β earmuff' fold continues into a slightly curved, long, helical region, with two helices of different subunits aligning antidromically but parallel in between the earmuffs to orient and stabilize the dimer. The central and bottom part of the earmuff folds are highly acidic, suggesting that they bind histones, and this was verified for H3–H4 by mutagenesis [19]. **(c)** Tandem PH–chaperones/Rtt106. Rtt106-M (PDB code 3GYP) is an exemplary member of the tandem plekstrin-homology-like (PH-like) histone chaperone family that includes Pob3-M (PDB code 2GCL) and Spt16-M (T Stuwe *et al.*, unpublished data). The PH-like fold consists of two anti-parallel β-sheets arranged in a specific angle to each other, with the open side covered by a capping helix. The C-terminal PH domains of the three histone chaperones are very similar in structure and might be a common site for histone H3–H4 interaction. For Rtt106, the interaction was mapped to the 'ITRLT' motif in a conserved loop of the second PH domain, an adjacent acidic patch of three conserved residues that might neutralize the charge of a bound histone dimer. **(d)** Spt16-N. The N-terminal domain of the FACT subunit Spt16 consists of an (enzymatically inactive) aminopeptidase-like fold (PDB codes 3CB5 and 3BIT), a β-sheet surrounded by α-helices. The domain binds both the globular cores, as well as the unstructured N-terminal tails of histones H3–H4 with low micromolar affinity, presumably through conserved surface patches.

can therefore directly take over H3–H4 from Asf1 and promote H3-H4 tetramer formation for nucleosome assembly [3••].

Concluding remarks and future challenges

An emerging feature of many histone chaperones is their ability to directly obstruct sites on their interacting histone partners that are normally engaged in DNA interactions within the NCP. So although nucleosome assembly is ultimately guided by a hierarchy of affinities between DNA, histones and chaperones [21,54,55•], the kinetic shielding of charged or hydrophobic histone–DNA and histone–histone interaction sites through formation of less stable histone–chaperone intermediates will allow the histones to slowly and gradually fold to the correct, DNA-bound structure and at the same time reduce the non-productive and unwanted formation of mis-structured histone-DNA aggregates. In addition, within fully assembled nucleosomes, the DNA ends of the NCP transiently detach from the histone surface [56], either spontaneously and depending on DNA sequence, or aided by loop-creating or torsion-creating motors such as the distinct ATP-dependent remodelers. Such events, in principle, may provide temporary access to normally hidden histone sites. This could help histone chaperones to further disassemble the nucleosome or to further destabilize histone–DNA interactions in order to promote the progression of RNA polymerase II, for example [57•]. In sum, recent structural evidence is highlighting how histone chaperones not only shield histones from unwanted interactions but also help them to engage in interactions other than with DNA in order to facilitate the dynamic remodeling of chromatin plasticity, which the chromatinized template depends on.

Acknowledgements

We would like to thank Andrew Bowman, Markus Hassler, Gytis Jankevicius, Dimitra Keramisanou and Tobias Stuwe for helpful discussion and comments on the manuscript. M.H. was the recipient of a predoctoral fellowship from the Boehringer Ingelheim Fonds and thanks the EU FP6 Marie Curie Research and Training Network 'Chromatin Plasticity' for support. We are grateful for further support to the European Molecular Biology Laboratory, the Ludwig Maximilians University of Munich and the EU FP7 Marie Curie Initial Training Network 'Nucleosome4D'.

References and recommended reading

Papers of particular interest, published within the period of review, have been highlighted as:

- • of special interest
- •• of outstanding interest

1. Feser J, Tyler J: **Chromatin structure as a mediator of aging**. *FEBS Lett* 2011, **585**:2041-2048.

2. •• Eitoku M, Sato L, Senda T, Horikoshi M: **Histone chaperones: 30 years from isolation to elucidation of the mechanisms of nucleosome assembly and disassembly**. *Cell Mol Life Sci* 2008, **65**:414-444.
In detail compendium of histone chaperones including a detailed description of their respective structure and function.

3. •• Das C, Tyler JK, Churchill ME: **The histone shuffle: histone chaperones in an energetic dance**. *Trends Biochem Sci* 2010, **35**:476-489.
Structural and biophysical classification of histone chaperone subfamilies. Interaction networks and histone binding affinities are merged into a thermodynamic model of nucleosome (dis)assembly.

4. • Park YJ, Luger K: **Histone chaperones in nucleosome eviction and histone exchange**. *Curr Opin Struct Biol* 2008, **18**:282-289.
Incorporation of histone variants alters chromatin stability and signaling. This review describes how certain histone chaperones recognize specific histone variants and therefore assigns them an active role in the maintenance of chromatin plasticity.

5. • Song JJ, Garlick JD, Kingston RE: **Structural basis of histone H4 recognition by p55**. *Genes Dev* 2008, **22**:1313-1318.
One of two papers (see [7•]) describing how the CAF-I chaperone subunits (RbAp46 in humans, p55 in Drosophila) recognize an isolated helical H4 peptide.

6. Ramos I, Martín-Benito J, Finn R, Bretaña L, Aloria K, Arizmendi JM, Ausió J, Muga A, Valpuesta JM, Prado A: **Nucleoplasmin binds histone H2A–H2B dimers through its distal face**. *J Biol Chem* 2010:33771-33778.

7. • Murzina NV, Pei XY, Zhang W, Sparkes M, Vicente-Garcia J, Pratap JV, McLaughlin SH, Ben-Shahar TR, Verreault A, Luisi BF, Laue ED: **Structural basis for the recognition of histone H4 by the histone-chaperone RbAp46**. *Structure* 2008, **16**:1077-1085.
See annotation to Ref. [5•]

8. •• Hu H, Liu Y, Wang M, Fang J, Huang H, Yang N, Li Y, Wang J, Yao X, Shi Y *et al.*: **Structure of a CENP-A-histone H4 heterodimer in complex with chaperone HJURP**. *Genes Dev* 2011, **25**:901-906.
One of two papers (see [9••]) describing structures of chaperones specifically recognizing the centromere-specific H3 variant. This paper describes the crystal structure of human HJURP in complex with CENP-A and H4. The authors show strong biochemical evidence that the characteristic ''targeting domain'' of the centromeric histone variant only increases the affinity to the chaperone but is not sufficient to exclude binding of canonical H3. Discrimination is effected outside this domain, through streric repulsion of a functionally conserved residue in canonical H3.

9. •• Zhou Z, Feng H, Zhou BR, Ghirlando R, Hu K, Zwolak A, Miller Jenkins LM, Xiao H, Tjandra N, Wu C, Bai Y: **Structural basis for recognition of centromere histone variant CenH3 by the chaperone Scm3**. *Nature* 2011, **472**:234-237.
See annotation to Ref. [8••]. NMR structure of yeast Scm3 in complex with Cse4–H4.

10. Park YJ, Chodaparambil JV, Bao Y, McBryant SJ, Luger K: **Nucleosome assembly protein 1 exchanges histone H2A–H2B dimers and assists nucleosome sliding**. *J Biol Chem* 2005, **280**:1817-1825.

11. •• English CM, Adkins MW, Carson JJ, Churchill ME, Tyler JK: **Structural basis for the histone chaperone activity of Asf1**. *Cell* 2006, **127**:495-508.
Together with (Ref. [12••] and others), this paper describes the first crystal structure of a chaperone–histone complex. English *et al*. solved the complex of yeast Asf1 with H3–H4 and support their structure with *in vivo* and *in vitro* studies. They suggest that tetrasome disassembly could be initiated by a ''strand-capture'' mechanism.

12. •• Natsume R, Eitoku M, Akai Y, Sano N, Horikoshi M, Senda T: **Structure and function of the histone chaperone CIA/ASF1 complexed with histones H3 and H4**. *Nature* 2007, **446**:338-341.
Together with (Ref. [11••] and others), the authors present the first crystal structure of chaperone–histone complexes. This paper describes the crystal structure of human CIA-I in complex with Xenopus histones H3–H4 and shows biophysical evidence of H3–H4 tetramer disruption.

13. English CM, Maluf NK, Tripet B, Churchill ME, Tyler JK: **ASF1 binds to a heterodimer of histones H3 and H4: a two-step mechanism for the assembly of the H3–H4 heterotetramer on DNA**. *Biochemistry* 2005, **44**:13673-13682.

14. Groth A, Ray-Gallet D, Quivy JP, Lukas J, Bartek J, Almouzni G: **Human Asf1 regulates the flow of S phase histones during replicational stress**. *Mol Cell* 2005, **17**:301-311.

15. • Tagami H, Ray-Gallet D, Almouzni G, Nakatani Y: **Histone H3.1 and H3.3 complexes mediate nucleosome assembly pathways dependent or independent of DNA synthesis**. *Cell* 2004, **116**:51-61.

Histone H3.1 is assembled during replicative nucleosome assembly, but during replication-independent nucleosome turnover the variant histone H3.3 gets incorporated. To decipher the pathway of histone H3 sorting, the authors immuno-purified complexes associated with the individual histones and found that different histone chaperones characterize each pathway, CAF-1 for replicative and HIRA for non-replicative nucleosome assembly.

16. Daganzo SM, Erzberger JP, Lam WM, Skordalakes E, Zhang R, Franco AA, Brill SJ, Adams PD, Berger JM, Kaufman PD: **Structure and function of the conserved core of histone deposition protein Asf1**. *Curr Biol* 2003, **13**:2148-2158.

17. Donham DC 2nd, Scorgie JK, Churchill ME: **The activity of the histone chaperone yeast Asf1 in the assembly and disassembly of histone H3/H4–DNA complexes**. *Nucleic Acids Res* 2011, **39**:5449-5458.

18. • Wang AY, Schulze JM, Skordalakes E, Gin JW, Berger JM, Rine J, Kobor MS: **Asf1-like structure of the conserved Yaf9 YEATS domain and role in H2A.Z deposition and acetylation**. *Proc Natl Acad Sci U S A* 2009, **106**:21573-21578.

This crystal structure of the YEATS chaperone domain shows an Ig-like β-sandwich fold highly similar to Asf1. The domain binds histones H3–H4 but not H2A–H2B *in vitro*, and genetic evidence suggests that it acts in a parallel pathway to Asf1 *in vivo*. The domain is required for H2A.Z deposition and acetylation.

19. Park YJ, Luger K: **The structure of nucleosome assembly protein 1**. *Proc Natl Acad Sci U S A* 2006, **103**:1248-1253.

20. Mosammaparast N, Ewart CS, Pemberton LF: **A role for nucleosome assembly protein 1 in the nuclear transport of histones H2A and H2B**. *EMBO J* 2002, **21**:6527-6538.

21. • Andrews AJ, Downing G, Brown K, Park YJ, Luger K: **A thermodynamic model for Nap1-histone interactions**. *J Biol Chem* 2008, **283**:32412-32418.

First description of a quantitative assay using fluorophore-tagged proteins to study histone affinities. See also Ref. [54].

22. Kepert JF, Mazurkiewicz J, Heuvelman GL, Tóth KF, Rippe K: **NAP1 modulates binding of linker histone H1 to chromatin and induces an extended chromatin fiber conformation**. *J Biol Chem* 2005, **280**:34063-34072.

23. • Bowman A, Ward R, Wiechens N, Singh V, El-Mkami H, Norman DG, Owen-Hughes T: **The histone chaperones Nap1 and Vps75 bind histones H3 and H4 in a tetrameric conformation**. *Mol Cell* 2011, **41**:398-408.

The authors use pulsed electron double resonance and protein cross-linking to show that Nap1 and Vps75 bind histones H3–H4 in a tetrameric conformation, which can be substrate to modification, whereas the chaperone Asf1 binds H3–H4 in a dimeric conformation.

24. Tang Y, Meeth K, Jiang E, Luo C, Marmorstein R: **Structure of Vps75 and implications for histone chaperone function**. *Proc Natl Acad Sci U S A* 2008, **105**:12206-12211.

25. Park YJ, Sudhoff KB, Andrews AJ, Stargell LA, Luger K: **Histone chaperone specificity in Rtt109 activation**. *Nat Struct Mol Biol* 2008, **15**:957-964.

26. • Berndsen CE, Tsubota T, Lindner SE, Lee S, Holton JM, Kaufman PD, Keck JL, Denu JM: **Molecular functions of the histone acetyltransferase chaperone complex Rtt109–Vps75**. *Nat Struct Mol Biol* 2008, **15**:948-956.

With structural, biochemical and genetic experiments the authors show that Vps75 stimulates the histone acetyltransferase activity of Rtt109 on histone H3 K9.

27. • Mazurkiewicz J, Kepert JF, Rippe K: **On the mechanism of nucleosome assembly by histone chaperone NAP1**. *J Biol Chem* 2006, **281**:16462-16472.

With quantitative gel electrophoresis and fluorescence anisotropy, the authors derive a kinetic model of Nap1-mediated mono-nucleosome assembly.

28. Dutta S, Akey IV, Dingwall C, Hartman KL, Laue T, Nolte RT, Head JF, Akey CW: **The crystal structure of nucleoplasmin-core: implications for histone binding and nucleosome assembly**. *Mol Cell* 2001, **8**:841-853.

29. Belotserkovskaya R, Oh S, Bondarenko VA, Orphanides G, Studitsky VM, Reinberg D: **FACT facilitates transcription-dependent nucleosome alteration**. *Science* 2003, **301**:1090-1093.

30. Foltz DR, Jansen LE, Black BE, Bailey AO, Yates JR 3rd, Cleveland DW: **The human CENP-A centromeric nucleosome-associated complex**. *Nat Cell Biol* 2006, **8**:458-469.

31. Lejeune E, Bortfeld M, White SA, Pidoux AL, Ekwall K, Allshire RC, Ladurner AG: **The chromatin-remodeling factor FACT contributes to centromeric heterochromatin independently of RNAi**. *Curr Biol* 2007, **17**:1219-1224.

32. Stuwe T, Hothorn M, Lejeune E, Rybin V, Bortfeld M, Scheffzek K, Ladurner AG: **The FACT Spt16 "peptidase" domain is a histone H3–H4 binding module**. *Proc Natl Acad Sci U S A* 2008, **105**:8884-8889.

33. VanDemark AP, Blanksma M, Ferris E, Heroux A, Hill CP, Formosa T: **The structure of the yFACT Pob3-M domain, its interaction with the DNA replication factor RPA, and a potential role in nucleosome deposition**. *Mol Cell* 2006, **22**:363-374.

34. Liu Y, Huang H, Zhou BO, Wang SS, Hu Y, Li X, Liu J, Zang J, Niu L, Wu J *et al.*: **Structural analysis of Rtt106p reveals a DNA binding role required for heterochromatin silencing**. *J Biol Chem* 2010, **285**:4251-4262.

35. • Xin H, Takahata S, Blanksma M, McCullough L, Stillman DJ, Formosa T: **yFACT induces global accessibility of nucleosomal DNA without H2A-H2B displacement**. *Mol Cell* 2009, **35**:365-376.

Careful study on the action of the histone chaperone FACT. The authors use nucleosome protection studies of nucleosomes in various chemical conditions and conclude that H2A–H2B dimers are not evicted but the nucleosome is converted to a looser, more dynamic structure upon FACT-mediated remodelling.

36. Kaplan CD, Laprade L, Winston F: **Transcription elongation factors repress transcription initiation from cryptic sites**. *Science* 2003, **301**:1096-1099.

37. Close D, Johnson SJ, Sdano MA, McDonald SM, Robinson H, Formosa T, Hill CP: **Crystal Structures of the *S. cerevisiae* Spt6 Core and C-Terminal Tandem SH2 Domain**. *J Mol Biol* 2011, **408**:697-713.

38. Diebold ML, Loeliger E, Koch M, Winston F, Cavarelli J, Romier C: **Noncanonical tandem SH2 enables interaction of elongation factor Spt6 with RNA polymerase II**. *J Biol Chem* 2010, **285**:38389-38398.

39. Sun M, Larivière L, Dengl S, Mayer A, Cramer P: **A tandem SH2 domain in transcription elongation factor Spt6 binds the phosphorylated RNA polymerase II C-terminal repeat domain (CTD)**. *J Biol Chem* 2010, **285**:41597-41603.

40. • McDonald SM, Close D, Xin H, Formosa T, Hill CP: **Structure and biological importance of the Spn1–Spt6 interaction, and its regulatory role in nucleosome binding**. *Mol Cell* 2010, **40**:725-735.

One of two papers (see Ref. [43]) describing the structure of Spn1(Isw1) in complex with a Spt6 peptide. This paper nicely shows that the same region of Spt6 binds to Spn1 or nucleosomes, and Spn1 can directly block the Spt6–nucleosome interaction. The authors speculate that this might have a regulatory role or enhance the turnover rate of the chaperone.

41. Formosa T, Eriksson P, Wittmeyer J, Ginn J, Yu Y, Stillman DJ: **Spt16–Pob3 and the HMG protein Nhp6 combine to form the nucleosome-binding factor SPN**. *Embo J* 2001, **20**:3506-3517.

42. Bortvin A, Winston F: **Evidence that Spt6p controls chromatin structure by a direct interaction with histones**. *Science* 1996, **272**:1473-1476.

43. Diebold ML, Koch M, Loeliger E, Cura V, Winston F, Cavarelli J, Romier C: **The structure of an Iws1/Spt6 complex reveals an interaction domain conserved in TFIIS, Elongin A and Med26**. *Embo J* 2010, **29**:3979-3991.

44. Mizuguchi G, Xiao H, Wisniewski J, Smith MM, Wu C: **Nonhistone Scm3 and histones CenH3–H4 assemble the core of centromere-specific nucleosomes**. *Cell* 2007, **129**:1153-1164.

45. Sekulic N, Bassett EA, Rogers DJ, Black BE: **The structure of (CENP-A–H4)(2) reveals physical features that mark centromeres**. *Nature* 2010, **467**:347-351.

46. Luger K, Mäder AW, Richmond RK, Sargent DF, Richmond TJ: **Crystal structure of the nucleosome core particle at 2.8 Å resolution**. *Nature* 1997, **389**:251-260.

47. Uhn-Soo C, Harrison SC: **Recognition of the centromere-specific histone Cse4 by the chaperone Scm3**. *Proc Natl Acad Sci U S A* 2011, **108**:9367-9371.

48. Black BE, Foltz DR, Chakravarthy S, Luger K, Woods VL Jr, Cleveland DW: **Structural determinants for generating centromeric chromatin**. *Nature* 2004, **430**:578-582.

49. •• Zhou Z, Feng H, Hansen DF, Kato H, Luk E, Freedberg DI, Kay LE, Wu C, Bai Y: **NMR structure of chaperone Chz1 complexed with histones H2A.Z–H2B**. *Nat Struct Mol Biol* 2008, **15**:868-869.
NMR-structure of the chaperone–histone complex. The authors show interesting backbone dynamics data and show that a truncated form of the chaperone can bind NCPs, suggesting that it might be involved in H2A–H2B dimer eviction during SWR1-catalyzed remodeling.

50. Jensen K, Santisteban MS, Urekar C, Smith MM: **Histone H2A.Z acid patch residues required for deposition and function**. *Mol Genet Genomics* 2011, **285**:287-296.

51. Fan JY, Rangasamy D, Luger K, Tremethick DJ: **H2A.Z alters the nucleosome surface to promote HP1alpha-mediated chromatin fiber folding**. *Mol Cell* 2004, **16**:655-661.

52. Tsubota T, Berndsen CE, Erkmann JA, Smith CL, Yang L, Freitas MA, Denu JM, Kaufman PD: **Histone H3–K56 acetylation is catalyzed by histone chaperone-dependent complexes**. *Mol Cell* 2007, **25**:703-712.

53. Li Q, Zhou H, Wurtele H, Davies B, Horazdovsky B, Verreault A, Zhang Z: **Acetylation of histone H3 lysine 56 regulates replication-coupled nucleosome assembly**. *Cell* 2008, **134**:244-255.

54. Andrews AJ, Luger K: **Nucleosome structure(s) and stability: variations on a theme**. *Annu Rev Biophys* 2011, **40**:99-117.

55. • Andrews AJ, Chen X, Zevin A, Stargell LA, Luger K: **The histone chaperone Nap1 promotes nucleosome assembly by eliminating nonnucleosomal histone DNA interactions**. *Mol Cell* 2010, **37**:834-842.
Along with Ref. [21], the authors use quantitative fluorescence measurements to determine the binding affinities of various intermediates in chaperone-mediated nucleosome assembly, such as chaperone–histone and histone–DNA affinities. They conclude that Nap1 acts not primarily by ensuring H2A–H2B supply but through prevention of non-specific histone–DNA aggregates.

56. Koopmans WJ, Brehm A, Logie C, Schmidt T, van Noort J: **Single-pair FRET microscopy reveals mononucleosome dynamics**. *J Fluoresc* 2007, **17**:785-795.

57. • Kulaeva OI, Gaykalova DA, Pestov NA, Golovastov VV, Vassylyev DG, Artsimovitch I, Studitsky VM: **Mechanism of chromatin remodeling and recovery during passage of RNA polymerase II**. *Nat Struct Mol Biol* 2009, **16**:1272-1278.
The authors use a reconstituted *in vitro* transcription elongation system to study nucleosome reorganization requirements during RNA polymerase II mediated transcription. They conclude that lifting the terminal 50 bp off the complete histone octamer is sufficient to allow RNA polymerase II passage through the nucleosome.

Molecular Cell
Previews

A Mitotic Beacon Reveals Its Nucleosome Anchor

Maria Hondele[1,2] and Andreas Ladurner[2,3,*]
[1]EMBL International PhD Programme
[2]Genome Biology Unit
[3]Structural and Computational Biology Unit
European Molecular Biology Laboratory, Meyerhofstrasse 1, 69117 Heidelberg, Germany
*Correspondence: ladurner@embl.de
DOI 10.1016/j.molcel.2010.09.001

Mitosis, nuclear envelope formation, and nucleocytoplasmic transport require chromosomes to identify themselves by enriching Ran-GTP around the chromatin fiber. In a recent *Nature* report, Makde et al. (2010) describe the structure of the Ran activator RCC1 anchored onto nucleosomes.

While chromatin's primary role is to package our DNA into an assembly that promotes the integrity of our genome, chromosomes need to identify themselves as a compartment during dynamic cellular events such as cell division. So how does a cell track the 3D coordinates of its genetic information in order to assemble a bipolar spindle around mitotic chromosomes, or to form a nuclear envelope once cells have divided and then tightly regulate who leaves and enters the nucleus? A key signal that identifies chromatin to the cell is a spherical Ran-GTP gradient that emanates from chromatin. The gradient is established, on the one hand, by the chromatin-bound RCC1 protein, the sole nucleotide exchange factor of Ran. RCC1 only efficiently activates Ran to bind GTP when bound to nucleosomes (Nemergut et al., 2001), the repeating fundamental unit of eukaryotic chromatin structure. Once activated, Ran-GTP diffuses away from chromatin. The cytoplasmatic GTPase-activating protein RanGAP then carries out the flipside to RCC1 action, promoting rapid hydrolysis to Ran-GDP. Thus, our packaged genome marks the anchor point for the establishment of a steep Ran-GTP to Ran-GDP gradient (Carazo-Salas et al., 1999), establishing a nucleocytoplasmatic 3D orientation that is required for mitotic spindle and nuclear envelope formation, as well as transport across the nuclear membrane (Clarke and Zhang, 2008). The mobile chromatin component RCC1 therefore gives directionality to processes that rely on steep nucleocytoplasmatic Ran-GTP gradients (Figure 1).

Chromatin recognition by factors such as RCC1 is crucial for signaling and cellular processes that require access to the DNA template, such as transcription and replication. Indeed, a wealth of genetic, biochemical, and structural evidence have identified and characterized hundreds of factors that recognize, chemically modify, and remodel nucleosomes, spherical complexes of ~145 base pairs of DNA wrapped around an octamer of histones. Decades of research have passed since Ada and Don Olins first glimpsed at nucleosomes under the electron microscope and since Karolin Luger, Timothy Richmond, and colleagues determined the structure of the nucleosome core particle at atomic resolution (Luger et al., 1997). Yet, until the recent *Nature* paper of Makde et al. (2010) our field had not seen a high-resolution structure of a protein directly interacting with the core nucleosome fold. The authors now present the crystal structure of a 145 base-pair nucleosome in complex with two copies of RCC1 (Makde et al., 2010). This structure represents a milestone in the structural analysis of nucleosome binding factors and offers insight into the mechanism of histone- and DNA-interaction by chromatin effectors.

RCC1 was known to bind nucleosomes in vitro and in vivo. Its core fold is composed of a toroid-shaped seven-bladed β-propeller (Renault et al., 1998), which binds histones H2A-H2B and Ran, as well as a short unstructured N-terminal tail, which interacts with DNA and is required for stable nucleosome interaction under high salt (England et al., 2010). Makde and colleagues determined the 2.9 Å resolution crystal structure of a nucleosome core particle bound to two copies of full-length *Drosophila* RCC1 (Makde et al., 2010). The authors liken their structure to the front wheel of a "tricycle," with two RCC1 "pedals" attached in a perpendicular orientation to the nucleosome "wheel." The interaction surface between RCC1 and the nucleosome is bipartite, with the major interaction occurring between an acidic patch on the surface of the histone H2A-H2B dimer and two Arg residues in one of the unstructured loops of RCC1 (named "switchback loop" for its sinuous path). In addition, a different loop of the same propeller-blade contributes a minor, unanticipated interaction with DNA phosphates of the major DNA groove near the sixth DNA helical turn (SHL6). Mutation of positively charged residues within this DNA-binding loop abrogates nucleosome binding, substantiating the binding cooperativity that is established by the bipartite RCC1-histone and RCC1-DNA interaction. While most of the DNA-binding N-terminal tail of RCC1 is not visible in the crystal structure of this complex, the authors' structure strongly suggests that the tail would recognize the minor groove around SHL6, thus contributing to the dynamic binding of RCC1 to chromatin. Consistently, nucleosome binding requires the unstructured N-terminal tail of RCC1.

The acidic patch on H2A-H2B contacted by RCC1 stands out in two ways: First, it is the only negatively charged patch on the otherwise positive or hydrophobic surfaces of histones. Thus, the triad of acidic residues on H2A (E61, D90, E92) establishes a unique binding surface on histones. Second, this region acts as a contact surface in the structures of the nucleosome in complex with RCC1 (Makde et al., 2010), the viral peptide LANA (Barbera et al., 2006), or the histone H4 N-terminal tail (Luger et al., 1997). In all cases, arginine residues within unstructured regions

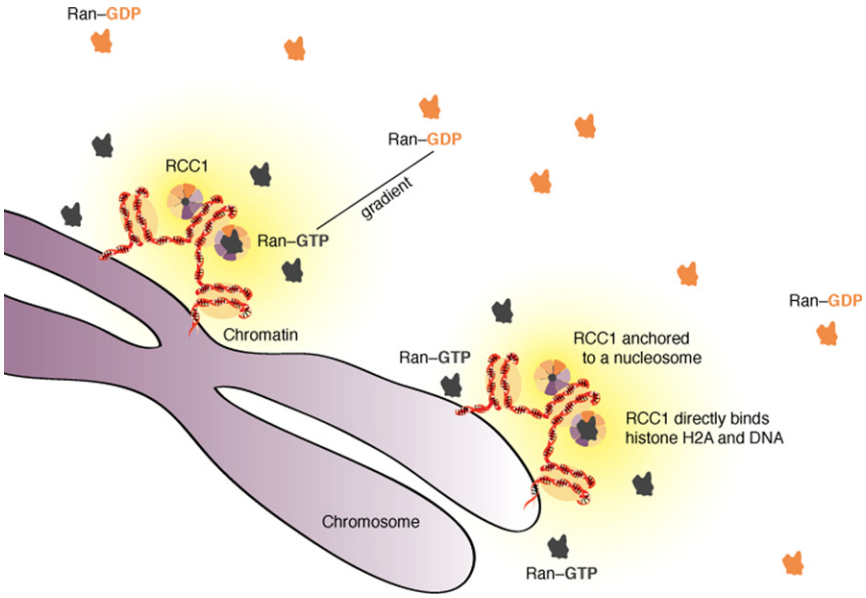

Figure 1. Anchoring of the Nucleotide Exchange Factor RCC1 to Nucleosomes Enriches Ran-GTP around Chromosomes

RCC1 binding to nucleosomes involves the direct recognition of histone H2A as well as the phosphate of the DNA backbone by loops connecting the 7-bladed structure of the Ran-nucleotide exchange factor RCC1. Makde et al. (2010) identify the molecular mechanism used by RCC1 to bind chromosomes, revealing how this regulator establishes a steep Ran-GTP to Ran-GDP gradient required for mitosis, nuclear envelope formation and nucleocytoplasmic transport.

contribute to H2A binding. In particular, the mode of interaction is strikingly similar for RCC1 and LANA, resembling the interaction typically formed between globular proteins and linear motifs. It is therefore quite likely that other nucleosome-binding proteins employ a similar, linear motif-like interaction with the acidic patch on the nucleosome surface. Further, the interaction between the positively charged N-terminal tail of histone H4 with the acidic H2A-H2B surface was first described in the original crystal structure of the nucleosome core particle, and later has been implicated in the formation of higher-order chromatin structures. While the H4 tail adopts a different conformation compared to the LANA peptide or RCC1 protein, and the interaction surface is less extended, the structures predict that proteins such as RCC1 or LANA could outcompete binding of the H4 tail, raising the possibility that nonhistone proteins or peptides that recognize this acidic H2A patch might influence, at least locally and/or temporally, the formation of higher-order chromatin structure.

Clearly, this structure shows us how RCC1 recognizes and intimately binds nucleosomes, establishing the mechanism that anchors RCC1 to chromosomes. But what does the structure tell us about how RCC1 binding to nucleosomes stimulates its nucleotide exchange activity on Ran, thus establishing the Ran-GTP gradient that is fundamental to its function as a signaling beacon? The switchback loop is on the same toroid face and in close proximity to the loop that mediates the major interactions with the nucleotide-binding site of Ran (Renault et al., 2001). When the authors superimposed their structure with the structure of the Ran-RCC1 complex, Ran would not contact the nucleosome, contrary to data indicating that Ran binds to chromatin also independently of RCC1. Makde and colleagues propose that conformational changes in Ran and/or RCC1, as observed in different crystal forms of the individual proteins, might contribute to RCC1's nucleotide exchange activity and lead to direct Ran-chromatin interactions. Specifically, the GTP-bound state of Ran had revealed an unstructured C-terminal 20 amino acids, which are folded into a helix in the GDP-bound state (and also in the complex structure with RCC1). Thus, when becoming unstructured in the GTP-bound state, this Ran region could mediate the previously observed direct interaction of Ran with H3-H4. Further, since RCC1 binding to histones occurs through the rather flexible switchback loop, it is possible that the RCC1 propeller core could pivot the RCC1-bound Ran for direct interactions with the nucleosome, in turn affecting the GDP to GTP exchange reaction. Moreover, higher-order packaging of nucleosomes into fibers creates a dense environment that could affect both RCC1 and Ran binding to nucleosomes and H3-H4, respectively, as well as RCC1's nucleotide exchange activity on Ran. Indeed, RCC1-Ran binding to chromatin may be coupled to the GDP-GTP exchange reaction (Li et al., 2003). With respect to our understanding of how chromatin contributes to establishing Ran-GTP gradients, the merit of this study clearly lies in its atomic description of how the signaling component RCC1 anchors itself onto chromatin. But the authors' successful first use of a distinct DNA template for nucleosome crystallization may also herald the long-sought opportunity of obtaining systematic insight into the structures of many further protein-nucleosome complexes involved in chromatin regulation. Looks like the nucleosome is finally set to reveal how it interacts with its many friends.

REFERENCES

Barbera, A.J., Chodaparambil, J.V., Kelley-Clarke, B., Joukov, V., Walter, J.C., Luger, K., and Kaye, J.C. (2006). Science *311*, 856–861.

Carazo-Salas, R.E., Guarguaglini, G., Gruss, O.J., Segref, A., Karsenti, E., and Mattaj, I.W. (1999). Nature *400*, 178–181.

Clarke, P.R., and Zhang, C. (2008). Nat. Rev. Mol. Cell Biol. *9*, 464–477.

England, J., Huang, J., Jennings, M., Makde, R., and Tan, S. (2010). J. Mol. Biol. *398*, 518–529.

Li, H.Y., Wirtz, D., and Zheng, Y. (2003). J. Cell Biol. *160*, 635–644.

Luger, K., Mader, A., Richmond, R., Sargent, D., and Richmond, T. (1997). Nature *389*, 251–260.

Makde, R.D., England, J.R., Yennawar, H.P., and Tan, S. (2010). Nature. Published online August 25, 2010. 10.1038/nature09321.

Nemergut, M.E., Mizzen, C.A., Stukenberg, T., Allis, C.D., and Macara, I.G. (2001). Science *292*, 1540–1543.

Renault, L., Nassar, N., Vetter, I., Becker, J., Klebe, C., Roth, M., and Wittinghofer, A. (1998). Nature *392*, 97–101.

Renault, L., Kuhlmann, J., Henkel, A., and Wittinghofer, A. (2001). Cell *105*, 245–255.

LETTER

doi:10.1038/nature12242

Structural basis of histone H2A–H2B recognition by the essential chaperone FACT

Maria Hondele[1,2]*, Tobias Stuwe[2]†*, Markus Hassler[1,2], Felix Halbach[3], Andrew Bowman[1], Elisa T. Zhang[2]†, Bianca Nijmeijer[2], Christiane Kotthoff[1], Vladimir Rybin[2], Stefan Amlacher[4], Ed Hurt[4] & Andreas G. Ladurner[1,2,5,6]

Facilitates chromatin transcription (FACT) is a conserved histone chaperone that reorganizes nucleosomes and ensures chromatin integrity during DNA transcription, replication and repair[1–6]. Key to the broad functions of FACT is its recognition of histones H2A–H2B (ref. 2). However, the structural basis for how histones H2A–H2B are recognized and how this integrates with the other functions of FACT, including the recognition of histones H3–H4 and other nuclear factors, is unknown. Here we reveal the crystal structure of the evolutionarily conserved FACT chaperone domain Spt16M from *Chaetomium thermophilum*, in complex with the H2A–H2B heterodimer. A novel 'U-turn' motif scaffolded onto a Rtt106-like module[7–10] embraces the α1 helix of H2B. Biochemical and *in vivo* assays validate the structure and dissect the contribution of histone tails and H3–H4 towards Spt16M binding. Furthermore, we report the structure of the FACT heterodimerization domain that connects FACT to replicative polymerases. Our results show that Spt16M makes several interactions with histones, which we suggest allow the module to invade the nucleosome gradually and block the strongest interaction of H2B with DNA. FACT would thus enhance 'nucleosome breathing' by re-organizing the first 30 base pairs of nucleosomal histone–DNA contacts. Our snapshot of the engagement of the chaperone with H2A–H2B and the structures of all globular FACT domains enable the high-resolution analysis of the vital chaperoning functions of FACT, shedding light on how the complex promotes the activity of enzymes that require nucleosome reorganization.

The essential heterodimeric chaperone FACT destabilizes nucleosomes to promote polymerase progression on chromatin templates[1–4,11] and maintains chromatin structure *in vivo*[5,6]. The recognition of the histone H2A–H2B heterodimer is crucial for the molecular functions of FACT[2]. To map the region(s) specifically responsible for H2A–H2B binding, we tested all globular domains within FACT using pull-down assays. Biochemical dissection of yeast FACT[12] (composed of the Spt16–Pob3 heterodimer) had identified four globular domains (the Spt16 amino-terminal domain (Spt16N)[13,14], the heterodimerization domain Spt16D–Pob3N, the middle domain of Spt16 (Spt16M) and the middle domain of Pob3 (Pob3M)[12]) and carboxy-terminal acidic stretches (Spt16C and Pob3C) (Fig. 1a). We find that only Spt16M, where most of the genetically identified, functionally deficient mutations cluster (Fig. 1a), recognizes H2A–H2B similarly to full-length Spt16 (Fig. 1b). Human Spt16M (encoded by the *SUPT16H* gene) also binds H2A–H2B (Fig. 1c), consistent with the evolutionary sequence

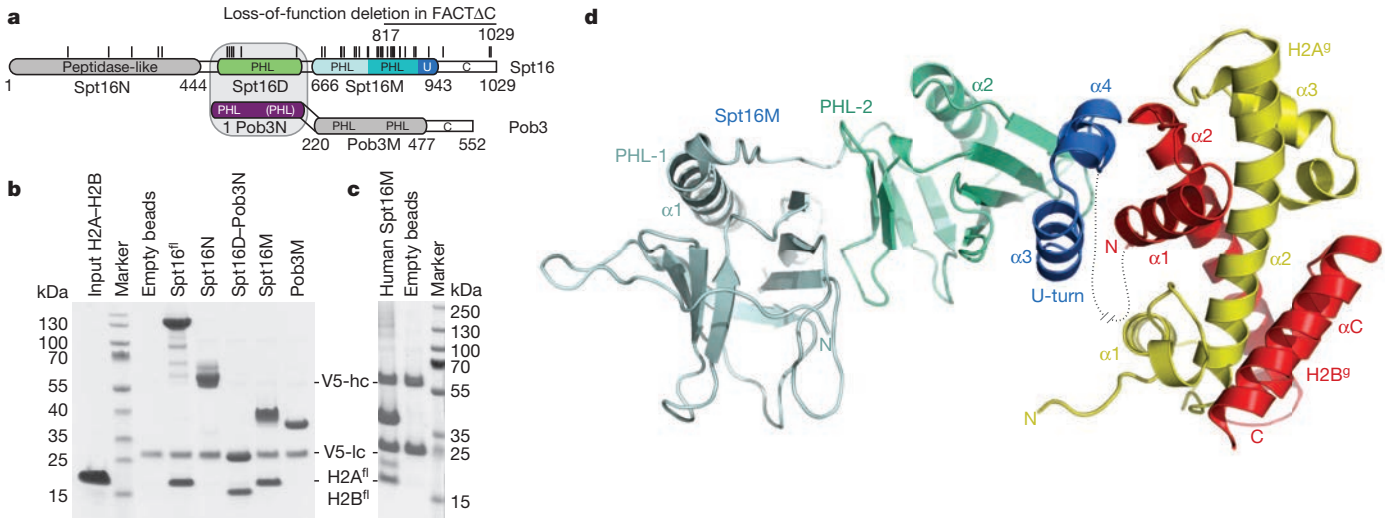

Figure 1 | The histone chaperone complex FACT recognizes the histone H2A-H2B heterodimer through the Spt16M domain of Spt16. a, Domain organization of yeast Spt16. Mutants isolated in *S. cerevisiae* (black lines) and a loss-of-function deletion in human Spt16 are indicated[2,15]. **b**, **c**, V5-immunoprecipitations of yeast (**b**) and human (**c**) Spt16M with H2A–H2B. V5-hc and V5-lc denote the heavy and light chain, respectively, of the V5 antibody. **d**, Crystal structure (2.35 Å) of the tethered (~25-residue linker, no electron density observed, grey dotted line) complex between *C. thermophilum* Spt16M (residues 647–950, green and blue), histone H2A (13–106, yellow) and histone H2B (24–122, red). $H2A^g$ and $H2B^g$ denote the globular domains.

[1]Department of Physiological Chemistry, Butenandt Institute and LMU Biomedical Center, Faculty of Medicine, Ludwig Maximilians University of Munich, Butenandtstrasse 5, 81377 Munich, Germany. [2]Genome Biology Unit and Structural & Computational Biology Unit, European Molecular Biology Laboratory, Meyerhofstrasse 1, 69117 Heidelberg, Germany. [3]Department of Structural Cell Biology, Max Planck Institute of Biochemistry, Am Klopferspitz 18, 82152 Martinsried, Germany. [4]Biochemistry Center, University of Heidelberg, Im Neuenheimer Feld 328, 69120 Heidelberg, Germany. [5]Munich Cluster for Systems Neurology (SyNergy), 81377 Munich, Germany. [6]Center for Integrated Protein Science Munich (CIPSM), 81377 Munich, Germany. †Present addresses: California Institute of Technology, Division of Chemistry and Chemical Engineering, 1200 East California Boulevard, Pasadena, California 91125, USA (T.S.); Department of Molecular and Cell Biology, Howard Hughes Medical Institute, University of California at Berkeley, Berkeley, California 94720-3204, USA (E.T.Z.).
*These authors contributed equally to this work.

conservation of FACT (Supplementary Fig. 1). This identifies Spt16M as a conserved binding module for H2A–H2B.

To characterize how Spt16M engages H2A–H2B, we determined the structures of free *Chaetomium thermophilum* Spt16M (2.0 Å resolution; Supplementary Fig. 2 and Supplementary Table 1) and a tethered complex with the globular H2A–H2B heterodimer (2.35 Å resolution; Fig. 1c and Supplementary Table 2). The core of Spt16M is composed of a tandem pleckstrin homology-like (PHL) module[9] (PHL-1 and PHL-2) structurally related to the H3–H4 chaperones Pob3M and Rtt106 (refs 7–10, 12 and Supplementary Fig. 3). Crucially, only Spt16M contains a C-terminal, α-helical U-turn motif that is patched onto the PHL-2 scaffold and recognizes H2A–H2B (Fig. 1d and Supplementary Fig. 3b). The U-turn motif is the most conserved and only extended hydrophobic patch on Spt16M (Supplementary Fig. 2). It forms a groove complementary to a hydrophobic patch on the N-terminal α1 helix of H2B (Fig. 2a, b and Supplementary Fig. 2c). The conserved Spt16M residues Leu 915, Val 919, Ile 920, Phe 931, Phe 939 and Leu 940 engage the H2B residues Ile 36 and Tyr 39. Additional interactions include those with loop L1 and helix α2 of H2B to establish a ~660 Å^2 interface with a free energy potential of −7.1 kcal mol^{-1}. Comparison of free (*C. thermophilum* and *Saccharomyces cerevisiae*[9]) and histone-bound Spt16M reveals few differences in the backbone of either chaperone or histones (Supplementary Fig. 4), suggesting rigid docking. Isothermal titration calorimetry (ITC) reveals endothermic binding with a ~400 nM dissociation constant (K_d) and 1:1 stoichiometry (Supplementary Fig. 5), consistent with the observed hydrophobic contacts between Spt16M and H2B.

To validate the interactions, we used biochemical, thermodynamic, site-directed mutagenesis and *in vivo* assays. Pull-down assays show that a construct containing the U-turn motif and PHL-2 is sufficient to recognize both full-length and tailless H2A–H2B (Supplementary Fig. 6a). Constructs consisting solely of the U-turn, or PHL-1/PHL-2 module, aggregate during purification, consistent with the hydrophobic core shared between PHL-2 and the U-turn. Wild-type Spt16M forms a complex with H2A–H2B in size-exclusion chromatography (SEC) that is consistent with 1:1:1 stoichiometry (Fig. 2c). By contrast, the Spt16M U-turn mutant Asn916Ser/Val919Ser/Ile920Ser/Thr923Ser (Spt16M^{NVIT}) fails to form a complex with full-length histones H2A–H2B by SEC and ITC (Fig. 2c, d), although its structure is preserved (Supplementary Fig. 6b).

On the histones' side, mutation of the hydrophobic H2B α1 helix residue Ile 36 reduces affinity 30-fold (Fig. 2e and Supplementary Fig. 5). By contrast, mutation of two other prominent hydrophobic surfaces on the H2A–H2B heterodimer, the C-terminal H2A region and Tyr 80 in helix α2 of H2B, does not alter the Spt16M interaction. In agreement, a H2B peptide spanning the H2B α1 helix (residues 26–48) binds Spt16M with low micromolar affinity. Together, these assays validate the hydrophobic, globular interface established by the U-turn and H2B α1 helix as a primary interaction region between the chaperone FACT and H2A–H2B.

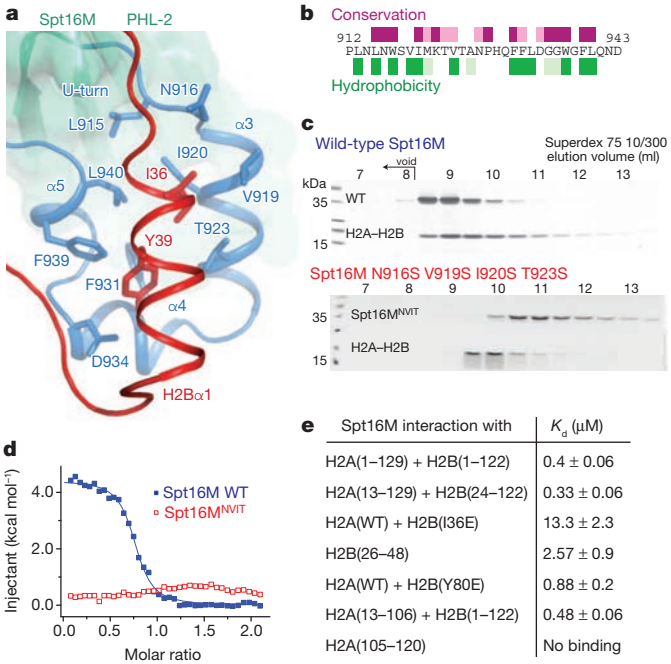

Figure 2 | A conserved, hydrophobic groove in the U-turn motif of Spt16M interacts with a hydrophobic patch of H2B. **a**, Close-up view of the Spt16M–H2A–H2B interface. Side chains of the H2B α1 helix (H2Bα1; red) nestle into the hydrophobic groove formed by the Spt16M (green) U-turn motif (marine). **b**, Primary sequence of residues in the U-turn motif. Hydrophobic residues (green) tend to be conserved (pink). **c**, **d**, Wild-type (WT) Spt16M but not an engineered U-turn mutant forms a complex with full-length H2A–H2B in gel-filtration experiments (**c**) and ITC (**d**). **e**, ITC between wild-type Spt16M and various histone constructs; ITC profiles and fitting data are given in Supplementary Fig. 5. Data are mean ± s.d.

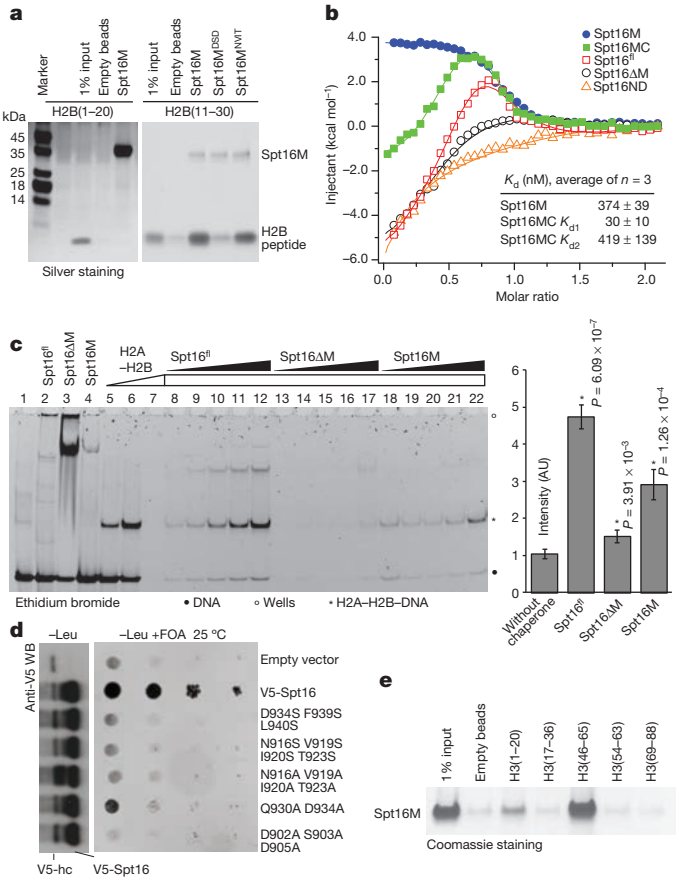

Figure 3 | Multiple interactions support histone binding by FACT, but Spt16M-mediated contacts are key to chaperoning function. **a**, V5-Spt16M pulls down an H2B N-terminal tail peptide encompassing residues 11–30, but not residues 1–20. Mutation of a conserved acidic patch on PHL-2 disrupts binding. **b**, ITC of various (truncated) Spt16 constructs shows that domains other than Spt16M contribute exothermically to the overall interaction with H2A–H2B. **c**, Chaperoning assay. Pre-incubation of H2A–H2B with full-length Spt16 (Spt16^{fl}) or Spt16M, but not Spt16ΔM, prevents histone-driven precipitation of DNA and rescues the soluble H2A–H2B–DNA complex (left). Quantification of the H2A–H2B–DNA complex (lanes 7, 12, 17 and 22) was carried out in quadruplicate (right). AU, arbitrary units. **d**, Wild-type Spt16 rescues a Δ*spt16* strain *in vivo*, whereas U-turn or acidic patch mutants mostly cannot. Protein expression was verified by western blot against an N-terminal V5-tag. FOA, 5-fluoroorotic acid. **e**, Streptavidin-mediated pull down of biotinylated H3 peptides.

Electrostatic interactions, often involving the basic histone tails, support histone–chaperone interactions. For Spt16M and H2A–H2B, the equilibrium dissociation constants are similar in the presence and absence of histone tails (Fig. 2e). However, deletion of the H2B N-terminal tail disrupts the chaperone–histone complex in SEC and accelerates disassembly of the complex (Supplementary Fig. 7a, b). Furthermore, a peptide encompassing H2B residues 11–30, but not 1–20, directly binds the chaperone (Fig. 3a). Interestingly, the Spt16M–H2A–H2B structure reveals an electrostatic crystal contact (450 $Å^2$, free energy potential of $+1.2\,kcal\,mol^{-1}$) mediated by Glu 899, Asp 902 and Asp 905 on PHL-2 and H2A Arg residues (Supplementary Fig. 7c), which could be replaced by positively charged residues of the H2B tail. Consistently, mutation of the acidic patch ($Spt16^{DSD}$; Asp902Ala, Ser903Ala Asp905Ala), but not mutation of the U-turn, abolishes interaction with H2B (11–30) (Fig. 3a) and lowers the K_d for full-length H2A–H2B ~4-fold (Supplementary Fig. 7d). Our data indicate that the H2B tail mediates the kinetic stability of the complex rather than determining its equilibrium stability, which depends on the interactions between the globular cores of H2A–H2B and the Spt16M U-turn.

Deletion of the C-terminal region of human Spt16 (termed FACTΔC) abrogates H2A–H2B binding, chaperone activity and cellular viability[2,15]. In light of our structure, it is clear that in addition to the acidic C-terminal tail of Spt16 (termed Spt16C; ref. 12), FACTΔC lacks the entire and essential U-turn motif and most of PHL-2 (Fig. 1a). To refine the contribution of Spt16M to histone binding and chaperone function further, we compared H2A–H2B binding by full-length Spt16 ($Spt16^{fl}$) with truncated constructs using ITC. Both Spt16M and Spt16M plus acidic C terminus (Spt16MC) display an endothermic binding site ($K_d \sim 400$ nM). However, Spt16MC adds a second, exothermic binding site ($K_d \sim 30$ nM; Fig. 3b), consistent with an independent, electrostatic histone interaction site mediated by Spt16C. These values compare favourably with the 30–90 nM H2A–H2B affinity reported for holo-FACT and full-length Spt16 using independent methods[15]. Furthermore, Spt16N and Spt16D together (Spt16ND) bind H2A–H2B exothermically, albeit with low affinity ($K_d = 10$–$100\,\mu M$). ITC profiles of full-length Spt16 and of Spt16 lacking Spt16M (Spt16ΔM) combine the characteristics of the isolated Spt16M, Spt16MC and Spt16ND domains. Thus, quantitative ITC reveals two high-affinity sites: the hydrophobic interaction seen in our Spt16–H2A–H2B complex, and an electrostatic Spt16C interaction.

Crucially, whereas full-length Spt16 prevents histone–DNA aggregates, a construct lacking Spt16M but containing the high-affinity, electrostatic Spt16C site (Spt16ΔM) cannot (Fig. 3c). By contrast, Spt16M alone resolves aggregates (Fig. 3c), indicating that the interaction of Spt16M with the globular H2A–H2B core is essential to chaperone function.

To test the role of key residues *in vivo*, we rescued the lethality of a yeast *spt16* deletion strain with mutant Spt16 proteins. Mutation of U-turn or acidic patch residues does not reduce the *in vivo* stability of Spt16, but mostly fails to rescue viability (Fig. 3d). Deletion of Spt16C is also lethal. However, because Spt16C contains a putative nuclear localization signal required for nuclear localization (Supplementary Fig. 8), the lethality cannot be directly attributed to a deficient nuclear function.

In addition to binding H2A–H2B, FACT recognizes H3–H4 (ref. 2). Because the tandem PHL core of Spt16M is structurally related to the H3–H4 chaperones Pob3M (ref. 12) and Rtt106 (refs 7, 8, 10), we tested H3–H4 binding and find that Spt16M binds both full-length and tailless H3–H4 (Supplementary Fig. 9a, b). Similarly, *S. cerevisiae* Spt16M binds H3–H4 with 2.5 μM affinity[9]. Importantly, U-turn mutants retain the H3–H4 interaction (Supplementary Fig. 10), suggesting that H3–H4 and H2A–H2B have distinct binding interfaces on Spt16M.

The interaction between Spt16M and H3–H4 probably occurs through a region encompassing histone H3 residues 46–65 (Fig. 3e), which is also recognized by Rtt106, preferentially in Lys 56-acetylated form[7,8]. Spt16M binding of the H3(46–65) peptide is preserved after Lys 56 acetylation (Supplementary Fig. 9d), although future work needs to clarify whether Lys 56 acetylation affects FACT function *in vivo*.

Furthermore, we solved the structure of the FACT heterodimerization domain (Fig. 4a and Supplementary Table 3). Spt16D–Pob3N also consists of PHL domains, a single PHL in Spt16D and a tandem PHL domain lacking the capping helix of the second domain in Pob3N. Interestingly, the PHL module of Spt16D–Pob3N does not interact with H2A–H2B. Nor does it bind H3–H4, in contrast to the tandem PHL modules of Spt16M, Pob3M and Rtt106 (Fig. 1b and Supplementary Fig. 9c). Yet, extended surface patches show high sequence conservation (Supplementary Fig. 11), suggesting a distinct but conserved molecular function. We used *S. cerevisiae* lysates expressing tandem affinity purification (TAP)-tagged proteins to screen for proteins co-precipitating with Spt16D–Pob3N, and identified the large subunit of the DNA polymerase α complex (Pol1) as a Spt16D interactor (Fig. 4b). Our assay suggests that the FACT heterodimerization domain couples FACT to the replication machinery, promoting nucleosome deposition during replication[12].

The high-resolution snapshot of the Spt16M–H2A–H2B complex, together with the structure of the FACT heterodimerization domain, completes the domain-by-domain dissection of FACT structure (Supplementary Fig. 12): Spt16N, Spt16M and Pob3M bind H3–H4, whereas Spt16M binds H2A–H2B. Consistent with the pleiotropic functions of FACT, the interaction between H2B and the Spt16M U-turn is unlikely to be directly affected by H2B heterodimers containing non-canonical H2A variants (for example, H2A.X and macroH2A) or by post-translational modifications including ubiquitination, which has a role in FACT function[16,17] (Supplementary Fig. 13).

Our structures serve as a platform for investigating the mechanism(s) by which holo-FACT couples H2A–H2B recognition to nucleosome reorganization. This can be illustrated by a superposition of Spt16M–H2A–H2B onto the nucleosome core particle (NCP) (Supplementary Fig. 14). We suggest that the solvent-accessible H2B N-terminal tail may mediate first interactions of FACT with the nucleosome. The Spt16M chaperone capitalizes on the dynamic nature of the NCP, in particular the constant and progressive unwrapping/rewrapping of DNA from the octamer core[18], to invade the NCP gradually and develop stronger interactions with the two DNA-covered binding patches on the H3 αN and H2B α1 helices. Shielding of a histones' DNA-interaction site is typical for histone chaperones[19–23]. Together, these multiple contact points establish an extended surface that coordinates the outermost ~30 base pairs[24–26]. Consistently, this DNA becomes hypersensitive to chemical modification in the presence of holo-FACT[27]. In perfect agreement with recent biochemical studies of FACT-facilitated Pol II transcription through nucleosomes[28], our structural data rationalize how FACT promotes nucleosome 'breathing'[15,26] and stabilizes reorganized, partially dissociated, more accessible nucleosome forms[27,29], assisting the passage of polymerases[30] without NCP disassembly to ensure chromatin integrity.

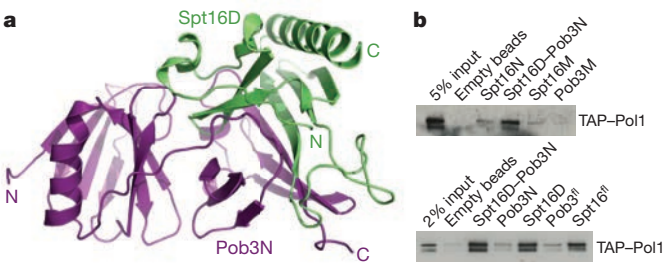

Figure 4 | The heterodimerization domain of FACT mediates interaction with the DNA replication machinery. **a**, Cartoon representation of the Spt16D (green) and Pob3N (magenta) PHL domains. **b**, The Spt16D domain of the FACT complex pulls down replicative Pol1 from yeast whole-cell extracts, as detected by western blot against TAP-tagged Pol1.

METHODS SUMMARY

The *C. thermophilum* Spt16M domain (residues 651–944) was fused to histone H2B (residues 24–122) by a 12-residue linker and was co-expressed with H2A (residues 13–106). Tetragonal crystals of the native complex (space group $P4_32_12$) were grown at 4 °C or 10 °C from hanging drops. High-resolution data sets were collected at beamlines PXIII (Swiss Light Source, Villigen, Switzerland) and ID23-2 (European Synchrotron Radiation Facility, Grenoble, France). ITC was performed at 20 °C in 200 mM NaCl, 25 mM Tris, pH 7.5.

Full Methods and any associated references are available in the online version of the paper.

Received 14 March 2012; accepted 3 May 2013.
Published online 22 May 2013.

1. Orphanides, G., Wu, W. H., Lane, W. S., Hampsey, M. & Reinberg, D. The chromatin-specific transcription elongation factor FACT comprises human SPT16 and SSRP1 proteins. *Nature* **400,** 284–288 (1999).
2. Belotserkovskaya, R. *et al.* FACT facilitates transcription-dependent nucleosome alteration. *Science* **301,** 1090–1093 (2003).
3. Mason, P. B. & Struhl, K. The FACT complex travels with elongating RNA polymerase II and is important for the fidelity of transcriptional initiation *in vivo*. *Mol. Cell. Biol.* **23,** 8323–8333 (2003).
4. Wittmeyer, J., Joss, L. & Formosa, T. Spt16 and Pob3 of *Saccharomyces cerevisiae* form an essential, abundant heterodimer that is nuclear, chromatin-associated, and copurifies with DNA polymerase alpha. *Biochemistry* **38,** 8961–8971 (1999).
5. Kaplan, C. D., Laprade, L. & Winston, F. Transcription elongation factors repress transcription initiation from cryptic sites. *Science* **301,** 1096–1099 (2003).
6. Lejeune, E. *et al.* The chromatin-remodeling factor FACT contributes to centromeric heterochromatin independently of RNAi. *Curr. Biol.* **17,** 1219–1224 (2007).
7. Su, D. *et al.* Structural basis for recognition of H3K56-acetylated histone H3–H4 by the chaperone Rtt106. *Nature* **483,** 104–107 (2012).
8. Zunder, R. M., Antczak, A. J., Berger, J. M. & Rine, J. Two surfaces on the histone chaperone Rtt106 mediate histone binding, replication, and silencing. *Proc. Natl Acad. Sci. USA* **109,** E144–E153 (2012).
9. Kemble, D. J. *et al.* Structure of the Spt16 middle domain reveals functional features of the histone chaperone FACT. *J. Biol. Chem.* **288,** 10188–10194 (2013).
10. Liu, Y. *et al.* Structural analysis of Rtt106p reveals a DNA binding role required for heterochromatin silencing. *J. Biol. Chem.* **285,** 4251–4262 (2010).
11. Orphanides, G., LeRoy, G., Chang, C. H., Luse, D. S. & Reinberg, D. FACT, a factor that facilitates transcript elongation through nucleosomes. *Cell* **92,** 105–116 (1998).
12. VanDemark, A. P. *et al.* The structure of the yFACT Pob3-M domain, its interaction with the DNA replication factor RPA, and a potential role in nucleosome deposition. *Mol. Cell* **22,** 363–374 (2006).
13. Stuwe, T. *et al.* The FACT Spt16 'peptidase' domain is a histone H3–H4 binding module. *Proc. Natl Acad. Sci. USA* **105,** 8884–8889 (2008).
14. VanDemark, A. P. *et al.* Structural and functional analysis of the Spt16p N-terminal domain reveals overlapping roles of yFACT subunits. *J. Biol. Chem.* **283,** 5058–5068 (2008).
15. Winkler, D. D., Muthurajan, U. M., Hieb, A. R. & Luger, K. Histone chaperone FACT coordinates nucleosome interaction through multiple synergistic binding events. *J. Biol. Chem.* **286,** 41883–41892 (2011).
16. Pavri, R. *et al.* Histone H2B monoubiquitination functions cooperatively with FACT to regulate elongation by RNA polymerase II. *Cell* **125,** 703–717 (2006).
17. Fleming, A. B., Kao, C.-F., Hillyer, C., Pikaart, M. & Osley, M. A. H2B ubiquitylation plays a role in nucleosome dynamics during transcription elongation. *Mol. Cell* **31,** 57–66 (2008).
18. Koopmans, W. J. A., Buning, R., Schmidt, T. & van Noort, J. spFRET using alternating excitation and FCS reveals progressive DNA unwrapping in nucleosomes. *Biophys. J.* **97,** 195–204 (2009).
19. Andrews, A. J., Chen, X., Zevin, A., Stargell, L. A. & Luger, K. The histone chaperone Nap1 promotes nucleosome assembly by eliminating nonnucleosomal histone DNA interactions. *Mol. Cell* **37,** 834–842 (2010).
20. Cho, U.-S. & Harrison, S. C. Recognition of the centromere-specific histone Cse4 by the chaperone Scm3. *Proc. Natl Acad. Sci. USA* **108,** 9367–9371 (2011).
21. Hu, H. *et al.* Structure of a CENP-A-histone H4 heterodimer in complex with chaperone HJURP. *Genes Dev.* **25,** 901–906 (2011).
22. Hondele, M. & Ladurner, A. G. The chaperone-histone partnership: for the greater good of histone traffic and chromatin plasticity. *Curr. Opin. Struct. Biol.* **21,** 698–708 (2011).
23. Zhou, Z. *et al.* NMR structure of chaperone Chz1 complexed with histones H2A.Z-H2B. *Nature Struct. Mol. Biol.* **15,** 868–869 (2008).
24. Luger, K., Mäder, A. W., Richmond, R. K., Sargent, D. F. & Richmond, T. J. Crystal structure of the nucleosome core particle at 2.8 A resolution. *Nature* **389,** 251–260 (1997).
25. Killian, J. L., Li, M., Sheinin, M. Y. & Wang, M. D. Recent advances in single molecule studies of nucleosomes. *Curr. Opin. Struct. Biol.* **22,** 80–87 (2012).
26. Hall, M. A. *et al.* High-resolution dynamic mapping of histone-DNA interactions in a nucleosome. *Nature Struct. Mol. Biol.* **16,** 124–129 (2009).
27. Xin, H. *et al.* yFACT induces global accessibility of nucleosomal DNA without H2A–H2B displacement. *Mol. Cell* **35,** 365–376 (2009).
28. Hsieh, F.-K. *et al.* Histone chaperone FACT action during transcription through chromatin by RNA polymerase II. *Proc. Natl Acad. Sci. USA* http://dx.doi.org/10.1073/pnas.1222198110 (22 April 2013).
29. Bondarenko, V. A. *et al.* Nucleosomes can form a polar barrier to transcript elongation by RNA polymerase II. *Mol. Cell* **24,** 469–479 (2006).
30. Kulaeva, O. I. *et al.* Mechanism of chromatin remodeling and recovery during passage of RNA polymerase II. *Nature Struct. Mol. Biol.* **16,** 1272–1278 (2009).

Supplementary Information is available in the online version of the paper.

Acknowledgements We thank J. Basquin, E. Conti, the MPI for Biochemistry and staff at beamlines Swiss Light Source PXII and European Synchrotron Radiation Facility ID23 for crystallographic support, P. Becker, S. Hake, J. Müller and G. Schotta for H3 peptides, and F. Bonneau, P. Cramer, T. Gibson, D. Gilmour, J. Griesenbeck, C. Häring, M. Hothorn, G. Jankevicius, D. Mokranjac, R. Russell, I. Schäfer, K. Scheffzek, C. Schultz, F. Wieland, M. Winter and E. Wolf for discussion. EMBL, LMU Munich, EC FP6 Marie Curie RTN Chromatin Plasticity (to A.G.L.) and Boehringer Ingelheim Fonds (to M.Ho. and F.H.) funded this research.

Author Contributions Crystallography on Spt16M–H2A–H2B was conducted by M.Ho., M.Ha. and F.H.; T.S. determined the structure of free Spt16M and Spt16D–Pob3N, with assistance from M.Ho. and E.T.Z.; M.Ho. and T.S. conducted biochemical assays; A.B. conducted the chaperoning assay; M.Ho., T.S. and B.N. purified proteins; M.Ho., C.K. and T.S. conducted yeast work; M.Ho. and V.R. carried out ITC; S.A. and E.H. provided *C. thermophilum* cDNA sequences; M.Ho., T.S., M.Ha., A.B. and A.G.L. designed the study; M.Ha. and A.G.L. supervised the work; M.H.o, M.Ha., A.B. and A.G.L. wrote the manuscript.

Author Information Atomic coordinates and structure factors have been deposited with the Protein Data Bank under accession codes 4KHA (Spt16M–H2A–H2B), 4KHO (Spt16M) and 4KHB (Spt16D–Pob3N). Reprints and permissions information is available at www.nature.com/reprints. The authors declare no competing financial interests. Readers are welcome to comment on the online version of the paper. Correspondence and requests for materials should be addressed to A.G.L. (andreas.ladurner@med.lmu.de).

METHODS

Protein expression and purification. The *C. thermophilum* Spt16M domain (residues 651–944) was cloned into pETMCN-6xHis, carrying an N-terminal 6×His tag and tobacco etch virus (TEV) protease cleavage site (leaving an N-terminal overhang of the residues Gly-Met-Glu, in which Glu corresponds to residue 647 of Spt16M; clone CL2537). For expression of the complex, the Spt16M construct was fused to a 12-residue GGSGGSGGSGGS linker and the globular domain of H2B (residues 24–122). The construct (clone CL2807) was co-expressed with globular H2A lacking the hydrophobic C terminus (residues 13–106). *C. thermophilum* Pob3N (residues 1–192) was cloned into pETMCN-6xHis (ampicillin selection), carrying an N-terminal 6×His tag and TEV protease cleavage site (leaving an N-terminal overhang of the residues Gly-Met-Glu (clone CL2060) and coexpressed with an untagged version of Spt16D (residues 521–651; clone CL2558) under kanamycin selection.

Constructs were transformed and grown in *Escherichia coli* BL21-CodonPLUS(DE3)-RIL cells to an attenuance (*D*) of 0.7 nm and induced with 0.4 mM isopropyl β-D-thiogalactoside (IPTG) in rich medium at 18 °C for 16 h. Selenomethionine-labelled protein was expressed in strain B834 (DE3) and induced for 18 h with 0.5 mM IPTG in TB media with 40 μg ml^{-1} seleno-L-methionine at 18 °C. Cells were resuspended in 50 mM Tris, pH 7.5, 500 mM NaCl, 10 mM imidazole, and EDTA-free protease inhibitor cocktail (Roche Complete), lysed by sonication, and centrifuged at 45,000*g* for 60 min. The supernatant was loaded onto a column packed with Ni-sepharose high performance beads (GE Healthcare), washed with lysis buffer, and eluted in the same buffer with a linear gradient of imidazole from 0 to 500 mM. Elutions were dialysed overnight in a buffer containing 25 mM Tris, pH 7.5, 400 mM NaCl and 5 mM dithiothreitol (DTT) and subsequently concentrated to 10 mg ml^{-1} using a Vivaspin 15R 10,000 molecular mass cut-off concentrator. The protein was then further purified on a Superdex 75 HR16/60 (for the chaperone–histone complex: SD 200 HR16/60) column (GE Healthcare). Fractions were pooled and the 6×His tag was cleaved with TEV protease for 20 h at 4 °C and dialysed into a buffer containing 25 mM Tris, pH 8.0, 150 mM NaCl and 5 mM DTT (chaperone–histone complex: 25 mM HEPES, pH 8.5, 500 mM NaCl, 2 mM DTT). The protein was bound to a MonoQ HR5/5 (heterodimerization domain: MonoS HR5/5, chaperone–histone complex: MonoS HR10/10) ion exchange column (GE Healthcare) and eluted running a linear gradient of 50 column volumes of elution buffer containing 25 mM Tris, pH 8.0, 1 M NaCl and 5 mM DTT. Fractions were pooled and dialysed against 25 mM Tris, pH 8.0, 150 mM NaCl and 5 mM DTT (complex: 25 mM HEPES, pH 8.5, 500 mM NaCl, 1 mM Tris(2-carboxyethyl)phosphine (TCEP)). Site-specific mutations were introduced by PCR and purified like wild-type Spt16M. Recombinant histones were purified and refolded, as described[31].

Crystallization and data collection. Orthorhombic crystals belonging to space group $P2_12_12_1$ of selenomethionine-labelled and native Spt16M (form A; Supplementary Table 1) were grown at room temperature from hanging drops composed of 1 μl of protein (3 mg ml^{-1}) and 1 μl of crystallization buffer (6% (v/v) PEG 8000, 100 mM Na-cacodylate, pH 5.5, 200 mM Ca-acetate hydrate) suspended over 0.5 ml of the latter. Crystals were transferred in 100% parathon N and frozen in liquid nitrogen. Single-wavelength anomalous dispersion data were collected at beamline PXII (Swiss Light Source (SLS), Villigen, Switzerland). A higher-resolution native data set was acquired at beamline ID-23-1 (European Synchrotron Radiation Facility (ESRF), Grenoble, France). Data processing and scaling were done with XDS[32,33]. Tetragonal crystals of the native complex (space group $P4_32_12$, Supplementary Table 2) were grown at 4 °C or 10 °C from hanging drops composed of 1 μl protein (15 mg ml^{-1}) and 1 μl crystallization buffer (7.25% (v/v) PEG 8000, 0.2 M $MgCl_2$, 0.1 M Tris, pH 7.8) suspended over 1 ml of the latter. Crystals were frozen in glycerol, stepwise soaking up to 20% in crystallization buffer, and frozen in liquid nitrogen. High-resolution data sets were collected at beamlines PXIII (SLS, Villigen, Switzerland) and ID23-2 (ESRF, Grenoble, France). Data processing and scaling were done with XDS and Scala[32,34,35]. Pob3N–Spt16D crystals grew in space group $P2_12_12_1$ (Supplementary Table 3) using the same set up as above in 2.2 M NH_4SO_4, 0.2 M Na-K-tartrate and 0.2 M Na_3-citrate, pH 5.6. Crystals of Pob3N–Spt16D were cryoprotected in crystallization buffer supplemented with 20% ethylene-glycol. Single-wavelength anomalous dispersion data were collected at beamline PX02 (SLS, Villigen, Switzerland). A higher-resolution native data set was acquired at beamline ID-23-eh1 (ESRF, Grenoble, France). Data processing and scaling were done with XDS.

Structure determination and refinement. For Spt16M and Spt16D–Pob3N, single-wavelength anomalous dispersion data were used to locate six selenium sites with Phenix Auto Solve[36] that further carried out site refinement, phasing, density modification and phase extension. Secondary structure elements were identified and an initial model was built using Arp/Warp[37,38]. The structure was completed in alternating cycles of model correction in COOT and restrained refinement in Refmac5 (refs 35, 37). The model was further used to determine the structure of the native data set by molecular replacement with PHASER[33]. For the structure of the complex, a PHASER molecular replacement solution was determined using the Spt16M structure determined here and the histone H2A–H2B heterodimer from the structure of the canonical nucleosome core particle[39]. The structure was finalized by iterative cycles of model adjustment in COOT and refinement in Refmac5 and PHENIX[36]. Structural visualization was done using Pymol. Electrostatic surface potentials were calculated using APBS[40]. Structural superpositions were calculated with 3dSS (ref. 41).

ITC. Binding affinities of wild-type Spt16M with H2A peptide, residues 108–130 (N-acetylated, with a C-terminal Tyr) and H2B peptides, residues 26–48 (N-acetylated, C-amidated), were determined at 25 °C by using VP-ITC and iTC200 calorimeters (GE Life Science, MicroCal). For peptide–protein interaction studies, proteins and peptides were dialysed against ITC buffer (25 mM Tris, pH 7.5, 50 mM NaCl). Injections consisted of 10 μl of peptide (600 μM) into 20 μM protein at 5-min intervals at 25 °C. For protein–protein interaction studies of Spt16M with constructs of histones H2A–H2B, proteins were dialysed against ITC buffer (25 mM Tris, pH 7.5, 200 mM NaCl). Injections on the VP-ITC instrument consisted of 10 μl of Spt16M (325 μM) into 20 μM H2A–H2B dimer at 5-min intervals at 25 °C and of 1 μl injections of 250 μM chaperone into 25 μM H2A–H2B on the iTC200. Data were analysed using Origin software (version 5.0). A single binding site model for Spt16M gave the best fit to the data, whereas Spt16MC had to be fitted with two independent binding sites. Errors are given as s.d. of the fit from the original data points.

Histone refolding and gel filtration. Histone refolding was performed as described[31], with modifications: full-length and globular histones were mixed at equimolar ratios to a final concentration of 1 mg ml^{-1} and refolded in 25 mM Tris, pH 7.5, 150 mM NaCl and 5 mM DTT. H2A–H2B dimers as well as $(H3–H4)_2$ tetramers were subsequently purified by gel-filtration chromatography using a Superdex75 HR16/60 column (GE Healthcare). Histones and Spt16M were mixed at equimolar ratios and incubated on ice for 30 min. Proteins were separated on a Superdex 75 or Superdex 200 10/300 GL column at 25 mM Tris, pH 7.5, 300 mM NaCl and 2 mM DTT.

Native PAGE analysis of Spt16 chaperoning function. Spt16^{fl} and Spt16ΔM were expressed and purified as Spt16M. A 54-base-pair DNA fragment was synthesized as two complementary oligomers, which were then annealed. The ratio of H2A–H2B to DNA that caused close to complete precipitation was determined experimentally at a ratio of three molar equivalents of histone dimer to DNA. Histone dimer (1.2 μM) was preincubated with 0.4, 0.8, 1.6, 3.2 and 6.4 μM of Spt16^{fl}, Spt16ΔM and Spt16M in 10 mM Tris-HCl, pH 7.4, 100 mM NaCl and 1 mM DTT. Binding of chaperone to histone was allowed to proceed at 25 °C for 15 min before the addition of DNA to a final concentration of 0.4 μM in a total reaction volume of 20 μl. In addition, controls containing chaperone at the concentration corresponding to the highest titration point with DNA alone were also carried out. Precipitation was carried out at 25 °C for 1 h before the addition of 5 μl of 20% (w/v) sucrose, removal of precipitates by centrifugation and separation of the remaining soluble complexes on a 9% polyacrylamide gel run in 0.2× TBE buffer. The gels were stained with ethidium bromide before visualization and quantification using a Fusion-FX7 Advance (PeqLab) imaging system. Statistics were calculated on a quadruplicate repeat of the experiment, with a two-tailed *t*-test assuming equal variance. Asterisks indicate *P* values of less than 0.05 when compared to the control without chaperone.

V5 immunoprecipitations. A total of 15 μl of anti-V5-agarose beads (Sigma) was incubated with 40 μg of *E. coli*-expressed, gel-filtration- and ion-exchange-purified V5-fused Spt16 or Pob3 construct for 30 min rotating at 4 °C in 25 mM Tris, pH 7.5, 150 mM NaCl and 0.05% Nonidet P-40 detergent. Beads were washed three times with 1 ml buffer. For interaction with histones, beads were incubated with refolded H2A–H2B in fivefold excess of histone for 1 h at 4 °C. Beads were washed five times with 25 mM Tris, pH 7.5, 200 mM NaCl and 0.05% Nonidet P-40. The samples were either directly boiled in SDS-loading buffer or eluted for 30 min with 25 μl V5 peptide (2 mg ml^{-1}) (sequence, Ac-YGKPIPNPLLGLDST) at room temperature. Samples were subsequently analysed by SDSPAGE. For interaction with H2B or H3 peptides, beads were washed twice with 25 mM Tris, pH 7.5, 600 mM NaCl and 0.05% Nonidet P-40 and twice with 25 mM Tris, pH 7.5, 0.05% Nonidet P-40 and 75 (H2B) or 150 (H3) mM NaCl. Two microlitres of 10 mg ml^{-1} peptide were incubated with the beads in 300 μl of the respective buffer for 2 h at 4 °C. Beads were washed four times with 1 ml buffer and bound peptides eluted twice with 10 μl 25 mM Tris, pH 7.5, 1 M NaCl and 0.05% Nonidet P-40. Samples were analysed by SDS–PAGE (NuPAGE BisTris 4–12%, run only for 75% of the length) and silver stain (Invitrogen SilverQuest kit).

Biotin–streptavidin immunoprecipitations. A total of 25 μl of streptavidin dynabeads (T1, Invitrogen) was saturated with 20 μl of 10 mg ml^{-1} H3 peptides for 1 h rotating at 4 °C in 25 mM Tris, pH 7.5, 150 mM NaCl and 0.05% Nonidet P-40 detergent. Beads were washed three times with 1 ml buffer. Recombinant

Spt16M was incubated with the beads for 2 h rotating at 4 °C. Beads were washed five times with 1 ml buffer, bound protein was eluted by boiling with Laemmli SDS loading buffer and analysed by SDS–PAGE and Coomassie staining.

Phenotypic analyses in *S. cerevisiae*. To determine the effect of Spt16M mutations on yeast cell growth[42], Spt16 was deleted from *S. cerevisiae* strain W303 by homologous recombination introducing a TRP cassette as selection marker. The associated lethal phenotype was rescued using a plasmid (YCplac33) carrying wild-type Spt16 from *S. cerevisiae* (clone CL2303) as well as the *URA3* gene that was co-transformed using the lithium acetate/PEG method. Spt16 from *C. thermophilum* (wild-type and mutants thereof; clones CL2924 (wild type), CL3046 (NVIT→A), CL3002 (NVIT→S), CL3001 (DFL→S), CL2978 (QD→A) and CL2977 (DSD→A)) with an N-terminal V5-tag was cloned into YCplac111 carrying the *LEU2* gene. The Δ*spt16* strain with the URA rescue plasmid was transformed with the mutant constructs under Leu selection und further on submitted to 5-fluoroorotic acid (FOA) selection. Thus, mutants depending on the presence of wild-type Spt16 cannot grow on FOA plates. Transformants growing on selective synthetic medium (SD − Leu) plates were grown for 5 h in YPAD medium and subsequently plated by spotting 4 µl of tenfold serial dilutions onto −Leu FOA plates and incubated at 24 °C for 4 days.

31. Dyer, P. N. *et al.* Reconstitution of nucleosome core particles from recombinant histones and DNA. *Methods Enzymol.* **375,** 23–44 (2003).
32. Kabsch, W. XDS. *Acta Crystallogr. D* **66,** 125–132 (2010).
33. McCoy, A. J. *et al.* Phaser crystallographic software. *J. Appl. Crystallogr.* **40,** 658–674 (2007).
34. Collaborative Computational Project, Number 4. The *CCP*4 suite: programs for protein crystallography. *Acta Crystallogr. D* **50,** 760–763 (1994).
35. Emsley, P. & Cowtan, K. Coot: model-building tools for molecular graphics. *Acta Crystallogr. D* **60,** 2126–2132 (2004).
36. Adams, P. D. *et al.* PHENIX: a comprehensive Python-based system for macromolecular structure solution. *Acta Crystallogr. D* **66,** 213–221 (2010).
37. Murshudov, G. N., Vagin, A. A. & Dodson, E. J. Refinement of macromolecular structures by the maximum-likelihood method. *Acta Crystallogr. D* **53,** 240–255 (1997).
38. Langer, G., Cohen, S. X., Lamzin, V. S. & Perrakis, A. Automated macromolecular model building for X-ray crystallography using ARP/wARP version 7. *Nature Protocols* **3,** 1171–1179 (2008).
39. Luger, K., Rechsteiner, T. J., Flaus, A. J., Waye, M. M. & Richmond, T. J. Characterization of nucleosome core particles containing histone proteins made in bacteria. *J. Mol. Biol.* **272,** 301–311 (1997).
40. Baker, N. A., Sept, D., Joseph, S., Holst, M. J. & McCammon, J. A. Electrostatics of nanosystems: application to microtubules and the ribosome. *Proc. Natl Acad. Sci. USA* **98,** 10037–10041 (2001).
41. Sumathi, K., Ananthalakshmi, P., Roshan, M. N. A. M. & Sekar, K. 3dSS: 3D structural superposition. *Nucleic Acids Res.* **34,** W128–W132 (2006).
42. Capozzo, C. *et al.* Gene disruption and basic phenotypic analysis of nine novel yeast genes from chromosome XIV. *Yeast* **16,** 1089–1097 (2000).

SUPPLEMENTARY INFORMATION

doi:10.1038/nature12242

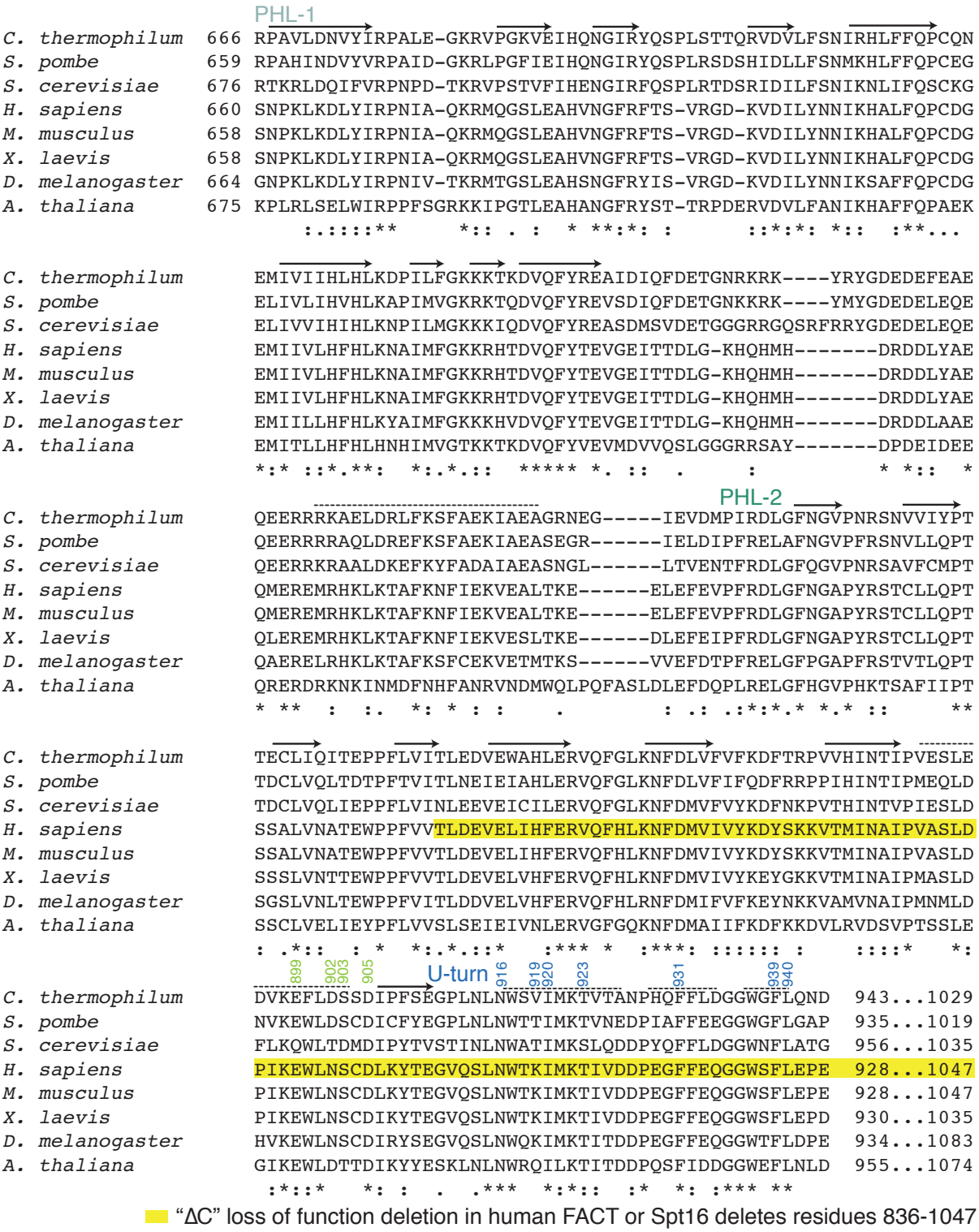

Supplementary Figure 1 | Sequence alignment of selected eukaryotic Spt16M domains. ClustalW2 alignments show absolutely conserved residues with asterisks below the sequence alignment and mostly conserved residues with two or one dots. Above the alignment, secondary structure elements are marked: β-sheets are marked with dotted lines, α-helices as arrows.

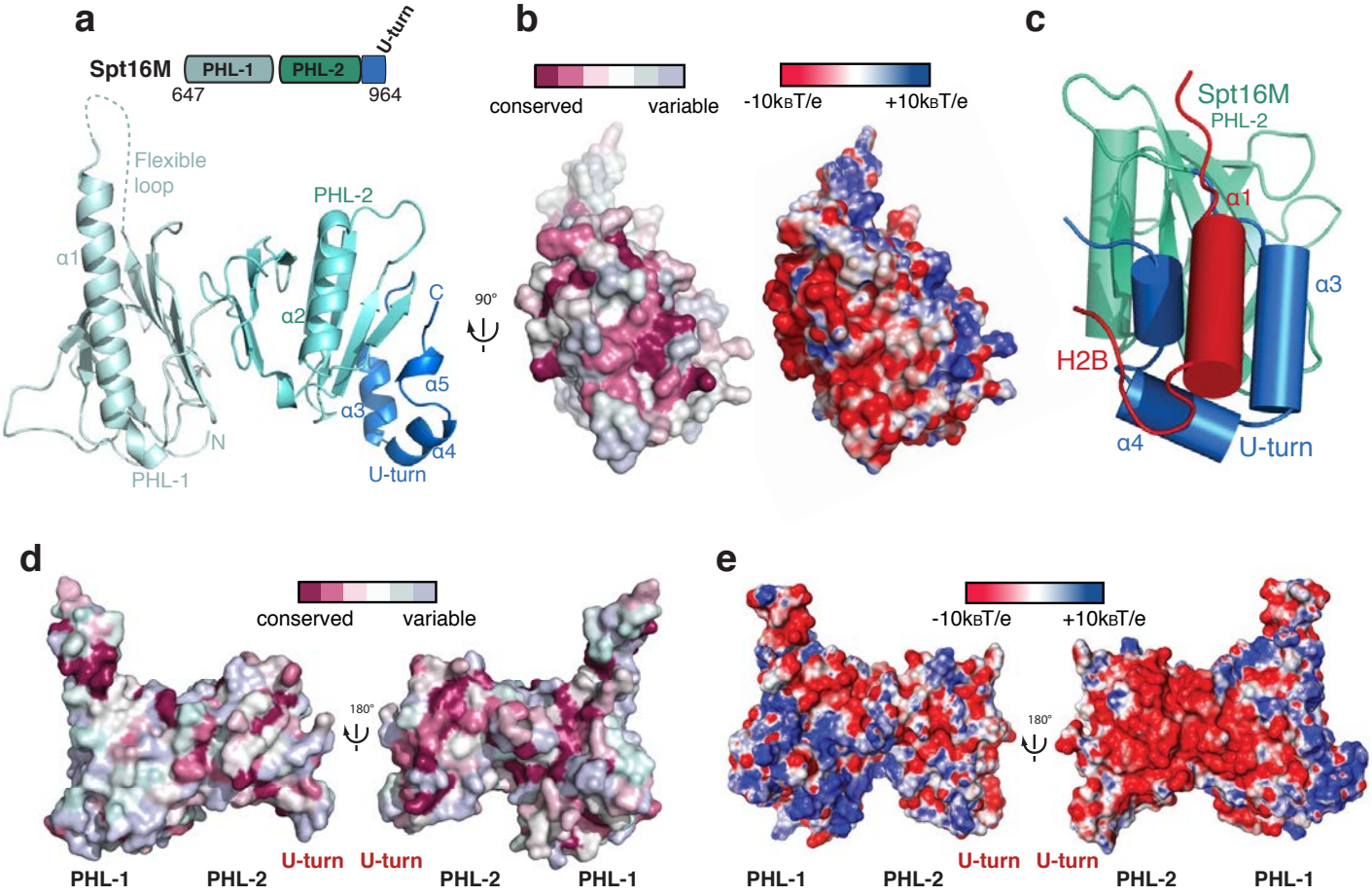

Supplementary Figure 2 | Analysis of the Spt16M surface.
a, 2.0 Å resolution crystal structure of *Ch. thermophilum* Spt16M (residues 647-950) in ribbon representation (PDB ID = 4KHO). **b,** Surface sequence conservation and electrostatics of the U-turn motif. **c,** Cartoon model of the N-terminal H2B helix (*red*) fitting into a groove formed by the three U-turn helices (*marine*) patched onto Spt16M PHL-2 (*green*). **d,** Surface sequence conservation of the tandem PHL module of Spt16M. The color code for the conservation score is shown at the bottom and is based on an alignment of 18 known sequences for Spt16 ranging from yeast to humans (alignment performed using ClustalW2). **e,** Electrostatic surface potential of Spt16M. The structure is shown in surface representation with contour levels from -10kBT/e (*red*=negative) to 10kBT/e (*blue*=positive). Electrostatic potential was calculated using APBS[40]. The PHL-1 domain displays positively charged surface patches. Further, the PHL-1 capping α 1-helix is atypically extended, with a Lys-Arg rich stretch connecting the β-barrel of PHL-1 to the capping α-helix, providing a positively charged surface that is conserved (b) and is required for viability (*data not shown*). PHL-2 displays an acidic surface, suited to neutralize histones.

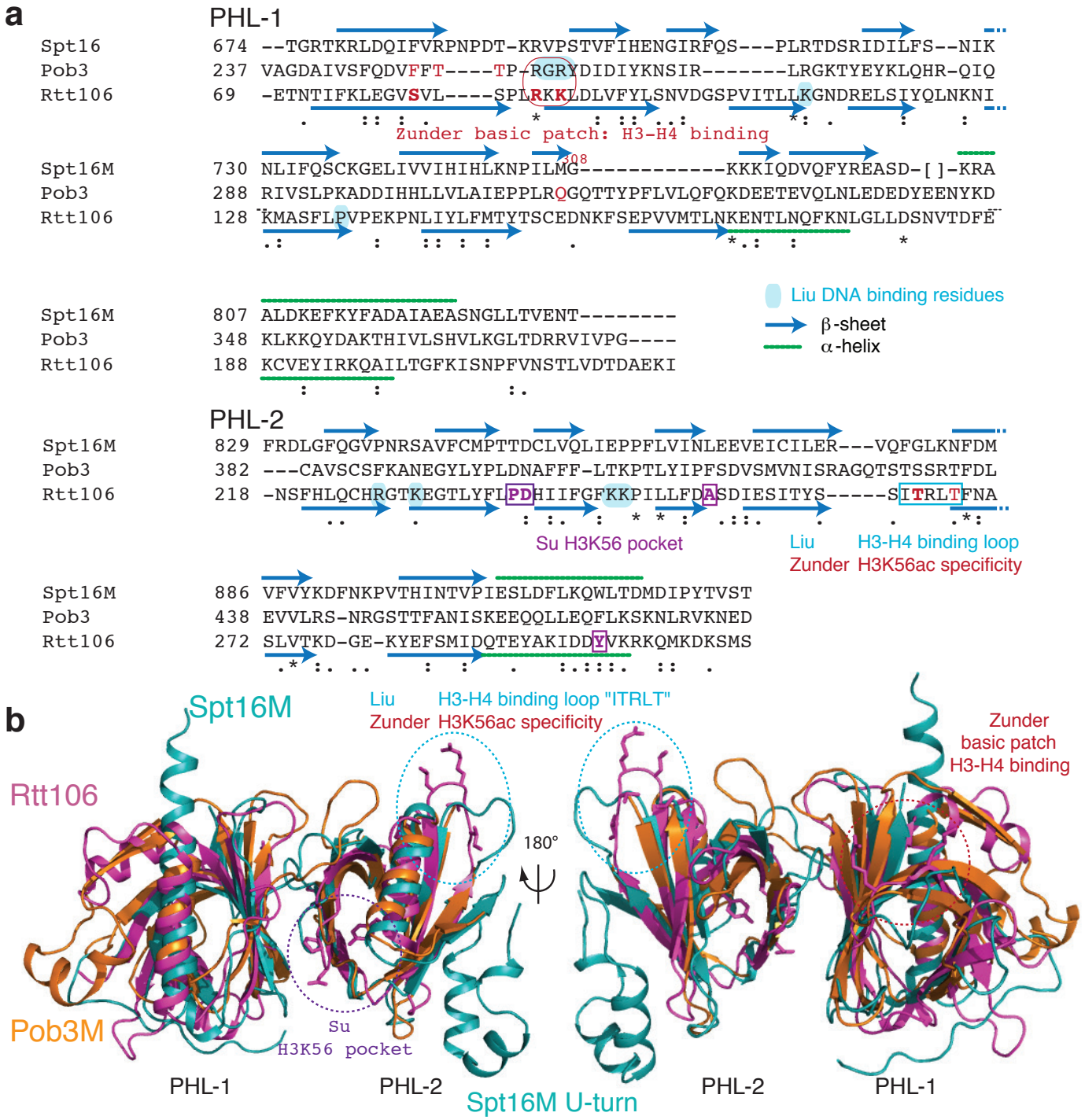

Supplementary Figure 3 | Spt16M is structurally related to the tandem PHL domains of the fungal H3-H4 binding chaperones Pob3M and Rtt106.

Reference is given to three publications that map histone binding onto the Rtt106 and Pob3M structures: Liu = Liu *et al.*, JBC 2010, Su = Su *et al.*, Nature 2012., Zunder = Zunder *et al.*, PNAS 2012 **a,** Structure-guided sequence alignment of the *S. cerevisiae* sequences for the three chaperone domains, split into individual PHL domains. Secondary structure elements are indicated as *blue* arrows (β-sheet) or *green* dashed lines (α-helix). **b,** Structural superpositions of the tandem PHL domains from Spt16M (*green,* PDB ID = 4KHA), Pob3M (*orange*, PDB ID = 2GCL; average r.m.s.d. of 2.4Å on 197 Cα-atoms for PHL-2) and Rtt106 (*pink*, PDB ID = 3TO1 from Zunder *et al.*; average r.m.s.d. of 3.2Å on 189 Cα-atoms for PHL-2). Putative histone H3 binding surfaces are labeled as described in the cited literature.

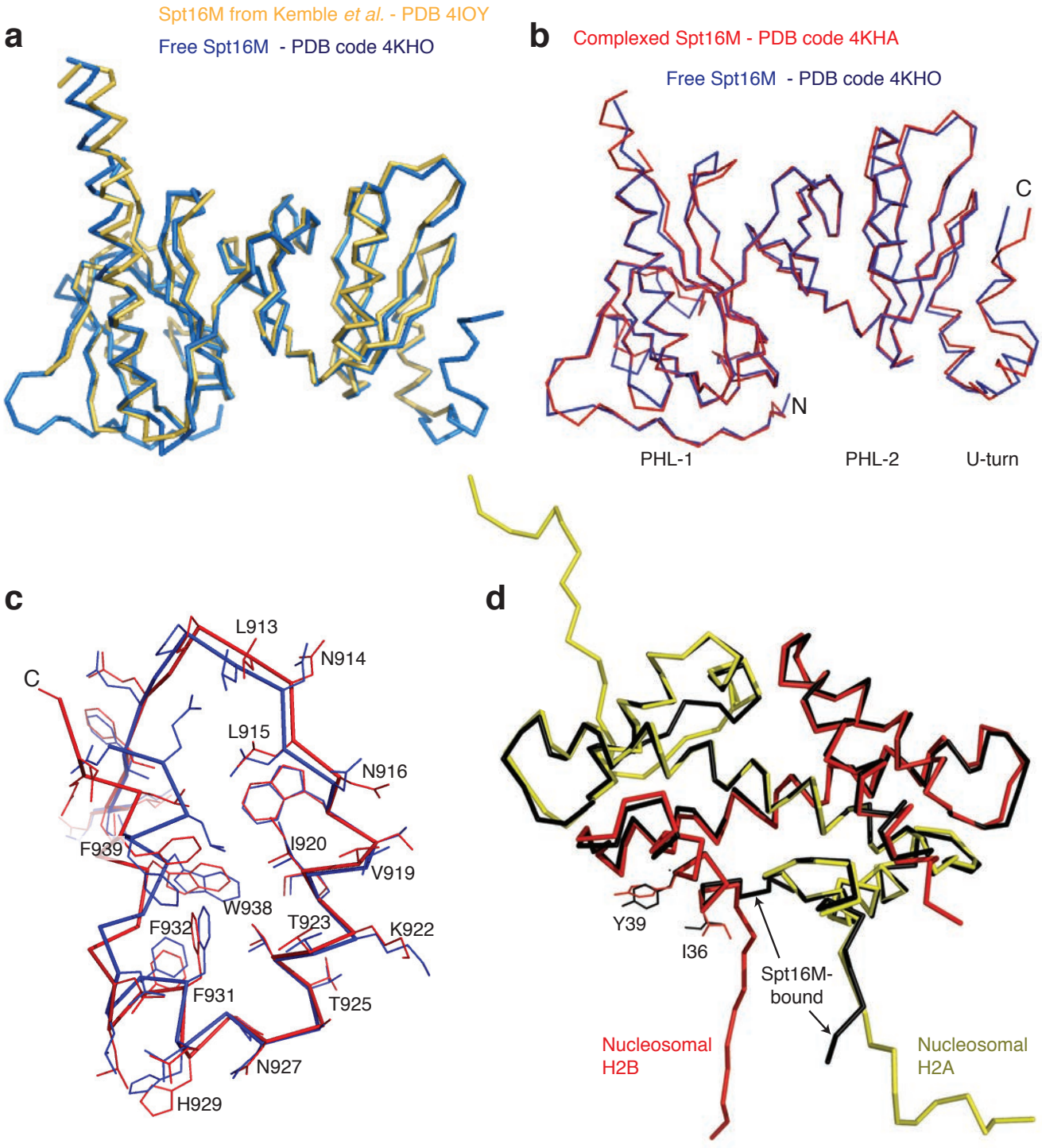

Supplementary Figure 4 | Superposition of the Spt16M–H2A-H2B complex relative to free Spt16M. **a,** Superposition of Spt16M crystallized in the free form, from this work (*C. thermophilum, blue,* PDB ID = 4KHO) and Kemble *et al., 2013* (*S. cerevisiae, yellow,* PDB ID = 4IOY) **b,** Superposition of Spt16M as crystallized in the free form (*blue,* PDB ID = 4KHO) and in complex with H2A-H2B (*red,* PDB ID =4KHA). R.M.S.D. of 1.14 Å on 271 Cα-atoms. **c,** Closeup view of the H2B-binding U-turn motif; sidechains are shown in line representation. **d,** Superposition of the H2A-H2B dimer as part of the nucleosome (*yellow / red,* PDB ID = 1AOI) or in complex with Spt16M (*black,* PDB ID = 4KHA). Average r.m.s.d. of 1.09Å on 193 Cα-atoms.

H2A(1-129) + H2B (1-122)

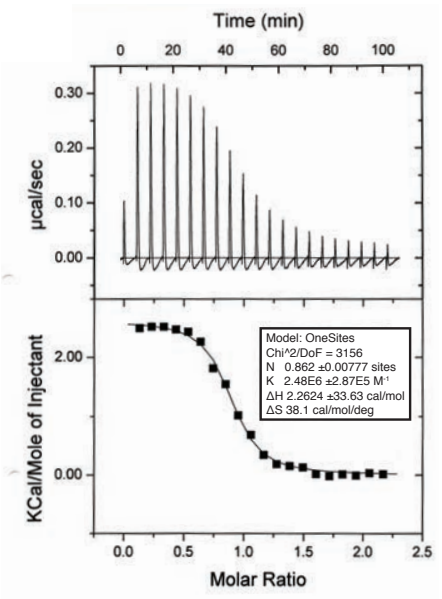

H2A(13-129) + H2B (24-122)

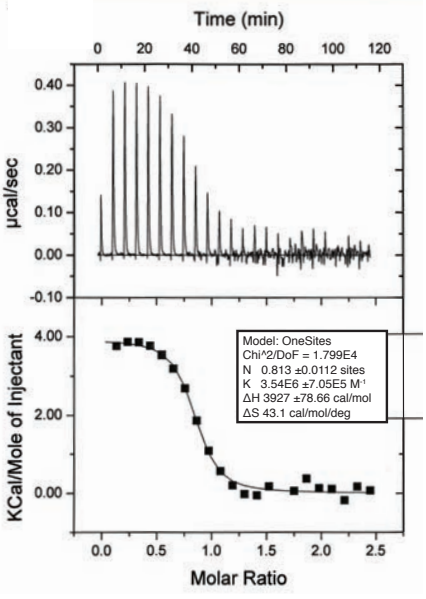

H2A(13-109) + H2B (1-122)

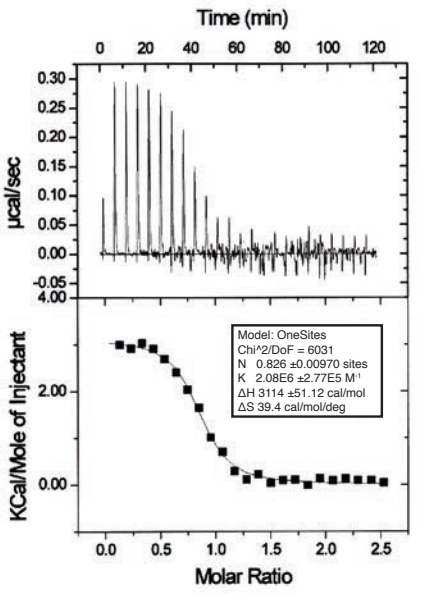

H2A(1-129) + H2B (1-122, Y80E)

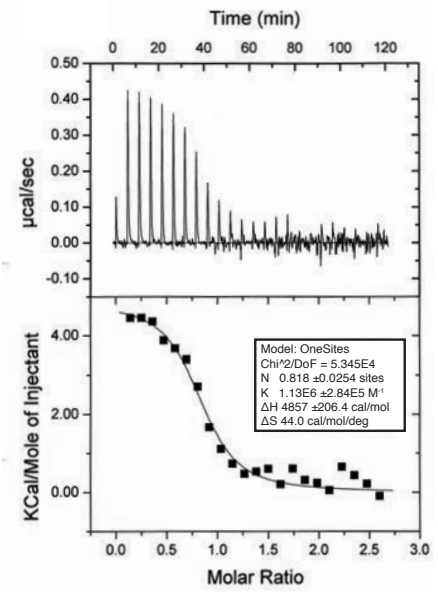

H2A(1-129) + H2B (1-122, I36E)

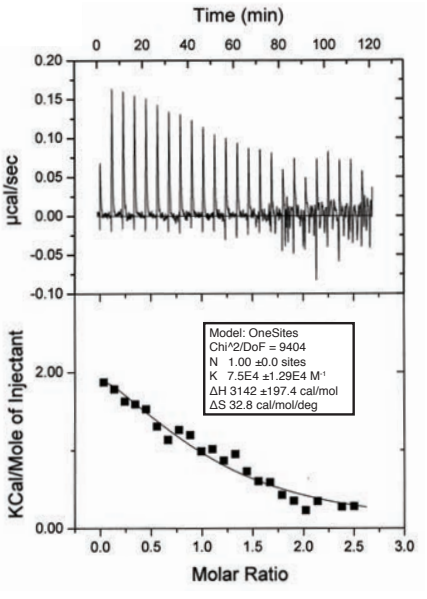

H2B (26-48)

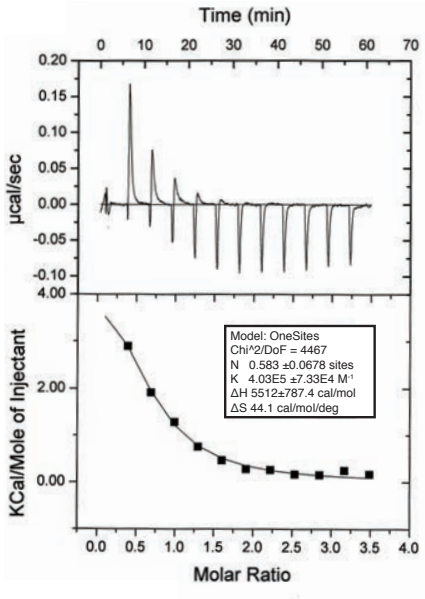

Supplementary Figure 5 | Raw isothermal titration calorimetry (ITC) data for the interaction between Spt16M and the H2A-H2B histone heterodimer and truncations thereof.
ITC assays using Spt16M as ligand reveals an endothermic interaction between Spt16M and histones H2A-H2B. All measurements were performed in 25 mM Tris, pH 7.5, and 200 mM NaCl at 25 °C.

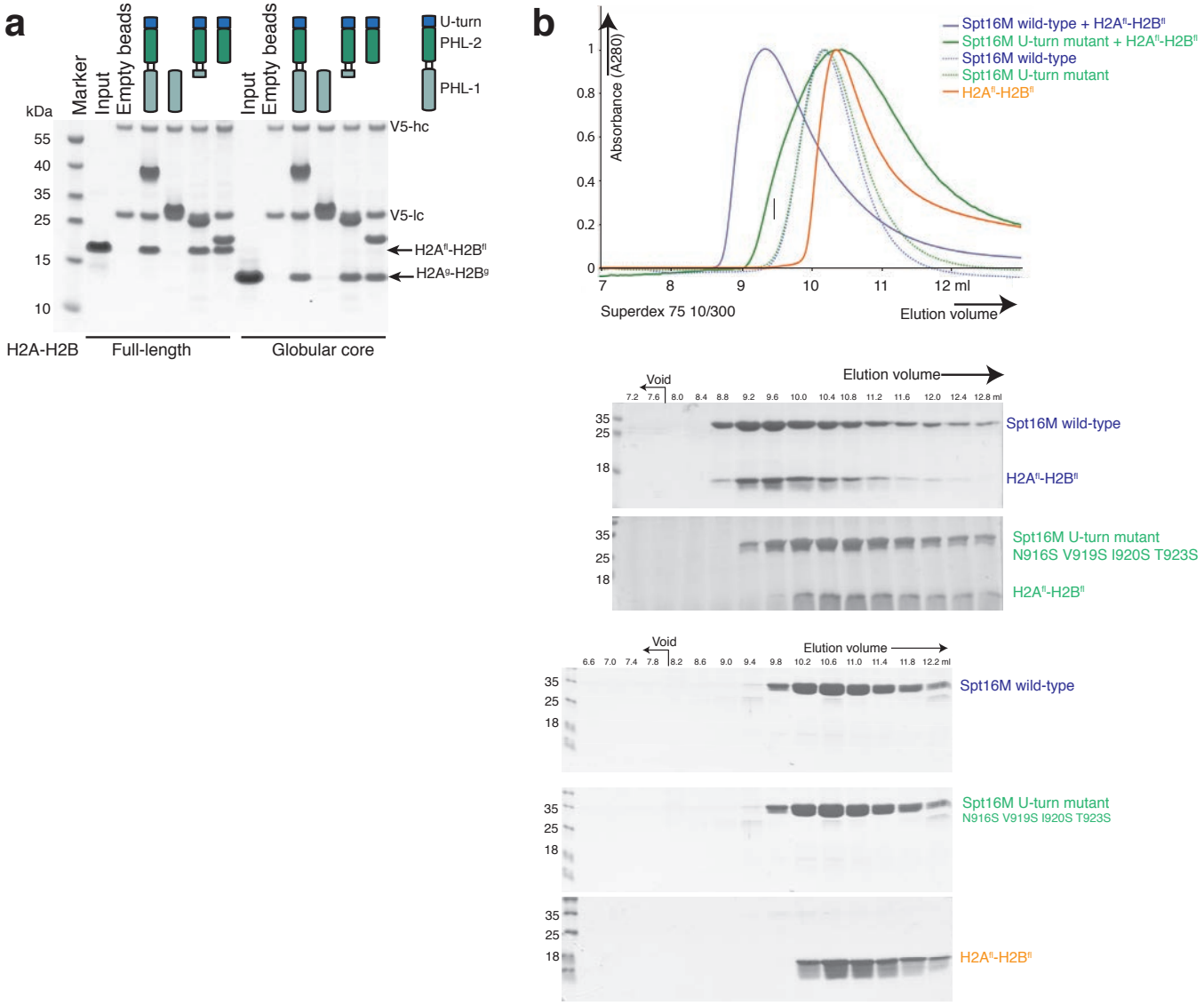

Supplementary Figure 6 | Biochemical mapping and size exclusion chromatography (SEC) of Spt16M with full-length H2A-H2B.

a, Pull-downs with V5-tagged Spt16M reveal interaction with full-length and globular H2A-H2B heterodimer. A C-terminal PHL2 and U-turn motif construct is necessary and sufficient for interaction. b, Wild-type Spt16M and the U-turn mutant were separated on a Superdex 75 10/300 column. UV absorption traces (280 nm wavelength) and corresponding SDS-PAGE of the eluted fractions show that mutation of the U-turn motif of Spt16M is sufficient to disrupt the complex between chaperone and H2A-H2B.

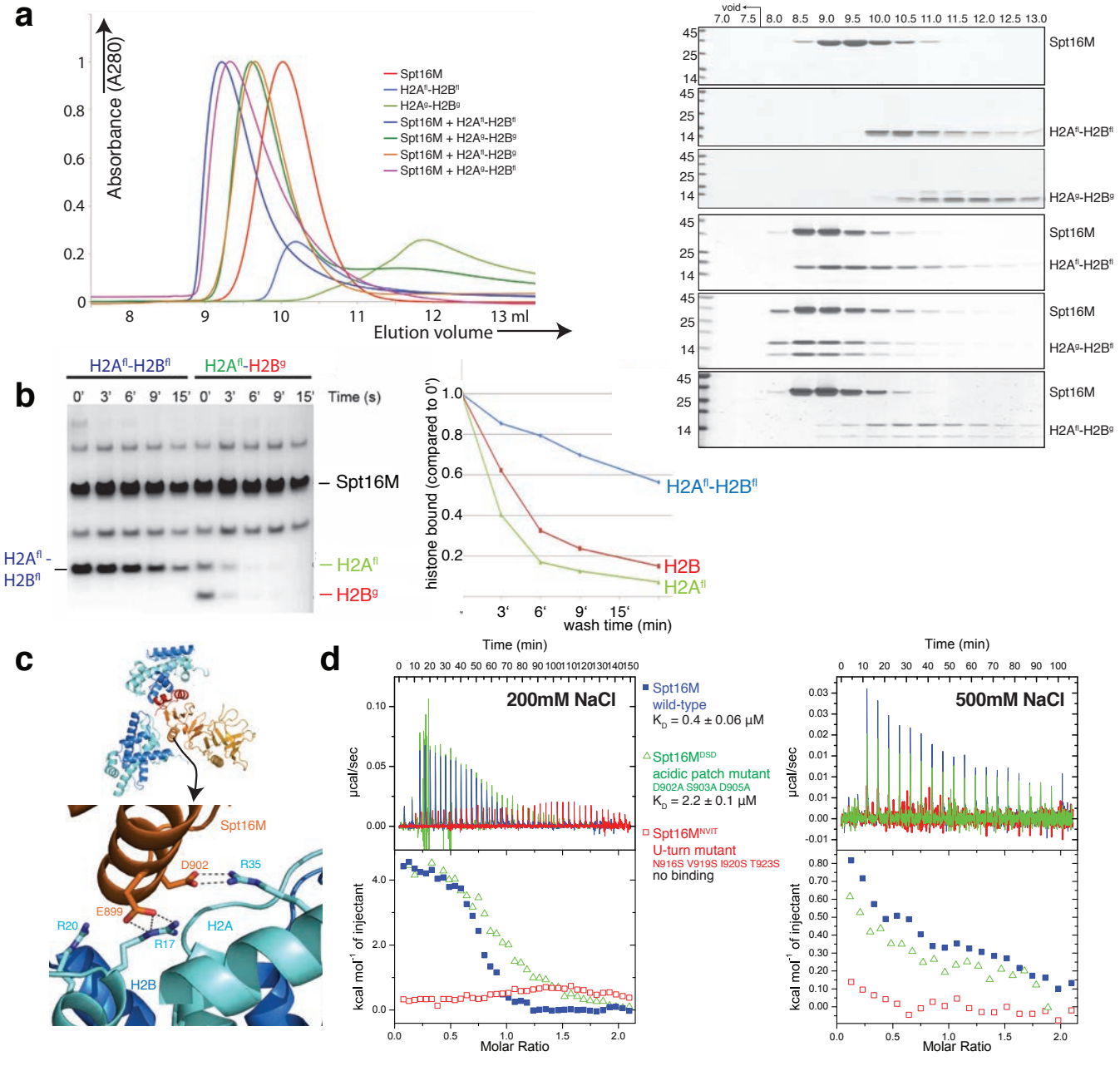

Supplementary Figure 7 | The H2B N-terminal tail contributes to the kinetics of complex formation.
a, The N-terminal tail of H2B, but not of H2A, is required for complex formation in SEC. Spt16M and histone H2A-H2B dimers were separated on a Superdex 75 10/300 column in buffer containing 300 mM NaCl. SEC profiles for individual proteins and complexes and SDS-PAGE of eluted fractions for the complexes are shown. It is worth noting that upon deletion of the H2B tail, Spt16M and the histone dimers elute in different peaks, but both peaks are shifted to an earlier elution volume. We speculate that this might be the result of an initially formed unstable complex that falls apart during the run. **b,** Histone dimers lacking the H2B tail dissociate more quickly from Spt16M than full-length H2A-H2B dimers. Spt16M was immobilized on V5-beads and saturated with the respective histone dimers. Beads were spun down and rotated at room temperature with 1 ml of washing buffer for the indicated time. Bound protein was eluted with Laemmli SDS-buffer and analyzed by SDS-PAGE and Coomassie staining. We refer to this assay as a `kinetic' pulldowns. **c,** Orientation of Spt16M and the H2A-H2B dimers from its own and the neighbouring asymmetric unit in the crystal lattice, and close-up view of an electrostatic crystal contact (450 Å^2, free energy potential of +1.2kcal/mol). A conserved acidic patch on PHL-2 of Spt16M (Glu899, Asp902, Asp905) contacts basic residues in the N-terminal tail and α1-helix of H2A. **d,** Raw ITC profiles and ΔH values for the interaction of Spt16M (wild-type, acidic patch mutant and U-turn mutant) with full-length H2A-H2B dimers measured in 25 mM Tris, pH 7.5, and 200 or 500 mM NaCl at 25° C. At 500 mM NaCl, the contribution of the acidic patch is negligible and the mutant behaves almost like wild-type protein.

a

b Sequence of Spt16C

```
951  EEEEDEDSAFEISESELEAASESSEEDSDYEDASEEESDAPPSEDDEGESWDELERKARKRDRESGLDDDDRGGKKRRR
                                                                        putative NLS

H. sapiens          RSMSRKRKASVHSSGRGSN-RGSRHSS--APPKKKRK 1047
M. musculus         RSMSRKRKASVHSSGRGSN-RGSRHSS--APPKKKRK 1047
C. thermophilum     --DEGESWDELERKARKRD-RESGLDDDDRGGKKRRR 1029
S. cerevisiae       ESEEGEDWDELEKKAARAD-RGANFRD---------- 1035
S. pombe            -EESGEDWDELERKARQEDAKHDAFEE--RPSKKRHR 1019
A. thaliana         -RRKMKAFGKSRPGTSGGG-GSSSMKN-MPPSKRKHR 1074
D. melanogaster     -SSSSGNKSSSKDKDRKRS-RDDSRDN-GHKSKKSRH 1083
X. laevis           --DRESLYEEVEEQKSGNR-KRKGHAPLPNPSKKRKK 1035
```

c

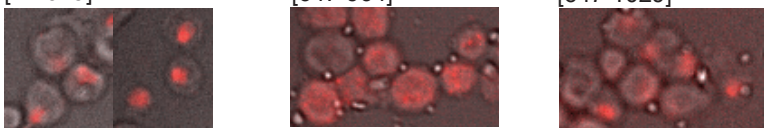

Supplementary Figure 8 | The Spt16C domain is required for viability.
a, A Spt16 protein lacking the Spt16C domain fails to rescue the lethality of a spt16 deletion strain in *S. cerevisiae.* **b,** The *Ch. thermophilum* Spt16C sequence contains a conserved putative NLS signal, predicted with the NucPred server (Brameier et al. 2007 Bioinformatics). **c,** Full-length Spt16 (*C. thermophilum*) and a construct spanning both Spt16M and Spt16C domains (Spt16 MC) localize to the nucleus, while a deletion of Spt16C (resulting in the Spt16 M construct) abrogates nuclear localization. The protein construct mostly localizes to the cytoplasm.

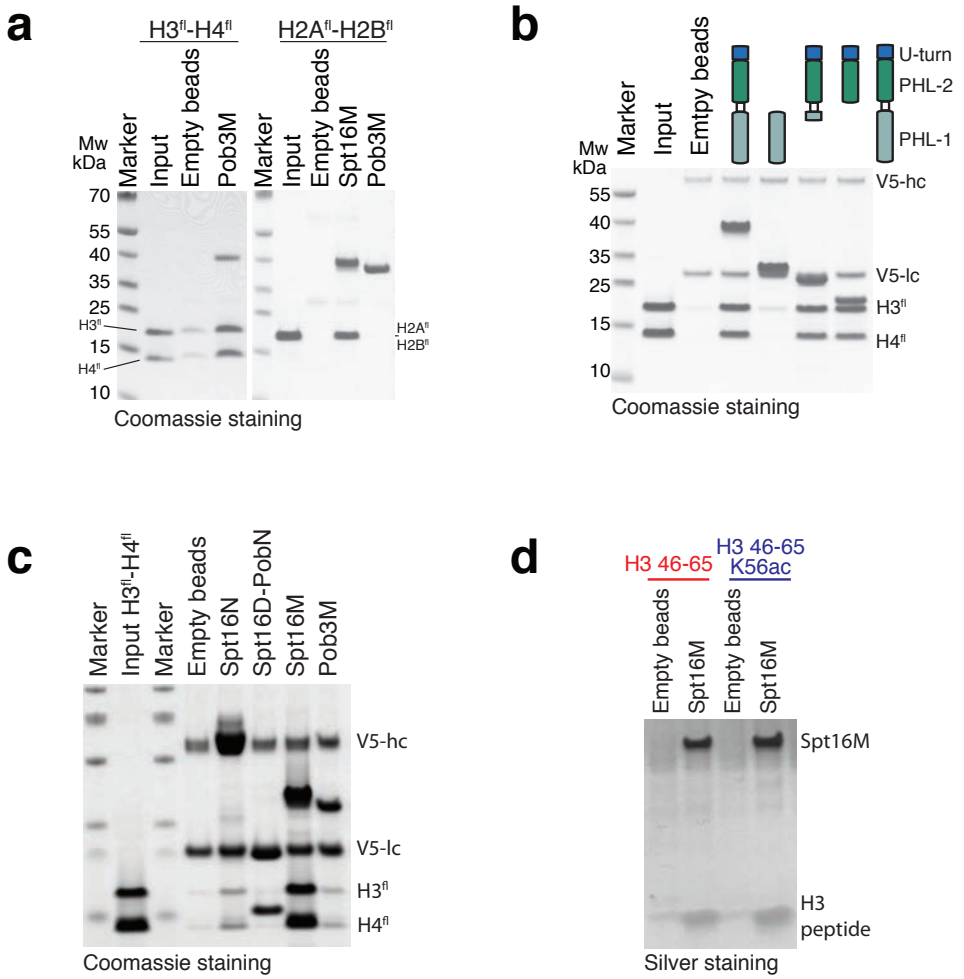

Supplementary Figure 9 | The Spt16M and Pob3M domains bind histones H3-H4.
a-c, V5-tagged Spt16 domains, Spt16M (or fragments thereof) or Pob3M were bound to beads, incubated with histones and washed extensively with 300 mM NaCl, unless indicated otherwise. Bound complexes were eluted with V5 peptide (**a**) or SDS loading buffer (**b, c**) and separated on 4-12% acrylamide gels. **a,** Pob3M forms a stoichiometric complex with full-length H3-H4 but not with H2A-H2B. **b,** The PHL-2 domain of Spt16 is necessary and sufficient for H3-H4 binding. **c,** V5-immunoprecipitations of FACT's globular domains with full-length histones H3-H4. Spt16M, Spt16N and Pob3M interact with histones H3-H4, but the heterodimerization domain Spt16D-Pob3N does not. **d,** V5-Spt16M pulls down H3 [46-65] peptides with and without acetylation of H3 K56, as detected by silver staining.

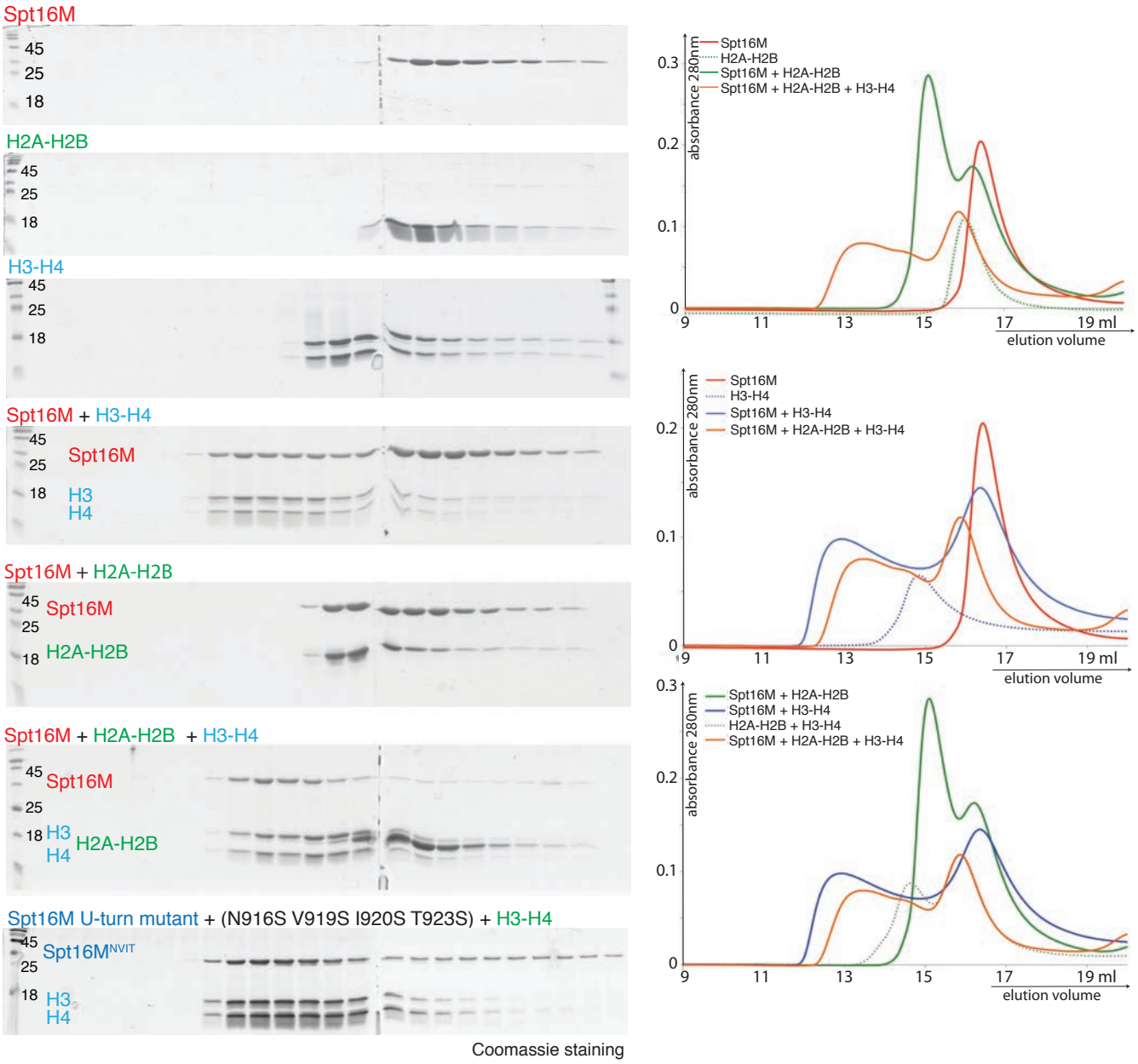

Supplementary Figure 10 | SEC of Spt16M with H2A-H2B and H3-H4.
Individually, both the H3-H4 and the H2A-H2B heterodimer form a soluble complex with Spt16M in SEC (size-exclusion chromatography, Superdex 200 10/300) at 300 mM NaCl. When Spt16M, H2A-H2B heterodimers and H3-H4 heterodimers are mixed all together in stoichiometric amounts, H3-H4 outcompetes H2A-H2B for binding to Spt16M. In contrast, the H2A-H2B-binding-defective Spt16M^{NVIT} U-turn mutant retains its ability to interact with histones H3-H4, indicating that the U-turn motif establishes a unique contact surface that is specific for H2A-H2B.

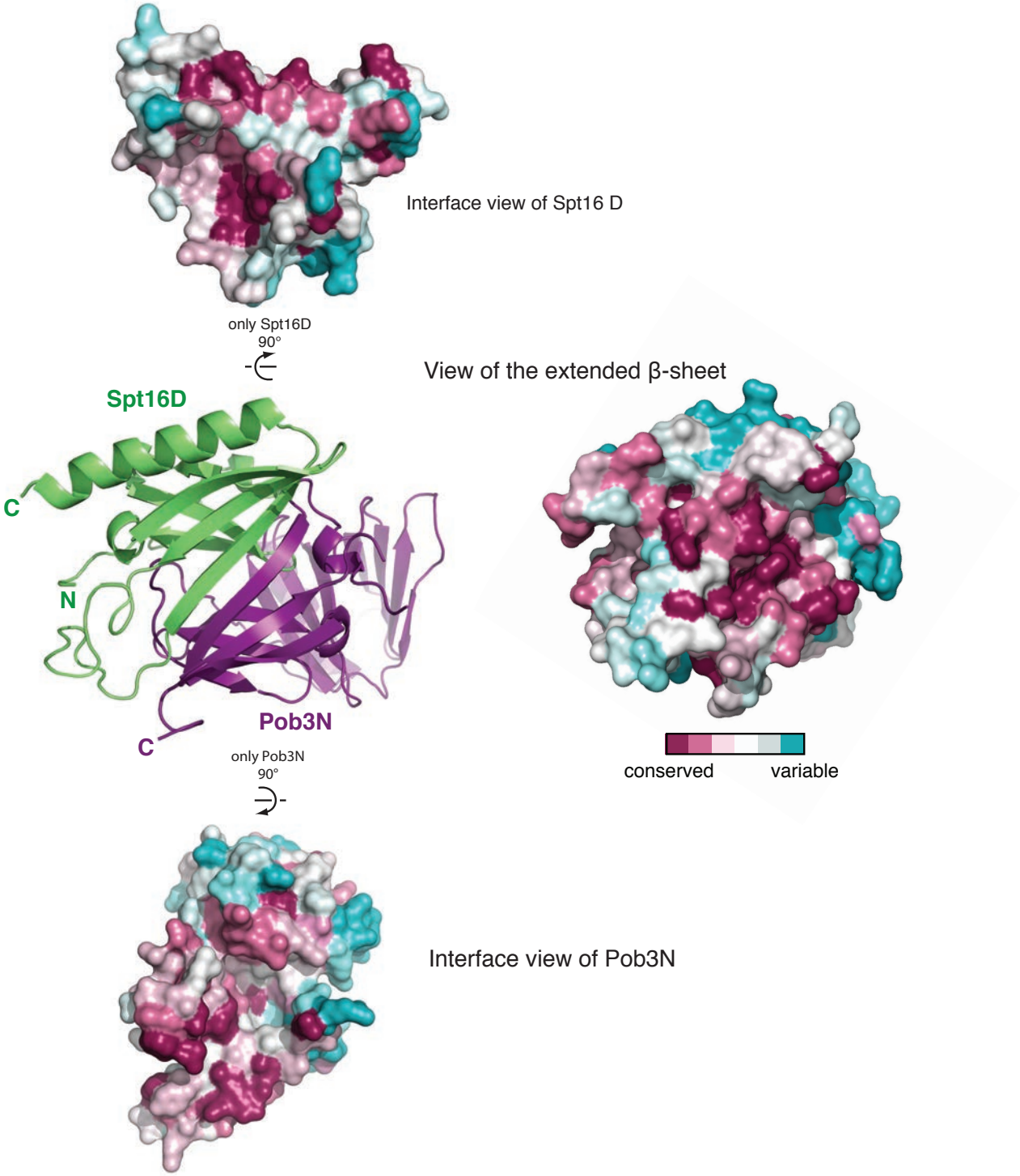

Supplementary Figure 11 | An extended beta-sheet surface on the heterodimerization domain of FACT is evolutionarily conserved.
Cartoon representation (*left,* PDB ID = 4KHB) with Spt16D (*green*) and Pob3N (*violet*) and surface view (*right*) of evolutionarily conserved residues (scale shown). To illustrate the high conservation of the interaction interface, a conservation view of these surfaces is represented without the binding partner.

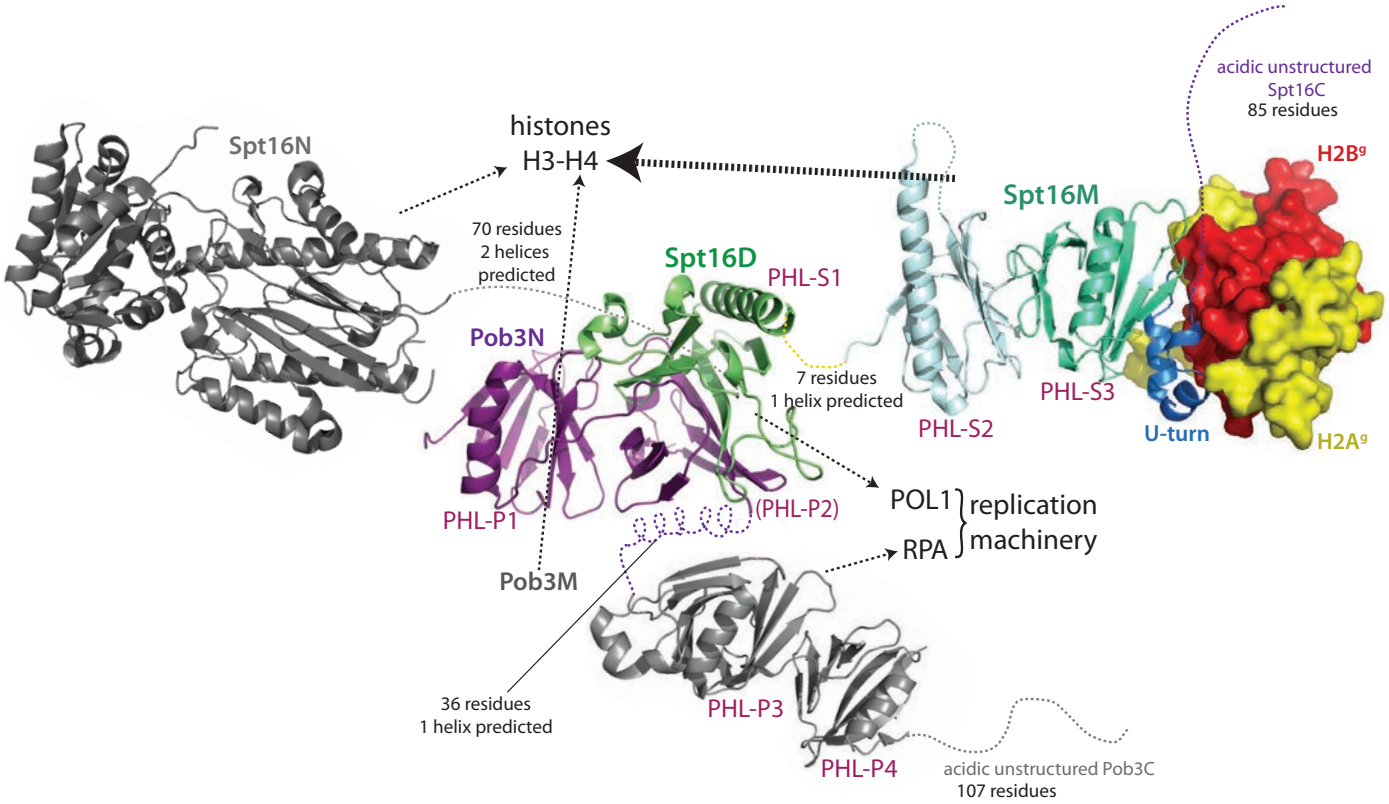

Supplementary Figure 12 | Schematic representation of the holo-FACT complex.
Crystal structures of all solved globular domains are shown in cartoon representation. Previous work (Spt16N, PDB 3CB5 and Pob3M, PDB 2GCJ) in *grey*, structures presented in this work (PDB ID = 4KHA and 4KHB) in *colour*. Linkers and unstructured regions are depicted as dotted lines. All globular domains except Spt16N consist of PHL domains with distinct molecular functions. The PHL domains are numbered according to the protein subunit, with PHL domains of Spt16 as PHL-S#, and PHL domains of Pob3 as PHL-P#. Spt16N, Pob3M and particularly Spt16M bind histones H3-H4, while Spt16M engages histones H2A-H2B specifically, as revealed by our crystal structure of the Spt16M–H2A-H2B complex. Spt16D and Pob3M bring the two subunits together and tether the comprehensive histone binding complex to the replication machinery.

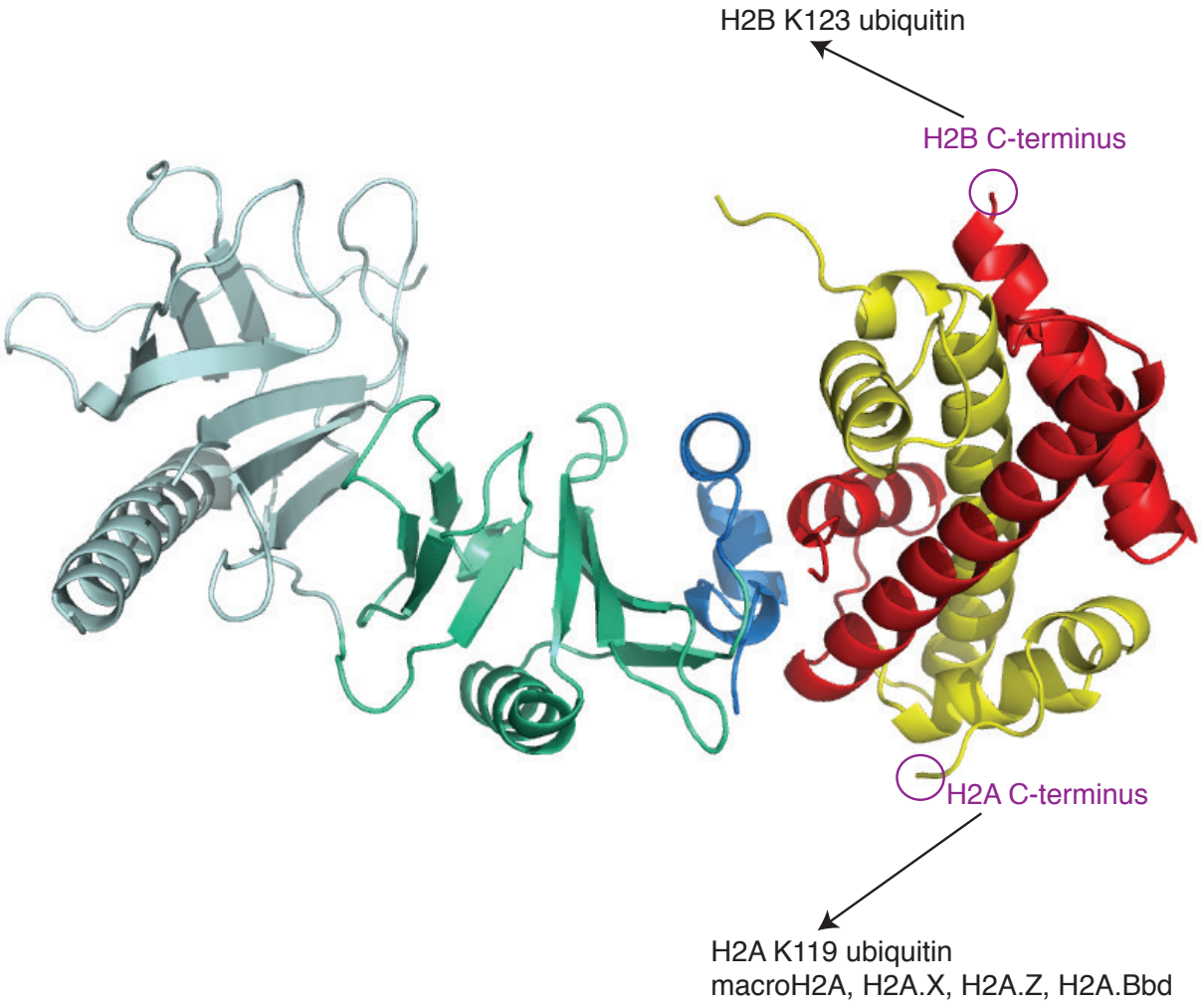

Supplementary Figure 13 | Ubiquitination and variants of H2A likely do not affect the chaperone-H2B interface.
Spt16M (*green-marine*) in surface / ribbon representation, H2B (*red*), H2A (*yellow*). The C-terminal ends of the histones are marked with *violet* circles. Location of ubiquitination sites or histone variant divergence to the canonical H2A sequence is indicated.

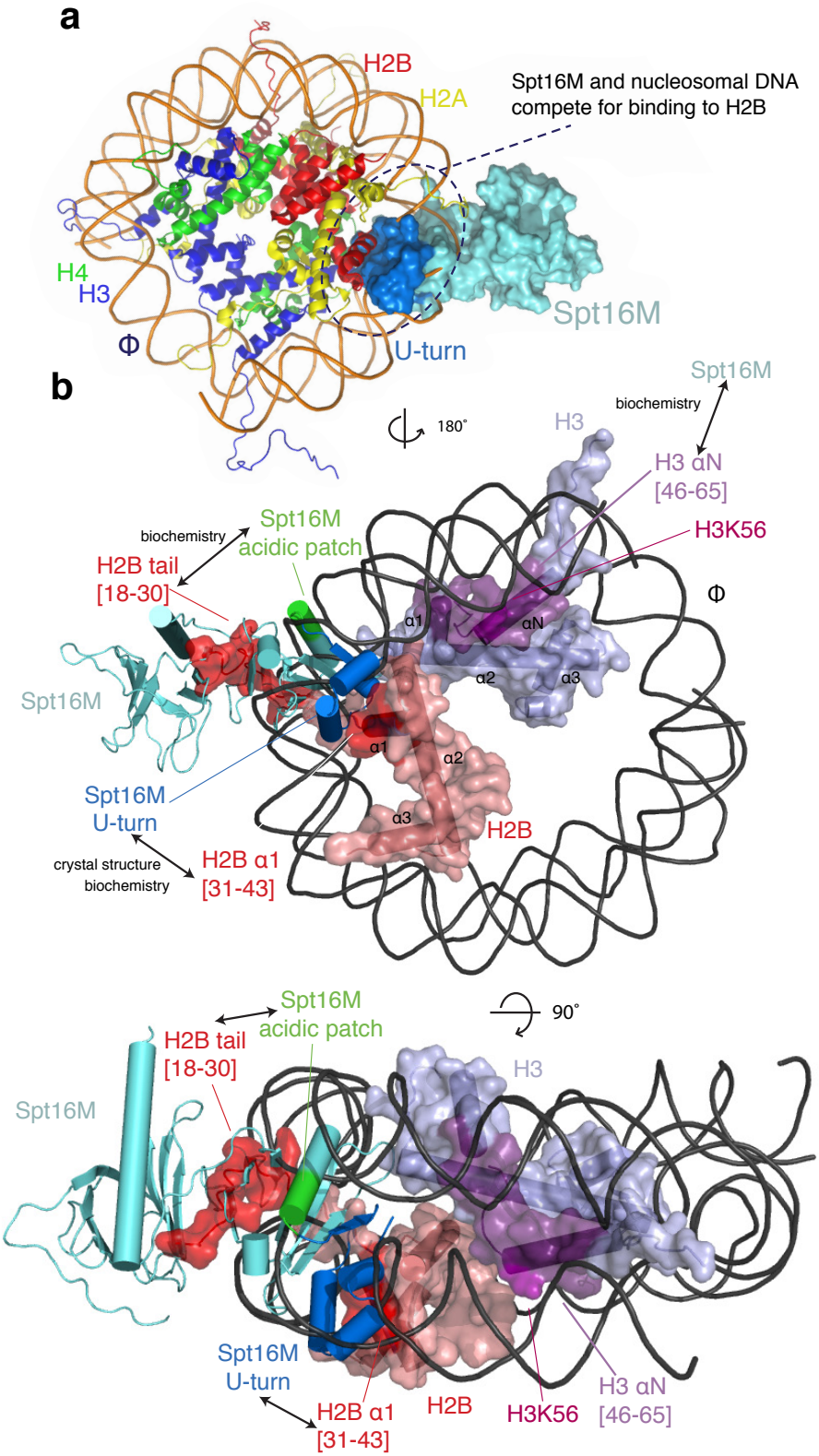

Supplementary Figure 14 | Superposition of the Spt16M-bound H2A-H2B heterodimer with one of the H2A-H2B heterodimers in the nucleosome core particle.

a, Superposition of our Spt16M-H2A-H2B complex (PDB ID = 4KHA) onto the structure of the nucleosome core particle (PDB ID = 1EQZ). The structure of the Spt16M–H2A-H2B complex was aligned to one H2A-H2B dimer in the nucleosome core particle structure. Spt16M (*green-marine*) in surface/ribbon representation, H2B (*red*), H2A (*yellow*), H3 (*blue*), H4 (*green*) and DNA (*orange*). The U-turn motif of Spt16M would be predicted to compete with DNA for binding to the hydrophobic patch on helices α1 and α2 of H2B.

b, For clarity, all histones but one copy of each H2B and H3 were removed. Spt16M is shown in cartoon representation; histones are shown as cylindrical helical cartoon representation with a transparent surface; H2B (*red*), H3 (*blue-violet*). Histone patches recognized by Spt16M are marked with darker shading and are labelled; the acidic patch on Spt16M that binds the H2B tail is coloured green. Together, the three patches recognized by Spt16M (H2B α1, the N-terminal tail of H2B and H3 αN) form a coherent surface that is partially solvent-exposed and is partially covered by the first ~30 bp of nucleosomal DNA.

Supplementary Table 1. Data collection, phasing and refinement statistics for the tandem PH-like Spt16M domain.

	Spt16M-Native	Spt16M-Se-Met
Data collection		
Space group	$P2_12_12_1$	$P2_12_12_1$
Cell dimensions		
a, *b*, *c* (Å)	61.47, 74.93, 142.53	61.06, 74.45, 141.78
Beamline	ESRF ID23-1	SLS PXII
Wavelength	0.931	0.979
Resolution (Å)	2.0 (2.1-2.0) *	2.11 (2.23-2.11)
R_{meas} [+]	0.083 (0.635)	0.055 (0.408)
$I/\sigma I$	17.0 (3.17)	14.0 (3.2)
Completeness (%)	98.7 (99.0)	99.7 (99.9)
Redundancy	7.5 (5.3)	3.6 (3.1)
Refinement		
Resolution (Å)	2.0	
No. reflections	52572	
R_{work}/ R_{free}	0.212 / 0.244	
No. atoms		
Protein	4343	
Water	430	
Ligands	9	
B-factors		
Protein	40.1	
Water	43.1	
R.m.s deviations		
Bond lengths (Å)	0.004	
Bond angles (º)	0.9	

*Highest resolution shell is shown in parenthesis.
[+]As defined in XDS (W.Kabsch, *Journal of Applied Crystallography* **26**, 795).

Supplementary Table 2. Data collection and refinement statistics for the Spt16M–H2A-H2B complex.

	Spt16M–H2A-H2B
Data collection	
Space group	$P4_32_12$
Cell dimensions	
a, *b*, *c* (Å)	108.4, 108.4, 117.8
Beamline	ESRF ID23-2
Resolution (Å)	2.3 (2.42-2.3) *
R_{merge}	0.072 (1.096)
$I/\sigma I$	19.6 (2.3)
Completeness (%)	99.9 (100.0)
Redundancy	8.8 (9.0)
Refinement	
Resolution (Å)	2.35
No. reflections	31807 (3140)
R_{work}/ R_{free}	0.191 / 0.228
No. atoms	
Protein	3411
Ligand/ion	10
Water	116
B-factors	
Protein	61.7
Ligand/ion	77.4
Water	52.0
R.m.s deviations	
Bond lengths (Å)	0.006
Bond angles (º)	0.896

*Highest resolution shell is shown in parenthesis.

Supplementary Table 3. Data collection and refinement statistics for the Spt16D–Pob3N complex.

	Spt16D–Pob3N native	Spt16D–Pob3N Se-Met
Data collection		
Space group	$P2_12_12_1$	
Cell dimensions		
a, *b*, *c* (Å)	85.39, 128.08, 132.33	85.63, 128.32, 132.13
Beamline	ESRF ID23-2	ESRF BM14
Resolution (Å)	2.4 (2.5-2.4) *	2.5 (2.77-2.53) *
R_{merge}	0.09 (0.87)	0.07 (0.64)
$I/\sigma I$	11.6 (1.9)	8.2 (1.6)
Completeness (%)	99.9 (100.0)	98.2 (97.9)
Redundancy	3.9 (3.9)	3.8 (3.7)
Refinement		
Resolution (Å)	2.4	2.5
No. reflections	57449	
$R_{work/}$ R_{free}	0.202/ 0.243	
No. atoms	9547	
Protein	9217	
Water	280	
Ligands	50	
B-factors		
Protein	23.4	
Water	18.0	
Ligands	38.8	
R.m.s deviations		
Bond lengths (Å)	0.004	
Bond angles (°)	0.912	

*Highest resolution shell is shown in parenthesis.